

Hello everybody,

If you intent to publish your data in connection with my data published in this PhD, you should contact me: **[U.Pueschner@unibas.ch](mailto:U.Pueschner@unibas.ch)**.

Any kind of publishing without my 'OK' is not allowed.

Dr. Ulrich R. Pueschner, 11.06.2002

---

**Very low-grade metamorphism in the Portage Lake Volcanics on the  
Keweenaw Peninsula, Michigan, USA**

**Inauguraldissertation**

zur  
Erlangung der Würde eines Doktors der Philosophie  
vorgelegt der  
Philosophisch-Naturwissenschaftlichen Fakultät  
der Universität Basel

von

Ulrich R. Püschner

aus Biberach an der Riss, Deutschland

Basel, 2001

---

---

Genehmigt von der Philosophisch-Naturwissenschaftlichen Fakultät  
auf Antrag von

PD Dr. Susanne Th. Schmidt, Prof. Dr. Theodore J. Bornhorst, Prof. Dr. Willem B. Stern

Basel, den 18.09.2001

---

## Dedication

This thesis is dedicated to my niece

- Miriam S. Püschner -

so she may grow up in a world of  
physical and mental freedom and  
peace.

Alles Lernen ist  
Nicht einen Heller  
Wert, wenn Mut  
Und Freude dabei  
Verloren gingen.

Pestalozzi

---

## **Acknowledgments**

First of all, I would like to thank PD Dr. S. Th. Schmidt and the late Prof. M. Frey (†, 9/2000).

They invited me to carry out the presented thesis and provided the financial and technical infrastructure of the project. More importantly, they introduced me to the topic of very low-grade metamorphism, which was, at that time, unfamiliar to me. After the tragic death of Prof. M. Frey, Prof. W. B. Stern kindly took on the role of the representative of the faculty. In many – direct and electronic - contacts they kindly provided scientific advice and suggestions.

I would also like to thank Prof. W. B. Stern for the introduction to the geochemical lab and for carrying out special measurements.

I would like to thank in Basel:

- W. Tschudin, our highly skilled technician, who is specialized in the preparation of very low-grade metamorphic rock thin sections and super polished fluid inclusion hand specimens.
- PD Dr. J. Mullis, for the introduction to the fluid inclusion studies, his measurements and for all the time he devoted to our discussions and the corrections.
- Prof. S. Graeser for sharing his expertise and for his help in special X-ray techniques.
- Prof. Ch. De Capitani for teaching me how to use the electron microprobe, and for his efforts to explain the secrets of thermodynamics to me.
- Prof. R. Abart, Dr. B. Schneider and K. Waite for discussions and quick corrections.
- Dr. R. Ferreiro Mählmann for discussion of a suite of topics.
- The best SEM images came from the Scanning Electron Microscope Lab of Basel University.
- My colleagues Dr. C. Hetherington and Dr. S. Potel for the discussions, encouragements and instrumental help.
- The former secretary S. Tobler and the new secretary B. Oberlein are thanked for saving me from administrative trouble.

In Bern I would like to thank Dr. B. Hofmann and Prof. G. C. Amstutz. With their kind help two reference samples of 'real' mining material from the Keweenaw Peninsula were obtained from the Natur-Historisches Museum of Bern/Switzerland.

---

At Geneva University I would like to thank Dr. R. Martini for teaching me how to use the cathode luminescence and Dr. R. Moritz for his efforts to find fluid inclusions in the native copper ore.

In the USA, especially on the Keweenaw Peninsula, Michigan, I would like to thank:

- The late Mr. G. Peterson for the kind permission to sample his privately owned drill core material, which ultimately made this thesis possible.
- Prof. Th. J. Bornhorst and Prof. B. Rose from the Michigan Technological University for their support, which was essential during fieldwork. I would also like to thank Prof. Th. J. Bornhorst for the time he devoted to the discussions and the corrections.

In Indiana at the University of Bloomington, I would like to thank:

- Prof. E. Ripley for the opportunity to work in his stable isotope lab,
- Dr. S. Studley for the good support at his Finniger Mat 252 mass spec
- and last but not least Dr. A. Schimmelmann for the right help just in time.

Most of the field expenses and traveling costs of this thesis were kindly funded by the Swiss National Science Foundation, project number 20.56.842.99. Some money was granted by the Travel Fund from the University of Basel. The Euro Clay Meeting in Krakow, Poland, was kindly founded by the Freiwillige Akademische Gesellschaft/Basel.

I would like to devote special thanks to all my friends and climbing partners in Europe (Germany, Switzerland, the Netherlands), in the USA (Michigan, Minnesota, Indiana), and to all my other friends spread all over the world. Thank you for your personal or electronic help in several stressful times during the last four years.

Finally, I want to thank my parents Dr. H. and E. Püschner who gave me the opportunity to obtain a good education, and who founded my studies in geology. Also a warm 'Thank you' to my sister Ursula, who was a great help, while lost in the 'soft rolling hills' of Bloomington /Indiana.

..... F. Gsell - showing me that there is more than 'academics' to live for.

---

## Table of Content

<b>ABSTRACT</b>	<b>1</b>
-----------------	----------

---

### **1**

<b>INTRODUCTION</b>	<b>3</b>
<b>MOTIVATION</b>	<b>4</b>
<b>STRATEGY</b>	<b>5</b>
SAMPLING STRATEGY	5
MACROSCOPICAL, MICROSCOPICAL AND TECHNICAL MINERAL DETERMINATION	7
ELECTRON MICROPROBE ANALYSES (EMP)	7
CHLORITE GEO-THERMOMETRY AFTER CATHELINÉAU (1988)	8
STABLE ISOTOPE INVESTIGATIONS (D, 13C, 18O)	8
FLUID INCLUSION STUDIES	8
SCANNING ELECTRON MICROSCOPY	8
CATHODE LUMINESCENCE	8

---

### **2**

<b>GENERAL GEOLOGY</b>	<b>9</b>
------------------------	----------

---

### **3**

---

#### **The very low-grade metamorphic history of the Portage Lake Volcanics on the Keweenaw Peninsula, Michigan – a new study on three diamond drill core profiles**

<b>INTRODUCTION</b>	<b>14</b>
<b>METHODS</b>	<b>14</b>
STRATEGY	15
X-RAY DIFFRACTION (XRD) AND X-RAY FLUORESCENCE (XRF)	16
ELECTRON MICROPROBE ANALYSES (EMPA)	16
SCANNING ELECTRON MICROSCOPE (SEM)	16
STABLE ISOTOPE (SI)	16
CATHODE LUMINESCENCE (CL)	17
<b>ALTERATION<sup>4</sup></b>	<b>17</b>
GENERAL PRIMARY CHARACTERISTICS OF THE PLV	17
MAJOR CHARACTERISTICS OF THE ALTERATION MINERALS	18
<i>Albite (ab)</i>	19
<i>Potassium-feldspar (kfs)</i>	19
<i>Epidote (epi)</i>	19
<i>Pumpellyite (pmp)</i>	20
<i>Prehnite (prh)</i>	21
<i>Phyllosilicate minerals (phy)</i>	22
<i>Quartz/Chalcedony</i>	23
<i>Calcite</i>	23
<i>Zeolites</i>	24
<i>Native Copper</i>	24
<i>Exotic secondary minerals</i>	24
ALTERATION-PATTERN	24
<b>STABLE ISOTOPE ANALYSES</b>	<b>26</b>
<b>DISCUSSION</b>	<b>30</b>
<b>CONCLUSIONS</b>	<b>32</b>

---

## 4

---

### **Phyllosilicates in the Portage Lake Volcanics: a record of very low-grade metamorphic alteration and reaction progress**

<b>INTRODUCTION</b>	<b>38</b>
<b>METHODS</b>	<b>38</b>
X-RAY DIFFRACTION	38
<i>Preparation of the sample material</i>	38
<i>Conditions for X-ray diffraction (XRD)</i>	39
ELECTRON MICROPROBE (EMP)	39
<i>Preparation of the sample material</i>	39
<i>Conditions for electron microprobe analyses (EMPA)</i>	41
<b>RESULTS</b>	<b>41</b>
DISTRIBUTION OF PHYLLOSILICATES IN THE PLV	44
CHLORITE THERMOMETRY	49
<b>DISCUSSION</b>	<b>51</b>
<b>CONCLUSIONS</b>	<b>52</b>

---

## 5

---

### **Native copper mineralisation in the Portage Lake Volcanics in context of the very low-grade metamorphic alteration on the Keweenaw Peninsula, Michigan**

<b>INTRODUCTION</b>	<b>54</b>
<b>METHODS</b>	<b>54</b>
FLUID INCLUSION MEASUREMENT	54
SCANNING ELECTRON MICROSCOPE (SEM)	54
CATHODE LUMINESCENCE (CL)	54
<b>RESULTS</b>	<b>55</b>
GENERAL OCCURRENCE OF NATIVE COPPER	55
NATIVE COPPER BESIDE QUARTZ	56
NATIVE COPPER BESIDE CALCITE	59
SHAPE OF NATIVE COPPER INCLUSIONS	61
FLUID INCLUSION RESULTS	61
DESCRIPTION OF THE FLUID INCLUSIONS OF AHMEEK AND COPPER HARBOR PROFILE	62
FLUID INCLUSIONS OF THE MINE SAMPLES	65
<b>DISCUSSION/INTERPRETATION</b>	<b>65</b>
COMPARISON OF FLUID INCLUSION DATA FROM THE KEWEENAW PENINSULA	66
NATIVE COPPER PRECIPITATION SCENARIOS	67
COMPARISON OF DIFFERENT MINE SITES, FROM SOUTH SHORE OF L.S.	68
<b>CONCLUSIONS</b>	<b>69</b>

---

## 6

<b>CONCLUSIONS</b>	<b>70</b>
<b>OPEN QUESTIONS &amp; OUTLOOK</b>	<b>73</b>

---

## 7

<b>REFERENCE</b>	<b>75</b>
------------------	-----------

---

## 8

<b>APPENDIX</b>	
A EMP ANALYSIS	<b>A 1 - 40</b>
B SEM & BSE IMAGES	<b>B 1 - 19</b>
C X-RAY DIFFRACTOGRAMS	<b>C 1 - 6</b>
D FLUID INCLUSION DATA	<b>D 1 - 7</b>



## Abstract

The Portage Lake Volcanics (PLV) on the Keweenaw Peninsula, Michigan, USA used to host one of most famous and biggest native copper mining areas in the world and are now closed. The rock sequence is also the locality of the first description of the low-grade metamorphic index mineral pumpellyite (Palache and Vassar, 1925). Exploration and mining of the native copper deposits in the approx. 5 km thick Keweenaw (Precambrian) Portage Lake Volcanics (PLV) on the Keweenaw Peninsula have provided many drill cores. Due to a lucky coincidence, 195 km of drill core material is still accessible. Part of this drill core is the basis for studying the history of the low-grade metamorphism of the basaltic rocks of the Portage Lake Volcanics. Ten drill cores were finally selected and studied, representing three vertical stratigraphic profiles through the PLV. The three profiles are located northeast of the former main mining area along the SW-NE striking PLV. They are correlated by interflow sediments. Furthermore, two samples from the Calumet mine were studied to complement the fluid inclusion data.

Amygdaloidal flow tops and veins with abundant secondary alteration minerals, less altered transition zones and massive flow interiors were sampled. The macroscopical and microscopical description combined with X-ray diffraction analysis lead to an overview of the mineral distribution in the studied area. The two already described low-grade metamorphic facies, a pumpellyite-prehnite and a zeolite facies, were confirmed (Jolly and Smith, 1972; Livnat, 1983). In contrast to the model of Jolly and Smith (1972) the samples do not indicate a stratigraphic zonation, which was demonstrated by Livnat (1983). His data support a low-grade metamorphic alteration plane, which crosscuts the stratigraphy of the PLV dipping towards the north at a shallower angle than the original bedding. In contrast, this study suggests an irregular and discontinuous distribution of the pumpellyite-prehnite index minerals with a slight trend to more pumpellyite-prehnite abundance in the SW towards the main mining area. The zeolite facies is a later, superimposed low-grade metamorphic alteration event related to late crosscutting veins. Based on the results of the microscopical studies, a three-stage alteration model of the PLV is postulated. These stages are subdivided into different pulses on the basis of electron microprobe analysis, fluid inclusion study and cathode luminescence data. The alteration minerals, such as quartz, pumpellyite and calcite, show major zonations, from 3 to 7 zones.

The investigation of alteration minerals in the different units of the PLV revealed that the growth of the low-grade metamorphic minerals was strictly controlled by the fluid/rock interaction and thus by the permeability of the surrounding rocks. In permeable rocks, secondary minerals like epidote, pumpellyite and prehnite are abundant as initial secondary alteration minerals. In non-permeable rocks such as massive flow interiors and in zones with non-connected small (<2 mm) amygdules, phyllosilicates dominate as minerals of initial alteration.

Phyllosilicates are the dominant minerals in the PLV. They can be considered as relative indicators of metamorphic grade (e.g. Kristmansdottir, 1979; Schiffman and Fridleifsson, 1991). In the Ahmeek profile, containing slightly more pumpellyite-prehnite index minerals, two distinct populations of phyllosilicates developed (chlorites and mixed-layered phyllosilicates). In contrast in the Copper Harbor profile, simultaneously with less abundant prehnite-pumpellyite facies index minerals, a continuous population of phyllosilicates (chlorite-corrensite-mixed-layered) is present.

The first and the third alteration stages are well distinguished on the basis of their  $\delta^{18}\text{O}$  values, where epidote, clinocllore and quartz of the first stage have a range of 5 – 15‰ and calcite of the third stage shows a range between 20 – 30 ‰.

The fluid inclusion studies in quartz and calcite close to the native copper precipitation revealed two main fluid inclusion populations. In the Copper Harbor profile, these populations can be divided into a high saline ( $> 30$  wt%) and a low saline ( $\leq 10$  wt%) population. Towards the southwest, the differences between the fluid populations vanish. In the studied mine samples, no populations could be distinguished so far.

Based on fluid inclusion and stable isotope data fluid mixing as suggested by Livnat (1983) was confirmed. The recently obtained data indicate that meteoric and metamorphic waters were mixed. The postulated seawater input (Livnat, 1983), however, could not be observed.

The process of native copper precipitation was probably different in the drill core profiles, where only little native copper occurs, and in the mine samples. In the mine samples corrosive fluids dissolved and precipitated quartz and calcite up to three times before the native copper precipitation occurred. The gangue minerals of the available mine samples are epidote and quartz. In the studied drill cores copper occurs together with prehnite. Two main types of native copper emplacements could be observed. The first type was likely precipitated as a result of a short, powerful, hydrothermal process such as pressure release, which is indicated by native copper droplets in vein quartz and in quartz cement of the conglomerates. The second type formed slowly as native copper sheets parallel to calcite cleavage or along grain boundaries. In contrast to the typical mine samples, no corrosion could be observed here.

The low-grade metamorphism in the PLV must have been related to a high heat flux, which was probably caused by an underplated gabbro at ca. 40km depth. Later thrusting along the Keweenawan fault did not change the metamorphic conditions considerably but generated new pathways for fluids depositing the same minerals or similar assemblages of alteration stage II. The deposition of the native copper ores is connected to this alteration stage. A late retrograde zeolite facies overprints the early alteration stages.

## **General Introduction**

## Introduction

In general, metamorphism is a process of solid-state change in the mineralogy, texture and chemistry of rocks (Frey and Robinson, 1999). Metamorphism includes low-grade metamorphism ( $<400\text{ }^{\circ}\text{C}$ ,  $<3\text{ kbar}$ ), high temperature metamorphism ( $>400\text{ }^{\circ}\text{C}$ ,  $>4\text{ kbar}$ ) and high pressure metamorphism ( $>10\text{ kbar}$ ). Metamorphic minerals are usually easily distinguished in high temperature-high pressure metamorphic rocks and therefore these types of metamorphism are well studied. Although being nearly omnipresent, low-grade metamorphism is comparatively little studied, because the minerals are not as easily identified. The first text book on very low-grade metamorphism was published in 1987 by Martin Frey and therefore, this branch in the geosciences may be considered to be relatively young. The low-grade metamorphic group of Basel under the head of the late Prof. Martin Frey († 2000) studied several areas of low-grade metamorphism in the Swiss Alps, (Wang et al. 1996 ; Schmidt et al., 1997), in the Andes of Chile (Belmar, 2000) and on New Caledonia (Potel, 2001)



**Figure 1:** Topographic map of the study area. Black quadrangles indicate the locations of the profiles and the single field-site (Keweenaw Point).

## Motivation

This thesis is concerned with the low-grade metamorphism of the Precambrian or Keweenaw basaltic rocks, named the Portage Lake Volcanics, on the south shore of Lake Superior in Northern Michigan, USA (**Fig. 1**). Based on selected material of drill cores, with a total length of 195 km (600 000 feet), which were recovered during mining activities; it examines the distribution of metamorphic minerals, the stable isotope composition of selected low-grade metamorphic minerals as well as the fluid inclusion populations in quartz and calcite. The main scope was to reinvestigate the proposed vertical metamorphic zonation, to generate a model how

the alteration could have taken place and to understand where the alteration fluids might have been derived from. In chapter 3 of this thesis the whole alteration history is described, discussed and a model of the alteration history is presented. In chapter 4 the occurrence of the phyllosilicates is discussed with the three common formation models of clinocllore, corrensite and smectite. Chapter 5 presents the observations of the fluid inclusion studies, which confirm the present hypothesis about fluid mixing during the alteration and especially during the native copper precipitation.

The Keweenaw Peninsula is famous for its rich native copper deposits, which were exploited from 1845 until the late 60ies of the 20th century. The area produced about 5 Mio t of refined copper (Weege and Pollack, 1971) and was at this time the biggest copper mine in the United States of America. The host rock of the native copper deposits is the unit of the Portage Lake Volcanics, abbreviated as PLV in the following text. Various studies concerning the genesis of the native copper deposits (e.g. Rath, 1874; Butler and Burbank, 1929; Broderick, 1931) were carried out. The metamorphic index mineral pumpellyite was recognized and described for the first time from this area by Palache and Vassar (1925).

Already as early as in 1959, Stoiber and Davidson recognized a stratigraphically dependent mineral zonation in the PLV. Jolly and Smith (1972) applied the new ideas of the low-grade metamorphic facies concept which was introduced by Coombs et al. (1959). They studied a diamond drill core profile through the PLV focusing on the alteration minerals and proposed three metamorphic zones with increasing stratigraphic depth. Livnat (1983) studied drill core samples, surface samples and dump hill material from the former copper mines and showed evidence that the secondary mineral zones and the  $\delta^{18}\text{O}$  isopleths of flow top minerals in the PLV dip at a shallower angle than stratigraphy. Based on the first stable isotope analyses Livnat (1983) initiated a discussion about seawater input during alteration processes of the PLV.

Low-grade metamorphism is also known from the Precambrian North Shore Volcanic Group on the south-western side of Lake Superior. Within the 8 000 km thick volcanic rocks of the North Shore Volcanic Group, a stratigraphically controlled metamorphic zonation is present spanning five low-grade metamorphic zones from low zeolite to beginning greenschist facies (Schmidt, 1990, 1993; Schmidt & Robinson, 1997)

## **Strategy**

### ***Sampling strategy***

It was first necessary to overview the 600 000 feet (195 km) of accessible drill core from the Portage Lake Volcanics stored in a building at Calumet, Michigan. The drill core is stored in wooden boxes, which are piled up to a height of more than several meters (Fig. 2). Drill site locations on the Keweenaw Peninsula and a short log-description of the rocks and minerals carried out at the time of drilling are still available. This information is stored on microfiche at the library of the Michigan Technical University in Houghton.

After a first examination of the drill core, the most suitable material was arranged in four drill core profiles, which are located between the Calumet mining area and the tip of the Keweenaw Peninsula (Fig. 1). This should allow a comparison of alteration close to the native copper main mining area and metamorphism unrelated to significant copper deposition.

Altered flow tops and bases, transition zones and less altered massive flow interiors were sampled. The flow tops and bases host the main amount of alteration minerals whereas the massive flow interiors are the least altered parts.

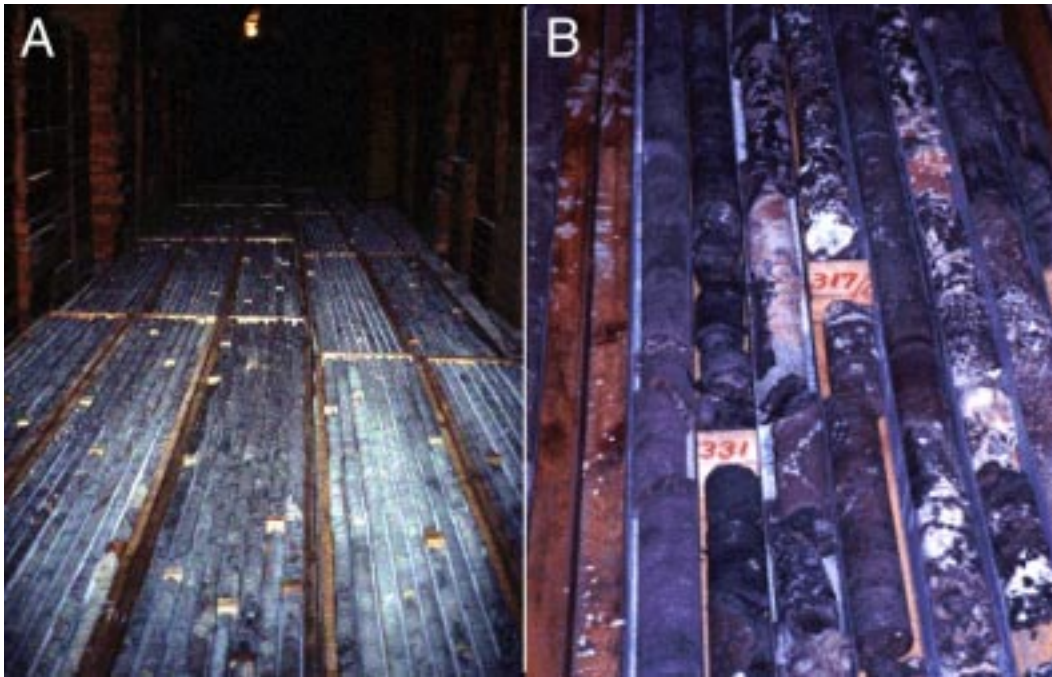


**Figure 2:** Part of the 195-km of diamond drill core. A) Drill core in the drill-core storage building in Calumet/Michigan (box-length about 2-m); B) Core diameter 3 cm, numbers indicate drill-depth in feet.

Initially, 912 samples from 17 different drill cores and an additional five surface samples were taken (Fig. 3). During the laboratory work the number of drill cores was reduced to 10 drill cores with a total number of 595 samples, and the surface samples were excluded.

The Copper Harbor profile, it is located in the eastern part of the Keweenaw Peninsula and consists of three individual drill cores. The second drill core profile - located about 25 km to the west of the Copper Harbor

profile - is the Eagle Harbor profile with five individual drill cores. These drill core section represents in part the same section which was also investigated by Stoiber & Davidson (1959a, b). The third profile, the Ahmeek profile, consists of three drill cores and is located in the vicinity of the Calumet mine. Three different interflow sediments are used as marker horizons for the stratigraphic correlation of the three profiles (Fig. 3).

For a descriptive purpose, the PLV are subdivided into four horizontal sections (A to D) from the stratigraphic top (A) of the volcanic lava flows down to the Keweenawen Fault (D), which cuts the PLV in a stratigraphically deeper level (Fig. 3).

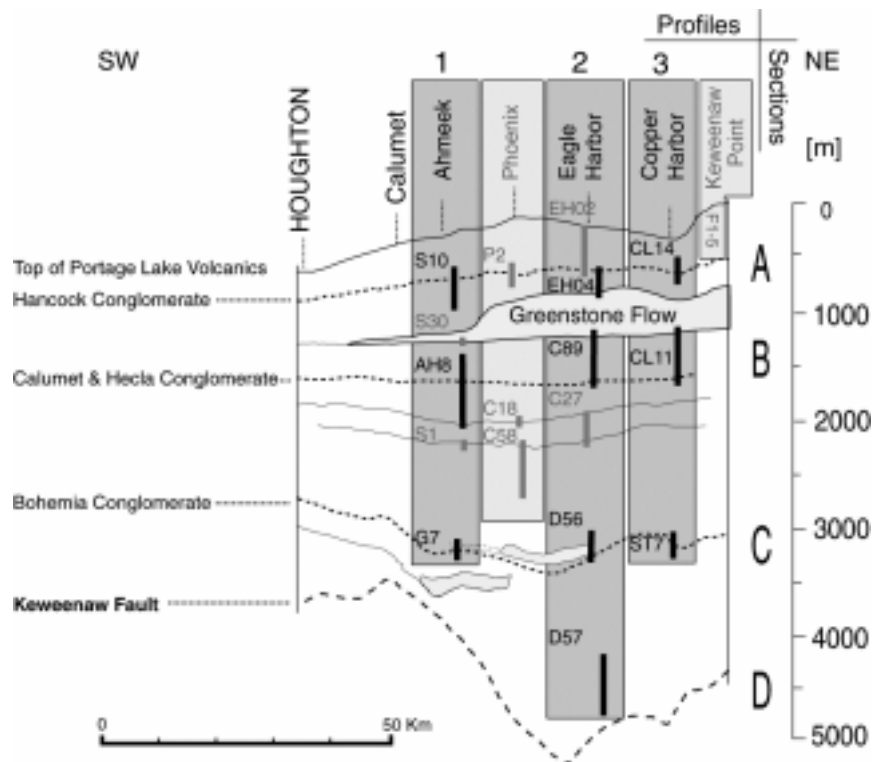


**Figure 3:** Schematic stratigraphic back-tilted profile through the Portage Lake Volcanics (PLV) on the Keweenaw Peninsula (after White, 1971). Indicated are the 17 sampled drill cores and one field-location (Keweenaw Point). Drill cores in bold are studied in detail in this thesis.

### **Macroscopical, microscopical and x-ray diffraction mineral determination**

While sampling the drill core, a brief sample description of the alteration minerals and the host rocks was obtained. A more detailed examination was carried out in the lab in Basel and a database of the occurrence and relative distribution of alteration minerals was obtained. With the help of the generated database, several key questions were asked and answered. Such as: What is the dominant mineral assemblage in the original stratigraphic levels? Is there a relation between mineral distribution and tilting or current stratigraphic deposition. In other words, do the mineral distributions show stratigraphic crosscutting relationships or is the distribution of alteration mineral zones controlled by stratigraphy, by later tectonic thrusting or by fluid movement?

The macroscopical descriptions were supported and supplemented by the X-ray diffraction technique to identify complex and individual mineral phases and by thin section microscopy. Thin section studies gave a more detailed idea about the relative mineral growth in amygdules and veins.

### **Electron microprobe analysis (EMPA)**

Due to restricted sample material, almost all thin-sections are highly polished ones, which are also suitable for electron microprobe measurements. Because of the fine-grained nature of the alteration minerals, electron microprobe analyses were necessary to identify the minerals. In addition, the chemical composition of minerals (e.g. pumpellyite, quartz, ...) was analyzed to obtain information about zonation. These chemical changes reflect changes in the physico-chemical conditions during formation, such as temperature, fugacity or variation in the

composition of the alteration fluid. They also might influence the formation of different mineral assemblages and generations in the amygdules, veins and the matrix itself.

### ***Chlorite geothermometry after Cathelineau (1988)***

Phyllosilicates are the most abundant alteration minerals in the PLV. Cathelineau (1988) introduced a chlorite geo-thermometer, which is based on the tetrahedral Aluminum content in an uncontaminated chlorite. Mixed-layering of chlorite is a common feature in the PLV. Therefore the geo-thermometer has its limitations and should not be applied. Nevertheless, the chlorite formation temperatures were calculated and approximate formation temperatures were obtained.

### ***Stable isotope investigations (D, <sup>13</sup>C, <sup>18</sup>O)***

The purpose of measuring stable oxygen and hydrogen isotopes was to reveal the nature and origin of the fluids, which altered the PLV. Livnat (1983) postulated that a seawater input and the abundant boron minerals likewise support such a theory.

The laboratory of Prof. Ripley (Indiana University of Bloomington) was chosen because its facility hosts an extraction-line for hydrogen from phyllosilicates (Ripley et al. 1998). Another reason was to be able to exchange experience and ideas with colleagues that were involved in similar projects. Therefore, this Ph.D. project included a 5.5 months stay at the stable isotope lab of the Geological Department at the Indiana University of Bloomington during spring and summer 2000.

### ***Fluid inclusion studies***

Fluid inclusions in low-grade metamorphic alteration minerals such as quartz and calcite contain essential information about the temperature formation of the host mineral and the composition of a fluid (Mullis, 1987). Various generations of low-grade metamorphic calcite and quartz were investigated from veins. Samples with abundant native copper were not available since the drill core with the native copper was probably removed immediately after drilling. Nevertheless, some samples contain small amounts of native copper.

### ***Scanning electron microscopy (SEM)***

Some of the highly polished thin sections, already used in the EMP analysis, were used to obtain highest quality back-scatter images. The SEM became an important tool in the context of the genesis and timing of formation of the native copper deposits and its relation to low-grade metamorphism. It allowed to generate in part a three-dimensional view of the native copper inclusions in quartz and calcite. From these and EMPA-BSE (back scatter electron) images, information about the mechanism of rapid copper precipitation could be derived.

### ***Cathode luminescence***

Cathode luminescence is mainly used in sedimentary geology to reveal the nature and generations of carbonatic cements. It is based on the variations of trace elements (mainly Mn and Fe) in minerals. In the PLV, different calcite generations usually contain different quantities of trace elements, therefore showing different cathode luminescence colors. It confirmed the results of stable isotope analysis to a certain extent.



## **General Geology**

## General Geology

The Keweenaw Peninsula is part of the North American Midcontinent Rift System extending from Kansas through the Lake Superior Region and to southern Michigan with a total length of about 2000 km (Fig. 1). The Mid-continent Rift System is the result of ex-tensional thinning of the Precambrian Superior block by an asthenospheric mantle plume which resulted in the extrusion and emplacement of large volumes of basaltic and rhyolitic rocks within the Rift (Hutchinson et al., 1990). The rift is filled, beneath Lake Superior, with a succession of subaerial volcanic deposits and clastic sedimentary rocks. Based on seismic profiles across the Lake Superior, the present day total thickness of the rift filling rocks is estimated to be around 35 km (Cannon, 1989; Hinze et al., 1990; Cannon and Hinze, 1992).

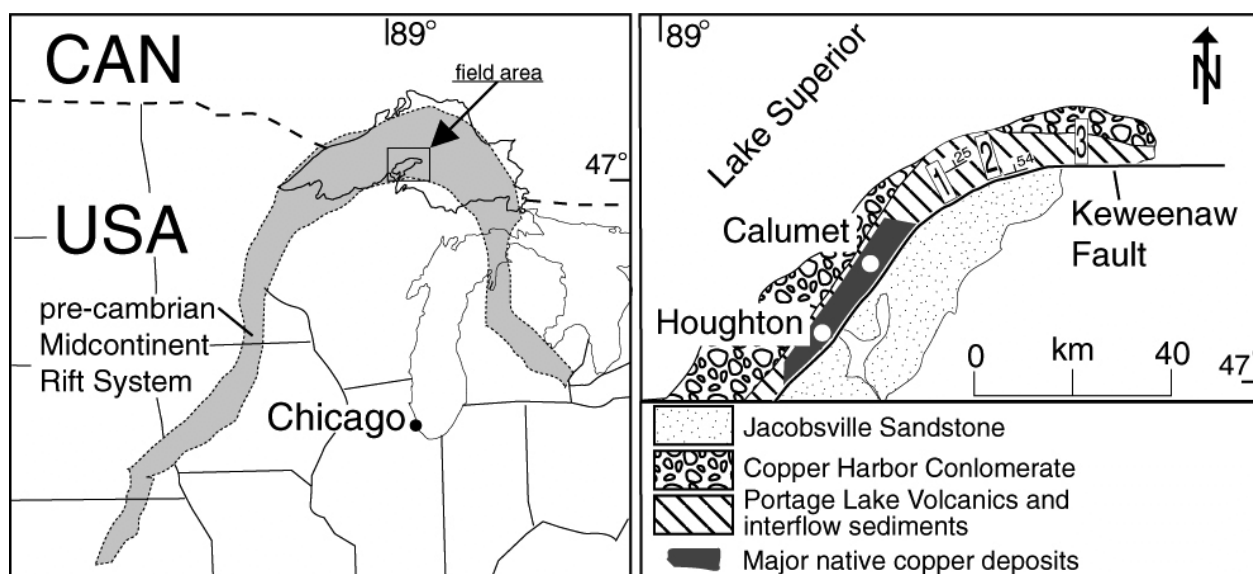


**Figure 1:** Context of the Keweenaw Peninsula in the Precambrian rift structure and general geology of the Peninsula itself (redrawn from Bornhorst, 1997). The numbers (1, 2, 3) in the schematic map indicate the approx. location of the studied drill core profiles.

Rift magmatism in the Lake Superior Region occurred ca. from 1.109 to 1.087 Ga. while the PLV erupted during a 2-3 Ma period around 1.095 Ga (Davis and Paces, 1990; Paces and Miller 1993). They are composed of at least 200 subaerial tholeiitic basaltic lava flows, with minor interbedded clastic sediments. The predominant rock type in the PLV is a fine-grained to ophitic, plagioclase-rich olivine tholeiite (Jolly, 1972; Jolly and Smith 1972). Sometimes, in bigger flows where in situ differentiation took place, the texture becomes pegmatitic (Cornwall 1951a, b, c; Lindsley et al. 1971). Less than 1 vol. % of the PLV are intermediate to felsic volcanic and subvolcanic rocks (Nicholson, 1987; Grimes, 1977).

Individual flows can have a consistent thickness over distances of 30-50 km and a few single flows can be recognized over distances of up to 100 km along strike. Flow thickness varies from one meter to over 500 m with an average of approx. 10 m (Paces, 1988). This average lava flow may contain 10 to 50 km<sup>3</sup> of magma. The largest flow within the PLV, and one of the largest flows on Earth, is the Greenstone Flow with a thickness of up to 500 m. It is estimated to contain more than 1500 km<sup>3</sup> of magma (Longo, 1983, 1984).

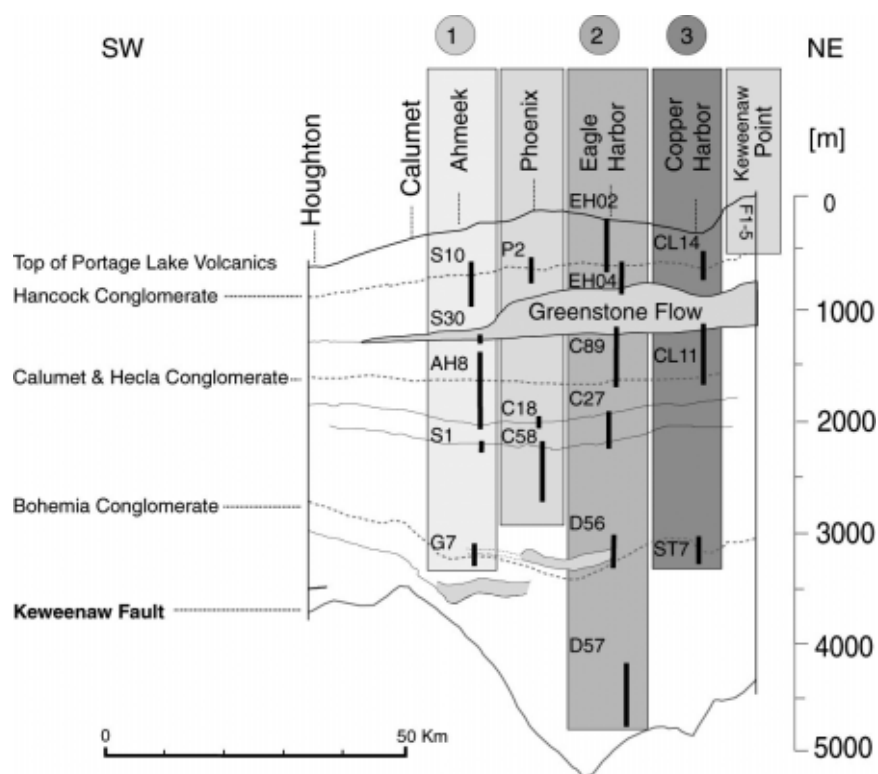


**Figure 2:** Schematic stratigraphic back-tilted profile through the Portage Lake Volcanics (PLV) on the Keweenaw Peninsula (after White, 1971). Indicated are the 17 sampled drill cores and one field-location (Keweenaw Point).

About 3% of the total volume of the PLV consists of interbedded sediments (Merk and Jirsa, 1982). These sediments are rare but an important feature within the PLV because they form relatively continuous marker horizons, which allow a stratigraphic correlation of the three drill core profiles of this thesis. In the PLV, there are 22 major interflow sedimentary horizons (Butler and Burbank, 1929; White, 1952; and Merk and Jirsa, 1982). On the Keweenaw Peninsula, the total stratigraphic thickness of the PLV is estimated to be 5000 m (Fig. 2).

The younger Keweenawan Copper Harbor Conglomerate covers the PLV. The PLV on the Keweenaw Peninsula dip in general  $25^{\circ}$  to  $70^{\circ}$  North towards the present axis of the Lake Superior syncline. These rocks are cut by a major thrust fault, the Keweenaw Fault, most of which is buried beneath a younger gently dipping to flat-lying sandstone of the Jacobsville Formation (Fig. 1).

The Keweenaw Fault transformed the original graben bounding normal fault into a high-angle reverse fault (Cannon, 1989). It shows several kilometers of lateral displacement. Within the rift-filling strata of the Keweenaw Peninsula, faults, fractures and broad open folds developed in response to this contractional event (White, 1968; Butler and Burbank, 1968). Cannon et al. (1994) has determined that the faulting occurred about  $1060 \pm 20$  Ma ago, using reset Rb-Sr biotite ages in older Precambrian basement rocks near the Michigan-Wisconsin border as argument. The probable cause of this compressional event is the continental collision along the Grenville front (Hoffman, 1989; Cannon and Hinze, 1992; Cannon, 1994).

A vertical section of a typical basaltic flow from the PLV can be subdivided into four parts (Fig. 3). The flow base consists of basalt with small and rare amygdules with a diameter of 2 mm. The

massive flow interior (MF) consists of massive basalt that is mostly impermeable, except for some cross cutting fractures. A transition zone (TZ) occurs between the MF and flow top. It consists of basalt with amygdules that increase in abundance upwards. The flow top (FT) consists often of a very porous, sometimes even cellular basaltic rock. In flow tops pipe-amygdules are often observed. They indicate with their elongated shapes where the surface of the lava flow was. Some FT's are brecciated and therefore infiltrated with clastic sediments in the open spaces.

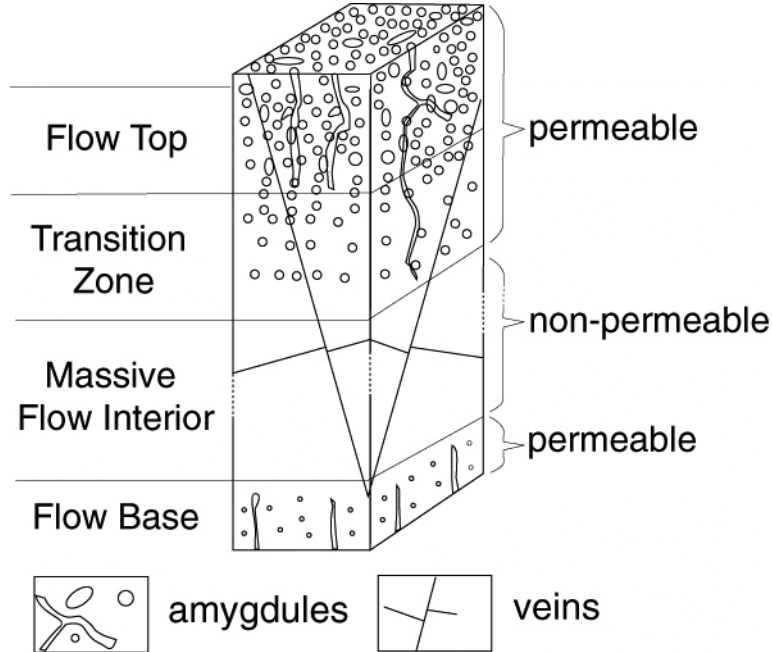


**Figure 3:** Schematic lava flow of the Portage Lake Volcanics.

The PLV of the Keweenaw Peninsula are famous for the rich native copper ore deposits (Fig. 1). Between 1845 and 1968, the refined copper production was ca. 5 Mio t (Weege and Pollack, 1971). About 96% of the production came from the area between Houghton and Calumet. The copper was deposited as part of the widespread metamorphic / hydrothermal alteration process of the PLV (Stoiber and Davidson, 1959). It is still unknown why the copper concentrations vary in that area, where specific enrichment processes were to form economic deposits (Broderick, 1931), and why other similar settings such as Isle Royale, Michigan, Wisconsin, Minnesota or Ontario, Canada do not show economic copper deposits (Cannon and McGervey 1991).

**The very low-grade metamorphic history of the Portage Lake Volcanics on the  
Keweenaw Peninsula, Michigan**

—

**a new study on three diamond drill core profiles**

Ulrich R. Püschner

Susanne Th. Schmidt

## Introduction

The study of Stoiber and Davidson (1959) documented a systematic regional zonation of prehnite, epidote and quartz within the Portage Lake Volcanics (PLV). Jolly and Smith (1972) studied diamond drill cores of the Eagle Harbor profile through the entire stratigraphy of the PLV. Applying the modern facies concept for low-grade metamorphic rocks described by Coombs (1971) in New Zealand, Jolly and Smith (1972) demonstrated a graduation from low-rank metamorphism of the zeolite facies in the stratigraphically upper sequence to a prehnite-pumpellyite facies in the stratigraphically lower sequence of the PLV. Livnat (1983) also carried out work on the low-grade metamorphism of the Keweenaw Peninsula using samples from drill core, mines and surface rock piles from the mines. His study aimed to model the metamorphic history and associated native copper mineralisation. He documented the same two facies as Jolly and Smith (1972) but according to his results planes of equal facies dip at an angle crosscutting the original stratigraphic depth. On the basis of a single stable isotope analysis he speculated about a seawater input to the metamorphic / hydrothermal fluids. The present study tries to generate a complete overview of the low-grade metamorphism of the Keweenaw Peninsula using the same drill cores studied by Jolly and Smith (1972) as well as two additional drill core profiles (**Fig. 1**).

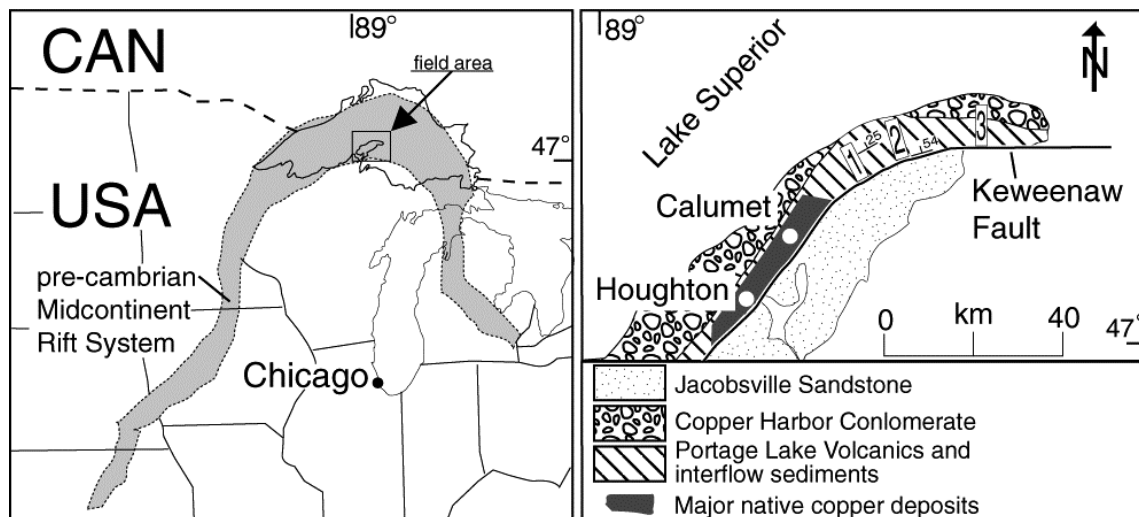


**Figure 1:** A) Location of the Keweenaw Peninsula with respect to the great North American Midcontinent Rift System. B) General geology of the Keweenaw Peninsula including major native copper deposits. (Modified from Bornhorst, 1997)

## Methods

During exploration for copper on the Keweenaw Peninsula many diamond drill holes were completed. Fortunately, 195 km (600 000 feet) (Weege, 1988) of diamond drill core were preserved in a building at Calumet Michigan owned by the late Mr. Peterson. The core with 3cm of diameter is stored in wooden boxes and the documentation of the drill core including details of drilling and a brief macroscopic description of the material at the time of the drilling is still available on microfiche at Michigan Technological University in Houghton, Michigan.

**Strategy**

Initially, 912 samples from 17 different drill cores were taken. During the laboratory work the number of drill cores was reduced to 10 drill cores with a total number of 595 samples. These 10 drill cores are located in 3 profiles between Calumet and Copper Harbor (**Fig. 2**). The distance between the different profiles is about 25 km. Three different interflow sediments are used as marker horizons for the correlation of the three profiles.

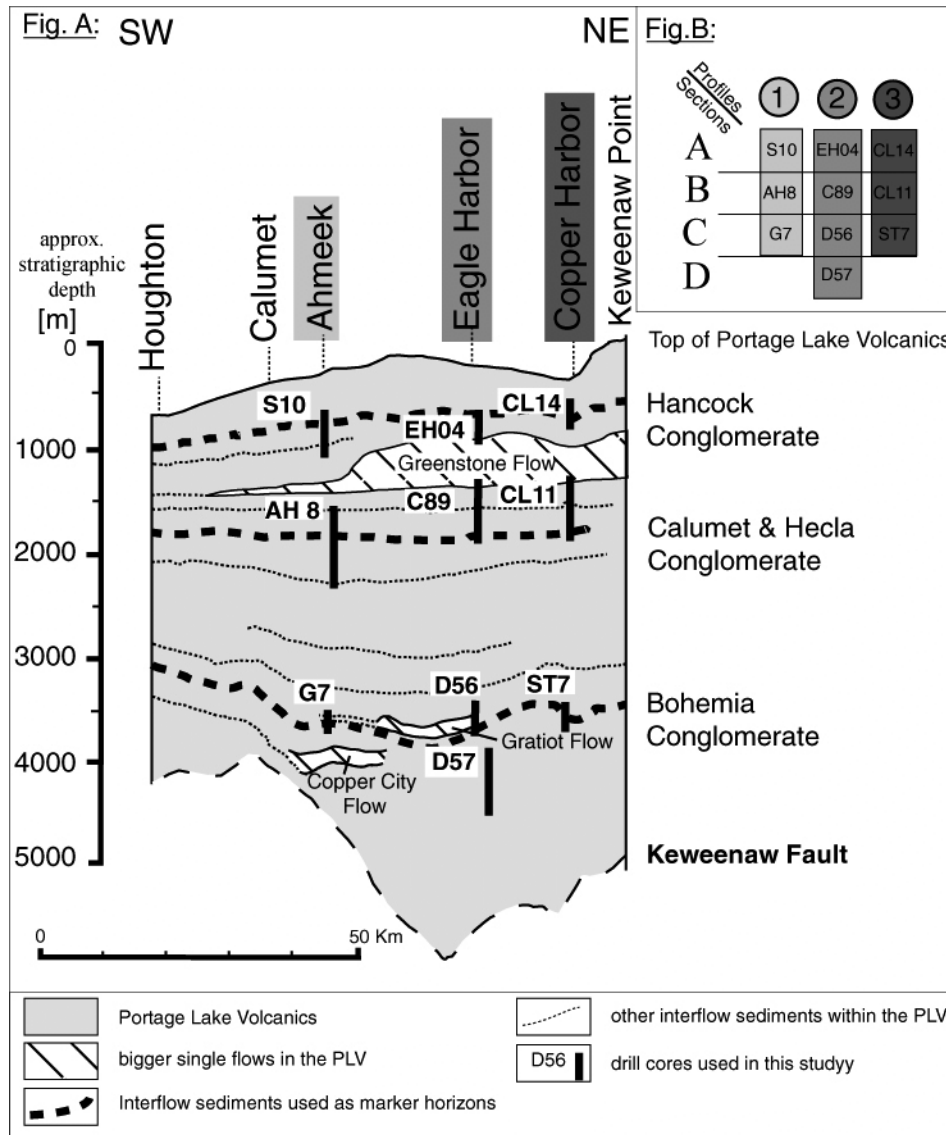


**Figure 2:** A) Back tilted stratigraphic cross-section of the Portage Lake Volcanics (PLV) along strike from Houghton in the southwest to the Keweenaw Point in the northeast. (Modified from White, 1971)  
B) Simplified sketch of cross-section for easy reference in text.

The samples were named after the shorthand expression of the drill core and assigned an additional number that increases with depth, e.g., drill core Eagle Harbor-No. 04, sample-No. 06 = EH04-06 or EH0406.

The material was studied macroscopically and microscopically. Because all the alteration products were fine-grained, a combination of X-ray powder diffraction technique (XRD), X-ray fluorescence (XFA), optical microscopy, electron microprobe analyses (EMPA) and back scattered electron imaging (BSE) were used for mineral identification.

#### **X-ray diffraction (XRD) and X-ray fluorescence (XFA)**

XRD was applied using the Cu-Tube in a SIEMENS/Bruker-AXS diffractometer (D5000), with copper radiation generator settings of 40 kV and 30 mA, variable divergence and antiscatter slits, and a secondary graphite monochromator. The standard measurement range was between 2 and 70° Theta with a scan speed of 1° 2-Theta/min, with a step size of 0.03 Theta.

XFA was applied by using an energy-dispersive spectrometer of Spectro Company®, Klebe (X-lab 2000) with Pd end-window tube and secondary excitation, optimized for low-, medium- and high-energy radiators; software package version 2.2 R 03 j.

Because only very small amounts of material were available from the amygdules and veins, a special preparation method was used. Using a small hand-held drill, the contents of amygdules were removed and ground by hand. A 20 mg portion was then mixed with a special fluid adhesive and spread over a 2 µm thick stretched polypropylene foil fixed across an aluminum ring (Handschin and Stern, 1992).

#### **Electron microprobe analyses (EMPA)**

Mineral analyses were obtained using a JEOL JXA-8600 superprobe from the Mineralogisch-Petrographisches Institut at Basel University. The elements Si, Al, Fe, Mg, Mn, Ca, Na, K were measured using wavelength dispersive spectroscopy, an accelerating voltage of 15 kV and a beam current of 10 nA. As standards natural minerals were used: albite for Na, wollastonite for Ca, graptone for Fe and Mn, orthoclase for K and Al and olivine for Mg and Si. In order to minimize evaporation of light elements (e.g. Na), the spot size was set to 2 µm, or the sample was measured in a scan-mode with a magnification of 20 000. The data were reduced with the PROZA correction function. Two types of microprobe samples were used: super polished thin section and the material separated for X-ray diffraction.

#### **Scanning electron microscope (SEM)**

The Philips XL30 FEG ESEM (scanning electron microscope) at the SEM lab at Basel University was used to obtain high quality back scattered electron (BSE) images from some thin sections.

#### **Stable Isotope (SI) measurement**

Stable isotope analyses (O, C and D) were carried out at the University of Indiana at Bloomington. Due to the restricted size of drill core, the material for stable isotope analysis was carefully extracted by microdrilling. The extracted powder was checked by X-ray diffraction techniques to ensure purity of the material. The samples were prepared using the BrF<sub>5</sub> method of Clayton and Mayeda (Clayton and Mayeda, 1963) to extract the oxygen from clinocllore, quartz and epidote. The method after Rosenbaum and Sheppard (1986) was used for calcite to generate CO<sub>2</sub>. The water was liberated from clinocllore, while melting the tubes using a slightly modified method of Vennemann and O'Neil (1993).

As standards North Carolina State University (NCSU) quartz (B. Showers, North Carolina State



University), BA66 (serpentinized komatiite, K. Kyser, Queen's University) and NBS20 calcite (Sollnhofen-Limestone) were used. NCSU quartz obtains  $\delta^{18}\text{O}$  values of  $9.6 \pm 0.2$  and  $11.45 \pm 0.2\text{‰}$ , the hydrogen isotopic composition for BA66 is  $-66 \pm 2\text{‰}$  and for carbonates NBS20  $\delta^{13}\text{C}$   $-1.27 \pm 0.2\text{‰}$  and  $\delta^{18}\text{O}$   $34.2 \pm 0.5\text{‰}$ . The stable isotope compositions were measured using a Finnigan MAT 252 mass spectrometer. Results for oxygen and hydrogen are in delta notation relative to Vienna Sea Mean Ocean Water (VSMOW) for oxygen and hydrogen and carbon is in delta notation relative to the PeeDee Belemnite (PDB).

### Cathode luminescence (CL)

Cathode luminescence was used to detect zonation in calcite. The TECHNOSYN® Cold Cathode Luminescence Model 8200 MK is setup on a Leica® microscope furnished with a photo camera. The vacuum chamber was under a 2.5 torr vacuum and the gun current was set to 570 to 600  $\mu\text{A}$  at 15 kV. The resulting images derive from exposed 1000 ASA films, with an exposure time up to 4 minutes.

## Alteration

### General primary characteristics of the PLV

The vertical section of a typical basaltic flow from the PLV can be subdivided into four parts (**Fig. 3**). The flow base consists of basalt with small and rare amygdules with a diameter of 2mm. The massive flow interior (MF) consists of massive basalt, which is mostly impermeable except for some cross cutting fractures. A transition zone (TZ) occurs between the MF and flow top. It consists of basalt with amygdules that increase in abundance upwards. The flow top (FT) is a highly amygdaloidal to sometimes cellulare basaltic rock. Some FT's are brecciated and infiltrated by clastic sediments.

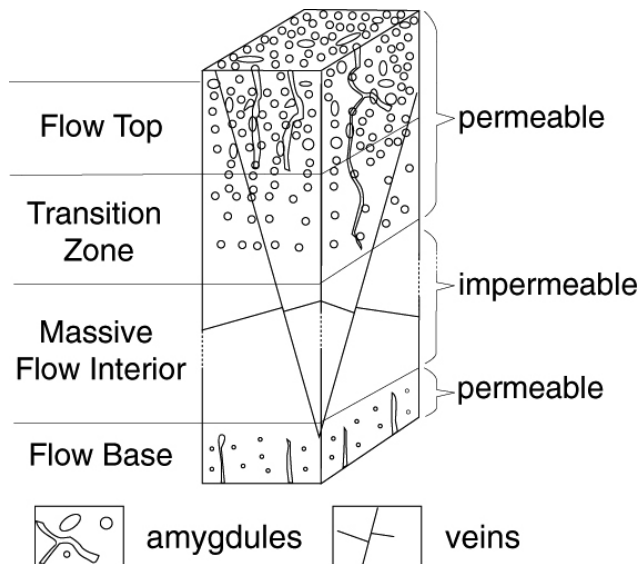


**Figure 3:** Schematic lava flow of the Portage Lake Volcanics.

In flow tops and bottoms pipe-amygdules are often observed. With their elongated shapes, caused by degassing, they point towards the surface of the lava flow.

The primary petrography and geochemistry of the PLV rocks have been studied in detail by Paces (1988). Primary, non-altered, magmatic plagioclase is  $\text{An}_{25}$  up to  $\text{An}_{75}$  (**Fig. 4**). The chemical

composition of pyroxene as determined by Paces (1988), as well as the lack of fresh olivine is in agreement with the results of this study (Fig. 5)

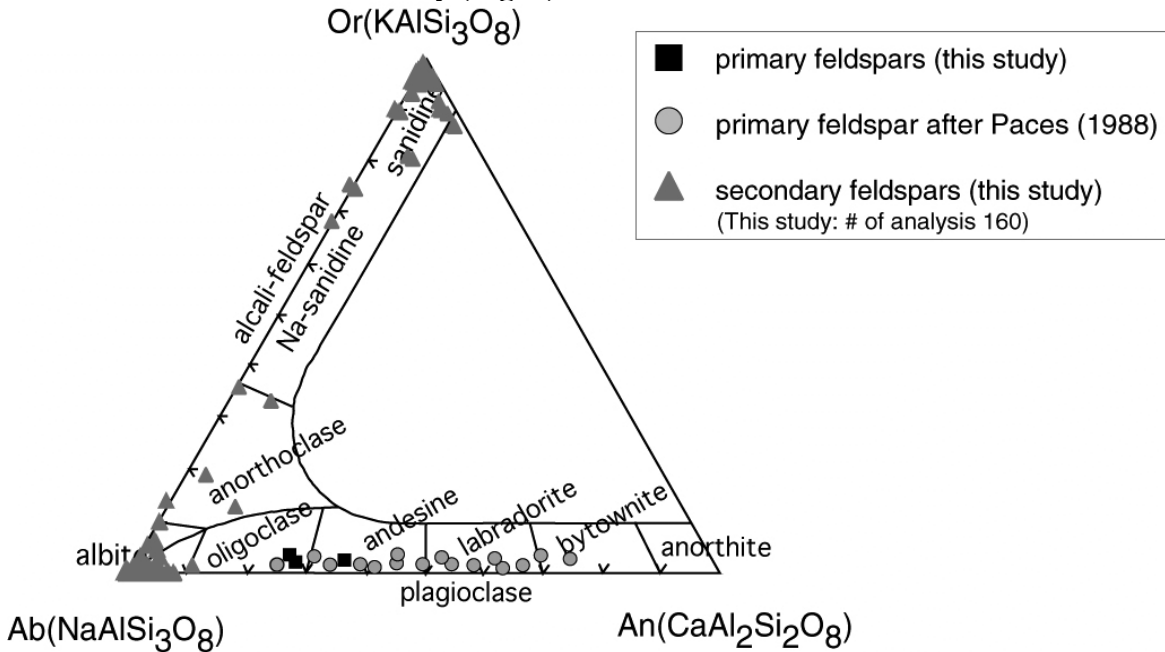


Figure 4: Compositional range of feldspar.

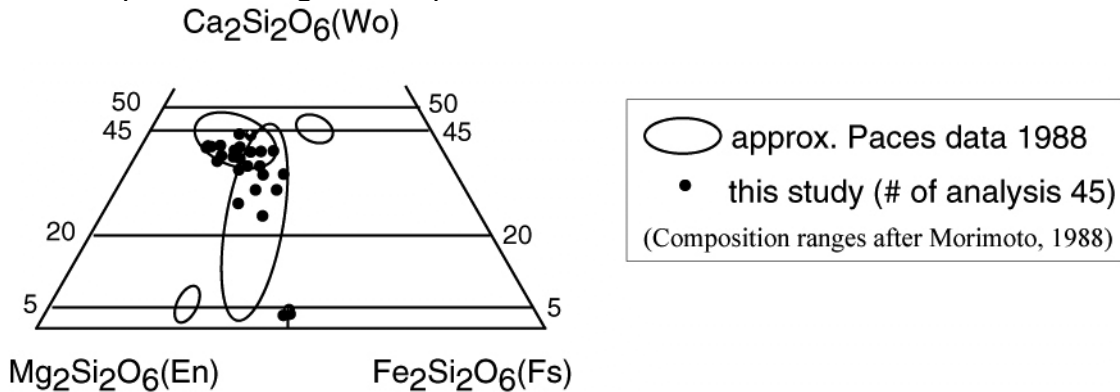


Figure 5: Compositional range of pyroxene.

**Major characteristics of the alteration minerals**

Alteration is present within all units of the examined flows. The amygdaloidal, cellular flow-top-zones are the most altered units; the least altered units are the massive flow interiors, which may only have secondary phyllosilicate minerals. The amount and proportion of the secondary minerals vary within and between the 10 drill cores due to the permeability of the host rock.

The early secondary minerals do not usually fill the amygdules completely. Often they cover only the rims (e.g. pumpellyite) or they grow as well shaped single crystals (e.g. epidote) into the center. Sometimes walls of the amygdules are covered so tightly by minerals of a given precipitation event that the access of a fluid and therefore the growth of additional minerals is inhibited resulting in a void center of the amygdule.

### Albite (Ab)

Albite was found in all flow units although more abundant in the permeable flow tops and transition zones. Albite replaces primary plagioclase in the matrix of the basalt, but is a newly grown mineral in amygdules and veins (**Fig. 6**). Primary plagioclase is partially to totally replaced by albite and partially replaced by other minerals such as pumpellyite, phyllosilicates, epidote or quartz. In thin section, albite does not show polysynthetic twinning but sometimes a cloudy appearance due to the occurrence of Fe-oxides/hydroxides.

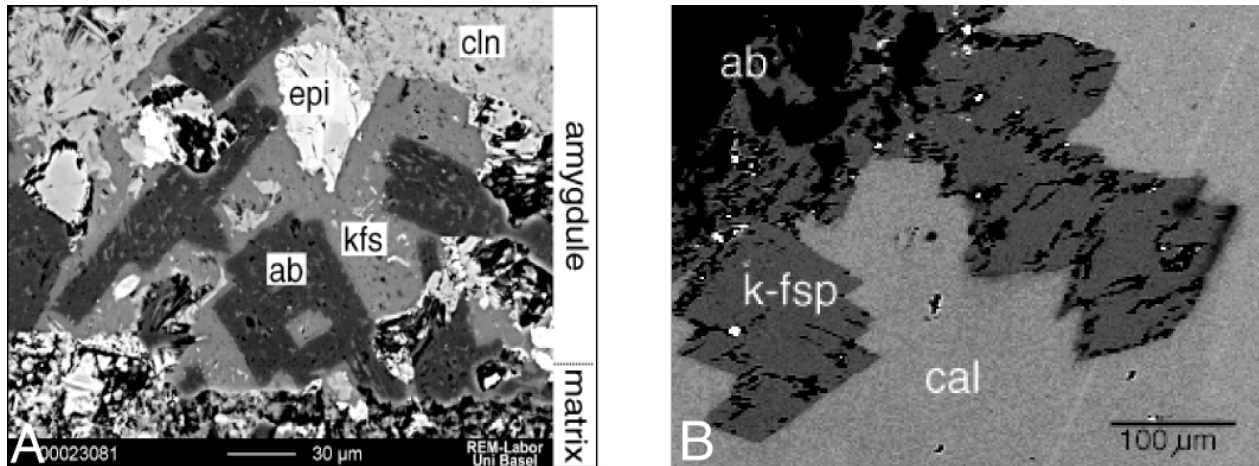


**Figure 6:** A) Recrystallized plagioclase, dark cores are albite; lighter rims are potassium feldspar, sample EH0409.

B) BSE image from EMP: Rim of secondary albite followed by euhedral potassium feldspar crystals. The amygdule was later filled with calcite, sample: C8907B.

The chemical composition of albite is shown in **figure 4**. Albite was found in all flow units although more abundant in the permeable flow tops and transition zones. Albite replaces primary plagioclase in the matrix of the basalt, but is a newly grown mineral in amygdules and veins (**Fig. 6**).

### Potassium-feldspar (Kfs)

Potassium-feldspar was found in all rocks studied. It often overgrows the secondary albite (**Fig. 6a**) in the matrix and sometimes in amygdules (**Fig. 06b**). The small compositional range of K-feldspar is shown in **figure 4**.

### Epidote (Epi)

Epidote is common in all three profiles, with a slight preponderance in drill G7. Macroscopically, it can be identified by its yellow-greenish color. Jolly and Smith (1972) identified epidote as pistazite. It occurs in amygdules and in veins. In so called 'meta-domains' it sometimes replaces all primary minerals while keeping the shape of the former minerals.

Generally epidote is euhedral and is an early mineral to grow in amygdules. Epidote occurs in dense irregular masses in later veins (e.g. crosscutting prehnite), always showing the typical green color. Euhedral epidote is often zoned (**Fig.7**). BSE images of single epidote crystals show often a darker gray center and lighter gray rim, which are due to variation in the Fe content.

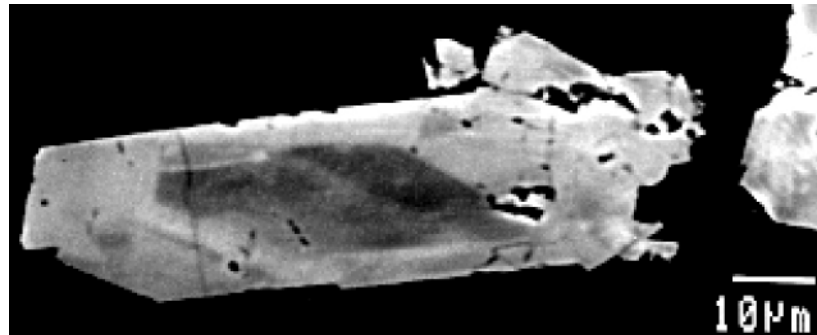


**Figure 7:** BSE image from EMP: zoned epidote crystal, showing a core with a composition poorer in Fe than the rim, sample: C8907B. (Areas with element of high Z-numbers show lighter gray in back scattered electron images.)

There exist at least two chemically similar epidote populations. They differ in their microscopical occurrence. The early alteration population is found in amygdules and in the epidote-domain rocks. The second later population is rare and occurs in small later veins in botryoidal prehnite. In rocks where epidote replaces the primary minerals, it is often found together with prehnite and/or pumpellyite. In smaller amygdules of section C, epidote forms the rims and quartz fills the amygdules. Sometimes epidote is dissolved by later phyllosilicates. These phyllosilicates (Chl) separate wall-grown epidote crystals of stage-I from the walls of the amygdules and suggest therefore a later epidote formation than the phyllosilicates.

#### Pumpellyite (Pmp)

Pumpellyite (Pmp) is recognized by its dark green color. It is found in amygdules and veins, where it often coats the walls. It can be the only mineral filling in the amygdule, but also occurs together with all other described minerals.

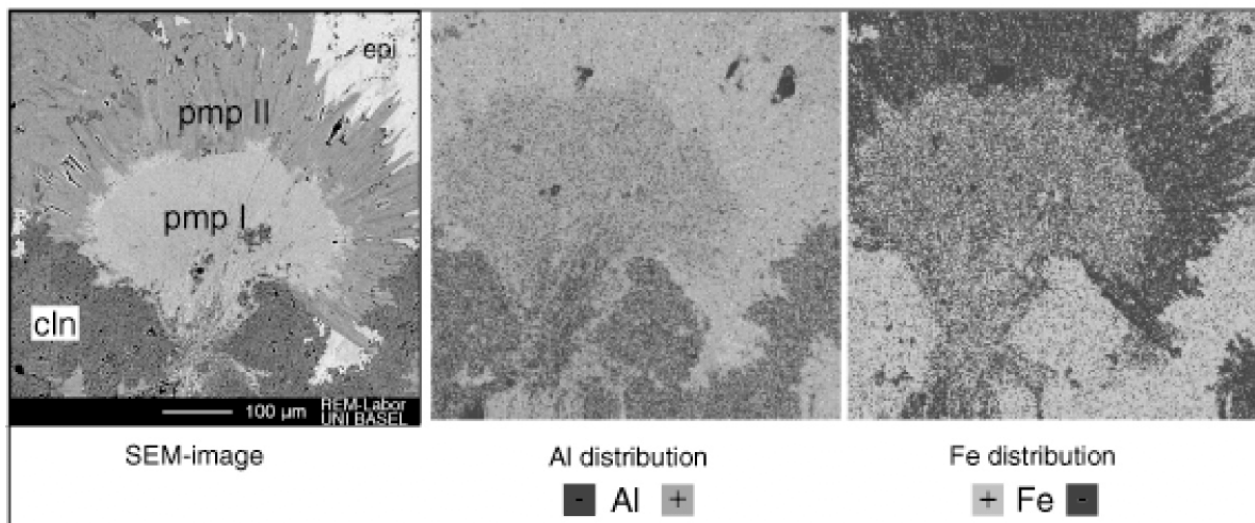


**Figure 8:** EMP X-ray map of two generations of pumpellyite (G706B).

Microscopically, pumpellyite is dark green translucent with strong yellow-green-bluish pleochroism. Pumpellyite often consists of concentrically grown acicular crystals or needles. It is a

frequent mineral in the alteration mineral assemblage. Jolly and Smith (1972) described two populations of pumpellyite and these are confirmed in this study by microscopic and EMPA work (Fig. 8). Based on the chemical composition a third population is present, which is depleted in iron (Fig.9). There was no trend in Fe/Al content of Pmp versus stratigraphic or real depth as already observed by Livnat (1983).

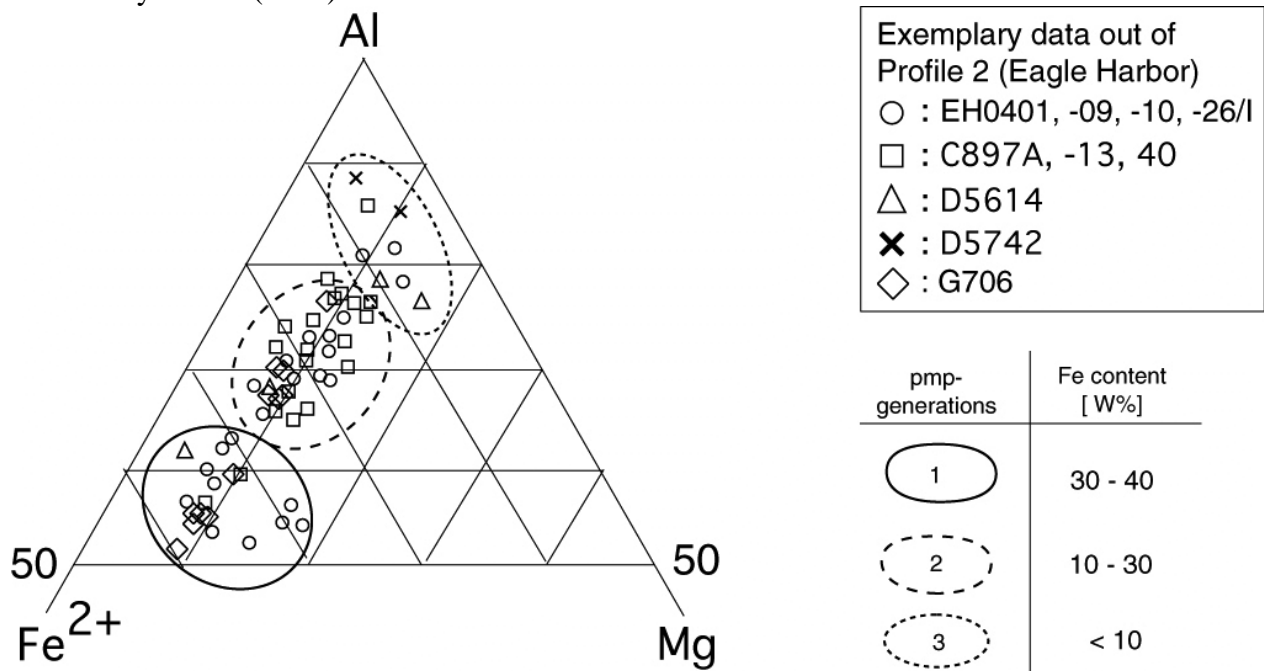


**Figure 9:** Fe-Al-Mg diagram of pmp, showing three different pmp populations.

Prehnite (Prh)

Macroscopically prehnite ranges in color from white to light and dark green shades. Prehnite is found in the matrix, in amygdules and in veins. Prehnite is pseudomorphic after primary minerals such as plagioclase and pyroxene. In amygdules and veins it occurs as the single infilling mineral as well as with other minerals described here. Prehnite usually forms after pumpellyite and, is often found in epidote-‘meta-domains’ but does not intergrow with epidote.

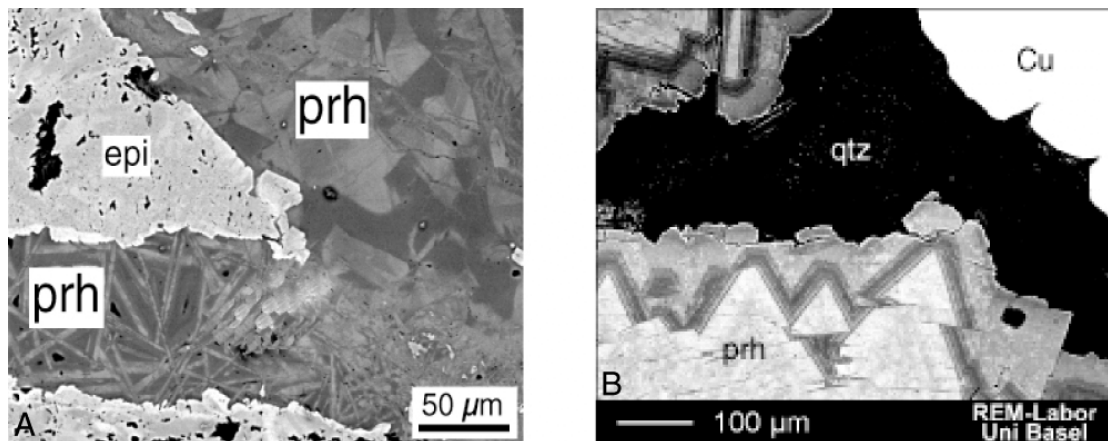


**Figure 10:** A) SEM image of two prehnite generations (botryoidal & needle-like) of identical chemical composition in epi-meta-domain rock, sample D5714.  
 B) Botryoidal prehnite with zonation along rims, sample ST742.

Prehnite has been found as big botryoidal masses, showing bright interference colors. It occurs in veins overgrowing earlier pumpellyite and in still or again open amygdules. On small veins (< 1 mm) or on new crosscutting veins, a fence-like prehnite is visible. From X-ray mapping or SEI images (**Fig. 10a**), there are no chemical differences evident. However bigger individuals show iron-rich and iron-depleted areas. In some samples up to four pulses of prehnite growth can be seen (**Fig. 10b**).

#### Phyllosilicate minerals (Phy)

The main phyllosilicates are clinochlore (Cln) and corrensite (Corr). Jolly and Smith (1972) described two different chlorite populations: dark green chlorite in small amygdules (< 2 mm) in the flow base and transition zones and the chlorite with different colors in the cellular flow tops. Clinochlore, the most abundant phyllosilicate of the Keweenaw Peninsula, occurs as dense masses in amygdules, veins and as patches in the slightly altered massive flow interior. In hand specimens it is usually dark-green colored, with sometimes lighter color and in thin section it displays a greenish pleochroism. Depending on the Mg/Fe ratio, an abnormal olive-green or violet-blue interference color is visible (Troeger, 1982). The chemical composition of the clinochlore does not show a significant variation. The entire clinochlore EMP-data plot close to the pure clinochlore point in a Si+Al+Fe+Mg+Mn versus Al<sub>(tot)</sub> diagram with a slightly trend towards the saponite point (**Fig. 11**).

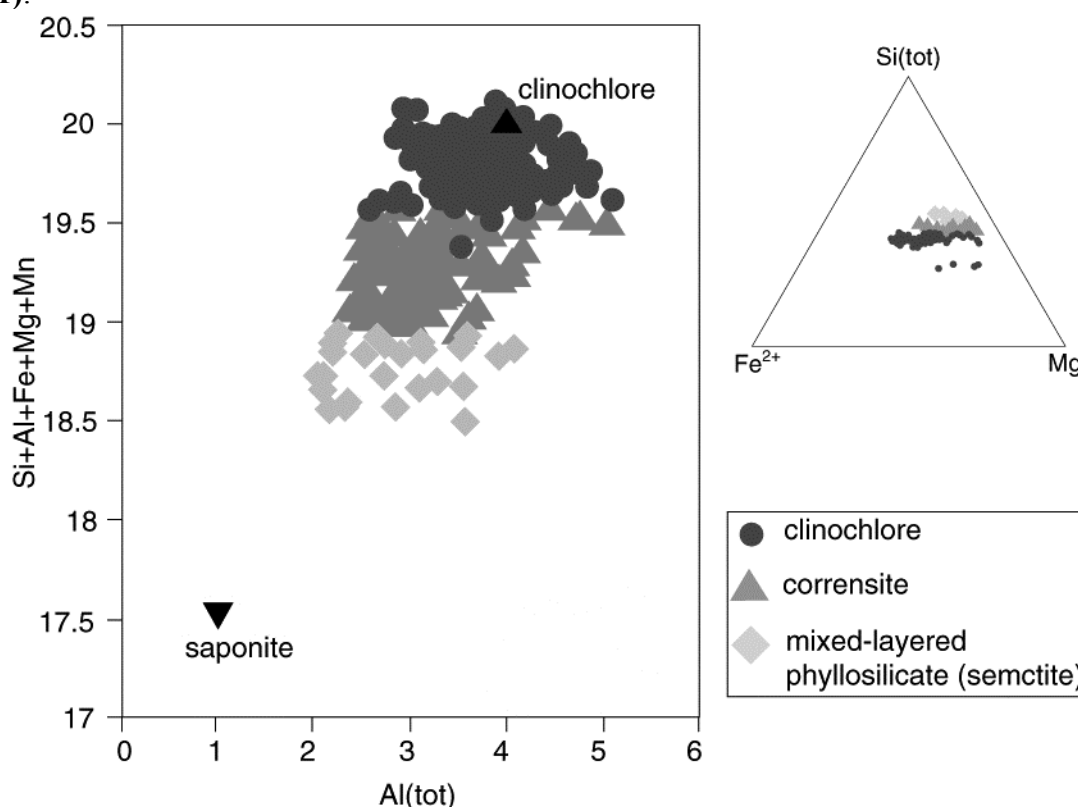


**Figure 11:** Al(tot) versus Si+Al+Fe+Mg+Mn of all phyllosilicate data.

Corrensite was detected by XRD and analyzed by EMP-techniques. It was found in all drill holes except G7. In the adjacent drill cores AH8, C89, D56 and D57 corrensite occurs mainly in veins and in amygdules of non-permeable TZ which are located in bigger flows. In all other drills,

corrensite was found in permeable and non-permeable parts of the different zones of the individual flows. Corrensite and clinocllore do not show any chemical zonation, while growing in the same amygdules. The evaluation of the data from electron microprobe, X-ray diffraction and optical microscopy shows that there is no correlation of the phyllosilicates in flow-top-zones (FT), transition zones (TZ) or massive flow interiors (MF) with stratigraphic depth nor current burial depth (also mentioned as real depth). There was also no ‘small’-scale zonation observed in amygdules or in veins. (Further observations about the formation of phyllosilicates see Chapter 4) As paragenetic youngest minerals in the PLV illite, vermiculite and saponite are found microscopically. They occur along cleavage planes of late stage minerals such as zeolites (laumontite) or in third-stage-calcite.

### Quartz/Chalcedony

Quartz (Qtz) / Chalcedony is also a common mineral in the PLV. Quartz occurs in amygdules as well as in veins, sometimes replacing plagioclase together with prehnite or epidote. In still open veins or bigger amygdules, quartz was found as well-shaped prismatic individuals. If quartz occurs together with calcite the rims are often solved by calcite.

It is sometimes difficult to distinguish quartz from zeolites microscopically because of quartz’s primary fibrous chalcedonic character. Larger individuals with prismatic or irregular shapes often show a high amount of fluid inclusions, which makes it easier to identify them as quartz. From the fluid inclusion studies (See Chapter 5) it was possible to identify up to three different quartz zones in prismatic individuals. Quartz is also often seen as a late mineral in prehnite veins, occurring commonly together with native copper.

### Calcite

Calcite (Cal) was detected during the drill-core sampling with HCl (10%). In thin sections, calcite is often visible in well-shaped crystals but also as anhedral latest mineral filling of still open amygdules and late cross cutting veins. With the help of the cathode luminescence it was possible to detect zonation in optically homogeneous calcite. Two calcite zones observed in the Ahmeek profile and up to seven calcite zones in the Copper Harbor profile (**Fig. 12**). Semi quantitative XFA analysis detected up to 2% Ba in calcite powder.

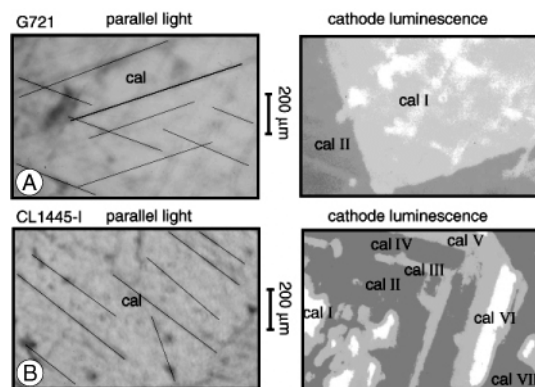


**Figure 12:** Calcite as seen under cathode luminescence, showing two (G7) to seven (CL14) growing zones.

### Zeolites

A wide range of zeolites was identified by XRD and XFA techniques. Laumontite is by far the most abundant zeolite. In the stratigraphically upper section (A) and within all of the drill cores of the most northeastern Copper Harbor profile, laumontite is a frequent mineral in amygdules and veins in flow tops. In the stratigraphically lower parts of the Ahmeek and Eagle Harbor profiles, it occurs in veins cross cutting the pumpellyite-prehnite assemblages. In addition, stellerite, stilbite, analcime, merlinoite, epistilbite, wairakite, philpsite and thomsonite are found in minor quantities and only locally. Wairakite was only observed in Section A below the Hancock Conglomerate and above the Greenstone flow.

### Native Copper

Native Copper was found in all profiles. The native copper rich drill cores were previously removed for assay. Native copper is a paragenetically late mineral in the sampled drill core and occurs always after the prehnite-pumpellyite formation. It is always associated with quartz and calcite (See Chapter 5).

### Exotic secondary minerals

During the XRD analyses, a range of other secondary minerals was identified. They have no significance for the low-grade metamorphic conditions. They occur only sporadically and locally. The boron minerals datolite ( $\text{CaBSiO}_4(\text{OH})$ ) and vonsenite ( $\text{Fe}_2\text{FeBO}_5$ ) were found mainly in the Copper Harbor profile. The minerals grow in dense rosettes in amygdules. Cuspidine ( $\text{Ca}_4\text{Si}_2\text{O}_7(\text{F},\text{OH})_2$ ) was also found by X-ray diffraction techniques in the stratigraphic lower parts of the holes G7, C89, D56, AH8 and ST7.

### **Alteration-pattern within the three profiles**

The distribution pattern of the main secondary minerals is summarized in **figure 13**. The index alteration mineral assemblages for FT/TZ and MF are listed separately, because the permeability of the different zones influences significantly the fluid circulation and therefore the development of the alteration minerals. It is evident that there is no alteration pattern related to stratigraphic depth or the Keweenawan fault, instead, every profile has its own characteristic alteration features.

The FT/TZ show for the different profiles the following patterns: The Ahmeek profile is dominated in the upper part of prehnite-pumpellyite or prehnite-epidote assemblages whereas in the lower part a pumpellyite-epidote assemblage occurs. Laumontite occurs only in crosscutting veins, which are considered to be part of the latest alteration stage under zeolite facies conditions.

In the of the Eagle Harbor profile the prehnite-pumpellyite assemblage is present together with epidote. The Copper Harbor profile shows at ca. 130 m within the drill core a prehnite-pumpellyite and a pumpellyite-epidote assemblage. In the lowest part of the section pumpellyite is the dominant mineral. The dominant alteration mineral in the Copper Harbor profile is the laumontite, which is superimposed on the scarce occurring pumpellyite-prehnite assemblage.

The massive flow interiors show a different alteration pattern. They are in general less altered than the FT/TZ. From the three profiles it is evident that the relative amount of prehnite-pumpellyite as well as epidote increases within the lower part of the Ahmeek-Profile (drill G7) as well as below the Greenstone flow in the Eagle Harbor Profile (drill C89). The relative amount of prehnite-



pumpellyite is obviously less in the most eastern Copper Harbor Profile (drill CL14), where the zeolite laumontite is apparently more abundant. In the other profiles laumontite is found mainly on late cross cutting veins indicating a superimposed event covering the whole Keweenaw Peninsula.

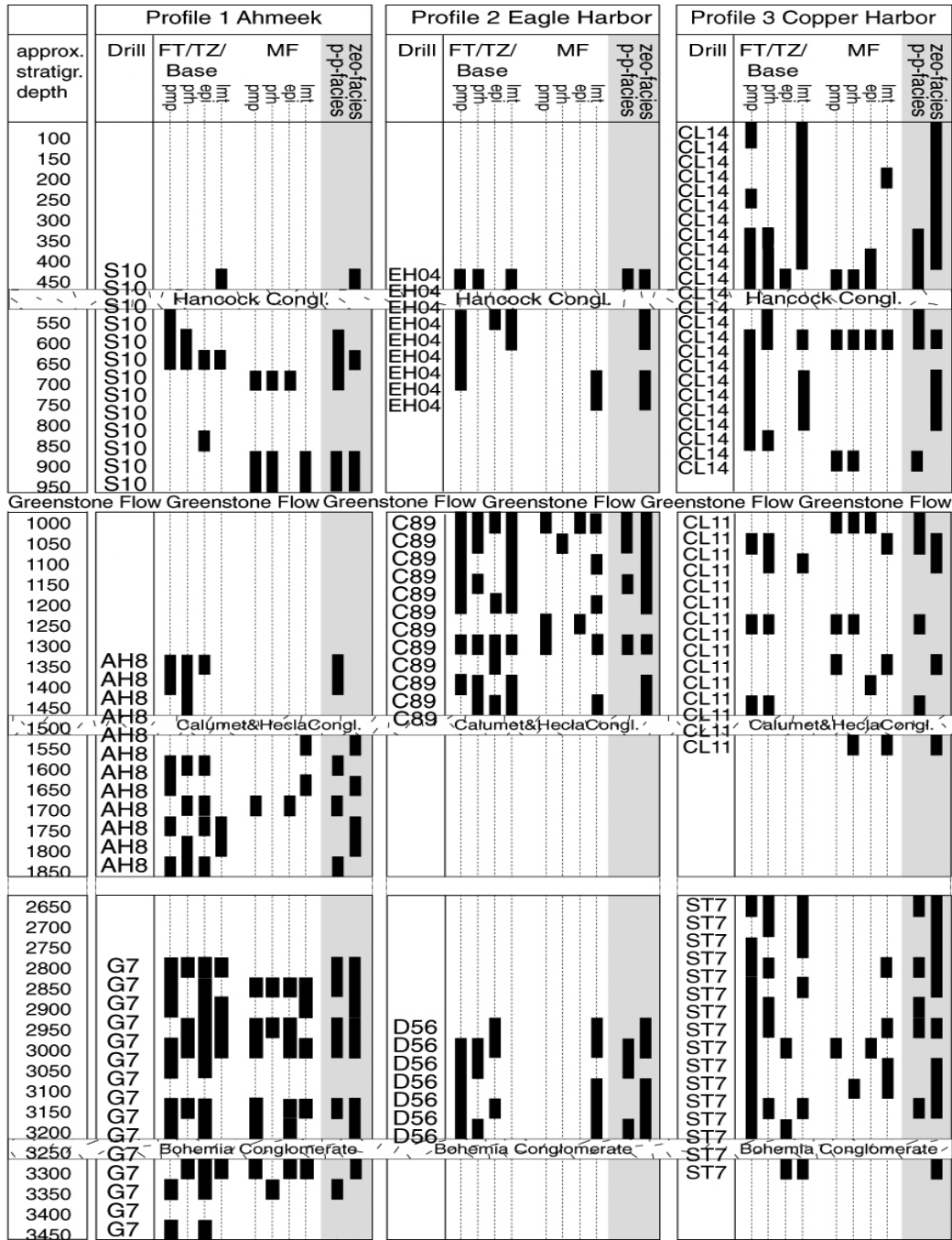


**Figure 13:** Summary of the results of the distribution of the alteration minerals within the studied three drill core profiles.

Legend: pmp: pumpellyite, prh: prehnite, epi: epidote, lmt: laumontite, FT: flow top, TZ; transition zone, MF: massive flow interior, p-p-facies: pumpellyite-prehnite-facies, zeo-facies: zeolite-facies. (Drill D57 is not shown because no significant data changes could be shown, and it would reduce the visibility of the data.)

## Stable isotope analyses

Stable isotope analyses ( $^{18}\text{O}$ , D,  $^{13}\text{C}$ ) were carried out on silicates and calcite. Four different types of alteration minerals were analyzed: clinocllore (Cln), corrensite (Corr), epidote (Epi), quartz (Qtz) and calcite (cal), in order to get a better understanding about the nature of the alteration fluids.

Table 1: Number of stable isotope sample analyzes

	cln	corr	epi	qtz	cal
$\delta\text{D}$	23	-	-	-	-
$\delta^{13}\text{C}$	-	-	-	-	32
$\delta^{18}\text{O}$	65	1	7	7	32
amygdules	33	-	-	1	3
veins	30	-	6	6	29
mixed	2	1	1	-	-

A total of 112 samples were analyzed (**Table 1**). Alteration minerals in amygdules and veins were analyzed. They are derived from all three morphological units of the lava flows, as well as from the three profiles. The  $\delta^{18}\text{O}$  values for clinocllore range from 4.2 to 19.0‰ with a mean at 8.7‰,  $\delta\text{D}$  values range from -153 to -26.5‰ with a mean at -57.3‰. There are no significant differences between the amygdule- and vein-samples. One single vein-value (19‰) is more enriched in  $^{18}\text{O}$  than the usual vein-values (15.8‰) which are in general comparable with the slightly lower values of amygdules (maximum 15.3‰). The minimums  $\delta^{18}\text{O}$  values of 5.5‰ from clinocllore amygdules are close to those of veins with 4.2‰. A single corrensite sample is from a TZ and has a  $\delta^{18}\text{O}$  value of 5.9‰ and a  $\delta\text{D}$  value of -42.9‰. The  $\delta^{18}\text{O}$  values of quartz range from 6.2‰ up to 18.3‰. The  $\delta^{18}\text{O}$  values of epidote range from 4.9‰ to 15.9‰ with a mean at 8.4‰. The  $\delta^{18}\text{O}$  values for calcite range from 17.7 to 29.6‰ and for  $\delta^{13}\text{C}$  from -7.1 to -0.2‰. (For stable isotope data see also **tables 2a) –c)** at the end of this chapter). From the cathode luminescence studies it is known, that calcite in the PLV show two up to seven calcite-growth-zones (**Fig. 12**). The stable isotope analyses of this and former studies (Livnat, 1983) do not resolve these fine structures and can only be considered as bulk analyses.

A general overview of the  $\delta^{18}\text{O}$  distribution in the three drill core profiles is given in **figure 14**. **Figure 14a)** shows  $\delta^{18}\text{O}$  compositions of the individual minerals as a function of stratigraphic depth, which presumably best represents the spatial relation during an early stage of metamorphism. **Figure 14b)** shows  $\delta^{18}\text{O}$  values as a function of depth below surface. It represents present day spatial relations and is appropriate to illustrate compositions of post metamorphic phases such as calcite. Because of microscopic textural reasons, **figure 14a)** is more accurate for  $\delta^{18}\text{O}$  of clinocllore, quartz and epidote, and **figure 14b)** for  $\delta^{18}\text{O}$  calcite (see also discussion/see below).

In all sampling profiles clinocllore and, where present, epidote have similar  $\delta^{18}\text{O}$  values. At a given stratigraphic (or real depth) position Qtz is generally (with one exception) enriched in  $^{18}\text{O}$  than clinocllore and epidote. The  $^{18}\text{O}$  fractionation between quartz and clinocllore, and quartz and epidote range from 1 to 10 ‰. These relations cannot be used as a thermometer, because different mineral separates were extracted from different hand specimen and thus do not represent equilibrium paragenesis. The observed sequence  $\delta^{18}\text{OQtz} > \delta^{18}\text{OCln} \approx \delta^{18}\text{OEpi}$  is, however,

comparable with a coeval oxygen isotope exchange of quartz, epidote and clinochlore with a common pore fluid, at least in a qualitative sense.

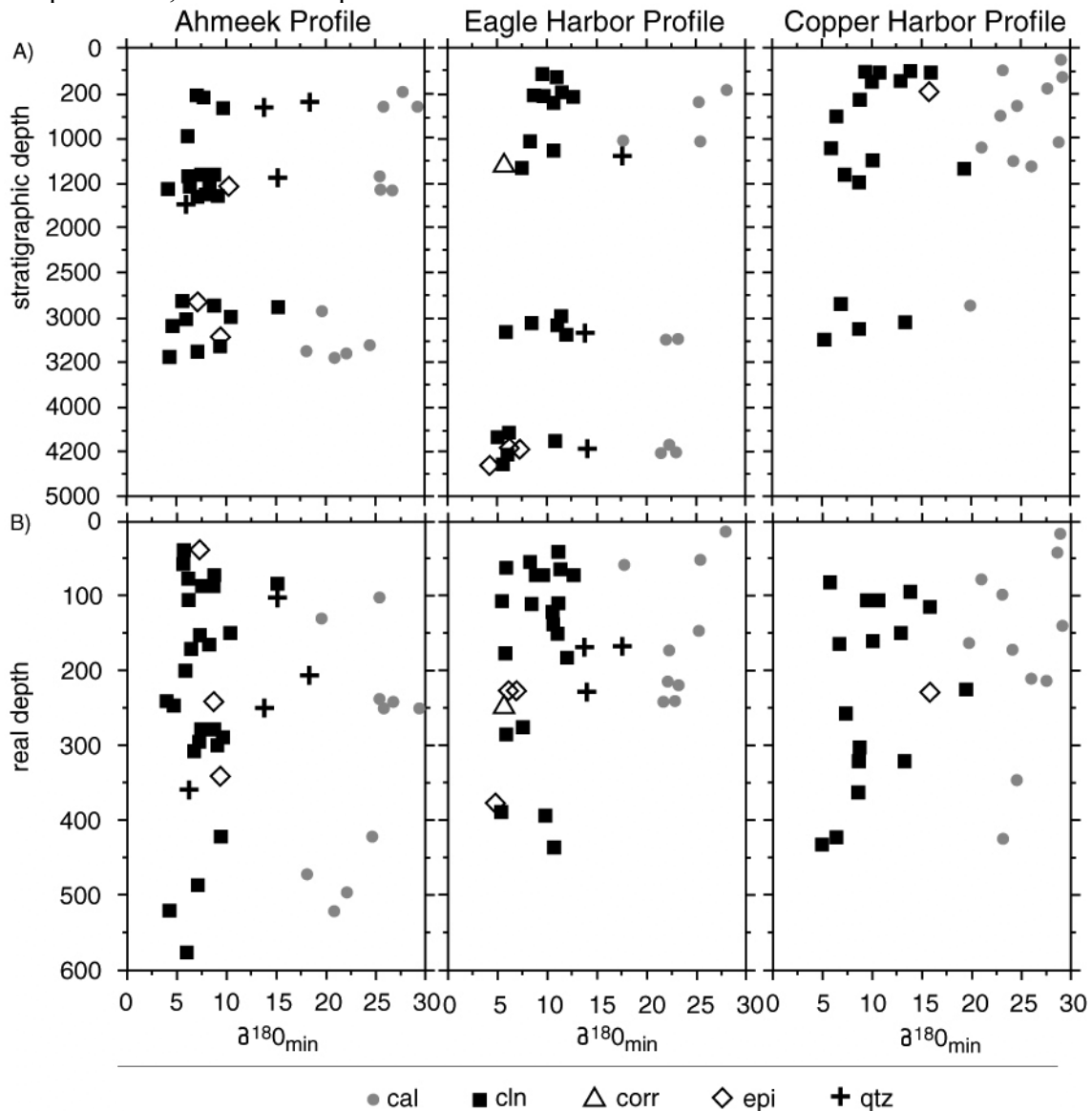


**Figure 14:** Distribution of  $\delta^{18}O_{\text{mineral}}$  values in the three drill core profiles, per mineral, cal: calcite, cln: clinocllore, corr: corrensite, epi: epidote, qtz: quartz.

A) versus original stratigraphic depth,

B) versus real depth under today's surface. (For explanation see text.)

If oxygen isotope equilibrium prevails, quartz is always more enriched in  $^{18}O$  than coexisting calcite, regardless of temperature (e.g. O'Neil, 1986). The fact that in the PLV samples calcite is generally enriched in  $^{18}O$  with respect to Qtz indicates that quartz and calcite did not coexist in oxygen isotope equilibrium. This suggests that quartz and calcite received their oxygen isotope signature during different alteration stages of the low-grade metamorphic evolution of the PLV in the Keweenaw Peninsula.

Quartz and clinocllore pertain to a prehnite-pumpellyite facies (Stage I). The shallow stratigraphic depth ( $\leq 5000$  m) results in a small pressure value, so that a temperature range from 200 – 275 °C is indicated (Frey et al., 1991). This is supported by fluid inclusion temperatures of this study, see Chapter 5, and by former authors (Stoiber and Davidson, 1959; Livnat, 1983). The temperatures for calculation of the fluid in equilibrium with calcite (stage III) derive from the fluid inclusion data from Livnat (1983), Stoiber and Davidson (1959) and data from this study, which are in the order of 100 – 150°C.

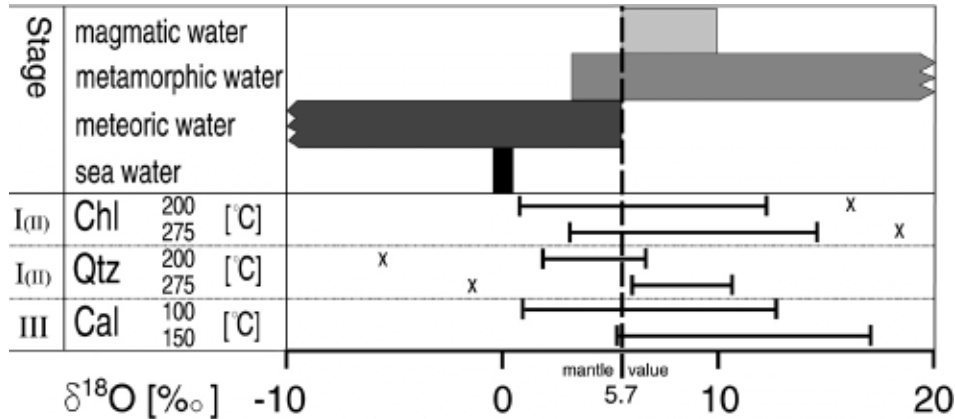


**Figure 15:** Diagram to derive the  $\delta^{18}\text{O}$  origin of the alteration fluids. Cln: clinocllore, qtz: quartz, cal: calcite, numbers: behind mineral abbreviations indicate the temperature range, which were used for calculations. Stage indicates the alteration stage in which the mineral grew (I, III likely, (II) less likely). (Diagram after Rollinson, 1993)

**Figure 15** shows the different water sources (modified after Rollinson, 1993) of the minerals after calculations with the different water-mineral fractionation factors (Taylor, 1974; Onuma et al, 1972; Sheppard, 1977; Graham and Harmon, 1983; and Hoefs, 1987). From the stable oxygen isotope analyses of this study no condensed data clusters could be found. The data range from meteoric, over metamorphic to magmatic  $\delta^{18}\text{O}$  sources.

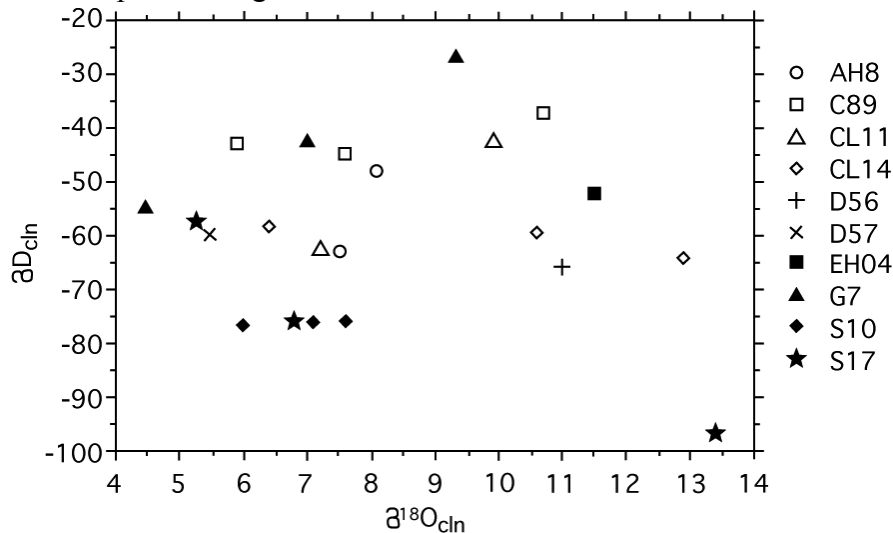


**Figure 16:**  $\delta^{18}\text{O}$  versus  $\delta\text{D}$ , showing no correlation over the three drill core profiles.

The 23 clinochlore  $\delta D$  values were plotted against  $\delta^{18}O$  values in **figure 16**. The  $\delta D$  values do not display any obvious trends. After calculation with assumed formation temperatures (see above), the data were plotted in a diagram suggested by Rollinson (1993) (**Fig. 17**). The character of the infiltrating water at Keweenaw times is not clearly displayed. The clinochlore-water calculations plot for temperatures of 275°C in some cases in the metamorphic water field. Provided the isotopic composition of seawater is taken as the present day  $\delta^{18}O$  value, there is no evidence for seawater input in the system assuming that the  $\delta^{18}O$  seawater has not changed during the Earth history (Longstaffe, 1987).

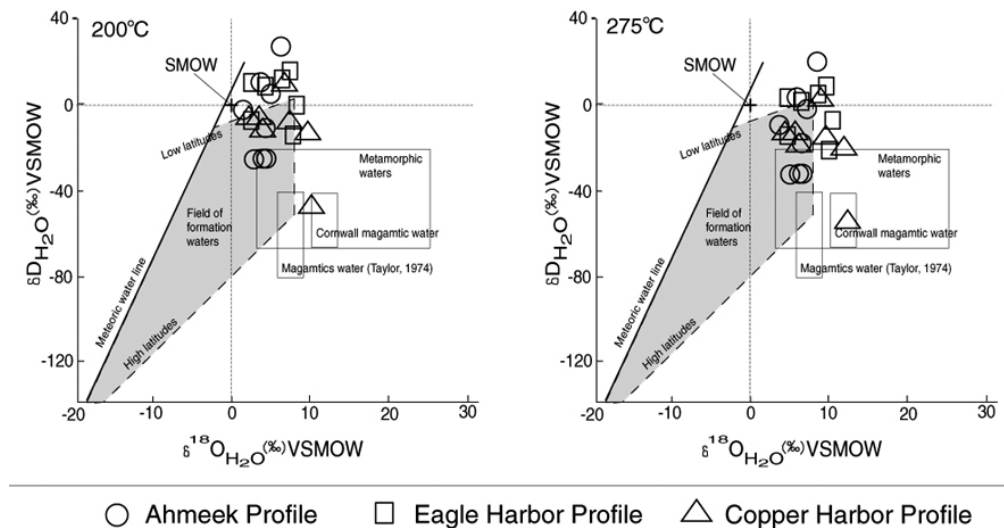


**Figure 17:** Plot of  $\delta D/\delta^{18}O$  for clinochlore, compositional fields for different water types are indicated. Metamorphic water field combines the values of Taylor (1974) and Sheppard (1981); Meteoric water line after Epstein et al. (1965) and Epstein (1970). Calculated for temperatures of 200°C and 275 °C;  $\delta^{18}O_{\text{clin-water}}$  after Cole (1985) and  $\delta D_{\text{clin-water}}$  after Taylor (1979).

A wide range of  $\delta^{18}O$  and  $\delta^{13}C$  values for calcite is obtained (**Fig. 18A**). There are no differences between values for amygdules and veins. In **figure 18B+C** the  $\delta^{18}O$  and  $\delta^{13}C$  values for calcite are plotted for the lowest stratigraphic section, drill core G7, in the southwest and the highest stratigraphic section, drill core CL14. A slight change in the  $\delta^{18}O$  composition versus G7 could be observed indicating higher temperatures towards the western Ahmeek profile. Within each individual drill core no correlation with real depth is observed. No significant changes could be observed for  $\delta^{13}C$  either.

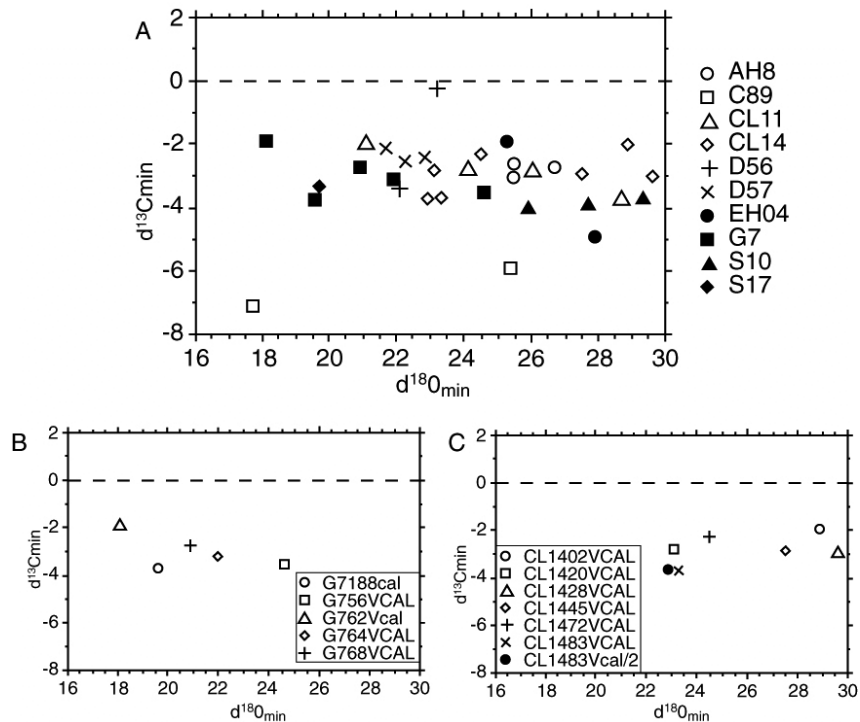


**Figure 18:** A) Plot of all calcite  $\delta^{13}\text{C}$  and  $\delta^{18}\text{O}$  values split by drills.

B) and C) The most western (Ahmeek) and the most eastern (Copper Harbor) profiles gives the lowest and the highest compositional  $\delta^{18}\text{O}$  range.

## Discussion

Low-temperature, hydrothermal alteration minerals have been known in the PLV rocks for more than 100 years. Stoiber and Davidson (1959) reported spatial mineral zoning in the PLV. They recognized three overlapping zones (prehnite, epidote, quartz). They note that laumontite is more abundant in flow tops in the upper part than in the lower part of the sequence. They named the process of alteration ‘regional hydrothermal metamorphism’ because of the combination of regional metamorphism and associated hydrothermal native copper deposit.

Jolly and Smith (1972) established three zones according to the stratigraphic depth: the lower epidote zone with albite, epidote, quartz and some pumpellyite, the middle pumpellyite zone with pumpellyite, albite, clinocllore and an upper laumontite zone with laumontite, prehnite, analcime and clinocllore. The zones were produced during regional metamorphism, which resulted in a localized metamorphic differentiation. Their metamorphic zonation is based on observations of one complete drill core profile at Eagle Harbor throughout the PLV. Livnat’s data (1983) show for the first time, that there is no stratigraphic zonation, but his data suggest a zoned metamorphic plane dipping another angle than the dipping of the PLV.

The metamorphic mineral distribution in the amygdules of the PLV shows a multiphase alteration history. In (Fig. 19) the paragenetic sequence of the alteration minerals is given.

A short remark for better understanding: the sequence of the PLV is not permeable equally in all three dimensions. There are better channel ways along the flow tops and bases, than through the veins and fractures of the massive flow interior. Therefore, the alteration minerals are more

abundant in permeable settings than in impermeable ones. The evolution of the alteration minerals of permeable or impermeable settings is simultaneous, but not the same minerals were formed as the microscopical studies showed.

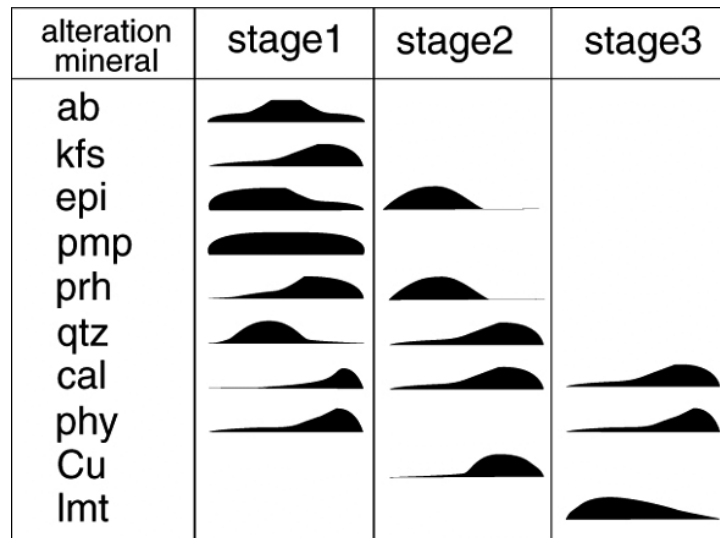


**Figure 19:** Mineral paragenetic sequence based on observations of the permeable units of the PLV. Mineral occurrence per alteration stage.  
 Legend: ab: albite; kfs: potassium feldspar; epi: epidote; pmp; pumpellyite; prh: prehnite; qtz: quartz; cal: calcite; phy: phyllosilicates (mainly clinocllore and corrensite); Cu: native copper; lmt: laumontite.

The early evolution of the alteration minerals in the PLV brought the widest range of alteration minerals in the permeable host rocks. The plagioclase begins to recrystallize to albite. This sets, Ca and Al free, which is usually used to form early zeolites (Frey and Robinson, 1999). Because of the already apparently high temperatures those elements, and Mg and Fe from the alteration of the olivines, form the first epidote and pumpellyite in permeable settings, whereas the same elements caused in non-permeable settings the growth of chlorite. This simultaneous evolution of chlorite in the massive flow interior veins and epidote of permeable settings is shown in **figure 14** with almost identical  $\delta^{18}\text{O}$  values. This stage displays also with its different generations of pumpellyite (**Fig. 9**) and prehnite (**Fig. 10**) that it was always a pulsing system. This early stage brought the pumpellyite-prehnite facies to the PLV.

Calculations with hydrogen and oxygen stable isotopes, after Taylor (1979) and Cole (1985), and assumed water temperatures from around 275°C show values close to today's seawater composition towards the metamorphic water fields (**Fig. 17**). Livnat (1983) in the PLV and Park (1995) in the North Shore Volcanics did imply that during the Precambrian the isotopic composition of seawater was the same as today. They assume both for their models seawater input. Calculations with the obtained  $\delta^{18}\text{O}$  values of this study, from quartz, clinocllore and calcite, using fractionation factors after O'Neil et al. (1969), Clayton et al. (1972) and Cole (1985), show that it is unlikely, that the proposed seawater input (Livnat, 1983) took place, even if a different seawater composition is assumed (Longstaff, 1987).

In non-permeable settings, like MF, from the beginning of the metamorphism clinocllore dominates the system as described by Jolly and Smith (1972) and by Paces (1988). Early

phyllosilicates form in a first stage as pseudomorphoses after olivine. In small amygdules they precipitate in dense, fine grained masses (Stoiber and Davidson, 1959) infilling the entire amygdules.

In permeable settings, in the already filled and now due to the ongoing alteration processes weak contacts between early amygdule minerals (epidote, pumpellyite) new phyllosilicates of mainly chloritic composition grow. The clinocllore EMPA data show often contamination because they are fine-grained and are as late alteration products grown as the expense of early minerals, so relicts of earlier now broken down minerals are still in the masses.

A second stage of epidote and prehnite is based on crosscutting fractures and veins that cut prehnite of stage I. No new pumpellyite was observed in that second stage. This could indicate that either the fluid had changed in composition and was depleted in Mg or there was lower pressure because of decreasing depth while the PLV as it was uplifted by the Keweenaw Fault. The second stage, is observed by microscope work, is only supported by the difference of one single amygdule-quartz-analysis with a very low  $\delta^{18}\text{O}$  value of 5‰, which is similar to early clinocllore from impermeable settings of the early alteration stage. Whereas the vein-quartz with enriched values of  $\delta^{18}\text{O}$  of a 15.4‰ mean can be placed, from microscopic textural observations, in a later event of that first stage or even displays a new second stage. However, based on single data point this is speculative. The final very low-grade metamorphic evolution stage is characterized by the zeolite laumontite and is related to the last movements of the formation of the Keweenaw Fault. The PLV are now in the tectonic position of today, which is confirmed by the fluid inclusions data which show similar homogenization temperatures Livnat (1983) and this study chapter 5 or appendix. Laumontite occurs in abundant quantities in cross cutting late veins throughout the whole sequence of the PLV and in all host rock settings. Those veins are then finally filled with high quantities of calcite. This late stage calcite (hand picked from late veins) shows higher  $\delta^{18}\text{O}$  values compared to the clinocllore, epidote and quartz  $\delta^{18}\text{O}$  values, indicating changing fluid conditions. On some rare calcite mineral fissures phyllosilicates, like vermiculite and saponite are observed – indicating late post metamorphic weathering processes.

The above results show that there is no distinct VLGM-mineral zonation versus stratigraphic depth (**Fig. 13**). The mineral assemblage of the prehnite-pumpellyite facies can be observed lateral (SE-NW) and vertical (NE-SW) over the whole three studied profiles. They cross cut the described epidote-, prehnite- out- and in-lines from Stoiber and Davidson (1959). The regional metamorphic pattern in the section studied is also in contrast to the metamorphic zonation observed by Schmidt (1990, 1993) and Schmidt and Robinson (1997) within the North Shore Volcanic Group on the western side of Lake Superior.

## Conclusions

Livnat (1983) was the first who doubted the stratigraphic zonation and postulated a zoned metamorphic plane dipping another angle than the PLV of today. With the data of this study we postulate a discontinuous distribution of the prehnite-pumpellyite facies and a superimposed zeolite facies metamorphism, from top of the PLV down to the closest sampled drill core to the Keweenaw Fault. There is a slight trend in the mineral assemblages, showing that there have been somewhat higher temperatures towards the Southwest (Ahmeek profile) and the native copper deposits. In stratigraphically lower levels of Section C and D pumpellyite-prehnite-epidote is more abundant than in the stratigraphic higher levels (A and B), whereas the zeolite facies with laumontite is superimposed on the pumpellyite-prehnite facies and developed on late cross cutting veins.



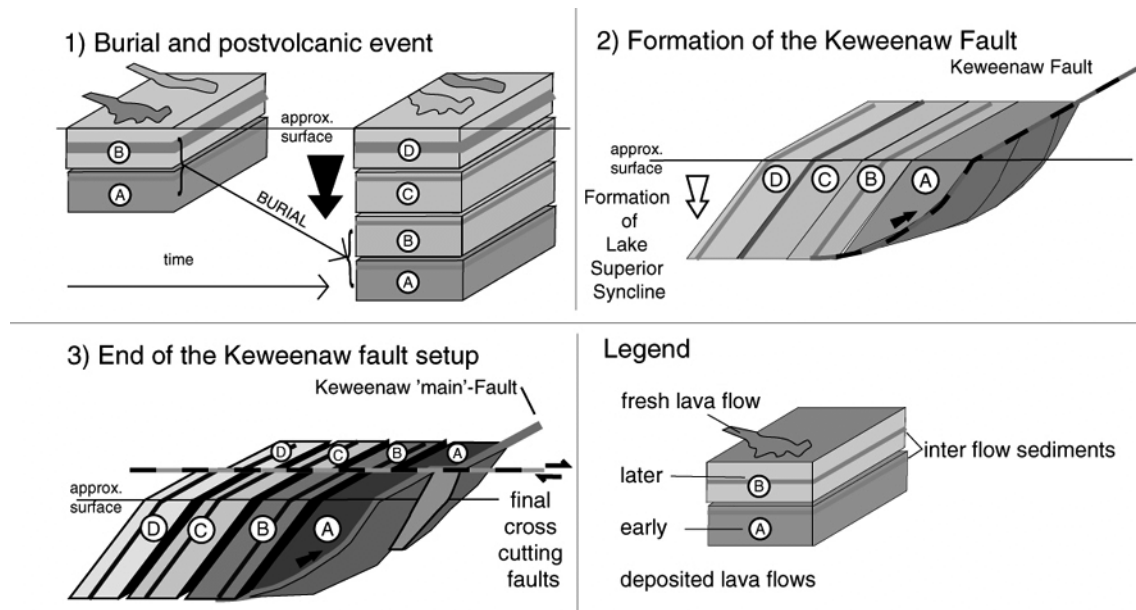


**Figure 20:** Tectonic evolution of the PLV on the Keweenaw Peninsula (simplified after Bornhorst, 1997).

A possible tectonic scenario for the development of the low-grade metamorphic alteration of the PLV is given in **figure 20**. Based on the microscopic observations of the early alteration minerals such as pumpellyite-prehnite-epidote the rise in temperature during the early burial event must have occurred rather fast, indicating to a high geothermal gradient. The heat source could be an underplated gabbro at 40 km depth (Woodruff et al., 1995). Thrusting along the Keweenaw Fault did not change the metamorphic conditions considerably but generated new pathways for fluids depositing the same minerals as stage 1 in the second alteration stage. The deposition of the native copper ores is connected to this second alteration stage. A late retrograde zeolite facies overprints the early stages. Woodruff et al. (1995) modeled the thermal history of the Midcontinent Rift region based on stratigraphic relationship, precise geochronology and multiple deep seismic reflection profiles. They suggest high heat flows at the southern margins of the rift rather than in the center. This conclusion is supported by this study of the metamorphism.

**For references see part 7 of this thesis.**

Table 2a: Stable isotope analysis, Ahmeek profile:

Profile	Section	Sample	HR	Vein	Amygdule	sec. Mineral	$\delta^{18}\text{O}_{\text{cal}}$	$\delta^{13}\text{C}_{\text{cal}}$	$\delta^{18}\text{O}_{\text{cln}}$	$\delta\text{D}_{\text{cln}}$	$\delta^{18}\text{O}_{\text{epi}}$	$\delta^{18}\text{O}_{\text{qtz}}$
							‰ VSMOW	‰ PDB	‰ VSMOW	‰ VSMOW	‰ VSMOW	‰ VSMOW
1	A	S1010AV	FT		A	cal	27.7	-3.9				
1	A	S1025B	TZ		A	cln			7.1	-75.4		
1	A	S1025B/2	TZ		A	cln			7.6	-75.4		
1	A	S1031V	FT	V		qtz						18.3
1	A	S1037V	FT	V		cal	29.3	-3.7				
1	A	S1037V/2	FT	V		cal	25.9	-4.0				
1	A	S1037Vqtz	FT	V		qtz						13.8
1	A	S1043V	MF	V		cln			9.5			
1	A	S1070V	TZ	V		cln			6.0	-76.4		
1	B	AH810BB	FT		A	cln			8.1	-47.7		
1	B	AH812BB	TZ		A	cln			6.5			
1	B	AH818V	TZ	V		cal	25.5	-3.0				
1	B	AH821V	FT	V		cln			4.2			
1	B	AH821V	FT	V		cal	26.7	-2.7				
1	B	AH821V	FT	V		epi					8.7	
1	B	AH823V	MF	V		cln			7.5	-62.6		
1	B	AH823V1	MF	V		cln			8.8			
1	B	AH823V2	MF	V		cln			7.7			
1	B	AH827B	TZ		A	cln			7.2			
1	B	AH827B/2	TZ		A	cln			9.1			
1	B	AH828BV	MF	V	A	cln			6.8			
1	B	AH836B	TZ		A	qtz						6.2
1	B	AH8IV	MF	V		cln			8.7			
1	B	AH8IVrim	MF	V		cln			7.6			
1	B	AH8JV	FT	V		cal	25.5	-2.6				
1	B	AH8JVq/2	FT	V		qtz						15.2
1	B	AH8LB	TZ		A	cln			6.3			
1	C	G706B/V	TZ	V	A	cln			5.6			
1	C	G706V	TZ	V	A	epi					7.0	
1	C	G708B	TZ	V	A	cln			5.6			
1	C	G710V	MF	V		cln			8.8			
1	C	G711V	MF		A	cln			6.2			
1	C	G712BB	FT	V	A	cln			15.3			
1	C	G718B	FT		A	cal	19.6	-3.7				
1	C	G722V	MF	V		cln			10.5			
1	C	G728B	TZ		A	cln			5.9			
1	C	G736V	MF	V		cln			4.5	-54.4		
1	C	G745dom	MF	V		epi					9.3	
1	C	G756V	MF	V		cln			9.3	-26.5		
1	C	G756V	MF	V		cal	24.6	-3.5				
1	C	G762V	TZ	V		cal	18.1	-1.9				
1	C	G763B	TZ		A	cln			7.0	-42.2		
1	C	G764V	TZ			cal	22.0	-3.2				
1	C	G768V	MF	V		cln			4.3			
1	C	G768V	MF	V		cal	20.9	-2.7				

Legend:

HR: host rock; FT: flow top; TZ: transition zone; MF: massive flow interior;

V: vein

A: Amygdule

sec. Mineral: secondary mineral

Cal: calcite; cln: clinocllore; qtz: quartz; epi: epidote; corr: corrensite

Table 2b: Stable isotope analysis, Eagle Harbor profile:

Profile	Section	Sample	HR	Vein	Amygdule	sec. Mineral	$\delta^{18}\text{O}_{\text{cal}}$	$\delta^{13}\text{C}_{\text{cal}}$	$\delta^{18}\text{O}_{\text{cln}}$	$\delta\text{D}_{\text{cln}}$	$\delta^{18}\text{O}_{\text{epi}}$	$\delta^{18}\text{O}_{\text{qtz}}$
							‰	‰	‰	‰	‰	‰
							VSMOW	PDB	VSMOW	VSMOW	VSMOW	VSMOW
2	A	EH0208B	TZ		A	cln			9.8	-41.2		
2	A	EH0216BB	MF		A	cln			10.9			
2	A	EH0216V	MF	V		cln			10.7			
2	A	EH0406V	TZ	V		cal	27.9	-4.9				
2	A	EH0409BB	TZ		A	cln			11.5	-51.8		
2	A	EH0410B	FT		A	cln			9.5			
2	A	EH0411B	TZ		A	cln			9.0			
2	A	EH0411V	TZ	V		cln			12.4			
2	A	EH0416B	TZ		A	cln			10.7			
2	A	EH0419B	TZ		A	cal	25.3	-1.9				
2	B	C8909V	MF			cal	25.4	-5.9				
2	B	C8912ABB	TZ		A	cln			8.3			
2	B	C8915V	MF			cal	17.7	-7.1				
2	B	C8920B	FT		A	cln			10.7	-37.0		
2	B	C8929V	TZ	V		qtz						17.4
2	B	C8938	TZ		A	corr*			5.9	-42.9		
2	B	C8940B	TZ		A	cln			7.6	-44.5		
2	C	D5609BB	TZ		A	cln			11.0			
2	C	D5620V	MF	V		cln			11.0	-65.5		
2	C	D5620V	MF	V		cln			8.5			
2	C	D5626V	MF	V		qtz						13.8
2	C	D5628V	MF	V		cln			5.9			
2	C	D5629V	MF	V		cln			11.8			
2	C	D5633V	MF	V		cal	22.1	-3.3				
2	C	D5634AV	MF			cal	23.2	-0.2				
2	D	D5707V	TZ	V		cln			5.8			
2	D	D5713VB	TZ	V	A	cln			5.5			
2	D	D5718BA	(FT)		A	cln			10.9			
2	D	D5720V	MF	V		cal	22.2	-2.5				
2	D	D5726Vdom	MF	V		epi					6.4	
2	D	D5726V	MF	V		epi					6.8	
2	D	D5726V	MF	V		qtz						13.9
2	D	D5728VA	MF	V		cal	22.8	-2.4				
2	D	D5728VB	MF	V		cal	21.7	-2.1				
2	D	D5731B	TZ	V		cln			5.9			
2	D	D5741dom	MF	V		epi					4.9	
2	D	D5742B	TZ		A	cln			5.5	-59.4		

Legend:

HR: host rock; FT: flow top; TZ: transition zone; MF: massive flow interior;

V: vein

A: Amygdule

sec. Mineral: secondary mineral

Cal: calcite; cln: clinocllore; qtz: quartz; epi: epidote; corr: corrensite

**Table 2c: Stable isotope analysis, Copper Harbor profile:**

Profile	Section	Sample	HR	Vein	Amygdule	sec. Mineral	$\delta^{18}\text{O}_{\text{cal}}$	$\delta^{13}\text{C}_{\text{cal}}$	$\delta^{18}\text{O}_{\text{cln}}$	$\delta\text{D}_{\text{cln}}$	$\delta^{18}\text{O}_{\text{epi}}$
							‰ VSMOW	‰ PDB	‰ VSMOW	‰ VSMOW	‰ VSMOW
3	A	CL1402V	MF	V		cal	28.9	-2.0			
3	A	CL1418V	FT	V		cln			13.8		
3	A	CL1420V	TZ	V		cal	23.1	-2.8			
3	A	CL1422B	FT		A	cln			10.6	-59.4	
3	A	CL1423B	FT		A	cln			9.5		
3	A	CL1425V	FT		A	cln			15.8		
3	A	CL1428V	FT	V		cal	29.6	-3.0			
3	A	CL1430V	MF	V		cln			12.9	-63.8	
3	A	CL1432B	FT		A	cln			9.9		
3	A	CL1445V	TZ	V		cal	27.5	-2.9			
3	A	CL1448V	MF	V		epi					15.9
3	A	CL1463B	TZ		A	cln			8.8		
3	A	CL1472V	MF	V		cal	24.5	-2.3			
3	A	CL1483V	MF	V		cln			6.4	-57.8	
3	A	CL1483V/1	MF	V		cal	23.3	-3.7			
3	A	CL1483V/2	MF	V		cal	22.9	-3.7			
3	B	CL1106B	FT		A	cal	28.7	-3.7			
3	B	CL1110V	TZ	V		cal	21.1	-2.0			
3	B	CL1112B	TZ		A	cln			5.8		
3	B	CL1125AB	TZ		A	cln			9.9	-42.1	
3	B	CL1127V	MF	V		cal	24.1	-2.7			
3	B	CL1131V	FT	V		cal	26.0	-2.8			
3	B	CL1135V	MF	V		cln			19.4		
3	B	CL1138B	TZ		A	cln			7.2	-62.4	
3	B	CL1148V	MF	V		cln			8.7		
3	C	ST707B	TZ		A	cln			5.3	-57.5	
3	C	ST713BE	TZ		A	cln			8.7		
3	C	ST720V	MF	V		cln			13.4	-96.4	
3	C	ST738V	FT	V		cln			6.8	-75.4	
3	C	ST738V	FT	V		cal	19.7	-3.4			

Legend:

HR: host rock; FT: flow top; TZ: transition zone; MF: massive flow interior;

V: vein

A: Amygdule

sec. Mineral: secondary mineral

Cal: calcite; cln: clinocllore; qtz: quartz; epi: epidote; corr: corrensite

**Phyllosilicates in the Portage Lake Volcanics: a record of very low-grade metamorphic alteration and reaction progress**

Ulrich R. Püschner

S. Th. Schmidt

W. B. Stern

## Introduction

Mafic phyllosilicates are the most common and ubiquitous alteration minerals in low-grade metamorphic basaltic rocks. Studies of the chemistry and structure as well as the nature of the transition of the phyllosilicate from smectite to chlorite during increasing metamorphism have been carried out in several places. Kristmansdottir (1979) and more recently Schiffman and Fridleifsson (1991) studied hydrothermally metamorphosed basalts in Iceland. Phyllosilicates were also investigated in DSDP Hole 504B (Shau and Peacor, 1992) as well as in ophiolitic sequences (Bettison and Schiffman, 1988). X-ray analyses and electron microprobe analyses have shown that phyllosilicates vary from smectite in lower grade metamorphic zones over mixed-layered chlorite/smectite in higher zeolite to prehnite-pumpellyite grade rocks and to chlorite in rocks of the beginning greenschist facies (Schmidt and Robinson, 1997). The nature of this transition is still under debate. Three models have been suggested for the smectite to chlorite transition: The traditional model involves the continuous sequence of smectite over continuous mixed-layering to chlorite. A second model assumes a discontinuous change from smectite to chlorite without chlorite-smectite mixed-layering. Corrensite - a 50:50 mixed-layered smectite/chlorite phase - occurs as an independent thermodynamically stable phase in this second model. A third model describes the transition between smectite to chlorite as a sharp step without any mixed-layering nor a formation of corrensite (Robinson and Zamora, 1999). The Portage Lake Volcanics (PLV) on the Keweenaw Peninsula in Michigan have experienced hydrothermal low-grade metamorphism reaching prehnite-pumpellyite facies conditions. Compared with other alteration minerals in the PLV such as prehnite or pumpellyite, phyllosilicates are the most abundant alteration minerals. They occur within the basaltic lava flows, in the most altered flow tops, but also in the massive flow interior where hardly any other alteration minerals are detected, as well as in the transition zone. A detailed X-ray and chemical study was carried out on the phyllosilicates of the PLV to gain a better understanding of the very low-grade metamorphism and the reaction progress in the phyllosilicates. The results indicate that there is a broad compositional range from mixed-layered phyllosilicates to clinocllore during not well established pumpellyite-prehnite facies in the northeastern Copper Harbor profile changing to three distinct phyllosilicates within the well established pumpellyite-prehnite facies of the Ahmeek profile in the southwest of the study area.

## Methods

### *X-ray diffraction*

#### Preparation of the sample material

Due to the limited amount of sample material from the drill core and the combination of analyses that should be carried out on one sample, a representative amount of phyllosilicate was extracted from amygdules and veins and analyzed by X-ray diffraction. The same material was then investigated by EPM and stable isotope analysis. For the X-ray diffraction analysis, a special technique developed by Handschin and Stern (1992) was applied which makes it possible to measure only 20 mg of powder material (**Fig. 1**). A total number of 444 samples were produced and measured. With a hand held drill, macroscopically pure material was extracted. Therefore this material was often a mixture of the amygdule fillings. It was not possible to extract any

defined amygdule rim or amygdule center material, because it was macroscopically never obvious how regular the amygdules were and therefore the distribution of the phyllosilicates was.

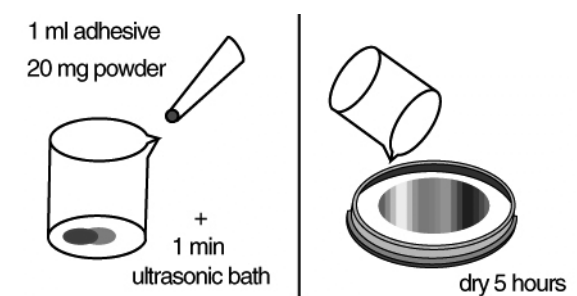


**Figure 1:** Preparation procedure for the X-ray diffraction of small powder amounts in the Siemens® D5000, according to Handschin and Stern (1992).

Only in the rarest cases, single-mineral filled amygdules contained more than 100 mg material. Due to the restricted amounts of sample material, the common clay lab techniques, such as separation of the 0.2-micron fraction, was not possible.

#### Conditions for X-ray diffraction (XRD)

XRD was applied using a SIEMENS/Bruker-AXS diffractometer (D5000), with copper radiation generator settings of 40 kV and 30 mA, variable divergence and antiscatter slits and a secondary graphite monochromator. The standard measurement range was between  $2^\circ$  to  $70^\circ$   $2\theta$  with a scan speed of  $1^\circ$   $2\theta$ /min, with a step size of 0.03  $\theta$ . The range for glycolated samples is set from  $1^\circ$  to  $22^\circ$   $2\theta$ , because in this range potential swelling will affect the crystal lattice.

#### *Electron Microprobe (EMP)*

##### Preparation of the sample material

The preparation of super polished thin sections of the phyllosilicates for use on the electron microprobe analyses was a difficult task. There is a wide variety of different hard and soft minerals, sometimes brittle or soft, which occur next to each other and which are difficult to be polished together. Quartz occurs next to zeolites or phyllosilicates next to feldspars or epidote. Zeolites cannot be exposed to high temperatures, because they can change their highly water bearing and brittle structures. Phyllosilicates together with zeolites or other harder minerals are often polished away and a mountain-and-valley structure remains, which is very difficult to handle during electron microprobe measurement. The danger of getting inaccurate data because of a split or miss-led beam is high. During the last 3 years the technique to produce high quality polished sections was improved by W. Tschudin. Today the cut rock samples are left in an epoxy bath for 10 min at a temperature of  $50^\circ\text{C}$  in a vacuum oven. This procedure fills the pores and leads to a hardening of the whole sample. Afterwards the piece is polished by hand on a metallic grinding disc with a Swiss polishing sand with a mesh size of '1500'. Then the pieces are polished on a grinding machine, where the plastic grinding discs become harder over the years, using a 1-3  $\mu\text{m}$  diamond-polishing-paste. This new technique produces good microprobe-ready thin-sections in less time (personal communication W. Tschudin 2001).

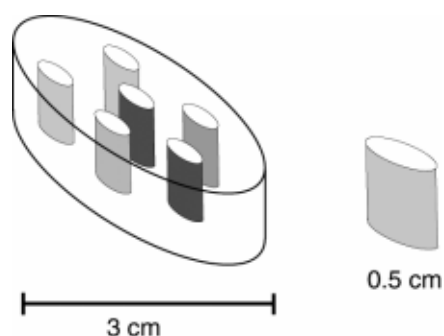


**Figure 2:** Special powder sample holder for EMP analysis

Some extracted powders from the amygdules, first measured by XRD were used for EMPA as well. In this case the sample powder was mixed with epoxy and mounted into a standard mineral holder (**Fig. 2**). With the aid of EMPA, sample of clinocllore assumed to be a single phase based on XRD were proved to be a mixture of various phases (**Fig. 3**).

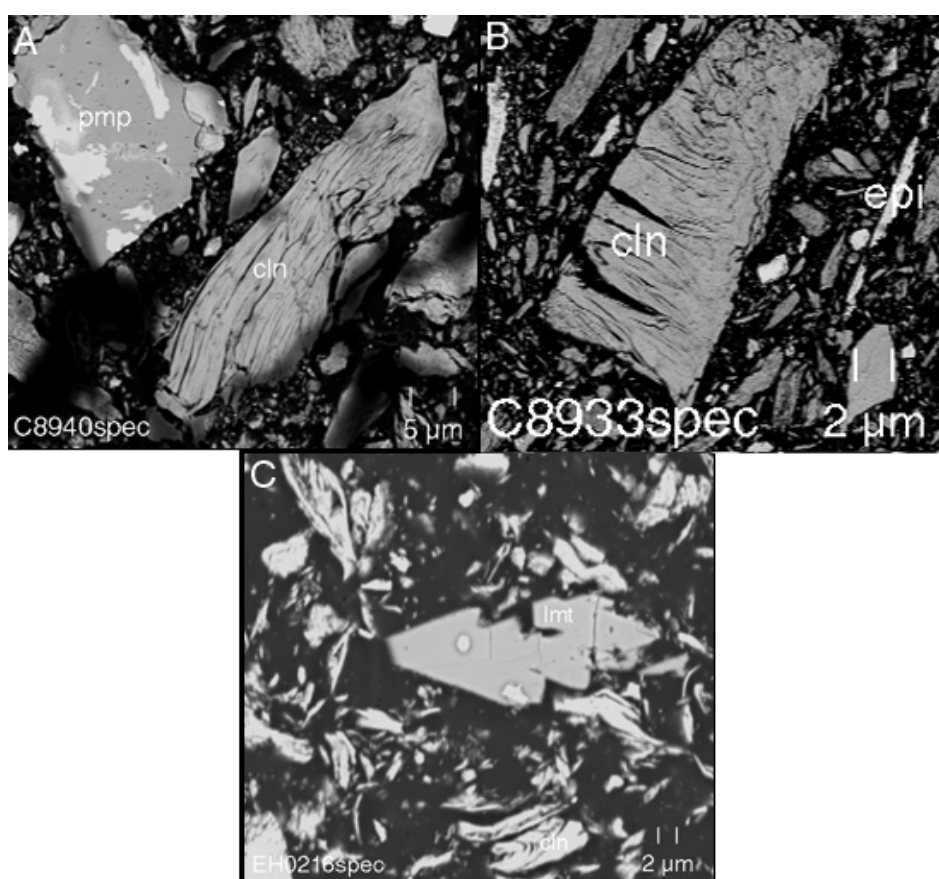


**Figure 3:** First XRD tested, assumed pure clinocllore amygdule extractions. A closer look with the EMPA reveals a mixture of different minerals of the low-grade metamorphic history of the Portage Lake Volcanics. A) Phyllosilicate (Phy) and pumpellyite (Pmp), dark background: epoxy ®. B) Phyllosilicate and epidote (Epi), dark background: epoxy ®. C) Phyllosilicate (all other) and laumontite (Lmt), dark background: epoxy®.



### Conditions for electron microprobe analysis (EMPA)

Mineral analyses were obtained using a JEOL JXA8600 superprobe at the Mineralogisch-Petrographisches Institut of Basel University. The elements Si, Al, Fe, Mg, Mn, Ca, Na, K were measured, using wavelength dispersive spectroscopy, an accelerating voltage of 15 kV and a beam current of 10 nA. As standards, natural minerals were used: albite for Na, wollastonite for Ca, graptolite for Fe and Mn, orthoclase for K and Al and olivine for Mg and Si. In order to minimize evaporation of light elements (e.g. Na), the spot size was set to 2  $\mu\text{m}$ , or the sample was measured in a scan-mode with a magnification of 20 000. The data were reduced with the PROZA correction function. It was difficult to obtain accurate electron microprobe data on the phyllosilicates. The topographical structure of the phyllosilicates in a thin section doesn't only depend on the preparation, but also on the orientation of the brittle material itself in the rock.

**Figure 4** gives an impression on the topography of a good sample. The 'black' colored spaces are holes. Because of the sheeted structure of phyllosilicates, more fractures become visible with higher magnification. The beam of the electron microprobe needs at least a clean patch of 3  $\mu\text{m}$  in diameter to give an accurate value.

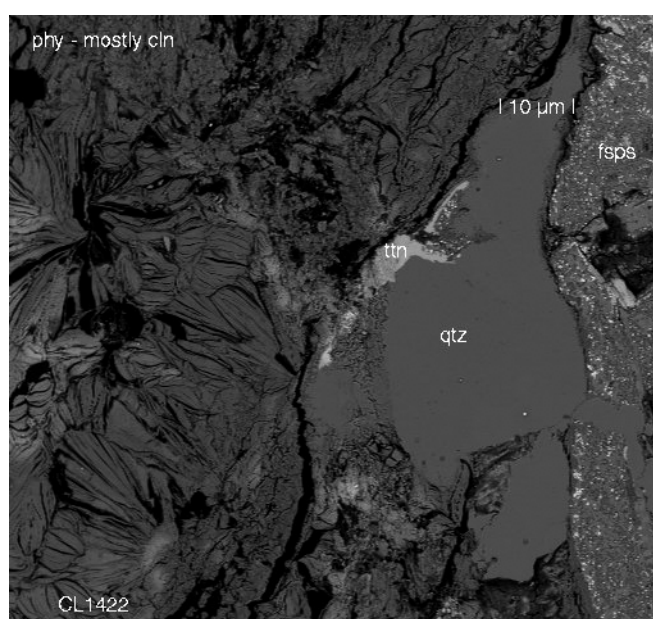


**Figure 4:** Early amygdule infilling minerals, titanite (ttn) and quartz (qtz) dissolved by phyllosilicates (clinocllore, cln) (CL1422).

## Results

The main phyllosilicates found in the PLV are clinocllore (Cln), corrensite (corr) and mixed-layered phases of chlorite and smectite (smc). In addition, vermiculite and illite were determined by XRD techniques.

Clinocllore, the most abundant phyllosilicate of the Keweenaw Peninsula, occurs as dense masses in amygdules and veins of the flow tops, the transition zone, and also in patches in the least altered ophitic massive flow interior of the lava flows. In hand specimen, it shows most often a dark green color, which can change to lighter green colors. In thin section, a light green to

dark green pleochroism is observed. Depending on the Mg/Fe ratio, an abnormal olive-green or violet-blue interference color is visible (Troeger, 1982).

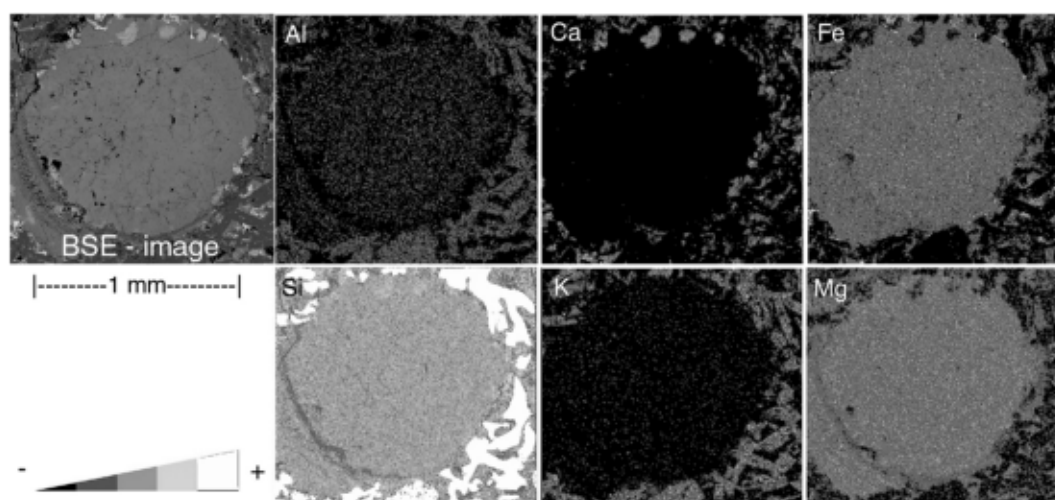


**Figure 5:** X-ray maps (EMPA) of a clinochlore amygdule (EH0426/I) showing homogeneous distribution of elements.

A detailed X-ray map of clinochlore in an amygdule (**Fig. 5**) shows a homogenous element distribution with titanite formation along the rim of the amygdule. This indicates stable growing conditions in small-scale amygdules (< 2mm) as reported by Jolly and Smith (1972). In bigger amygdules (> 2cm) a change in grain size from rim to center could be observed, indicating a probable rise in temperature (Merriman and Peacor, 1999).

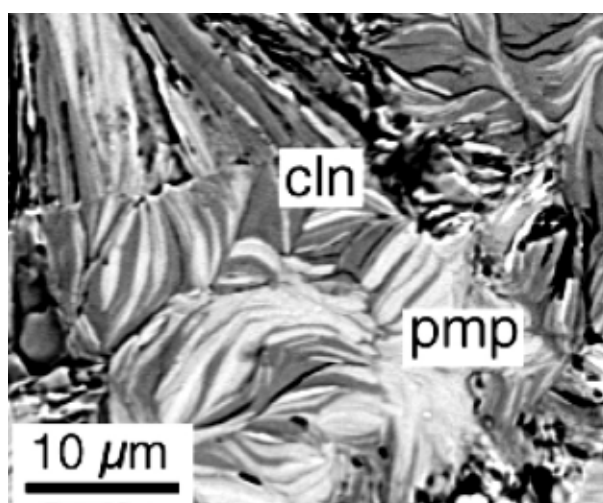


**Figure 6:** Acicular clinochlore (cln) intergrown with acicular pumpellyite (pmp) (D5742).

Clinochlore and pumpellyite are also sometimes intergrown. Both minerals form acicular-shaped minerals, which alternate as observed in an early vein of D5742 (**Fig. 6**). In **figure 7** clinochlore occurs as worms, together with a matrix of mixed-layered phyllosilicates, in an amygdule of a transition zone. In bigger amygdules clinochlore occurs often macroscopically as the first mineral grown along the rim. Microscopical and electron microscope BSE images show clearly that most of the phyllosilicates (Cln) in the permeable sections are products of pervasive alteration

affecting also earlier formed alteration minerals. In **figure 4** the first alteration mineral assemblage of a flow top amygdale shows quartz and titanite and is dissolved by a later grown phyllosilicate. In the matrix, often phyllosilicates (Cln) with a higher Mg content are observed in alternating layers of quartz (**Fig. 8**). In veins of early stage prehnite, later filled with quartz and native copper, phyllosilicates are found also as final vein infilling (**Fig. 9**). Other phyllosilicates, like vermiculites are found also on third stage veins along the cleavage of laumontite and calcite.

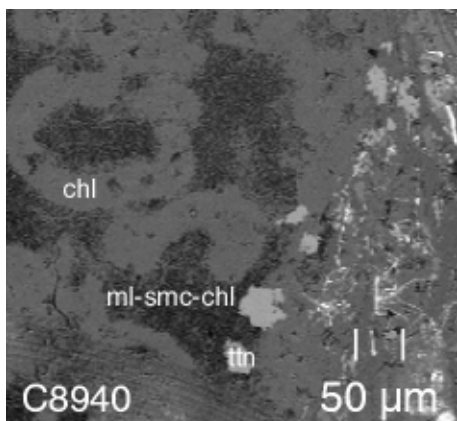


**Figure 7:** Phyllosilicates in amygdule, worms of clinochlore (chl) in a mixture with mixed-layered phyllosilicates (ml-smc-chl), and titanite (tn) at the host rock walls (C8940).

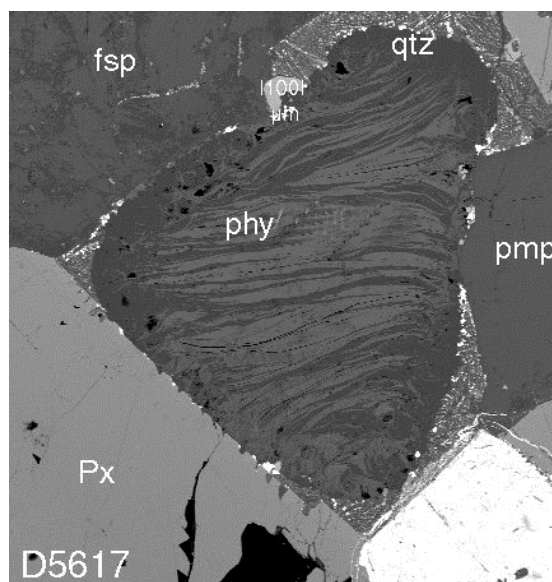


**Figure 8:** Matrix setting: quartz (qtz) intergrown with clinochlore of high Mg content (D5617).

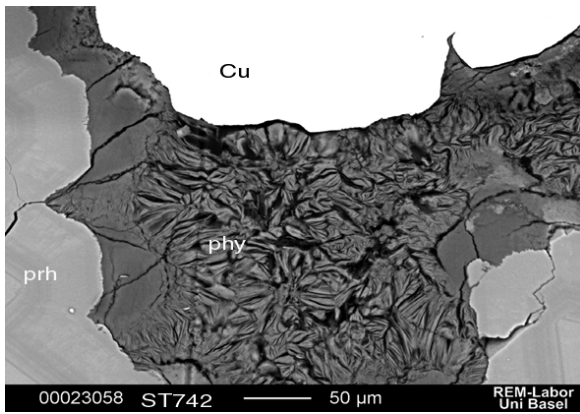


**Figure 9:** Vein of early alteration stage prehnite (prh), filled by stage II native copper (Cu), showing phyllosilicate (phy) as final infilling from the last alteration stage (ST742).

### *Distribution of phyllosilicates in the PLV*

Based on a total of 444 X-ray diffractograms, no clear trend of phyllosilicate distribution is observed. Pure clinocllore occurs within all drill core sections in amygdules of flow tops and transition zones (**Fig. 10**). Corrensite occurs in the upper stratigraphic sections A and B mainly in amygdules of the transition zones and flow tops. In the deeper sections C and D, it occurs mainly in veins of massive flow interiors. It is first well crystallized in Section B below the Greenstone Flow (**Fig. 11**). It occurs frequently together with clinocllore and only sometimes as single infilling of amygdules. Smectite is never observed as a single phase within amygdules or veins but is normally intergrown with clinocllore. Its occurrence seems to be limited to veins in the massive flow interior within all drill core sections (**Fig. 12**)

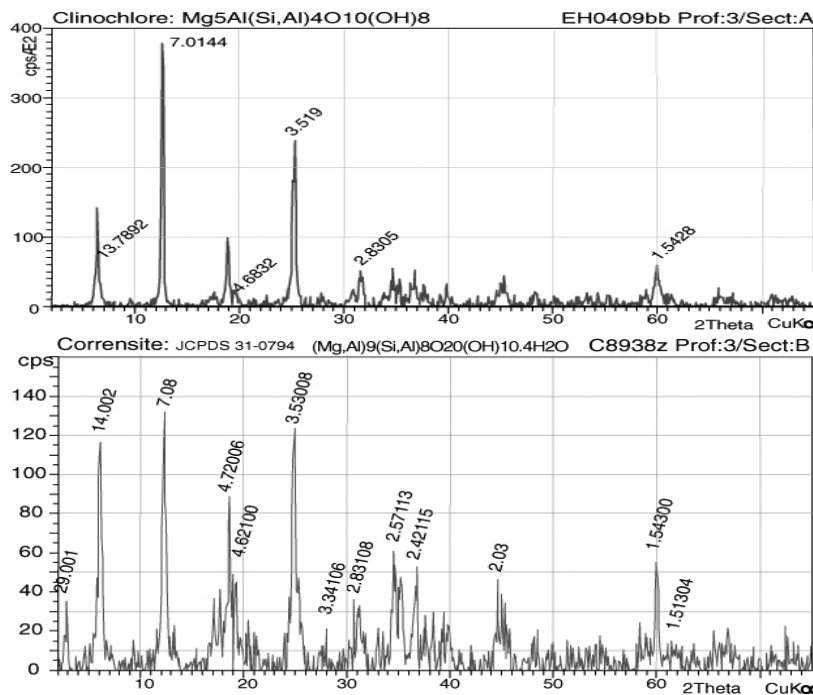


**Figure 10:** X-ray diffractogram of pure clinocllore (air dry).

**Figure 11:** X-ray diffractogram of pure corrensite (air dry).

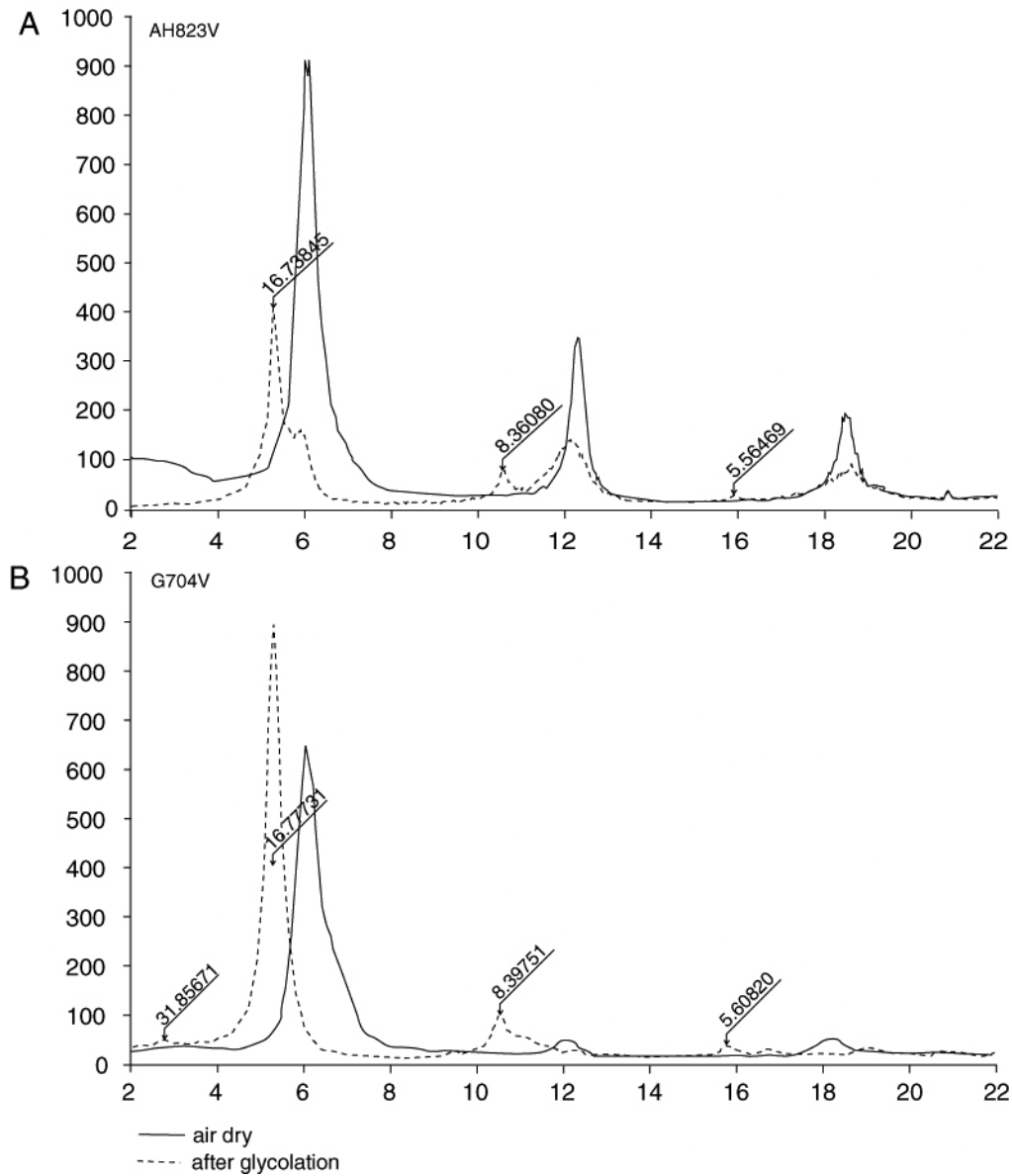


**Figure 12:** X-ray diffractogram of mixed-layered phyllosilicate A) air dry and B) glycolated.

The chemical composition of the phyllosilicates based on 360 individual electron microprobe analyses within the three drill cores is shown in the diagram of total non-interlayered cation (NIC) versus total Al. This same diagram is plotted three times in **figure 13** but samples are labeled differently. Plot A) is the general plot of the samples within one drill core profile, plot B) represents the site of phyllosilicate occurrence (vein, matrix, amygdale) and plot C) plots the samples according to the flow morphology.

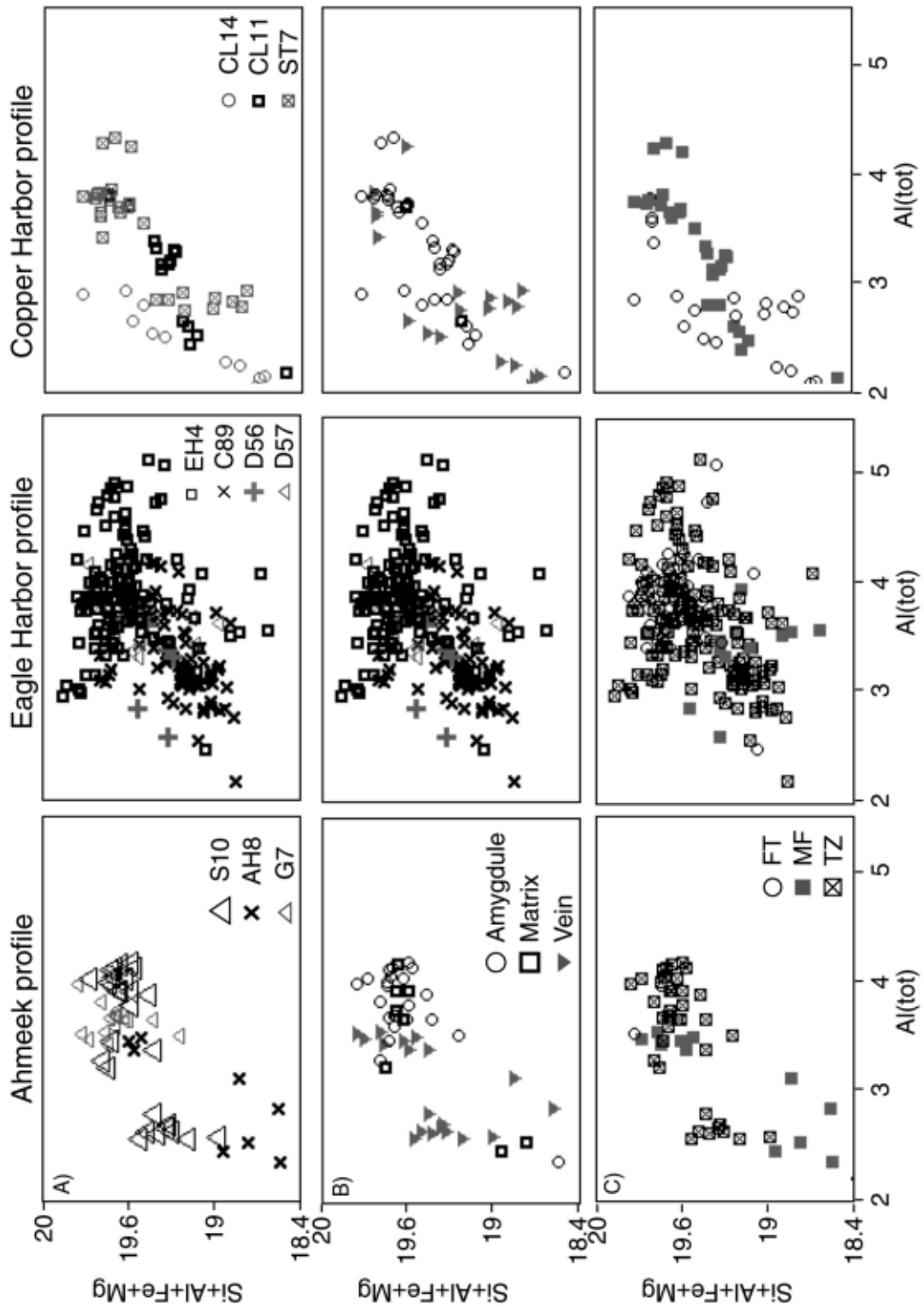


**Figure 13:** Plot of Al(tot) versus Si+Al+Fe+Mg: split by: A) drill samples, B) site of occurrence in host rock, C) Host rock unit, MF: massive flow interior, TZ: transition zone, FT: flow top.

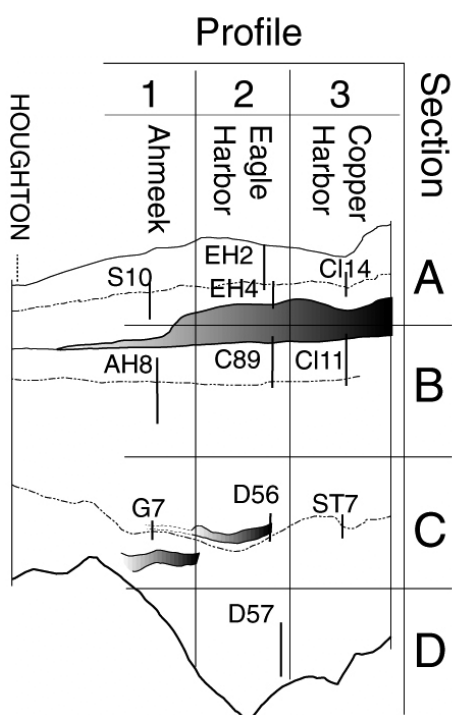


**Figure 14:** Schematic sketch of the PLV including the three drill core profiles and four stratigraphic sections, for easy reference.

A schematic overview of the drill core profiles is shown in **figure 14**. By carefully comparing the plots of the three drill core profiles, the following facts become evident.

- 1) Chlorite as well as mixed-layered phyllosilicates were identified but no pure smectite was found, which theoretically would plot at 17.8 non-interlayer cation (NIC) atom. These results confirm the result of the X-ray study.
- 2) None of the profiles shows a stratigraphic depth-related compositional zonation of the phyllosilicates. There is a significant overlap of the chemical composition of samples from the various drill core sections.
- 3) The phyllosilicates with the highest mixed-layered component, and probably related to lower-grade metamorphic conditions, are found in the stratigraphically lower part of the most western Ahmeek profile and occur within a early vein as well as in massive flow interiors.
- 4) The most eastern Copper Harbor Profile shows the widest and a continuous compositional range in total aluminum content. In contrast, phyllosilicates from the most western Ahmeek Profile show two distinct phyllosilicate populations: a mixed-layered population and a chloritic population (samples G7 and part of samples S10). The Eagle Harbor Profile shows a compositional and continuous range as well.
- 5) The most chloritic composition is found in the stratigraphically upper part of the Eagle Harbor Profile (EH4). As has been shown in **figure 10**, the peaks of the X-ray diffractograms of sample EH409bb are extremely thin and sharp, indicating a well crystallized chlorite.
- 6) In general no correlation is found between the chemical composition of the phyllosilicate, the site of the occurrence of the phyllosilicate (amygdule, vein or matrix) and the flow morphology.
- 7) Samples from the massive flow interiors plot relatively more towards the mixed-layered compositions than samples from the transition zone or the flow top. This is true for EH04 in the Eagle Harbor profile, for AH8 in the Ahmeek profile and to a certain extend for ST7 in the Copper Harbor profile.

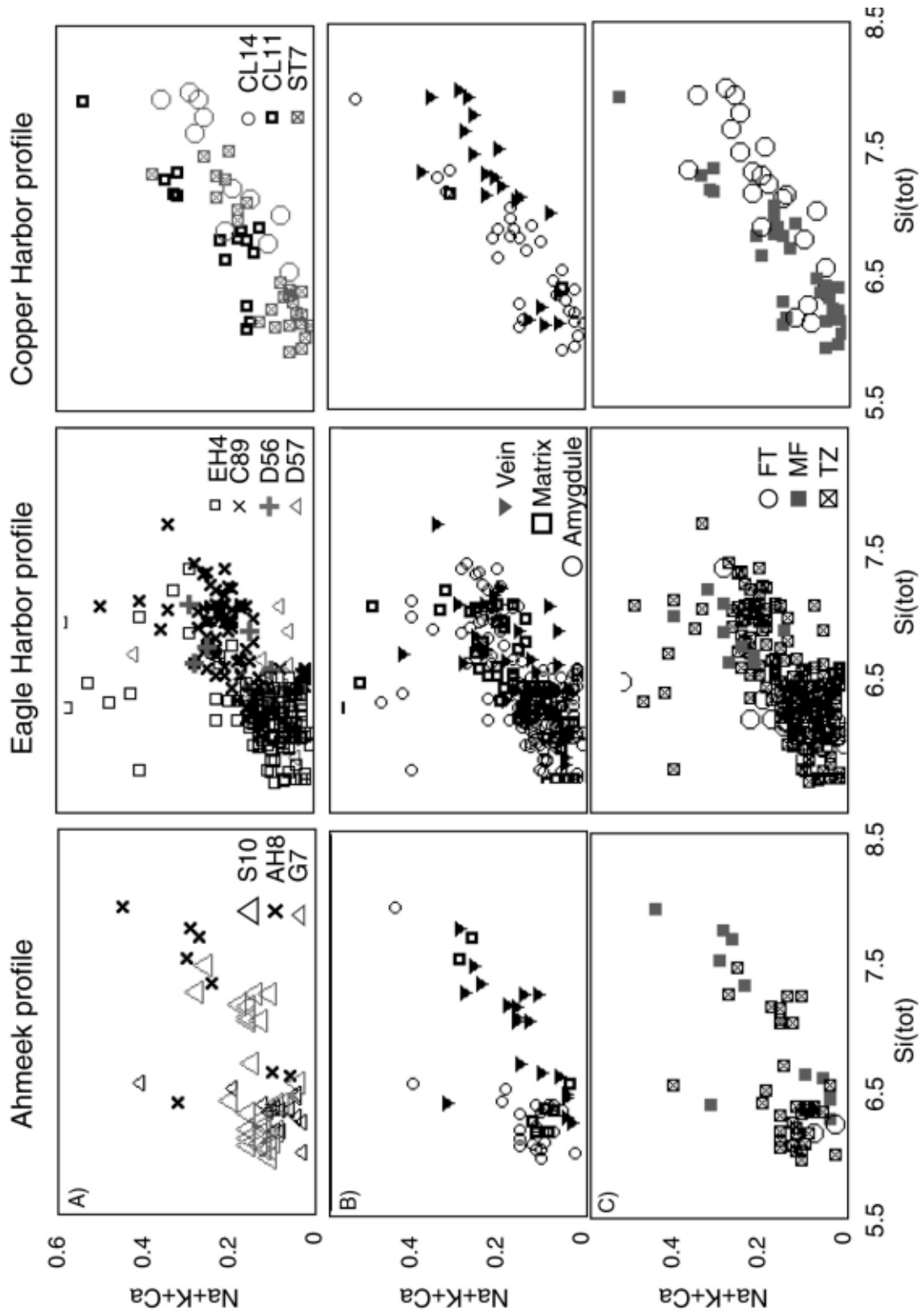


**Figure 15:** Total EMPA data in a plot of Si(tot) versus Na+K+Ca: split by: A) drill samples, B) site of occurrence in host rock, C) Host rock unit in a lava flow of the Portage Lake Volcanics (PLV), MF: massive flow interior, TZ: transition zone, FT: flow top.



The plot of interlayered cations (IC) of phyllosilicates versus total Si can be understood as an indicator of mixed-layering (**Fig. 15**). Similar as in figure 13, samples were plotted according to drill site (A), to the site of phyllosilicate occurrence (B) and according to the flow morphology (C). Samples in the Copper Harbor drill core profile show high concentrations of IC indicating variations in the mixed-layered composition. The western Ahmeek profile shows more samples with lower IC values especially the lowest G7 drill core. Also ST7 and EH04 show a low contamination with ICs. In **figure 15/B**, the above trend can be observed for amygdules, matrix and vein settings. To a certain extent amygdules show less contaminated phyllosilicates than veins or matrix samples. From **figure 15/C** it is evident that samples from massive flow interiors show more often a high content of ICs above 0.2 than samples analyzed from flow tops or transition zones.

From the different diagrams it is evident that the distribution of the phyllosilicates is not controlled by stratigraphic depth or site of phyllosilicate occurrence or flow morphology. There is some evidence that the different morphology of a flow – vein in the massive flow interior versus flow top or transition zone has a controlling factor on phyllosilicate formation. A continuous spectrum of phyllosilicate composition is present in the Eagle Harbor profile and the Copper Harbor profile. At a certain degree of alteration the phyllosilicate population splits up into two distinct populations as seen in the Ahmeek profile, a chloritic and a mixed-layered one.

**Figure 16(A/B/C)** displays a plot  $Al^{(iv)}$  versus  $Na+K+2Ca$  including hypothetical mixtures of chlorite with other minerals (after Schmidt et al. 1997), displayed as vectors. The diagram confirms the observation of contamination. A contamination with mixed-layered minerals is displayed. Also a slight trend to illite/muscovite contamination can be observed, which is supported by X-ray diffraction which detected muscovite in a sample of drill G7. **Figure 16/B** displays that the phyllosilicates in the veins are more often contaminated than amygdules and **figure 16/C** shows that the less contaminated phyllosilicates are located in the FTs.

### **”Chlorite thermometry”**

Cathelineau and Nieva (1985) and Cathelineau (1988) proposed a chlorite geo-thermometer, which relates the tetrahedral Al content of chlorite to temperature and was calibrated in the Los Azufres geothermal system in Mexico. This geo-thermometer was applied and criticized by many petrologists since it seemed to be an elegant tool for estimating temperature but did not work in many cases (de Caritas, 1993; Essence, 1995; Hillier, 1991; Jahren, 1991 and 1992; Jiang, 1994; Schmidt, 1997). Shau et al. (1990) and Jiang et al. (1994) documented by TEM observations that chlorite is usually contaminated by the presence of mixed-layer smectite. Such a phase is not a thermodynamically stable phase, which is one of the basic requirements for a geo-thermometer.

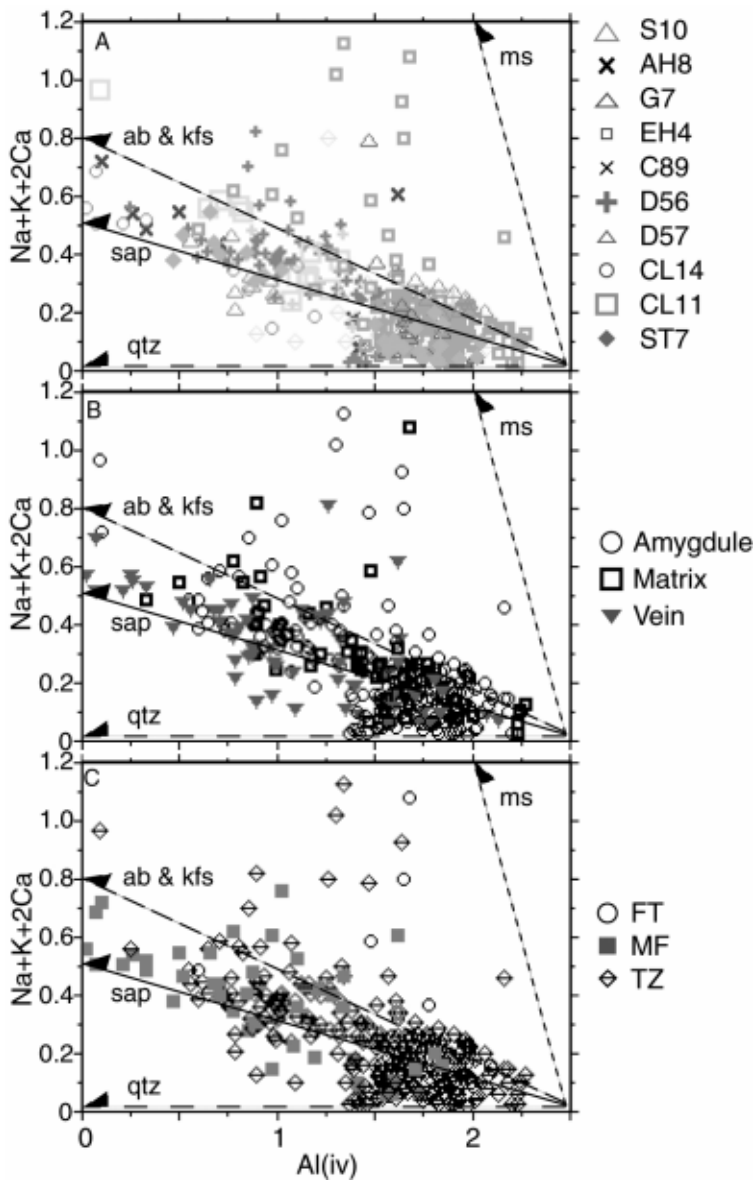


**Figure 16:** Al(IV) versus Na+K+2Ca. Hypothetical mixtures of chlorite with other phases are shown as arrows (modified after Schmidt et al., 1997). Qtz; quartz, sap: saponite, ab & kfs: albite and potassium feldspar, ms: muscovite; split by: A) drill samples, B) site of occurrence in host rock, C) Host rock unit, FT: flow top, TZ: transition zone, MF: massive flow interior.

Nevertheless, the chlorite geo-thermometer was applied to 70 chlorite analyses. The derived values have a minimum of 95°C (vein sample CL14) and a maximum of 340°C (amygdule sample EH04). The average calculated temperature is around 230°C. Other values were calculated for AH8 (vein material; 165-195°C), C89 (vein/amygdule material; 160-200°C), G7 (vein material; 190-225°C) and D57 (vein material 150-230°C).

Temperatures in single amygdules were calculated from drill EH04 (**Table 1**). In one individual thin section of sample EH0409, a variance of calculated temperatures of 130°C can be observed. No continuous trend could be observed for increasing or decreasing temperatures from amygdule rim to amygdule center.

**Table 1:** Amygdule rim to center temperatures in drill EH04, after calculations from Cathelineau (1988)

Sample	Amygdule	Rim [°C]	trend	Center [°C]
EH0409	1	200	>	170
	1	240	>	170
	2	300	=	300
	3	250	<	290
	3	250	>	210
	4	245	>	190
	4	295	>	255
EH0410	8	230	>	210
EH0426	1	240	<	256
	2	210	<	245
	3	238	<	244

## Discussion

The PLV are completely recrystallized in the flow tops and the bases. Therefore these parts must have experienced high water rock ratios. As has been shown in the Ahmeek profile, the permeability and porosity-control play a role in the formation of phyllosilicates and prevent or favor the transformation of the phyllosilicate series. It is evident that the distribution of the phyllosilicates is not controlled by stratigraphic depth or site of phyllosilicate occurrence. Instead there is evidence that the different morphology of a flow – vein in the massive flow interior versus flow top or transition zone - has a controlling impact on phyllosilicate formation. A continuous spectrum of phyllosilicate composition is present in the two eastern profiles. At a certain grade of alteration, the phyllosilicate population splits up into two distinct populations as seen in the Ahmeek profile: a chloritic and a mixed-layered one. This process can be explained by a reaction progress where the transformation of smectite to chlorite proceeds either by a continuous or a discontinuous step. Three reaction pathways have been proposed for this transformation:

- 1) a continuous smectite-corrensite-chlorite series,
- 2) a discontinuous smectite-corrensite-chlorite series and
- 3) a direct smectite to chlorite transition.

Our results indicate that in the eastern Copper Harbor profile there is a continuous transformation of smectite to chlorite, which occurs at zeolite facies grade. In the prehnite-pumpellyite zone of the most western Ahmeek profile, the reaction progress of the smectite-chlorite transformation has proceeded and two distinct phyllosilicate populations are present.

Various parameters control this mineralogical transformation. Temperature is certainly one important parameter. Direct measurements of temperature and phyllosilicate formation were correlated in Iceland (Kristmansdottir, 1979) and in the Chipilapa system in El Salvador (Robinson and Zamora, 1999). Chlorite appearance temperature varies from 210 to 270 °C in the Icelandic System. In the Chipilapa system, chlorite occurs as a minor phase at a temperature of 120 °C while it becomes the main phase at 160 °C.

Fluid/rock ratios have also been considered as controlling the phyllosilicate transformation (Schiffman and Staudigel, 1995; Alt, 1999). Intensive re-crystallization of the host rock points to high water/rock ratios. Schmidt (1990, 1993) and Schmidt and Robinson (1997) have shown that not only fluid/rock ratios play an important role, but also the mode of fluid transport. Areas with high permeability and porosity such as amygdaloidal flow tops will permit advective fluid flow, whereas areas with low permeability and porosity will allow a restricted diffusive transport.

## Conclusions

The transformation of tri-smectite-corrensite-chlorite is a common mineralogical process during low-grade metamorphism of basic rocks. Progress in the understanding of this transformation and the tri-smectite-corrensite-chlorite transformation, have been made mainly through detailed TEM studies (Jiang, 1994, Shau et al., 1990). Essence and Peacor (1995) suggested interpreting the transformation of this reaction pathway in terms of reaction progress. The main control on reaction progress is considered to be kinetic.

The results of this study confirm the concept of reaction progress. At the low metamorphic grade, mixed-layering is present and as the compositional range of the phyllosilicates is high. At a certain stage of metamorphism, the reaction progress has advanced and only 2 distinct populations are now present as seen in the Ahmeek profile, where the pumpellyite-prehnite facies is slightly better developed than in the more eastern profiles.

In many low-grade metamorphic rocks, characteristic Ca-Al-assemblages are lacking and phyllosilicates are the only metamorphic minerals. Estimation of the metamorphic grade is therefore difficult. In the Portage Lake Volcanics, the Ahmeek profile displays two distinct phyllosilicate populations. Prehnite-pumpellyite alteration is abundant in these rocks and quantitatively more dominant than in the Eagle Harbor profile. In the Copper Harbor profile, a continuous compositional range can be seen and prehnite-pumpellyite assemblages are less frequent and laumontite is still present.

It is proposed that the smectite-corrensite-chlorite transition is a very sensitive indicator of low-grade metamorphism grade if Ca-Al-silicates are not present. In addition, it can also be used as a relative indicator of grade within the prehnite-pumpellyite facies.

**For references see part 7 of this thesis.**

**Native copper mineralisation in the Portage Lake Volcanics in context of the very  
low-grade metamorphic alteration on the Keweenaw Peninsula, Michigan**

Ulrich R. Püschner

Josef Mullis

Susanne Th. Schmidt

## Introduction

The Keweenaw Peninsula is famous for its rich native copper deposits, which were exploited until the late 60ies (Weege and Pollack 1971) as one of the biggest native copper mining areas in the world. Therefore, the native copper ore has been studied since the beginning of the exploration, in the middle of the 19<sup>th</sup> century by several authors (Pumpelly, 1871; Palache and Vassar, 1925; Broderick, 1929; Butler and Burbank, 1929; and Broderick, 1946).

The rich native copper ore parts were already removed from the drill cores for assay. There was only material available with few flakes of native copper. Thus, the presented study about fluid inclusions adjacent to the native copper ore is a by-product of studying the low-grade metamorphic alteration minerals. The data of this chapter 5 derive from the Ahmeek and the Copper Harbor profiles (See also Chapter 1 - Introduction). Therefore the conditions of native copper precipitation may differ from the occurrence in the mines as it was studied by other authors (e.g. Stoiber and Davidson, 1959; Livnat, 1983).

To recognize significant differences between mining material and the studied profiles two mine samples from Keweenaw Peninsula Mines out of the collection of the Swiss Natural Historical Museum in Bern/Switzerland were used. Native copper flakes were found in all types of host rock in the studied drill cores especially in conglomerates, where 40% of the native copper was mined (Bornhorst, 1997). The investigated samples include only one conglomerate specimen, because sediments usually do not contain significant amounts of secondary alteration minerals, and were therefore not collected within the topic of this study.

## Methods

### Fluid inclusion measurement

Fluid inclusion data on vein quartz and calcite were obtained by micro-thermometry as described in Mullis (1987). The measurements were performed on a Laborlux microscope equipped with a freezing-heating stage (Chaixmeca), designed to work within a range of  $-180^{\circ}\text{C}$  to  $+450^{\circ}\text{C}$ . The precision of measurements is  $0.2^{\circ}\text{C}$  in the range of  $-60^{\circ}\text{C}$  to  $+40^{\circ}\text{C}$ , and  $1^{\circ}\text{C}$  otherwise. The salinity was estimated after Potter et al. (1977).

### Scanning electron microscope (SEM)

The Philips XL30 FEG SEM (scanning electron microscope) at the SEM lab at Basel University was used to obtain high quality back scattered electron (BSE) images from a few well chosen EMPA thin sections and other native copper bearing samples. In addition, a semi-quantitative X-ray mapping was performed with the same equipment.

### Cathode luminescence (CL)

Cathode luminescence was used to detect zonation in calcite. The TECHNOSYN® Cold Cathode Luminescence Model 8200 MK is setup on a Leica® microscope furnished with a photo camera. The vacuum chamber was under a 2.5 torr vacuum and the gun current was set between 570 to 600  $\mu\text{A}$  at 15 kV. The resulting images were taken with 1000 ASA films, with an exposure time of up to 4 minutes.

## Results

### General occurrence of native copper

From the microscopical studies, it is evident, that in the volcanic host rocks, native copper is often related to the occurrence of prehnite (**Table 1**). Younger prehnite (stage II) veins cross cutting preferentially prehnite of the first alteration stage are characterized by lighter gray rims, which are related to enriched high-Z elements such as Fe. These can be visualized in the back-scatter-electron images (BSE) of the EPM or SEM (**Fig. 1 and 2**). These enriched zones were only observed close to the native copper precipitation. In most cases the native copper ore within these veins is precipitated with a mineral assemblage of quartz and/or calcite in the prehnite veins.

Table 1: Mineral assemblages of native copper in thin sections (profiles and mines)

P	S	HR	Sample	realD	sec. min. assemblage	Cu 'host' min.	Cu reported by	metamorphic-facies
ND	ND	FT	MineKP	ND	epi, qtz, cal, Cu	qtz/cal	this study	
ND	ND	FT	MineKP	ND	epi, qtz, cal, Cu	qtz/cal	this study	
ND	ND	FT	CallMine	ND	epi, qtz, Cu	epi/qtz	this study	
1	A	FT	S10-31	205	prh, prh, prh, qtz, Cu	prh/qtz	this study	
1	A	FT	S10-35	241	pmp, prh, qtz, Cu, zeo, cal, phy	prh/qtz	this study	pmp-prh and zeo
1	A	FT	S10-37	251	epi, prh, pmp, qtz, cal, qtz, prh, Cu, qtz	prh/qtz	this study	pmp-prh
1	B	FT	AH8-0J	102	prh, cal, prh, qtz, qtz, Cu	prh/qtz	this study	
1	B	FT	AH8-21	242	epi, pmp, phy, qtz, epi, prh, qtz, Cu, qtz, cal	prh/qtz	this study	pmp-prh
1	B	MF	AH8-23	277	qtz, phy, zeo, cal, phy	cal	drill log data	zeo
1	B	TZ	AH8-27	298	phy, pmp, qtz, phy	qtz	drill log data	
1	B	MF	AH8-29	318	epi, pmp, phy, qtz, cal, pmp, qtz, cal, phy	qtz/cal	drill log data	
1	B	TZ	AH8-32	345	epi, prh, cal, epi, prh, qtz, Cu, qtz	prh/qtz	this study	
1	B	TZ	AH8-46	444	kfs, prh, qtz, Cu, cal, phy, zeo	prh/qtz	this study	zeo
1	B	FT	AH8-47	456	epi, pmp, prh, qtz, cal, Cu, cal	qtz/cal	this study	pmp-prh
1	C	TZ	G7-06	40	pmp, pmp, epi, epi, qtz, Cu, phy	epi/qtz	this study	
1	C	MF	G7-21	144	pmp, prh, qtz, Cu, phy, zeo, phy, cal, phy	prh/qtz	this study	pmp-prh
1	C	MF	G7-25	195	pmp, epi, ab, qtz, Cu, phy, qtz, phy	epi/qtz	this study	
2	A	TZ	EH04-24	205	epi, pmp, cal, phy	pmp/cal	drill log data	
2	A	MF	EH04-25	206	ab, qtz, pmp, phy, cal	?	drill log data	
2	B	FT	C89-02	17	epi, pmp, prh, Cu, zeo, cal, phy	prh/cal	this study	pmp-prh and zeo
2	B	TZ	C89-12	55	prh, zeo	prh	drill log data	
2	B	MF	C89-13	56	pmp, pmp, pmp, prh, Cu, pmp, prh, phy	prh	this study	pmp-prh
2	B	TZ	C89-31	174	ab, epi, pmp, phy	?	drill log data	zeo
3	A	TZ	CL14-45	215	prh, prh, cal, Cu, cal	prh/cal	this study	
3	A	MF	CL14-48	227	prh, cal, phy, phy	prh/cal	drill log data	
3	A	MF	CL14-83	426	prh, qtz, cal, Cu, qtz, pmp, cal, phy, phy	prh/qtz	this study	pmp-prh
3	B	FT	CL11-06	42	pmp, ab, prh, Cu, cal	prh/cal	this study	pmp-prh
3	B	MF	CL11-24	158	pmp, prh, cal, phy	prh/cal	drill log data	pmp-prh
3	B	TZ	CL11-25	160	prh, ab, phy, pmp, phy	prh/qtz	drill log data	pmp-prh
3	C	MF	ST7-20	323	zeo, phy	prh/qtz	drill log data	zeo
3	C	TZ	ST7-21	7	pmp, prh, prh, prh, Cu, cal, cal	prh/cal	this study	pmp-prh
3	C	FT	ST7-22	9	pmp, prh, zeo, cal, phy	prh/cal	drill log data	pmp-prh and zeo
3	C	FT	ST7-31	45	prh, phy, zeo, cal, phy, phy	prh/cal	drill log data	
3	C	TZ	ST7-42	180	pmp, prh, cal, prh, qtz, Cu, qtz	prh/qtz	this study	pmp-prh
3	C	MF	ST7-43	201	phy	?	drill log data	
3	C	FT	ST7-44	174	pmp, epi, qtz, prh, epi, prh, qtz, Cu, cal	prh/qtz	this study	pmp-prh
3	C	TZ	ST7-58	315	phy	?	drill log data	

P: drill core profile; (1: Ahmeek; 2: Eagle Harbor; 3: Copper Harbor); S: section, HR: host rock, FT: flow top, MF: massive flow interior, TZ: transition zone, realD: today's depth under surface, ab: albite, cal: calcite, Cu: native copper, epi: epidote, prh: prehnite, pmp: pumpellyite, zeo: zeolite, qtz: quartz, phy: phyllosilicates (chlorites, corrensite, smectites), kfs: potassium feldspar, (Mineral abbreviations according to Kretz, 1983).

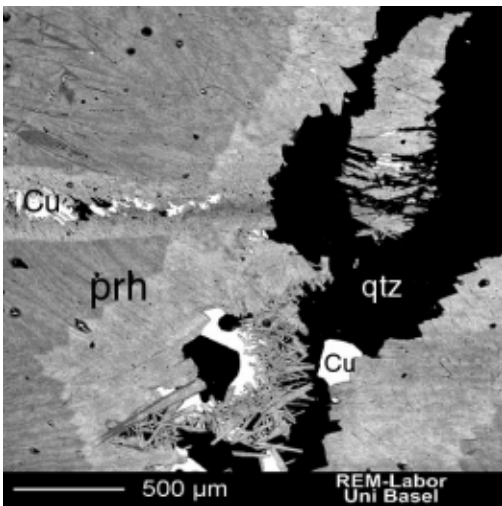


**Figure 1:** Prehnite vein with native copper and quartz, sample ST742.  
(Abbreviations see Table 1)

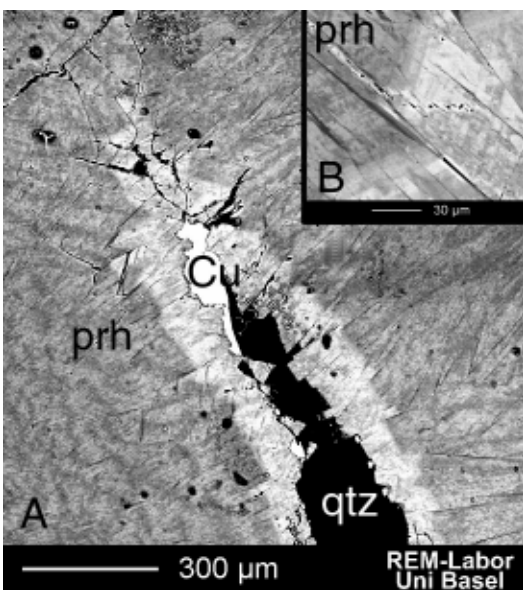


**Figure 2:** Prehnite displaying compositional zonation as evidenced by the lighter gray color along the rim which is probably due to fluid infiltration and quartz and native copper precipitation, sample ST742.

A) Overview, note: reaction zone (light gray) only in contact to the Cu/qtz assemblage.

B) Detail, showing the border of the reaction in prh. (Abbreviations see Table 1)

#### Native copper beside quartz

The studied volcanic rock samples of the drill cores from the Ahmeek and the Copper Harbor profile show mostly quartz, which forms euhedral planes adjacent to native copper (**Fig. 1 and 3**). The quartz rims are translucent in thin sections because of very few fluid inclusions. Quartz shows more fluid inclusions if native copper droplets occur directly in quartz, which could be observed in the conglomerate sample. In quartz of the studied conglomerate sample from the drill core AH8 of the Ahmeek profile, native copper was found as droplets apparently as part of the quartz matrix, which serves as a cement in the conglomerates (**Fig. 4**). The rare fluid inclusions indicate young quartz of the second alteration stage. In the massive flow interiors of the Ahmeek profile in drill core G7, native copper was detected in first alteration stage epidote veins adjacent to early secondary quartz (**Fig. 5**). In the Copper Harbor profile, native copper was found in small quantities in quartz veins (e.g. CL1483). Within an alteration zone small native copper bodies are arranged around a main native copper body (**Fig. 6**). At least two generations of quartz occur in this vein, distinguished by the decreasing amount of fluid inclusions in the younger quartz generation.



The studied mine samples show prismatic quartz of the first alteration stage which shows due to fluid inclusions, up to three distinguishable zones before native copper precipitation (**Fig. 7**). Different from the observations of the drill core profiles Ahmeek and Copper Harbor is that a second form of native copper precipitation can be observed, which is characterized by the corrosion of the quartz / copper contact planes (**Fig. 8**).

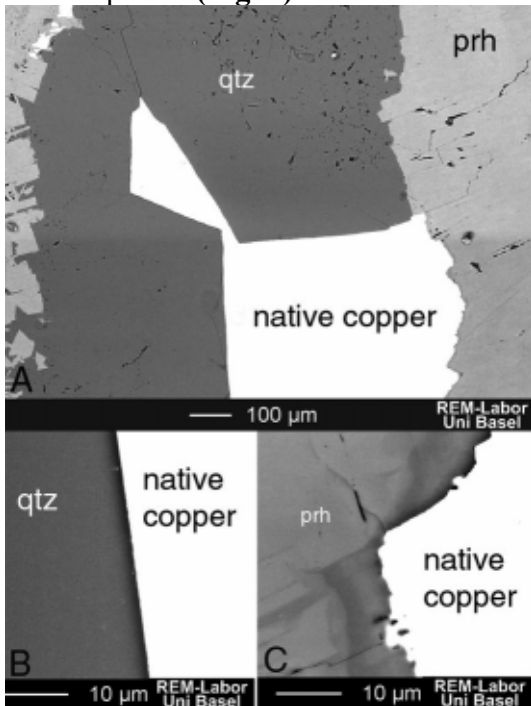


**Figure 3:** BSE images from the phase contact of native copper/quartz, -/prehnite. A) Overview; sample ST742. B) Sharp border to quartz, sample ST742. C) Corroded prehnite; sample ST742. (Abbreviations see Table 1)

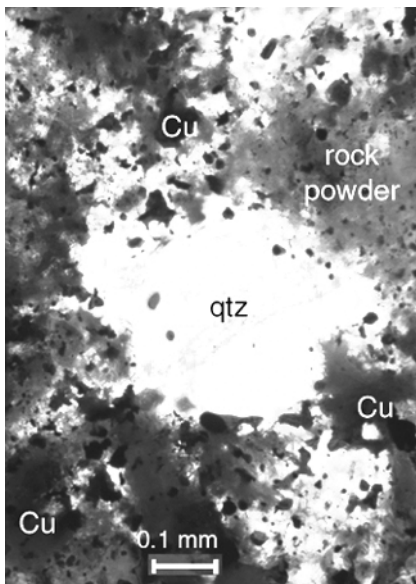


**Figure 4:** Optical microscopic image of fine disseminated native copper and rock powder in quartz cement of a conglomerate in the PLV, sample AH847.

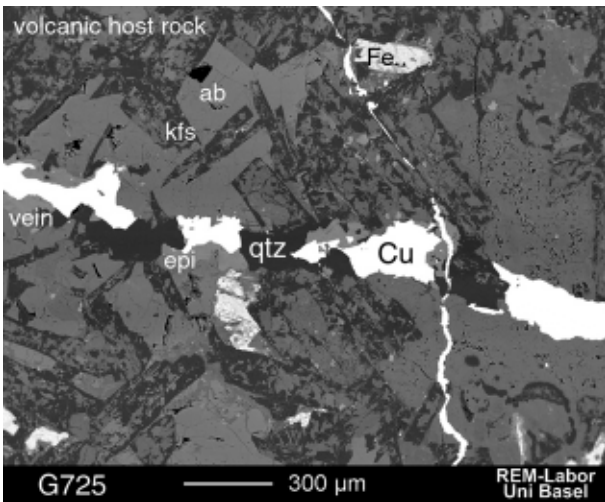


**Figure 5:** Native copper in a massive flow interior on a later cross cutting vein, in a mineral assemblage with epidote and quartz, sample G725.

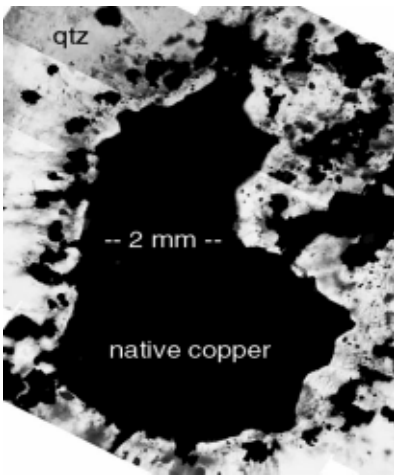


**Figure 6:** Native copper ‘splash’, witness of a fast event? Native copper looking like drops in quartz, sample CL1483, (Abbreviations see Table 1).

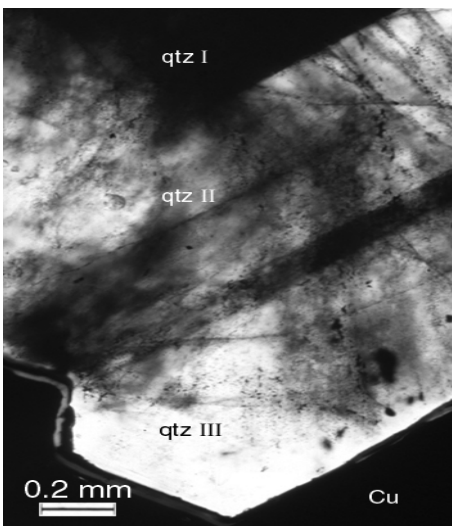


**Figure 7:** Zoned prismatic quartz showing three zones, distinguished by the amount of fluid inclusions (Mine sample). [Gray line between ‘Cu’ and ‘qtz’ is epoxy®].

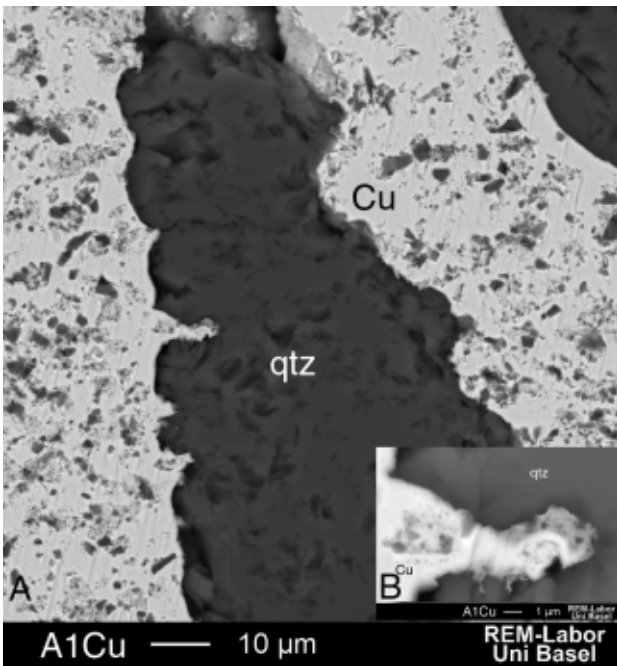


**Figure 8:** SEM image; corrosive contact of quartz and native copper in a sample from the main mining area, sample: KP Mines.

#### Native copper beside calcite

Calcite is an abundant mineral in the PLV during the entire low-grade metamorphic evolution. The main calcite precipitation took place after the final superimposed zeolite facies which is stage three. But there is also earlier calcite related to the fading pumpellyite-prehnite facies (alteration stage II). It occurs mainly in veins, only seldom in amygdules.

The luminescence of trace elements in calcite was used to detect any kind of zonations (Denniston et al. 1997, Wogelius et al., 1997). Calcite from the main mining area with native copper (**Fig. 9/A**) shows no zonation. The sample from G7 (Ahmeek profile) shows two generations (**Fig. 9/B**), whereas the samples from the Copper Harbor profile (**Fig. 9/C and 9/D**) show up to seven generations. But calcite from the Copper Harbor profile adjacent to native copper shows only two different zones (**Fig. 9/E**). Three types of native copper occurrence in calcite are observed. In the main mining area precipitation is characterized by proceeding corrosion. Droplets of native copper are found along early secondary fluid inclusion planes without any relation to the cleavage (**Fig. 10A**). Type 2 of native copper precipitation is the sheet-like native copper, along cleavages or fractures is more common (**Fig. 10B**). For type 3 observations from the Copper Harbor profile show that the native copper does not corrode the calcite surface, rather the native copper precipitates as pustules on the surface of calcite (**Fig. 11**).

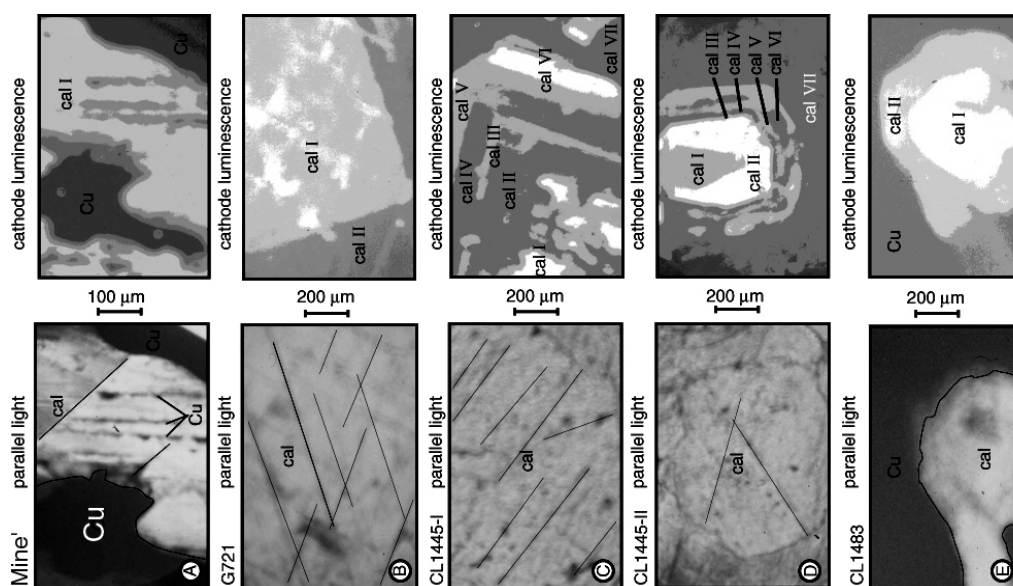


**Figure 9:** Light microscope images (left) and cathode luminescence images (right) of calcite. A) Mine sample (Southwest of the three drill core profiles) showing no zonation. Darker gray lines in calcite of the right image indicate the site of the native copper. B) Sample from drill core G7 of the Ahmeek profile showing two generations of calcite. C, D) Sample from drill core CL14 of the Copper Harbor profile, showing up to seven different calcite zones. E) Sample from drill core CL14 of Copper Harbor profile with only two generations of calcite and native copper.

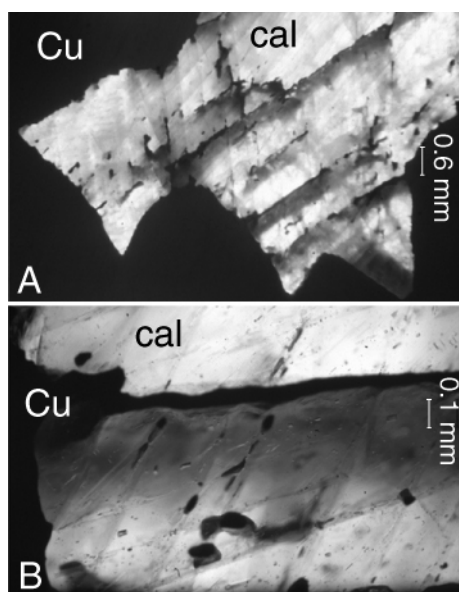


**Figure 10:** Native copper in calcite; sample: KP Mine (A1C), A) Overview, B) Detail – Note: native copper planes are not parallel to the mineral cleavage.

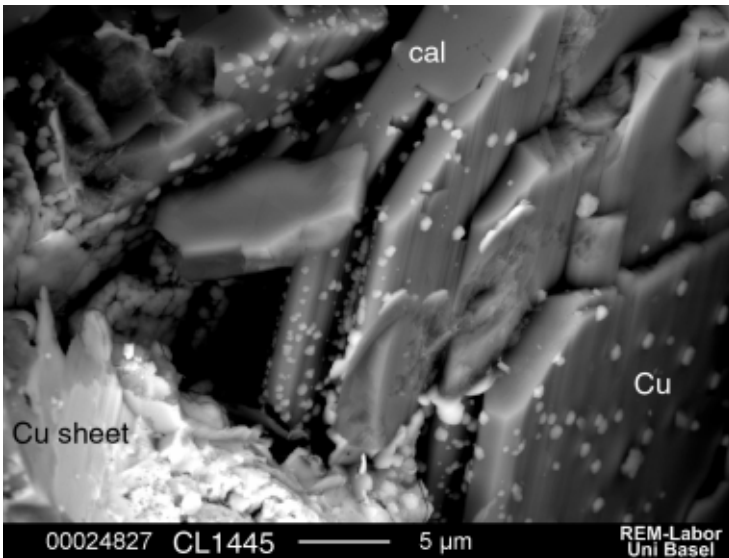


**Figure 11:** SEM image of calcite with non-corrosive native copper occurrence, sample: CL1445.

### Shape of native copper inclusions

Two types of native copper inclusions are found in all different samples, namely sub rounded droplets or copper-wire-like structures (**Fig. 12**). No fluid inclusions could be found within the native copper.

### **Fluid inclusion results**

Fluid inclusions are abundant in the secondary minerals such as quartz, calcite and epidote. Apparently, little research has been done on fluid inclusions (Stoiber and Davidson, 1959; and Livnat, 1983). It is beyond the scope of this chapter to display an entire fluid inclusion data-set of the alteration minerals in the PLV. Instead this study describes the fluids, which might be closest related to the precipitation of the native copper and therefore the alteration stage II (See also chapter III).

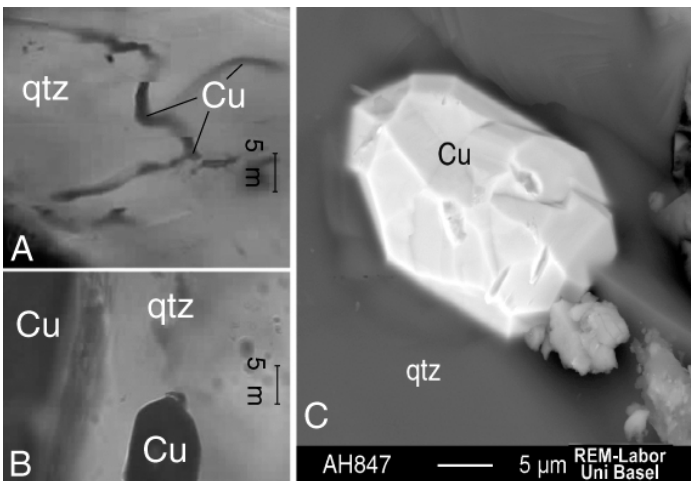


**Figure 12:** Native copper inclusions in quartz of the mine samples (A & B); (microscopical studies) and C) in conglomerate matrix cement of sample AH847 (C) SEM image).

Table 2: Fluid inclusion population data

Profile	Location	HR	pop	HM / gen	fis [ $\mu\text{m}$ ]	gas [V %]	T <sub>1MP</sub> [°C]	T <sub>MP</sub> [°C]	T <sub>hom</sub> [°C]	NaCl <sub>equ</sub> [w %]	n
Mine	MineKP	FT	1	qtz I/II / cal II	19 3/30	9 3/30	-19 -23.3/-11	-0.8 -2.7/-0.1	177 151/285	1.4 0.2/4.5	48
	CalMine	FT	1	qtz I/II	30	14 4/40	-16.5 -17/-11	-1 -1.8/-1.0	266 122/352	1.8 0.2/3	17
Ahmeek	S10	FT	1	qtz II / cal II	9	4.5	-66 -68/-65	-15 -16/-14	100 99/101	18.8 17.9/19.8	3
Ahmeek	S10	FT	2	qtz II / cal II	25 11/40	6 4/8	-54 -57/-50	-6 -10/-1	143 102/237	8.8 1.6/14	34
Ahmeek	AH8	FT	1	qtz II / cal II	6	5.5 4/7	-62 -65/-59	-19.3 -28/-10.4	157 56/206	23 14/30	42
Ahmeek	AH8	FT	2	qtz II / cal II	N.D.	5 4/7	-59	-4 -8/-0.5	91 78/104	6 0.4/12	10
Ahmeek	G7	TZ	1	qtz I / cal II	6 6/6	3.5	-70	-20 -23/-17	78 63/87	24 20.4/30	3
Ahmeek	G7	TZ	2	qtz I / cal II	5.5 5/6	3.5	-69 -81/-53	-6 -11/-2	81 60/104	8.6 3.4/15	16
Copper Harbor	CL14	TZ	1	qtz II / cal II	N.D.	3	-76 -87/-71	-32 -44/-23	52 31/66	> 24	31
Copper Harbor	CL14	TZ	2	qtz II / cal II	7/44	3	-55	-1.7 -2.6/-0.5	65 48/77	2.8 0.4/4.3	12
Copper Harbor	ST7	TZ	1	qtz II / cal II	16 7/30	5	-77 -79/-74	-44 -45/-43	60 46/69	> 24	15
Copper Harbor	ST7	TZ	2	qtz II / cal II	19 17/20	5 4/6	-82	-11 -16/-5	167 149/204	14.6 8.1/19.8	19

Profile: area where the sample came from; Location: Mine or drill core; HR: host rock; Pop: fluid inclusion population (1 approx. early; 2 approx. late), HM / gen : host mineral / I, II mineral generation (according to alteration history); fis: fluid inclusion size [ $\mu\text{m}$ ]; first value: mean, values below minimum/maximum values  
gas: size of gas bubble in fluid inclusion [V %], T<sub>1MP</sub>: first melting temperature of ice (eutectic temperature)  
T<sub>MP</sub>: melting of ice phase, T<sub>hom</sub>: homogenization temperature of fluid inclusions, (liquid + vapor= liquid), NaCl<sub>equ</sub>: NaCl equivalents [w %] (after Potter et al. 1977); n: number of studied fluid inclusions

### Description of the fluid inclusions of the Ahmeek and Copper Harbor profile (*table 2*)

Two fluid inclusion populations are significant in the upper part of the Copper Harbor profile in drill core CL14, and are found in quartz and calcite of alteration stage II. A first population of high salinity (>24 wt% NaCl equivalents (NaCl<sub>eq</sub>)), low gas content and with a few inclusions of daughter minerals of unknown material occurs mainly in quartz of alteration stage II, which is cut by several fluid inclusion trails (**Fig. 13**).

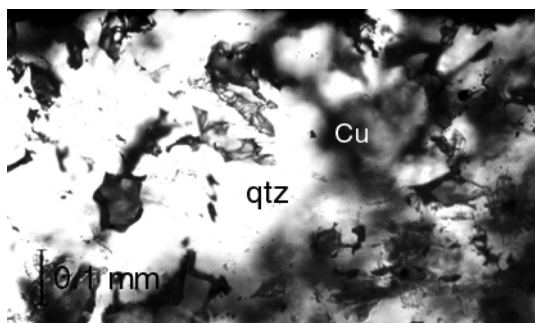


**Figure 13:** Fluid inclusions of population one and two in quartz. Populations are only distinguished based on the melting temperature of ice. The black areas indicate ore precipitation in healed cut bands, sample; S1037.

Calcite sometimes shows fluid inclusions with negative crystal shapes (**Fig. 14**). A later secondary population shows lower salinity (2.8 wt% NaCl<sub>equ</sub>). Both fluids can be described as syn- to post-copper precipitation. The homogenization temperatures ( $T_{\text{hom}}$ ) of both fluid inclusion populations are very low. Their mean values are 52°C in population 1 and 65°C in population 2. The first fluid inclusion population often shows healing structures where irregular native copper flakes are left on healing bands adjacent to still gas- and fluid-filled inclusions.

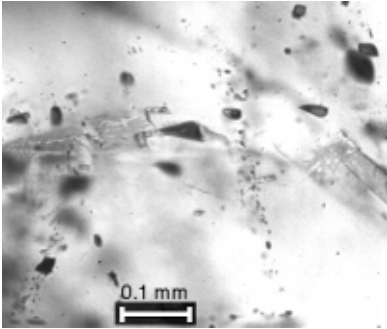


**Figure 14:** Fluid inclusions in calcite, mostly low saline inclusions, sample S1037.

In the upper part of the most western Ahmeek profile in drill core S10, calcite and quartz from alteration stage II, show similar fluid inclusion populations as described above. Fluid inclusions of population 1 were observed and measured more often in calcite (stage II). The high saline fluids with 18.8 wt% NaCl<sub>equ</sub> in population 1 more often show well healed fluid inclusion shapes, sometimes with daughter minerals, whereas the lower salinity fluids of population 2 with 9 wt% NaCl<sub>equ</sub> occur in irregularly formed fluid inclusions. The homogenization temperature of population 2 (143°C in mean) is significantly higher than those of population 1 (100°C). Because of the enormous scattering of the  $T_{\text{hom}}$  in population 2 it is assumed that calcite could have been stretched during healing. Fluid inclusions in calcite of the third, final alteration stage show hardly any salinity, which means they are late fluid inclusions, postdating the copper precipitation. (These fluids are not reported in table 2 because of low data density and without any relation to the native copper precipitation.) In section C (compare Chapter 1 – Introduction) of the Ahmeek profile in drill core AH8 similar fluid inclusions to those described above are observed in quartz and calcite of alteration stage II. Quartz of stage II shows fluid inclusions in irregular shapes along cut bands. The same can be seen in calcite. Fluid inclusions in quartz contain some rare non-isotropic daughter minerals and can be necked down. Calcite of alteration stage III shows less, but better healed inclusions. Salinity of fluid inclusion population 1 is 23 wt% and that of population 2 is 6 wt% NaCl<sub>equ</sub>. Population 1 shows homogenization temperatures around 157°C and population 2 around 91°C.

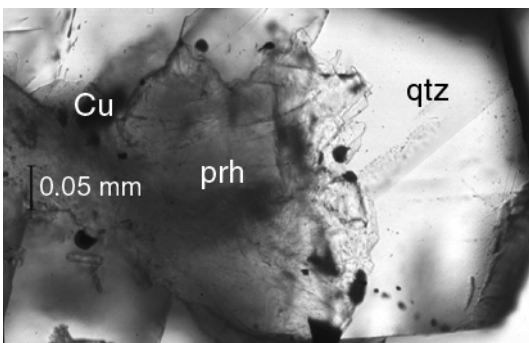


**Figure 15:** Native copper inclusions in prehnite and quartz, sample: ST721.

The fluid inclusions observed in drill core G7 of section C of the Ahmeek profile are in contrast to the described above located in quartz of the first alteration stage, no quartz of second alteration stage could be observed. But the studied fluid inclusions are also observed in calcite of the second alteration stage.

The both minerals contain fluid inclusions of high salinity in population 1 (24 wt%  $\text{NaCl}_{\text{equ}}$ ) and lower salinity in population 2 (8.6 wt%  $\text{NaCl}_{\text{equ}}$ ). No native copper flakes could be observed. The mean values of the homogenization temperature are low, with 78°C in population 1 and 81°C in population 2. In contrast the fluid inclusions in quartz and calcite of alteration stage II of the Copper Harbor profile of section C in drill ST7 show two fluid inclusion populations with markedly different salinity: Population 1 with > 24 wt%  $\text{NaCl}_{\text{equ}}$  and population 2 with 14.6 wt%  $\text{NaCl}_{\text{equ}}$ . Their homogenization temperatures are 60°C in the 1<sup>st</sup> fluid inclusion population and much higher in the 2<sup>nd</sup> population with a mean of 167°C. The same samples show prehnite beside quartz and two types of copper precipitation (**Fig. 15**). A precipitation after corrosion of the prehnite and the precipitation of native copper inclusions on healed fluid bands in quartz.

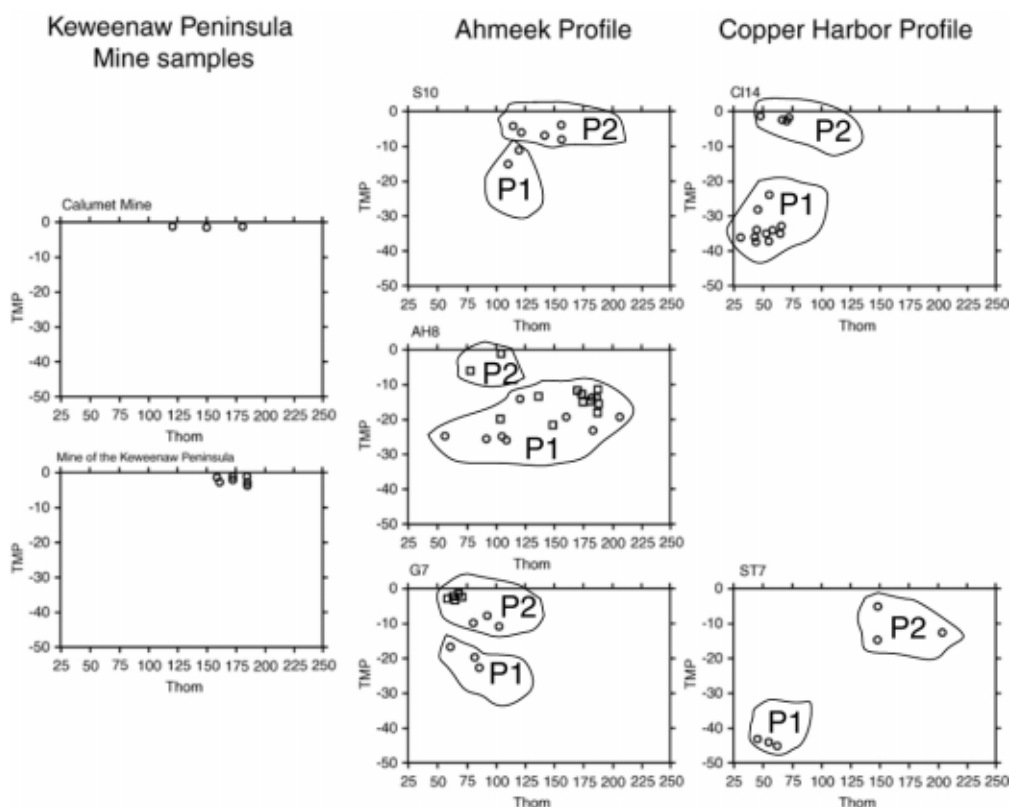


**Figure 16:** Plot of TMP (temperature of the melting point of ice) versus Thom (homogenization temperature), to distinguish characteristic populations (P1, P2) and to get an approx. overview of the distribution over the Keweenaw Peninsula. Quartz and calcite are not distinguished, because the different fluid inclusion populations are often found in both minerals. The fluid inclusions of the mine samples do not indicate any populations. The numbers ‘1’ and ‘2’ of the populations do not indicate a relative age.

The fluid inclusion studies of material from the Ahmeek profile and the Copper Harbor profile reveal certain similarities. In **figure 16** it is shown that in the different drill cores two distinct populations can be distinguished. The populations are found in calcite as well as in quartz of the second alteration stage (except quartz of drill core of G7). The fluid inclusions described in **table 2** as first population, show a very low melting temperature ( $T_{\text{MP}}$ ) of  $-32$  and  $-44$ °C in the drill core samples of Copper Harbor profile. This corresponds to a very high salinity of approximately > 24 wt%  $\text{NaCl}$  equivalents. In contrary to that the first populations in the Ahmeek profile do not display such a well defined first



population. They have low melting temperatures and the salinity ranges from 18 to 24 wt%. Population 2 in the Ahmeek profile samples is similar to other observed populations of the Copper Harbor profile but has a relative low salinity of 3 to 15 wt% NaCl<sub>equ</sub>.

### Fluid inclusions of the Mine Samples:

The paragenesis of the available mine sample is different from the drill core profiles. The fluid inclusions are studied in quartz of an early alteration stage, which is indicated by the lack of any prehnite or pumpellyite minerals quartz is growing directly on epidote. Calcite is considered to be a product of the second alteration stage, while growing on the prismatic quartz of stage I. The populations and the native copper is observed in both minerals, indicating syn or post calcite native copper precipitation. The studied fluid inclusions of the mine samples are much better shaped than those described in the drill core samples. **Figure 16** and **table 2** display, that either the fluid inclusion history in the main mining areas has been completely different from that of the drill core samples, or that it was just not possible to detect any measurable fluid inclusions of high salinity. Only low salinity fluid inclusions of 1.4 to 1.8 wt% NaCl equivalents could be determined. The much bigger gas bubbles, up to 40 v%, and high homogenization temperatures of 177 and 266°C (range 122 – 352°C) indicate that there must have existed boiling conditions (**Fig. 17**).

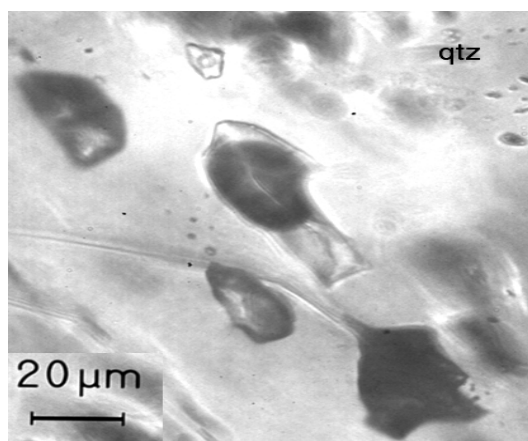


**Figure 17:** Fluid inclusions in a mine sample. The big gas bubbles indicate a boiling of the fluid during entrapment.

As described above, the borderlines between native copper/ prehnite, -/quartz, -/calcite indicate at least three repeated events of corrosion and precipitation of quartz or calcite prior to native copper precipitation. During this study it was not possible, to measure fluids in these zones, because they are too tiny (< 1 µm) and cannot be resolved with the best magnification available.

Unfortunately, even with the improved optical microscopic equipment, we were not able to detect or measure the ultimate native copper fluid. New techniques allow measuring fluid inclusions in non-translucent material such as hematite. Even by applying this new technique at the University of Geneva, it was not possible to observe any fluid inclusion in the native copper ore of the available sample material.

## **Discussion/Interpretation**

The host rock of the native copper ore deposits, the PLV and the interflow sediments underwent a low-grade metamorphic alteration as evidenced by secondary alteration minerals such as pumpellyite, prehnite and laumontite (e.g. Stoiber and Davidson, 1959; Jolly and Smith, 1972; and Livnat, 1983).

Due to still unknown processes and incidents in the PLV, rich native copper deposits formed (Broderick, 1931). According to Chapter 3, the alteration history of the PLV can be divided into three stages. Only two stages can be distinguished using the stable isotope signatures. In the following interpretation of the obtained fluid inclusion data, the results are discussed and interpreted on the hypothesis of the three stages alteration model (**Fig. 18, see also chapter III**). Stage II could also be considered as the waning of the main alteration stage I, which is responsible for the low-grade metamorphic prehnite-pumpellyite facies of the PLV.

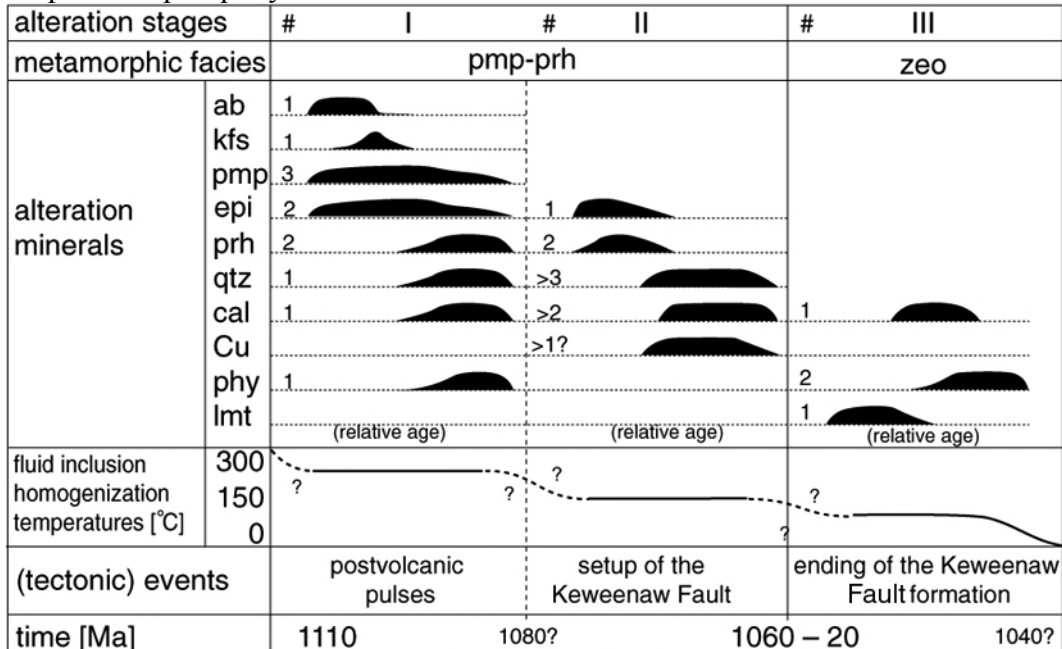


**Figure 18:** Native copper in context with the secondary alteration mineral assemblage and tectonic history of the PLV on the Keweenaw Peninsula. (Time scale and tectonic events after Cannon, 1989; and Bornhorst, 1997) Abbreviations see Table 1; # indicates pulses of mineral growth observed in one stage. The dashed line between stage I and II refers to the discussion of the existence of an independent second stage.

#### Comparison of fluid inclusion data of the PLV

The fluid inclusion study did not reveal a unique native copper fluid but most of the problems that Livnat (1983) reported from his samples could not be confirmed. For example necking down does occur, but not in all samples of this study. A major problem of comparing the obtained fluid inclusion data of this study with those from Stoiber and Davidson (1959) and Livnat (1983) is that those authors didn't distinguish any mineral generations or alteration stages. Nevertheless it is assumed that they studied material adjacent to native copper ore occurrence. Their data sets are probably incomplete compared to studies of today. Both studies do not report any melting temperatures or NaCl-equivalents (Potter et al., 1977; Mullis, 1987). Therefore their reported data could not be differentiated and compared to the fluid inclusion populations as described in this study.

Stoiber and Davidson (1959) reported data from personal communication of D. H. Richter. The obtained homogenization temperatures from 295-360°C (\*) in quartz are, compared to those from Livnat (1983) of 200°C and to data from mine samples of this study, with 40-100°C higher in the mine area. (\* Similar data are expected but not measured in quartz shown in **Fig. 7**, because these fluid inclusion populations are situated in early quartz and not correlated to the copper precipitation.)

Compared to the obtained data of the drill core samples (**Table 2**) the temperatures of the mine samples, according to Stoiber and Davidson (1959) and/or Livnat (1983), are up to 250°C higher, indicating different conditions towards the Keweenaw Peninsula Tip.

Fluid inclusions from calcite of the above mentioned mine samples of the three data sources (Stoiber and Davidson, 1959; Livnat, 1983; this study) are within an overlapping range of 60 to 160°C. Fluid inclusion data of the drill core profiles are within this same range as well. One possible interpretation is that similar conditions of a late hydrothermal system in the PLV affect the whole Keweenaw Peninsula in a late alteration stage. This hypothesis could also be confirmed by the macroscopical and microscopical observations concerning the superimposed late stage (stage III) of the low-grade metamorphic zeolite facies. Here laumontite is observed on late crosscutting veins, which occurs in all samples of the three drill core profiles. No mine samples with that superimposed zeolite facies were available for study during this thesis.

### Native copper precipitation scenarios

The SEM-, BSE- and optical- images give some new input to the discussion about the development of the native copper ore deposits in the PLV of the Keweenaw Peninsula north east of the former main mining area, but cannot give a solution for the native copper precipitation.

The different fluid inclusion populations of this study support the fluid mixing process (Livnat, 1983; Bornhorst, 1997) often discussed for the drill core profiles.

For the mines it can only be assumed because no evidence has been found so far. For both sites some characteristics of the fluid inclusions are similar. The corrosive character of the fluids could be observed in e.g. ST7, where the prehnite shows corrosion (**Fig. 3**), but also in the mine samples (**Fig. 8**) where quartz is corroded.

The light prehnite rims in contact with native copper and quartz in ST7 are probably caused by a reaction, which is not related to the initial growth of the prehnite (stage I), as shown in **figure 2**. The prehnite in **figure 2a**) shows a lighter gray than the prehnite being not in direct contact with native copper and quartz, and **2b**) displays a sharp contact between the two chemically distinct zones. In the mine samples, no prehnite was observed, but up to three corrosion and precipitation events of quartz and calcite can be distinguished before the precipitation of native copper finally takes place.

The alteration system in the PLV can be regarded as a pulsing system of varying intensity. In calcite (**Fig. 9**) the observed differences between the mine samples (no zonation), and the drill core profiles (up to seven growth-zones) suggest that the conditions where more copper precipitated can be assumed as more constant than the conditions further northeast towards the Keweenaw Tip where less copper occurs.

Another scenario of precipitation is described by observations like those in **figure 6 and 17**. The native copper bodies, surrounded by drop-like native copper bodies, suggest the hypothesis of a fast and quick precipitation event caused, probably, by mixing of fluids of different temperatures, salinity, pH or boiling of the fluids. This model assumes a buildup of pressure beneath blockages in veins caused by precipitation of secondary minerals (e.g. quartz). The rapid expulsion of the near-critical fluids and mixing with overlying ground waters would provide ideal conditions for the precipitation of the native copper (Hedenquist and Henley, 1985b; Nelson and Giles, 1985). This scenario seems to be possible on a small scale, but the fact that there exist native copper masses of several meters in diameter (Wilson and Dyl, 1992) suggests that also long-time pulses or several pulses must have occurred. The model of boiling causing copper precipitation can not be invoked with the absolute certainty because the observed vapor-enriched fluid inclusions predate the copper formation and no boiling indicating fluid inclusions were detected within **figure 6**.

Quartz and native copper are also reported from the scarcely studied conglomerate samples suggesting fast and powerful events because of the occurrence finely distributed rock powder (**Fig. 4**). Richards and Spooner (1989) suggest from Mamainse Point, Canada, that brecciated rocks in veins with quartz-matrix indicate explosive hydraulic activities which were important for the formation of the ore deposits. This could also be valid for the PLV.

Almost all the SEM-, BSE-images suggest, that corrosion precedes the native copper precipitation. Occasionally native copper bodies form on the surfaces of euhedral calcite planes, which suggests a different, minor, maybe bacterially controlled precipitation (**Fig. 10**).

Looking at the melting temperature of the measured fluid inclusions of the drill core samples, an infiltration of a saline fluid from the northeast can be assumed. The relative proportion of the  $\text{NaCl}_{\text{equ}}$  from the Copper Harbor decrease towards the Ahmeek profile (**Fig. 16 and table 2**). The rich native copper ore deposits of the Hancock-Houghton area (e.g. Butler and Burbank, 1929) outline, that there must have been also other sources of high saline fluids, which were able to transport native copper in solution (e.g. Fernekcs, 1907).

As could be shown with the cathode luminescence (**Fig. 9**), there exist up to seven zones of calcite. Therefore, the stable isotope data from calcite and quartz need to be used with precaution and be interpreted as a bulk analysis of multiple pulses during one alteration stage. In **figure 19** the homogenization temperature of the available quartz and calcite and the measured isotope composition are used to calculate the composition of the fluid in equilibrium with the respective mineral. (For temperatures evidence see Chapter 3.) It can be shown that a mixing of meteoric and metamorphic waters is a likely explanation for the native copper precipitation. This result agrees with Livnat (1983) in terms of fluid mixing and confirms the hypothesis of Bornhorst (1997).

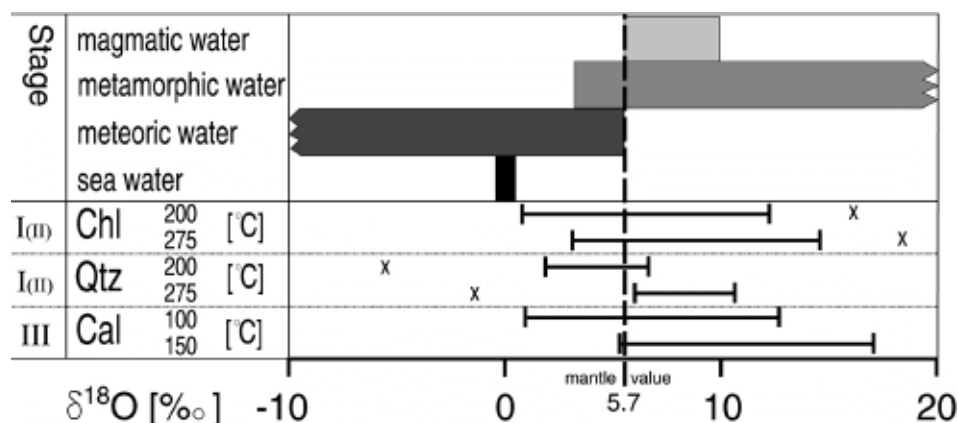


**Figure 19:** Different water types of  $\delta^{18}\text{O}$  fluid reservoir compared with data from this study. Stage indicates the alteration stage in which the mineral grew (I, III likely, (II) less likely). (Data from Taylor, 1974; Onuma et al., 1972; Sheppard, 1977; Graham and Harro, 1983; and Hoefs, 1987; after an idea of Rollinson, 1993).

#### Comparison of different copper mine sites, from the south shore of Lake Superior

The native copper deposits from the Keweenaw Peninsula are not unique in this area. The White Pine Mine, for instance, is located about 100 km in the south west of the Houghton-Calumet main mining area. The copper bearing layer is the Nonesuch-Shale containing 1-3% copper sulfides. Above this formation some native copper flakes are reported in conglomerates (Mauk et al.; 1992a, b).

Furthermore, some minor copper deposits are located at Mamainse Point 200 km to the southeast in

Canada, where the copper is found in the continuation of the PLV. Native copper is here reported from quartz veins in rocks with the same alteration assemblage as observed on the Keweenaw Peninsula (R. J. Rupert, 1976, unpubl. rept., out of Richardson and Spooner, 1989).

The copper mineralisation of the Keweenaw Peninsula is often discussed in connection with the sulfur and minor native copper mineralisation of the White Pine Mine. Arehart (1990) carried out stable isotope work on the native copper ore. From inter-metallic water, he obtained values for  $\delta D$  varying from  $-55$  to  $-45\text{‰}$  and for  $\delta^{18}O$  varying from  $-12$  to  $-6\text{‰}$ . Additionally, stable oxygen data from Mamainse Pointe are available. Values of quartz  $\delta^{18}O$  range from 2.5 to 10.7‰, and calcite has values from  $-6.9$  to 4.8‰ (Richards and Spooner, 1989). These values show no correlation with the obtained values from the PLV on the Keweenaw Peninsula. The  $\delta^{18}O$  data of the quartz of stage II from the Keweenaw Peninsula shows values from 13.8 to 18.3‰ and for calcite from 17.7 to 19. ‰. It could be inferred that the development of the native copper ore deposits in the PLV on the Keweenaw Peninsula has its own unique development history.

In spite of the above observation, the literature reports similar formation ages. Bornhorst (1988) used the Rb-Sr method on amygdule-filling microcline, calcite, epidote and chlorite calculating a mineralisation age of 1060 and  $1047 \pm 20$  Ma. In comparison with **figure 18** this displays an overview age, maybe of the whole very low-grade metamorphic alteration history. For White Pine Ruiz (1984) obtained an age of  $1040 \pm 20$  Ma. Therefore similar formation ages can be assumed.

Still, a genetic very low-grade metamorphic link between the Coppercrop Mine from Mamainse Point and the Keweenaw Peninsula may exist. Richards and Spooner (1989) observed, in their proposed 4<sup>th</sup> stage, a gangue mineralisation of native copper, quartz, calcite and chlorite which is similar to the 2<sup>nd</sup> stage of the very low-grade metamorphic alteration history in the PLV. This could be a hint that the conditions in the Lake Superior area were similar in a wide regional area over a long time span. No explanation was found so far, where the heat and fluid source of this system was located.

## Conclusions

The fluid inclusion results of the studied profile samples indicate that most of the observed native copper deposits were precipitated while two different fluid inclusion populations - a) a high saline and b) a low saline fluid – were mixed. This is different from the mine samples, where only a low saline fluid could be observed. The homogenization temperatures of the mine samples are high (177-266°C), compared to the bulk average of the fluid inclusions of the drill core samples (52-167°C; (225°C)), which could indicate different native copper precipitation conditions.

Fluid mixing was already suggested by Livnat (1983) who also proposed seawater input to the system. This was not confirmed by the data of this study. The stable isotope work of Chapter 3 supports mixing of fluids of meteoric and metamorphic signatures (magmatic origin is also not excluded).

The native copper ore deposits observed in the sample material are embedded, based on microscopical studies, between stage II and III of the low-grade metamorphic alteration history of the PLV in the Keweenaw Peninsula.

The copper ore introducing fluid generally shows a corrosive character. In the mines mainly quartz and/or calcite of early alteration stage are corroded, whereas in the drill core samples prehnite shows corrosion. Therefore the proposed best-fit-model is: High saline brines bring dissolved copper and corrode quartz, calcite and/or prehnite. Meteoric waters mix with the ore bearing fluids and precipitate native copper, quartz and calcite. The meteoric fluids were until now not documented.

In the drill core samples only small-scale observations are possible. Some of these pulses display powerful fast events, in other samples there must have been several pulses because of the big size of

native copper ore deposits. Other mechanisms of copper precipitation are also possible. SEM-images of euhedral calcite cleavage indicate a late and minor copper precipitation possibly controlled by bacteriological activity, an assumption which is highly speculative for Precambrian rocks and needs further investigations.

**For references see part 7 of this thesis.**

## Conclusions

The scope of this study was to reinvestigate the proposed vertical metamorphic zonation in the Portage Lake Volcanics, to generate a model how the alteration could have taken place and to understand where the alteration fluids might have been derived from. Based on the data of the three drill core profiles it could be shown that there exists no vertical stratigraphic zonation as proposed by Jolly and Smith (1972). Livnat (1983) also showed a non-stratigraphic zonation. His data suggested an alteration plane, which dips at a shallower angle than the today's dipping of the PLV. In contrast, this study suggests a discontinuous distribution of the pumpellyite-prehnite facies index minerals throughout the entire studied area.

Quantitatively, pumpellyite-prehnite assemblages are more dominant and frequent towards the SW or the main mining area. Superimposed on the prehnite-pumpellyite facies is a zeolite facies occurring in cross cutting veins.

A three stages alteration model of the PLV is postulated. In addition, the main alteration stages themselves are subdivided in different pulses as evidenced from microscopical study, electron microscope analysis, fluid inclusion studies and cathode luminescence. Alteration minerals like quartz, pumpellyite and calcite show major zonations from two up to seven zones. The first and third stages are distinguishable by variations in the  $\delta^{18}\text{O}$  values: epidote, clinocllore and quartz show  $\delta^{18}\text{O}$  values between 5 – 15‰, while calcite of the third stage gives a range between 20 – 30‰  $\delta^{18}\text{O}$ .

The stable isotope and fluid inclusion data indicate fluid mixing of a metamorphic- and meteoric-water, as already postulated by Livnat (1983). No indicators for seawater input as suggested by Livnat (1983) could be found.

The investigation of alteration minerals in the different units of the PLV revealed that the growth of the low-grade metamorphic minerals was strictly controlled by fluid/rock interaction and thus by the permeability of the surrounding rocks. In permeable rocks such as flow tops, alteration minerals like epidote, pumpellyite and prehnite are abundant. In non-permeable rocks such as massive flow interiors and in zones with non-connected small (<2 mm) amygdules phyllosilicates are the dominant minerals of initial alteration.

According to several authors (e.g. Kristmánsdóttir, 1979; Schiffman and Fridleifsson, 1991) phyllosilicates can be considered as indicator of relative grade in the low-grade metamorphic facies. Phyllosilicates are the dominant minerals in the PLV. In the Ahmeek profile, where pumpellyite-prehnite assemblages are more frequent, two distinct populations of phyllosilicates developed (chlorites and mixed-layered phyllosilicates). In contrast the Copper Harbor profile contains a continuous population of phyllosilicates (chlorite-corrensite-mixed-layered phyllosilicates) that developed in rocks with less abundant prehnite-pumpellyite assemblages.

The fluid inclusion studies revealed two main fluid inclusion populations, which are considered to be related to the event of native copper precipitation. In the Copper Harbor

profile, the populations show a high saline ( $> 24$  wt%  $\text{NaCl}_{\text{equivalents}}$ ) and a low saline ( $\leq 10$  wt%  $\text{NaCl}_{\text{equivalents}}$ ) population, respectively. Towards the southwest, the differences between the fluid populations vanish. In the studied mine samples, no populations could be distinguished.

The mineral assemblages in which the native copper ore is located in the profiles and in the mine samples are different. In the mine samples, corrosive fluids dissolved and precipitated quartz of the first alteration stage and calcite of the second alteration stage up to three times, before the native copper precipitation occurred. The gangue minerals of the available mine samples are epidote (stage I) and quartz (stage I), whereas in the drill core profiles, copper is mostly related to a gangue mineralisation with prehnite (stage II). This suggests changes in the physico-chemical conditions such as changes in the composition of the fluid, temperature or even a difference in time might be possible. This study might not have included representative mine samples, because prehnite is reported as well as a common gangue mineral in some mines (Butler and Burbank, 1929).

In the studied drill core where only minor occasional copper precipitation occurred, two main types of native copper emplacements could be observed. The first type was likely precipitated as a result of a short powerful, hydrothermal process such as a pressure release, which is indicated by native copper droplets in vein quartz and in quartz cement of the conglomerates. The second type was formed as native copper sheets along calcite cleavage or on euhedral crystal faces. In contrast to the typical mine samples, the drill core samples do not show signs of corrosion.

The three stages model of the low-grade metamorphic evolution in the PLV shows different flow infiltration regimes:

- During the first stage, the fluids mainly circulated along strike in the flow tops and interbedded sediments, flowing from SW to NE, with a heat source in the SW. This is outlined, by the relatively more abundant prehnite-pumpellyite occurrence in the Ahmeek profile, and in early fluid inclusions of quartz (G7).
- During the second stage at least two fluid sources existed based on the fluid inclusion data. In the studied profiles, the pulses from the high saline fluids originated from the NE, as evidenced by a decrease of fluid inclusion salinity towards the SW. Because of the rich native copper deposits in the SW of the three profiles, an additional second source of fluid is needed.
- In a third stage a low-grade metamorphic zeolite facies is superimposed over the whole studied area, and is found on cross cutting veins. It is not clear where the fluids are derived from.



## Open questions

The analysis of fine-grained, volatile – containing minerals brought the available technical equipment to their limits. A main question remains: whether the correlation of distant profiles 10 to 50 km apart, is feasible, based on mineral studies in  $\mu\text{m}$  or even nm scale – problems of dimensionality will remain. In addition we still do not know well enough the processes of fluid flow and precipitation in minerals in rock. Although we have learned a lot in the last decades, we still have to understand what parameters (pressure, temperature, main and trace elements in the rock, elements in the fluid or reaction kinetics) are involved in the formation of secondary minerals, and what their respective importance is.

## Outlook

Further interesting projects in the PLV of the Keweenaw Peninsula derive from the following problems:

- Studying the fluid inclusions with respect to the native copper inclusions will help to determine the number of fluid inclusion generations and populations and their differences along strike. This will enable solving the question where the fluids (geographically) originated, if there have been more than two sources of fluids, and along which pathway they traveled along.
- Laser supported stable isotope measurements may help revealing why there are up to seven zones in calcite within the Eagle Harbor profile, and why there are only two zones in samples related to native copper of the main mining area.
- The phyllosilicates hold the potential for further investigation. The obtained X-ray diffractograms of this study show usually very well-shaped clinoclone peaks. A similar study in Chile (Belmar, 2000) was done in an area of similar low-grade metamorphic facies. But here the diffractograms of the phyllosilicates show less well-shaped peaks. What influences, beside temperature and variation in permeability, the formation of phyllosilicates?
- The investigations of native copper inclusions with the help of the SEM raises the question how the native ores precipitate within the veins. What are the mechanisms of the emplacements of the native copper – pressure release, temperature drop? Are the copper droplets common in other world deposits?



## **General Reference**

- Alt J. C., 1999, Hydrothermal alteration and mineralization of oceanic crust; mineralogy, geochemistry, and processes, *in* Barrie-C. T., and Hannington M. D., eds., *Reviews in Economic Geology: Volcanic-associated massive sulfide deposits; processes and examples in modern and ancient settings: Socorro, NM, United States*, Society of Economic Geologists, p. 133-155.
- Arehart G. B., O'Neil J. R., and Mauk J. L., 1990, Stable isotope compositions of fluid inclusions in native copper from White Pine, Michigan, *in* Annual Meeting, Dallas, Texas, v. 22, p. 251.
- Behnke D., 1983, Copper Country Microminerals: Mineral Record, v. 14, no. 4, p. 219-226.
- Belmar M., 2000, Low-grade metamorphism in Central Chile at 35° S [Ph.D. thesis]: Basel University.
- Bettison L. A., and Schiffman P., 1988, Compositional and structural variations of phyllosilicates from the Point Sal ophiolite, California: *American Mineralogist*, v. 73, p. 62-76.
- Bornhorst Th. J., 1997, Tectonic context of native copper deposits of the North American Midcontinent Rift System: Geological Society of America, no. Special Paper 312.
- Bornhorst Th. J., Paces J. B., Grant N. K., Obradovich J. D., and Huber N. K., 1988, Age of native copper mineralisation, Keweenaw Peninsula, Michigan: *Economic Geology*, v. 83, p. 619-625.
- Broderick T. M., 1929, Zoning in the Michigan copper deposits and its significance: *Economic Geology*, v. 24, p. 149-162, 311-326.
- Broderick T. M., 1931, Fissure vein and lode relations in Michigan copper deposits: *Economic Geology*, v. 41, p. 675-725.
- Broderick T. M., 1946, Recent contributions to the geology of the Michigan copper district: *Economic Geology*, v. 41, p. 675-725.
- Butler B. S., and Burbank W. S., 1929, The copper deposits of Michigan: US Geological Survey Professional Paper, v. 144, p. 238.
- Cannon W. F., 1989, The North American Midcontinent Rift beneath Lake Superior from GLIMPCE seismic reflection profiling: *Tectonics*, v. 8, p. 305-332.
- Cannon W. F., 1994, Closing of the Midcontinent rift - a far-field effect of Grenvillian compression: *Geology*, v. 22, p. 155-158.
- Cannon W. F., and Hinze W. J., 1992, Speculations on the origin of the North American Midcontinent Rift: *Tectonophysics*, v. 213, p. 49-55.
- Cannon W. F., and McGervey T. A., 1991, Map showing mineral deposits of the Midcontinent Rift, Lake Superior region, United States and Canada: U.S. Geological Survey, scale 1:500 000.
- Cannon W. F., Peterman Z. E., and Sims P. K., 1993, Crustal-scale thrusting and origin of the Montreal River monocline-A 35-km-thick cross section of the Midcontinent Rift in northern Michigan and Wisconsin: *Tectonics*, v. 12, p. 728-744.
- Cathelineau M., 1988, Cation site occupation in Chlorites and Illites as a Function of Temperature: *Clay Minerals*, v. 23, p. 471-485.
- Cathelineau M., and Nieva M., 1985, A chlorite solid solution geothermometer The Los Azufres (Mexico) geothermal system: *Contributions to Mineralogy and Petrology*, v. 91, p. 235-244.
- Clayton R. N., and Mayeda T. K., 1963, The use of bromine pentafluoride in the extraction of oxygen from oxides and silicates for isotopic analysis.: *Geochimica et Cosmochimica Acta*, v. 27, p. 43-52.

- Clayton R. N., O'Neil J. R., and Mayeda T. K., 1972, Oxygen isotope exchange between quartz and water: *Journal of Geophysical Research*, v. 77, p. 3057-3067.
- Cole D. R., 1985, A preliminary evaluation of oxygen isotopic exchange between chlorite-water., *in Geological Society of America Annual Meeting, Orlando FL*, v. 17.
- Cole D. R., Mottl M. J., and Ohmoto H., 1987, Isotopic exchange in mineral-fluid systems. II. Oxygen and hydrogen isotopic investigations of the experimental basalt-seawater system: *Geochimica et Cosmochimica Acta*, v. 51, p. 1523-1538.
- Coombs D. S., 1971, Present status of the zeolite facies, *in Society, A. C., ed., Molecular Sieve Zeolites - Advances in Chemistry Series*, p. 312-327.
- Coombs D. S., Ellis A. J., Fyfe W. S., and Taylor A. M., 1959, The zeolite facies, with comments on the interpretation of hydrothermal synthesis: *Geochimica et Cosmochimica Acta*, v. 17, p. 53-107.
- Cornwall H. R., 1951a, Differentiation in lavas of the keweenaw series and the origin of the copper deposits of Michigan: *Bulletin of the Geological Society of America*, v. 62, p. 159-202.
- Cornwall H. R., 1951b, Differentiation in magmas of the keweenaw series: *Journal of Geology*, v. 59, p. 151-172.
- Cornwall H. R., 1951c, Ilmenite, magnetite, hematite and copper in lavas of the keweenaw series: *Bulletin of the Geological Society of America*, v. 46, p. 51-67.
- Dalla Torre M., Livi K. J. T., and Frey M., 1996, Chlorite textures and compositions from high-pressure/low-temperature metashales and metagraywackes, Franciscan Complex, Diablo Range, California, USA: *European Journal of Mineralogy*, v. 8, p. 825-846.
- Davis D. W., and Paces J. B., 1990, Time resolution of geologic events on the Keweenaw Peninsula and implications for development of the Midcontinent Rift System: *Earth and Planetary Science Letters*, v. 97, p. 54-64.
- de Caritat P., Hutcheon I., and Walshe J. L., 1993, Chlorite geothermometry: a review.: *Clays and Clay Minerals*, v. 41, p. 219-239.
- Denniston R. F., Shearer C. K., Layne G. D., and Vaniman D. T., 1997, SIMS analyses of minor and trace element distribution in fracture calcite from Yucca Mountain, Nevada, USA: *Geochimica et Cosmochimica Acta*, v. 61, no. 9, p. 1803-1818.
- Epstein S., 1970, Antarctic ice sheet: stable isotope analysis of Byrd Station covers and interhemispheric climatic implications.: *Science*, v. 168, p. 570-572.
- Epstein S., Sharp R. P., and Gow A. J., 1965, Six year record of hydrogen and oxygen isotope variations in South Pole fur.: *Journal of Geophysical Research*, v. 70, p. 1809-1814.
- Essene E. J., and Peacor D. R., 1995, Clay mineral thermometry - a critical perspective.: *Clays and Clay Minerals*, v. 43, p. 540-553.
- Fernekes G., 1907, Precipitation of copper from chlorite solution by means of ferrous chlorite: *Economic Geology*, v. 2, p. 580-584.
- Frey M., and Robinson D., 1999, *Low-grade Metamorphism*: Oxford, UK.
- Frey M. ed., 1987, *Low Temperature Metamorphism*: Glasgow, Blakie and Son Ltd.
- Graham C. M., and Harmon R. S., 1983, Stable isotope evidence on the nature of crust-mantle interactions, *in Hawkesworth C. J., and Norry M. J., eds., Continental basalts and mantle xenoliths.*: Natwich, Shiva, p. 20-45.
- Grimes J. G., 1977, *Geochemistry and petrology of Keweenaw Rhyolithes and associated rocks, Portage Lake Volcanics, Michigan.* [unpubl. MS thesis]: Michigan Technological University.

- Handschin R. G., and Stern W. B., 1992, Crystallographic Lattice Refinement of Human Bone: Calcified Tissue International, v. 51, p. 111-120.
- Hedenquist J. W., and Henley R. W., 1985, Hydrothermal eruptions in the Waiotapu geothermal system, New Zealand: Their origin, associated breccias, and relation to precious metal mineralization: Economic Geology, v. 80, p. 1640-1668.
- Hillier S., and Velde B., 1991, Octahedral occupancy and the chemical composition of diagenetic (low-temperature) chlorites: Clay Minerals, v. 26, p. 149-168.
- Hinze W. J., Braile L. W., and Chandler V. W., 1990, A geophysical profile of the southern Margin of the Midcontinent Rift System in western Lake Superior: Tectonics, v. 9, p. 303-310.
- Hoefs J., 1987, Stable isotope geochemistry: Berlin, Springer-Verlag.
- Hoffman P. F., 1989, Precambrian geology and tectonic history of North America, in Bally A. W., and Palmer A. R., eds., The Geology of North America-An overview: Boulder, Colorado, Geological Society of America, p. 447-512.
- Hutchinson D. R., White R. S., Cannon W. F., and Schulz K. J., 1990, Keweenaw hot spot: Geophysical evidence for a 1.1 Ga mantle plume beneath the Midcontinent Rift System.: Journal of Geophysical Research, v. 95, p. 10.869 - 10.884.
- Jahren J. S., 1991, Evidence of Ostwald ripening related recrystallization of diagenetic chlorites from reservoir rocks offshore Norway.: Clay Minerals, v. 26, p. 169-178.
- Jahren J. S., and Aagaard P., 1992, Diagenetic illite-chlorite assemblages in arenites. I. Chemical evolution.: Clays and Clay Minerals, v. 40, p. 540-546.
- Jiang W. T., Peacor D. R., Merriman R. J., and Roberts B., 1990, Transmission and analytical electron microscopic study of mixed-layer illite/ smectite formed as an apparent replacement product of diagenetic illite: Clays and Clay Minerals, v. 38, no. 5, p. 449-468.
- Jolly W. T., 1972, Degradation (Hydration) - Aggradation (Dehydration) and Low-Rank Metamorphism of Mafic Volcanic Sequences, in 24th IGC.
- Jolly W. T., 1974, Behavior of Cu, Zn and Ni during prehnite - pumpellyite rank metamorphism of the Keweenaw basalts, northern Michigan: Economic Geology, v. 69, p. 1118-1125.
- Jolly W. T., and Smith R. E., 1972, Degradation and Metamorphic Differentiation of the Keweenawan Tholeiitic Lavas of Northern Michigan, U.S.A.: Journal of Petrology, v. 13, p. 273-309.
- Kretz R., 1983, Symbols for rock-forming minerals: American Mineralogist, v. 68, p. 277-279.
- Kristmannsdottir H., 1979, Alteration of basaltic rocks by hydrothermal activity at 100-300°C.: Developments in Sedimentology, v. 27, p. 359-367.
- Lindsley D. H., Smith D., and Haggerty S. E., 1971, Petrography and mineral chemistry of a differentiated flow of Picture Gorge Basalt near Spray, Oregon., Carneg Instit Wash Yearbook, p. 264-285.
- Liou J. G., Kim H. S., and Maruyama S., 1983, Prehnite - epidote equilibria and their petrologic applications: Journal of Petrology, v. 24, p. 321-341.
- Lippmann F., 1956, Clay minerals from the Roet member of the Triassic near Goettingen, Germany: Journal of Sedimentary Petrology, v. 26, p. 125-139.
- Livnat A., 1983, Metamorphism and copper mineralisation of the Portage Lake Lava series, northern Michigan. [dissertation thesis]: University of Michigan.
- Longo A. A., 1983, A geochemical correlation of a Precambrian flood basalt: the Greenstone Flow, Upper Michigan [abstr.]: Eos Trans Am Geophys Union, v. 64, p. 888.

- Longo A. A., 1984, A correlation for a middle Keweenaw flood basalt: The Greenstone Flow, Isle Royale and Keweenaw Peninsula, Michigan. [unpubl. MS thesis]: Mich. Technical University.
- Longstaffe F. J., 1987, Chapter 6. An introduction to stable oxygen and hydrogen isotopes and their uses as fluid tracers in sedimentary systems, *in* Kyser T. K., ed., *Stable isotope geochemistry of low temperature processes*: Toronto, ON, Canada,, Mineralogical Association of Canada, p. 115-121.
- Matrin-Vivaldi J. L., and MacEwan D. M. C., 1960, Corrensite and swelling chlorite: *Clay Mineralogical Bulletin*, v. 4, p. 173-181.
- Mauk J. L., Brown A. C., Seasor R. W., and Eldridge C. S., 1992a, Geology and stable isotope and organic geochemistry of the white Pine sediment-hosted stratiform copper deposit, *in* Geologists, S. o. E., ed., *Guidebook Series*, p. 63-98.
- Mauk J. L., Kelly W. C., van der Pluijm B. A., and Seasor R. W., 1992b, Relations between deformation and sediment-hosted copper mineralisation: Evidence from the White Pine portion of the Midcontinent Rift system: *Geology*, v. 20, p. 427-430.
- Merk G. P., and Jirsa M. A., 1982, Provenance and tectonic significance of the Keweenaw interflow sedimentary rocks: *Geological Society of America*, v. 156, p. 97-105.
- Merriman R. J., and Peacor D. R., 1999, Very low-grade metapelites: mineralogy, microfabrics and measuring reaction progress, *in* Frey M., and Robinson D., eds., *Low-Grade Metamorphism*: Oxford, UK, p. 10-60.
- Morimoto N., 1988, Nomenclature of pyroxenes: *Mineralogical Magazine*, v. 52, p. 535-550.
- Mullis J., 1987, Fluid inclusion studies during very low grade metamorphism, *in* Frey, M., et al., ed., *Low temperature metamorphism*: Glasgow, Blackie, p. 162-199.
- Nelson C. E., and Giles D. L., 1985, Hydrothermal eruption mechanisms and hot spring gold deposits: *Economic Geology*, v. 50, p. 1633-1639.
- Nicholson S. W., 1987, Stratigraphic and geochemical characteristics of rhyolites associated with the Portage Lake Lava Series, Keweenaw Peninsula, northern Michigan [abstr.], *in* North Central, North Central, v. 19, p. 236.
- O'Neil J. R., 1986, Theoretical and Experimental aspects of isotopic fractionation, *in* Valley J. W., Taylor H. R. jr., and O'Neil J. R., eds., *Stable Isotopes in high temperature geological processes*: Blacksburg, Virginia, USA,, Mineralogical Society of America, p. 1-37.
- O'Neil J. R., Clayton R. N., and Mayeda T. K., 1969, Oxygen isotopic fractionation in divalent metal carbonates: *Journal of Chemical Physics*, v. 51, p. 5547-5558.
- Onuma N., Clayton R. N., and Mayeda T. K., 1972, Oxygen isotope cosmothemometer: *Geochimica et Cosmochimica Acta*, v. 36, p. 169-188.
- Paces J. B., 1988, Magmatic processes, evolution and mantle source characteristics contributing to the petrogenesis of the Midcontinent Rift basalts: Portage Lake Volcanics, Keweenaw Peninsula, Michigan [Ph.D. thesis]: Michigan Technological University, 413 p.
- Paces J. B., and Miller J. D. Jr., 1993, Precise U-Pb ages of Duluth Complex and related mafic intrusions, northeastern Minnesota: Geochronological insights to physical, petrogenetic, paleomagnetic and tectomagnetic processes associated with the 1.1 Ga Midcontinent Rift System: *Journal of Geophysical Research*, v. 98, p. 13997-14013.
- Palache C., and Vassar H. E., 1925, Some minerals of the Keweenaw copper deposits: *American Mineralogist*, v. 10, p. 412-418.
- Park Y. R., and Ripley E. M., 1998, Hydrothermal flow systems in the Midcontinent Rift: Oxygen and Hydrogen Isotopic Studies of the North Shore Volcanic Group and Related Hypabyssal Sills, Minnesota: *Geochimica et Cosmochimica Acta*, v. 63, p. 1787-1804.

- Potel S., 2001, Very low-grade metamorphism of northern New Caledonia [Ph.D. thesis]: Basel University.
- Potter R. W., Babcock R. S., and Brown D. L., 1977, A new method for determining the solubility of salts in aqueous solutions at elevated temperatures: US Geological survey Journal of Research, v. 5, p. 389-395.
- Pumpelly R., 1871, The paragenesis and derivation of copper and its associates on Lake Superior: American Journal of Science, v. 2, no. 3rd Ser., p. 188-98; 243-58; 347-55.
- Rath G. vom, 1878, Einige krystallographische Beobachtungen am kupfer vom Oberen See.: Zeitschrift fuer Kristallographie und Mineralogie, v. 2, p. 169-173.
- Richards J. P., and Spooner E. T. C., 1989, Evidence for Cu-(Ag) Mineralization by Magmatic-Meteoric Fluid Mixing in Keweenaw Fissure Veins, Mamainse Point, Ontario.: Economic Geology, v. 84, p. 360-385.
- Ripley E. M., Butler B. K., and Taib N. I., 1992, Effects of devolatilization of the hydrogen isotopic composition of pelitic rocks in the contact aureole of the Duluth Complex, northeastern Minnesota.: Chemical Geology, v. 102, p. 185-197.
- Robinson D., and Zamora De A. S., 1999, The smectite to chlorite transition in the Chipilapa geothermal system, El Salvador: American Mineralogist, v. 84, p. 607-619.
- Roedder E., 1963, Studies of fluid inclusions II: Freezing data and their interpretation.: Economic Geology, v. 58, p. 167-211.
- Rollinson H. R., 1993, Using geochemical data: evaluation, presentation, interpretation: Essex, Addison Wesley Longman Limited.
- Rose A. W., 1976, The effects of cuprous chloride complexes in the origin of Red-Bed Copper and related deposits.: Economic Geology, v. 71, p. 1036-1048.
- Rosenbaum J., and Sheppard S.M.F., 1986, An isotopic study of siderites, dolomites, and ankerites at high temperatures.: Geochimica et Cosmochimica Acta, v. 50, p. 1147-1150.
- Ruiz J., Jones L. M., and Kelly W. C., 1984, Rubidium-strontium dating of ore deposits hosted by Rb-rich rocks using calcite and other common Sr-bearing minerals: Geology, v. 12, p. 259-262.
- Schiffman P., and Fridleifsson G. O., 1991, The smectite-chlorite transition in drillhole NJ-15, Nesjavellir geothermal field, Iceland: XRD, BSE and electron microprobe investigations: Journal of Metamorphic Geology, v. 9, p. 679-696.
- Schiffman P., and Liou J. G., 1980, Synthesis and stability relations of Mg-pumpellyite: Journal of Petrology, v. 21, p. 441-474.
- Schiffman P., and Staudigel H., 1995, The smectite to chlorite transition in a fossil seamount hydrothermal system: the Basement Complex of La Palma, Canary Islands: Journal of Metamorphic Geology, v. 13, p. 487-498.
- Schmidt D., Schmidt S. Th., Mullis J., Ferreira Maehlmann R., and Frey M., 1997, Very low grade metamorphism of the Taveyanne formation of western Switzerland: Contributions to Mineralogy and Petrology, v. 129, p. 385-403.
- Schmidt S. Th., 1990, Alteration under conditions of burial metamorphism in the North Shore Volcanic Group, Minnesota - Mineralogical and geochemical zonation: Heidelberger Geowissenschaftliche Abhandlungen, v. 41, p. XIV+309.
- Schmidt S. Th., 1993, Regional and local patterns of low-grade metamorphism in the North Shore Volcanic Group, Minnesota, USA: Journal of Metamorphic Geology, v. 11, p. 401-414.
- Schmidt S. Th., and Robinson D., 1997, Metamorphic grade and porosity and permeability controls on mafic phyllosilicate distributions in a regional zeolite to greenschist facies



- transition of the North Shore Volcanic Group, Minnesota: Geological Society of America Bulletin, v. 6, p. 683-697.
- Shau Y. H., and Peacor D. R., 1992, Phyllosilicates in hydrothermally altered basalts from DSDP Hole 504B, Leg83: A TEM and AEM study: Contributions to Mineralogy and Petrology, v. 112, p. 119-133.
- Sheppard S. M. F., 1977, The Cornubian batholith, SW England: D/H and 18O/16O studies of kaolinite and other alteration minerals: Journal of Geological Sciences, v. 133, p. 573-591.
- Stoiber R. E., and Davidson E. S., 1959a, Amygdule Mineral Zoning In The Portage Lake Lava Series, Michigan Copper District; Part II: Economic Geology, v. 54, p. 1444-1460.
- Stoiber R. E., and Davidson E. S., 1959b, Amygdule Mineral Zoning In The Portage Lake Lava Series, Michigan Copper District; Part I: Economic Geology, p. 1250-1277.
- Taylor H. P. jr., 1974, The application of oxygen and hydrogen isotope studies to problems of hydrothermal alteration and ore deposits.: Economic Geology, v. 69, p. 843-883.
- Taylor H. P. jr., 1979, Oxygen and hydrogen isotope relationships in hydrothermal mineral deposits., Geochemistry of Hydrothermal Ore Deposits: New York, Wiley Interscience, 236-277 p.
- Troeger W. E., 1982, Optische Bestimmung der Gesteinsbildenden Minerale: Stuttgart, E.Schweizerbart'sche Verlagsbuchhandlung.
- Vennemann T. W., and O'Neil J. R., 1993, A simple and inexpensive method of hydrogen isotope and water analyses of minerals and rocks based on zinc reagent.: Chemical Geology, v. 103, p. 227-234.
- Wang H., Frey M., and Stern W. B., 1996, Diagenesis and metamorphism of clay minerals in the Helvetic Alps of Eastern Switzerland: Clays and Clay minerals, v. 44, p. 96-112.
- Weege R. J., 1988, The Keweenawan diamond drill core library: private report MTU,.
- Weege R. J., and Pollack J. O., 1971, Recent developments in native copper district of Michigan, *in* Field Conference, Michigan Copper District, p. 18-43.
- White W. S., 1952, Imbrication and initial dip in a Keweenawan conglomerate bed: Journal of Sedimentary Petrology, v. 22, p. 189-199.
- White W. S., 1968, The native copper deposits of northern Michigan, *in* Ridge, J. D., ed., Ore deposits of the United States, 1933-1967 (the Graton Sales volume): New York, American Institute of Mining, Metallurgical and Petroleum Engineering, p. 303-325.
- White W. S., 1971, Geological settings of the Michigan Copper District, *in* Field conference, Michigan Copper District, p. 3-17.
- Wilson M. L., and Dyl St. J., 1992, The Michigan copper country: Mineral Record, v. 23, no. 2, p. 4-16 and 24-76.
- Wogelius R. A., Fraser D. G., Wall G. R. T., and Grime G. W., 1997, Trace element and isotopic zonation in vein calcite from the Mendip Hills, UK, with spatial-process correlation analysis: Geochimica et Cosmochimica Acta, v. 61, no. 10, p. 2037-2051.
- Woodruff L.G., Daines M.J., Cannon W.F., and Nicholson S.W., 1995, The thermal history of the Midcontinent Rift in the Lake Superior Region: implications for mineralization and partial melting., *in* International Geological Correlation Program, Field Conference and Symposium on the Petrology and metallogeny of volcanic and intrusive rocks of the mid Continent rift system, Duluth, Minnesota, v. 336, p. 213-214.

**Appendix A: EMPA data**

## Entire EMPA data from epidote

Mineral Sample	epi C8902	epi C8902	epi C8902	epi C8902	epi C8902	epi C8907A	epi C8907A	epi C8907A	epi C8907A	epi C8907B	epi C8907B
SiO2	35.84	35.89	36.87	35.81	35.51	37.69	36.95	36.22	36.91	36.54	37.18
TiO2	0.00	0.00	0.00	0.00	0.00	0.00	0.00	0.00	0.00	0.00	0.00
Al2O3	16.98	17.78	22.43	17.79	18.16	21.10	19.28	18.28	18.42	17.23	20.85
Cr2O3	0.00	0.00	0.00	0.00	0.00	0.00	0.00	0.00	0.00	0.00	0.00
FeO	18.04	16.33	11.04	17.56	16.63	13.17	14.14	15.56	16.11	16.49	13.11
MnO	0.00	0.08	0.67	0.00	0.00	0.80	0.16	0.12	0.00	0.05	0.81
MgO	0.00	0.00	0.00	0.00	0.00	0.00	0.07	0.00	0.00	0.00	0.00
CaO	22.12	22.02	22.45	22.53	21.71	21.69	21.82	21.67	22.33	21.96	21.63
Na2O	0.00	0.01	0.00	0.02	0.00	0.03	0.00	0.02	0.03	0.00	0.00
K2O	0.08	0.00	0.01	0.01	0.00	0.00	0.03	0.01	0.00	0.05	0.09
TOTAL	93.06	92.11	93.47	93.72	92.01	94.48	92.45	91.88	93.80	92.32	93.67
Si	3.03	3.05	3.04	3.00	3.02	3.08	3.09	3.07	3.07	3.09	3.07
Altotal	1.69	1.78	2.18	1.76	1.82	2.03	1.90	1.82	1.80	1.72	2.03
Fetotal	1.27	1.16	0.76	1.23	1.18	0.90	0.99	1.10	1.12	1.17	0.90
Ti	0.00	0.00	0.00	0.00	0.00	0.00	0.00	0.00	0.00	0.00	0.00
Mn	0.00	0.01	0.05	0.00	0.00	0.06	0.01	0.01	0.00	0.00	0.06
Mg	0.00	0.00	0.00	0.00	0.00	0.00	0.01	0.00	0.00	0.00	0.00
Ca	2.00	2.00	1.98	2.02	1.97	1.90	1.96	1.97	1.99	1.99	1.91
Na	0.00	0.00	0.00	0.00	0.00	0.00	0.00	0.00	0.00	0.00	0.00
K	0.01	0.00	0.00	0.00	0.00	0.00	0.00	0.00	0.00	0.01	0.01
Total	8.00	7.99	8.00	8.01	7.99	7.96	7.96	7.97	7.98	7.97	7.97
O=12.5	12.50	12.50	12.50	12.50	12.50	12.50	12.50	12.50	12.50	12.50	12.50

Mineral Sample	epi C8907B	epi C8907C	epi C8907C	epi C8907C	epi C8907C	epi D5614	epi D5614	epi D5714	epi D5714	epi D5714	epi D5742V	B
SiO2	36.77	36.08	36.17	36.87	36.32	36.28	37.14	36.18	36.25	37.00	37.05	
TiO2	0.00	0.00	0.00	0.00	0.00	0.00	0.00	0.00	0.00	0.00	0.00	0.00
Al2O3	19.22	17.47	17.55	22.37	18.11	19.35	23.09	19.62	20.64	22.73	19.18	
Cr2O3	0.00	0.00	0.00	0.00	0.00	0.00	0.00	0.00	0.00	0.00	0.00	0.00
FeO	14.88	17.14	17.86	11.55	16.49	14.22	10.76	14.82	13.93	10.02	14.98	
MnO	0.15	0.02	0.07	0.74	0.04	0.07	0.13	0.12	0.16	0.07	0.00	
MgO	0.00	0.00	0.00	0.00	0.00	0.45	0.05	0.38	0.55	0.04	0.04	
CaO	22.31	21.64	22.01	21.41	22.29	21.44	22.18	22.55	22.88	23.81	23.69	
Na2O	0.02	0.02	0.00	0.00	0.00	0.00	0.09	0.01	0.00	0.01	0.05	
K2O	0.07	0.04	0.07	0.03	0.02	0.01	0.03	0.00	0.00	0.03	0.00	
TOTAL	93.42	92.41	93.73	92.97	93.27	91.82	93.47	93.68	94.41	93.71	94.99	
Si	3.06	3.05	3.03	3.05	3.04	3.06	3.04	3.01	2.98	3.04	3.04	
Altotal	1.88	1.74	1.73	2.18	1.79	1.92	2.23	1.92	2.00	2.20	1.85	
Fetotal	1.03	1.21	1.25	0.80	1.15	1.00	0.74	1.03	0.96	0.69	1.03	
Ti	0.00	0.00	0.00	0.00	0.00	0.00	0.00	0.00	0.00	0.00	0.00	
Mn	0.01	0.00	0.00	0.05	0.00	0.00	0.01	0.01	0.01	0.00	0.00	
Mg	0.00	0.00	0.00	0.00	0.00	0.06	0.01	0.05	0.07	0.00	0.00	
Ca	1.99	1.96	1.97	1.89	2.00	1.94	1.95	2.01	2.02	2.09	2.08	
Na	0.00	0.00	0.00	0.00	0.00	0.00	0.01	0.00	0.00	0.00	0.01	
K	0.01	0.00	0.01	0.00	0.00	0.00	0.00	0.00	0.00	0.00	0.00	
Total	7.99	7.97	7.99	7.97	7.99	7.98	7.98	8.02	8.04	8.03	8.02	
O=12.5	12.50	12.50	12.50	12.50	12.50	12.50	12.50	12.50	12.50	12.50	12.50	

## Entire EMPA data from epidote, continuation:

Mineral Sample	epi EH0409B	epi EH0426/I	epi EH0426/I	epi EH0426/I	epi EH0426/I
SiO2	36.13	38.52	37.04	38.23	37.35
TiO2	0.17	0.00	0.00	0.00	0.00
Al2O3	20.18	23.64	17.68	23.67	18.59
Cr2O3	0.00	0.00	0.00	0.00	0.00
FeO	17.89	9.74	15.98	9.42	15.75
MnO	0.01	0.05	0.02	0.39	0.01
MgO	0.00	0.02	0.00	0.00	0.00
CaO	21.29	22.97	22.64	22.35	22.79
Na2O	0.00	0.00	0.00	0.00	0.01
K2O	0.05	0.02	0.02	0.00	0.00
TOTAL	95.72	94.96	93.38	94.06	94.50
Si	2.94	3.09	3.09	3.10	3.08
Altotal	1.94	2.24	1.74	2.26	1.80
Fetotal	1.22	0.65	1.12	0.64	1.08
Ti	0.01	0.00	0.00	0.00	0.00
Mn	0.00	0.00	0.00	0.03	0.00
Mg	0.00	0.00	0.00	0.00	0.00
Ca	1.86	1.97	2.03	1.94	2.01
Na	0.00	0.00	0.00	0.00	0.00
K	0.01	0.00	0.00	0.00	0.00
Total	7.97	7.96	7.98	7.96	7.98
O=12.5	12.50	12.50	12.50	12.50	12.50

## Titanite EMPA data

Mineral Sample	ttn C8938	ttn C8940B	ttn EH0409B	ttn EH0409B	ttn EH0409B	ttn EH0409B	ttn EH0409B	ttn EH0409B
SiO <sub>2</sub>	30.69	29.89	31.19	32.45	27.75	30.51	30.21	26.45
TiO <sub>2</sub>	29.99	35.01	23.69	26.68	33.12	22.58	27.96	28.08
Al <sub>2</sub> O <sub>3</sub>	2.77	2.99	7.05	3.91	4.87	6.20	4.09	3.35
FeO	3.67	2.84	8.46	3.81	9.25	10.66	3.49	3.75
MnO	0.00	0.00	0.15	0.11	0.14	0.01	0.00	0.09
MgO	0.63	0.00	3.13	2.29	0.00	4.55	1.13	0.28
CaO	25.95	27.13	20.27	25.07	22.33	19.82	25.74	24.10
Na <sub>2</sub> O	0.11	0.03	0.03	0.18	0.33	0.03	0.05	0.03
K <sub>2</sub> O	0.05	0.01	0.10	0.18	0.03	0.13	0.03	0.02
total	93.86	97.90	94.07	94.68	97.82	94.49	92.70	86.15
Si	1.04	0.98	1.03	1.07	0.92	1.00	1.03	0.98
Ti	0.76	0.87	0.59	0.66	0.82	0.55	0.71	0.78
Al	0.11	0.12	0.27	0.15	0.19	0.24	0.16	0.15
Fe <sup>3+</sup>	0.10	0.08	0.23	0.10	0.26	0.29	0.10	0.12
Mn	0.00	0.00	0.00	0.00	0.00	0.00	0.00	0.00
Mg	0.03	0.00	0.15	0.11	0.00	0.22	0.06	0.02
Ca	0.94	0.96	0.72	0.88	0.79	0.69	0.94	0.96
Na	0.01	0.00	0.00	0.01	0.02	0.00	0.00	0.00
K	0.00	0.00	0.00	0.01	0.00	0.01	0.00	0.00
Σ cations	3.00	3.00	3.00	3.00	3.00	3.00	3.00	3.00

Mineral Sample	ttn EH0409B	ttn EH0409B	ttn EH0409B	ttn EH0409B	ttn EH0410	ttn EH0410	ttn EH0410	ttn EH0410
SiO <sub>2</sub>	29.83	31.79	31.24	31.10	30.12	30.91	31.03	31.61
TiO <sub>2</sub>	31.06	29.07	27.58	30.15	34.21	28.92	28.79	28.16
Al <sub>2</sub> O <sub>3</sub>	3.89	7.08	6.98	3.86	2.01	5.92	6.07	7.14
FeO	1.27	1.49	1.59	3.02	1.98	1.47	2.29	1.47
MnO	0.00	0.14	0.10	0.09	0.00	0.00	0.00	0.02
MgO	0.00	0.00	0.00	0.00	0.41	0.00	0.54	0.00
CaO	27.34	26.99	27.61	26.85	26.67	27.87	27.30	28.04
Na <sub>2</sub> O	0.01	0.64	0.10	0.11	0.05	0.03	0.02	0.12
K <sub>2</sub> O	0.04	0.00	0.03	0.00	0.03	0.04	0.05	0.06
total	93.44	97.20	95.23	95.18	95.48	95.16	96.09	96.62
Si	1.01	1.02	1.02	1.04	1.01	1.02	1.01	1.02
Ti	0.79	0.70	0.68	0.76	0.87	0.72	0.71	0.68
Al	0.16	0.27	0.27	0.15	0.08	0.23	0.23	0.27
Fe <sup>3+</sup>	0.04	0.04	0.04	0.08	0.06	0.04	0.06	0.04
Mn	0.00	0.00	0.00	0.00	0.00	0.00	0.00	0.00
Mg	0.00	0.00	0.00	0.00	0.02	0.00	0.03	0.00
Ca	1.00	0.93	0.97	0.96	0.96	0.99	0.95	0.97
Na	0.00	0.04	0.01	0.01	0.00	0.00	0.00	0.01
K	0.00	0.00	0.00	0.00	0.00	0.00	0.00	0.00
Σ cations	3.00	3.00	3.00	3.00	3.00	3.00	3.00	3.00

Zeolite EMPA data:

No of anions on basis of 48 oxygen (O, OH) calculated for laumontite formula.

Res Sample	lmt C8922	lmt C8922	lmt C8922	lmt C8922	lmt D5620V	lmt D5620V	lmt D5620V
SiO <sub>2</sub>	52.94	52.94	53.84	54.10	51.83	51.66	51.78
TiO <sub>2</sub>	0.00	0.00	0.00	0.00	0.00	0.00	0.00
Al <sub>2</sub> O <sub>3</sub>	20.87	20.87	20.43	21.06	19.42	19.31	20.18
FeO	0.05	0.05	0.01	0.04	0.00	0.02	0.01
MnO	0.00	0.00	0.02	0.06	0.00	0.00	0.08
MgO	0.00	0.00	0.00	0.00	0.08	0.13	0.06
CaO	10.38	10.38	9.39	9.45	8.55	10.08	9.70
Na <sub>2</sub> O	0.06	0.06	0.18	0.09	0.10	0.03	0.04
K <sub>2</sub> O	0.12	0.12	0.14	0.12	0.30	0.18	0.17
total	84.42	84.42	84.01	84.91	80.29	81.40	82.02
Si	16.17	16.17	16.67	16.40	16.83	16.54	16.50
Ti	0.00	0.00	0.00	0.00	0.00	0.00	0.00
Al	7.51	7.51	7.46	7.52	7.43	7.29	7.58
Fe	0.92	0.92	0.19	0.73	0.00	0.38	0.19
Mn	0.00	0.00	0.01	0.02	0.00	0.00	0.02
Mg	0.00	0.00	0.00	0.00	0.04	0.06	0.03
Ca	3.40	3.40	3.12	3.07	2.97	3.46	3.31
Na	0.07	0.07	0.22	0.11	0.13	0.04	0.05
K	0.09	0.09	0.11	0.09	0.25	0.15	0.14
Σ cations	28.16	28.16	27.76	27.94	27.64	27.91	27.81

## EMPA-data from pyroxene:

Mineral	px	px	px	px	px	px	px	px	px	px	px
Sample	AH8-13	AH8-13	C8913	C8913	C8922	C8922	C8922	C8931	C8940B	CL1125AB	CL1125AB
SiO2	52.13	50.40	49.47	48.76	49.26	47.99	49.16	49.71	49.14	48.21	47.88
TiO2	0.00	0.00	0.00	0.00	0.00	0.00	0.00	1.13	0.00	0.00	0.00
Al2O	1.70	2.59	3.20	2.78	3.60	3.78	2.76	1.29	2.82	1.97	1.29
FeO	7.96	10.19	12.48	11.15	10.54	11.33	12.07	12.45	11.16	13.85	14.97
MgO	16.12	14.92	13.44	13.62	12.36	11.77	12.75	12.74	13.78	12.12	11.04
MnO	0.12	0.33	0.29	0.23	0.26	0.22	0.30	0.42	0.31	0.19	0.27
CaO	18.76	18.38	18.13	18.66	20.15	19.21	19.07	18.61	18.15	18.14	18.46
Na2O	0.29	0.31	0.34	0.33	0.34	0.37	0.27	1.27	0.34	0.25	0.81
K2O	0.03	0.00	0.01	0.01	0.00	0.00	0.00	0.00	0.00	0.01	0.02
Total	97.11	97.12	97.36	95.54	96.51	94.67	96.38	97.62	95.70	94.72	94.75
Al	0.08	0.12	0.15	0.13	0.17	0.18	0.13	0.06	0.13	0.09	0.06
Ti	0.00	0.00	0.00	0.00	0.00	0.00	0.00	0.03	0.00	0.00	0.00
Si	1.97	1.93	1.91	1.92	1.92	1.91	1.92	1.93	1.92	1.94	1.94
Fe	0.25	0.33	0.40	0.37	0.34	0.38	0.40	0.40	0.37	0.47	0.51
Mg	0.91	0.85	0.78	0.80	0.72	0.70	0.74	0.74	0.80	0.73	0.67
Mn	0.00	0.01	0.01	0.01	0.01	0.01	0.01	0.01	0.01	0.01	0.01
Ca	0.76	0.76	0.75	0.79	0.84	0.82	0.80	0.78	0.76	0.78	0.80
Na	0.02	0.02	0.03	0.03	0.03	0.03	0.02	0.10	0.03	0.02	0.06
K	0.00	0.00	0.00	0.00	0.00	0.00	0.00	0.00	0.00	0.00	0.00
Σ cation	4.00	4.02	4.03	4.03	4.01	4.02	4.02	4.05	4.02	4.03	4.06

Mineral	px	px	px	px	Px	px	px	px	px	px
Sample	CL1125AB	D5620V	D5620V	D5620V	Augit	D5714	EH0207	EH0207	EH0214	EH0217
SiO2	41.26	48.23	48.81	40.06	51.16	49.16	49.17	49.29	50.62	49.26
TiO2	0.00	0.00	0.00	0.00	0.00	0.00	1.45	1.48	0.72	1.93
Al2O	0.98	2.62	1.55	6.61	1.55	2.75	1.87	1.60	1.65	3.40
FeO	20.09	12.50	12.92	14.45	10.28	9.25	14.97	16.44	12.48	14.11
MgO	12.42	13.59	13.91	5.94	15.25	14.80	12.74	13.98	12.79	12.60
MnO	0.49	0.33	0.32	0.29	0.09	0.08	0.42	0.33	0.21	0.25
CaO	17.63	16.00	17.75	25.15	19.16	20.28	17.08	14.67	19.69	19.43
Na2O	0.45	0.57	0.27	1.16	0.31	0.28	0.29	0.28	0.33	0.37
K2O	0.00	0.08	0.00	0.04	0.00	0.00	0.00	0.04	0.04	0.02
Total	93.31	93.92	95.53	93.70	97.80	96.60	97.99	98.11	98.53	101.37
Al	0.05	0.12	0.07	0.33	0.07	0.13	0.09	0.07	0.07	0.15
Ti	0.00	0.00	0.00	0.00	0.00	0.00	0.04	0.04	0.02	0.05
Si	1.78	1.93	1.93	1.70	1.95	1.90	1.91	1.91	1.94	1.85
Fe	0.72	0.42	0.43	0.51	0.33	0.30	0.49	0.53	0.40	0.44
Mg	0.80	0.81	0.82	0.38	0.87	0.85	0.74	0.81	0.73	0.71
Mn	0.02	0.01	0.01	0.01	0.00	0.00	0.01	0.01	0.01	0.01
Ca	0.81	0.69	0.75	1.15	0.78	0.84	0.71	0.61	0.81	0.78
Na	0.04	0.04	0.02	0.10	0.02	0.02	0.02	0.02	0.02	0.03
K	0.00	0.00	0.00	0.00	0.00	0.00	0.00	0.00	0.00	0.00
Σ cation	4.22	4.03	4.04	4.18	4.03	4.05	4.01	4.02	4.01	4.03

## EMPA-data from pyroxene, continuation:

Mineral Sample	px EH0217	px EH0217	px EH0222	px EH0401	px EH0401	px EH0401	px EH0401	px EH0409B	px EH0409B	px EH49B
SiO <sub>2</sub>	48.99	48.10	49.22	50.17	50.58	49.62	49.96	51.25	50.47	50.82
TiO <sub>2</sub>	1.47	1.22	0.69	1.27	1.05	0.94	0.78	0.92	1.06	1.01
Al <sub>2</sub> O <sub>3</sub>	3.08	4.47	0.80	3.83	3.75	3.81	2.93	1.92	1.63	2.72
FeO	14.59	13.20	18.26	8.24	7.98	8.47	9.99	13.93	16.00	12.92
MgO	12.33	12.94	12.36	14.95	15.40	15.41	16.03	13.65	12.96	14.22
MnO	0.17	0.15	0.53	0.24	0.11	0.16	0.30	0.39	0.49	0.34
CaO	19.16	19.16	14.81	18.88	19.41	19.13	18.25	17.36	15.86	17.12
Na <sub>2</sub> O	0.36	0.31	0.30	0.35	0.28	0.31	0.30	0.30	0.28	0.28
K <sub>2</sub> O	0.02	0.00	0.02	0.00	0.01	0.00	0.00	0.00	0.10	0.03
Total	100.17	99.55	96.99	97.93	98.57	97.85	98.54	99.72	98.85	99.46
Al	0.14	0.20	0.04	0.17	0.17	0.17	0.13	0.09	0.07	0.12
Ti	0.04	0.04	0.02	0.04	0.03	0.03	0.02	0.03	0.03	0.03
Si	1.87	1.84	1.95	1.89	1.89	1.88	1.89	1.94	1.94	1.92
Fe	0.47	0.42	0.61	0.26	0.25	0.27	0.32	0.44	0.52	0.41
Mg	0.70	0.74	0.73	0.84	0.86	0.87	0.90	0.77	0.74	0.80
Mn	0.01	0.00	0.02	0.01	0.00	0.01	0.01	0.01	0.02	0.01
Ca	0.78	0.78	0.63	0.76	0.78	0.78	0.74	0.70	0.65	0.69
Na	0.03	0.02	0.02	0.03	0.02	0.02	0.02	0.02	0.02	0.02
K	0.00	0.00	0.00	0.00	0.00	0.00	0.00	0.00	0.00	0.00
Σ cation	4.03	4.04	4.02	4.00	4.00	4.02	4.03	4.00	4.00	4.00

Mineral Sample	px EH0409B	px EH0409B	px EH0409B	px EH0409B	px EH0409B	px S1025B	px S1025B	Px S1070V	Px S1070V	Px S1070V	Px S1070V
SiO <sub>2</sub>	50.97	49.98	50.88	48.21	50.16	51.99	50.98	51.34	50.66	50.92	51.28
TiO <sub>2</sub>	1.06	0.74	0.95	1.65	0.92	0.00	0.00	0.00	0.00	0.00	0.00
Al <sub>2</sub> O <sub>3</sub>	1.25	1.53	1.89	2.83	1.52	1.89	2.11	0.47	0.58	0.55	0.56
FeO	11.74	19.14	13.28	13.11	16.15	7.49	10.37	28.63	29.10	29.59	12.78
MgO	14.47	11.83	13.95	13.38	14.69	15.15	15.43	17.41	16.66	16.82	12.61
MnO	0.25	0.58	0.31	0.14	0.43	0.18	0.20	0.40	0.45	0.74	0.43
CaO	18.47	14.93	17.92	18.23	15.25	19.87	18.86	1.65	1.74	1.65	21.49
Na <sub>2</sub> O	0.21	0.26	0.26	0.24	0.30	0.27	0.29	0.02	0.04	0.02	0.21
K <sub>2</sub> O	0.00	0.08	0.05	0.00	0.00	0.00	0.05	0.00	0.02	0.02	0.00
Total	98.42	99.07	99.49	97.79	99.42	96.83	98.29	99.92	99.25	100.30	99.36
Al	0.06	0.07	0.08	0.13	0.07	0.08	0.09	0.02	0.03	0.03	0.03
Ti	0.03	0.02	0.03	0.05	0.03	0.00	0.00	0.00	0.00	0.00	0.00
Si	1.94	1.94	1.93	1.87	1.92	1.98	1.94	1.98	1.98	1.97	1.96
Fe	0.37	0.62	0.42	0.43	0.52	0.24	0.33	0.92	0.95	0.96	0.41
Mg	0.82	0.69	0.79	0.77	0.84	0.86	0.87	1.00	0.97	0.97	0.72
Mn	0.01	0.02	0.01	0.00	0.01	0.01	0.01	0.01	0.01	0.02	0.01
Ca	0.75	0.62	0.73	0.76	0.63	0.81	0.77	0.07	0.07	0.07	0.88
Na	0.02	0.02	0.02	0.02	0.02	0.02	0.02	0.00	0.00	0.00	0.02
K	0.00	0.00	0.00	0.00	0.00	0.00	0.00	0.00	0.00	0.00	0.00
Σ cation	4.01	4.01	4.01	4.03	4.03	3.99	4.03	4.01	4.01	4.02	4.03



## EMPA-feldspar data:

mineral	fsp	fsp	fsp	fsp	fsp	fsp	fsp	fsp	fsp	fsp	fsp
Sample	C8902	C8902	C8902	C8902	C8902	C8906	C8907A	C8907B	C8907B	C8907B	C8907B
SiO2	63.02	64.26	63.37	63.45	63.13	62.72	64.67	63.91	50.55	63.91	64.43
Al2O3	19.26	17.30	17.25	17.47	17.13	17.04	17.36	17.35	13.78	16.98	17.71
FeO	0.27	0.51	0.23	0.14	0.14	0.06	0.02	0.01	0.64	0.00	0.03
MgO	0.95	0.66	0.01	0.03	0.03	0.00	0.01	0.00	0.31	0.01	0.00
MnO	0.00	0.06	0.11	0.01	0.09	0.05	0.06	0.10	0.05	0.05	0.02
CaO	0.73	0.19	0.27	0.13	0.04	0.03	0.04	0.04	0.01	0.00	0.00
Na2O	7.98	0.17	0.07	0.18	0.03	0.05	0.12	0.08	0.13	0.08	0.10
K2O	3.02	10.97	14.53	12.88	16.92	16.83	15.51	16.34	13.98	16.08	14.36
total	95.23	94.12	95.84	94.29	97.51	96.78	97.79	97.83	79.45	97.11	96.65
D=	2.79	2.86	2.88	2.89	2.87	2.89	2.82	2.84	3.55	2.86	2.84
Si	2.93	3.06	3.03	3.05	3.01	3.01	3.04	3.02	2.98	3.04	3.04
Al	1.05	0.97	0.97	0.99	0.96	0.97	0.96	0.97	0.96	0.95	0.99
Fe	0.01	0.02	0.01	0.01	0.01	0.00	0.00	0.00	0.03	0.00	0.00
Mg	0.07	0.05	0.00	0.00	0.00	0.00	0.00	0.00	0.03	0.00	0.00
Mn	0.00	0.00	0.00	0.00	0.00	0.00	0.00	0.00	0.00	0.00	0.00
Ca	0.04	0.01	0.01	0.01	0.00	0.00	0.00	0.00	0.00	0.00	0.00
Na	0.72	0.02	0.01	0.02	0.00	0.00	0.01	0.01	0.01	0.01	0.01
K	0.18	0.67	0.89	0.79	1.03	1.03	0.93	0.99	1.05	0.98	0.86
Σ Ions	4.99	4.79	4.93	4.86	5.02	5.02	4.95	4.99	5.07	4.98	4.90

mineral	fsp	fsp	fsp	fsp	fsp	fsp	fsp	fsp	fsp	fsp	fsp
Sample	C8907C	C8907C	C8907C	C8907C	C8907C	C8922	C8938	C8938	CL1125AB	D5614	D5614
SiO2	61.99	56.08	58.89	63.03	62.95	53.36	66.09	62.15	65.15	62.10	63.13
Al2O3	17.26	15.25	15.82	17.28	17.61	15.51	19.82	17.52	19.20	18.13	17.38
FeO	0.35	0.21	0.18	0.11	0.17	0.72	0.08	0.48	0.07	0.06	0.37
MgO	0.34	0.11	0.00	0.00	0.00	0.92	0.00	0.03	0.03	0.03	0.01
MnO	0.00	0.00	0.00	0.04	0.03	0.00	0.03	0.05	0.00	0.00	0.00
CaO	0.04	0.03	0.03	0.00	0.21	0.15	1.40	0.03	1.38	0.01	0.11
Na2O	0.05	0.02	0.03	0.07	0.06	0.44	10.66	0.17	10.71	0.16	0.12
K2O	17.59	11.35	14.66	17.36	16.30	13.75	0.05	16.04	0.04	17.25	17.52
total	97.62	83.05	89.61	97.89	97.33	84.85	98.13	96.47	96.58	97.74	98.64
D=	2.89	3.28	3.09	2.86	2.86	3.30	2.68	2.89	2.73	2.87	2.85
Si	2.98	3.06	3.03	3.00	3.00	2.93	2.95	2.99	2.96	2.97	2.99
Al	0.98	0.98	0.96	0.97	0.99	1.01	1.04	0.99	1.03	1.02	0.97
Fe	0.01	0.01	0.01	0.00	0.01	0.03	0.00	0.02	0.00	0.00	0.01
Mg	0.02	0.01	0.00	0.00	0.00	0.08	0.00	0.00	0.00	0.00	0.00
Mn	0.00	0.00	0.00	0.00	0.00	0.00	0.00	0.00	0.00	0.00	0.00
Ca	0.00	0.00	0.00	0.00	0.01	0.01	0.07	0.00	0.07	0.00	0.01
Na	0.00	0.00	0.00	0.01	0.01	0.05	0.92	0.02	0.94	0.01	0.01
K	1.08	0.79	0.96	1.06	0.99	0.96	0.00	0.99	0.00	1.05	1.06
Σ Ions	5.08	4.85	4.97	5.04	5.00	5.07	4.99	5.01	5.00	5.06	5.06

## EMPA-feldspar data; continuation:

mineral	fsp	fsp	fsp	fsp	fsp	fsp	fsp	fsp	fsp	fsp	fsp
Sample	D5614	D5614	D5620V	D5620V	D5620V	EH0214	EH0214	EH0222	EH0222	EH0222	EH0401
SiO <sub>2</sub>	64.18	63.71	62.05	63.46	63.46	62.99	64.21	59.28	55.26	60.93	67.08
Al <sub>2</sub> O <sub>3</sub>	17.24	17.64	16.61	16.80	16.80	17.36	17.39	22.77	23.41	23.18	20.06
FeO	0.20	0.36	0.09	0.00	0.00	0.09	0.02	0.68	0.62	0.45	0.23
MgO	0.04	0.01	0.02	0.02	0.02	0.01	0.00	0.02	0.07	0.06	0.06
MnO	0.03	0.01	0.08	0.03	0.03	0.06	0.00	0.02	0.01	0.01	0.07
CaO	0.00	0.04	0.03	0.02	0.02	0.00	0.00	5.41	7.63	3.80	1.13
Na <sub>2</sub> O	0.06	0.12	0.12	0.08	0.08	0.07	0.06	8.23	7.28	5.59	9.99
K <sub>2</sub> O	17.72	17.31	15.12	15.86	15.86	15.40	14.54	0.69	0.42	0.41	0.07
total	99.47	99.20	94.12	96.27	96.27	95.98	96.22	97.10	94.70	94.43	98.69
D=	2.82	2.83	2.94	2.88	2.88	2.88	2.85	2.77	2.86	2.78	2.66
Si	3.01	3.00	3.04	3.04	3.04	3.02	3.05	2.73	2.63	2.82	2.97
Al	0.95	0.98	0.96	0.95	0.95	0.98	0.97	1.24	1.31	1.26	1.05
Fe	0.01	0.01	0.00	0.00	0.00	0.00	0.00	0.03	0.02	0.02	0.01
Mg	0.00	0.00	0.00	0.00	0.00	0.00	0.00	0.00	0.00	0.00	0.00
Mn	0.00	0.00	0.00	0.00	0.00	0.00	0.00	0.00	0.00	0.00	0.00
Ca	0.00	0.00	0.00	0.00	0.00	0.00	0.00	0.27	0.39	0.19	0.05
Na	0.01	0.01	0.01	0.01	0.01	0.01	0.01	0.74	0.67	0.50	0.86
K	1.06	1.04	0.94	0.97	0.97	0.94	0.88	0.04	0.03	0.02	0.00
Σ Ions	5.04	5.04	4.96	4.97	4.97	4.96	4.91	5.04	5.06	4.81	4.94

mineral	fsp	fsp	fsp	fsp	fsp	fsp	fsp	fsp	fsp	fsp	fsp	fsp
Sample	EH0409B	EH0409B	EH0409B	EH0409B	EH0409B	EH0409B	EH0409B	EH0409B	EH0409B	EH0409B	EH0409B	EH0409B
SiO <sub>2</sub>	66.75	64.22	57.58	66.50	66.34	66.48	66.41	56.91	65.93	64.17	65.03	
Al <sub>2</sub> O <sub>3</sub>	18.20	16.47	14.13	17.82	17.20	18.28	19.51	14.39	21.68	17.74	17.47	
FeO	0.73	2.36	3.87	0.36	1.21	1.67	0.63	1.42	1.26	0.45	1.06	
MgO	0.04	3.20	4.73	0.08	1.13	0.16	0.19	0.70	0.10	0.04	0.28	
MnO	0.00	0.00	0.00	0.07	0.03	0.00	0.00	0.00	0.01	0.07	0.00	
CaO	0.09	0.77	0.32	0.06	0.95	0.15	0.27	7.25	0.09	0.00	0.07	
Na <sub>2</sub> O	6.70	8.43	0.10	2.86	9.92	10.15	9.50	0.20	3.06	0.48	0.08	
K <sub>2</sub> O	5.96	0.07	13.09	13.28	0.23	1.82	0.95	12.43	10.70	17.38	17.34	
total	98.47	95.52	93.82	101.03	97.01	98.71	97.46	93.30	102.83	100.33	101.33	
D=	2.72	2.77	3.02	2.73	2.72	2.70	2.70	3.05	2.65	2.80	2.77	
Si	3.02	2.96	2.89	3.02	3.01	2.99	2.98	2.89	2.91	2.99	3.00	
Al	0.97	0.90	0.84	0.95	0.92	0.97	1.03	0.86	1.13	0.97	0.95	
Fe	0.03	0.09	0.16	0.01	0.05	0.06	0.02	0.06	0.05	0.02	0.04	
Mg	0.00	0.22	0.35	0.01	0.08	0.01	0.01	0.05	0.01	0.00	0.02	
Mn	0.00	0.00	0.00	0.00	0.00	0.00	0.00	0.00	0.00	0.00	0.00	
Ca	0.00	0.04	0.02	0.00	0.05	0.01	0.01	0.39	0.00	0.00	0.00	
Na	0.59	0.75	0.01	0.25	0.87	0.88	0.83	0.02	0.26	0.04	0.01	
K	0.34	0.00	0.84	0.77	0.01	0.10	0.05	0.81	0.60	1.03	1.02	
Σ Ions	4.96	4.97	5.11	5.02	4.98	5.02	4.94	5.09	4.96	5.06	5.04	

## EMPA-feldspar data; continuation:

mineral	fsp	fsp	fsp	fsp	fsp	fsp	fsp	fsp	fsp	fsp	fsp
Sample	EH0409B	EH0409B	EH0409B	EH0409B	EH0409B	EH0409B	EH0409B	EH0409B	EH0409B	EH0410	EH0410
SiO <sub>2</sub>	63.36	62.74	62.93	63.71	63.08	64.28	63.17	64.48	64.68	57.13	57.13
Al <sub>2</sub> O <sub>3</sub>	17.06	17.25	17.40	17.18	16.98	20.99	20.96	21.12	20.82	17.09	17.09
FeO	1.15	0.93	0.75	0.58	0.84	0.68	0.56	0.65	0.48	4.20	4.20
MgO	0.52	0.27	0.10	0.44	0.55	0.36	0.08	0.00	0.22	6.20	6.20
MnO	0.06	0.00	0.00	0.00	0.01	0.00	0.00	0.00	0.02	0.08	0.08
CaO	0.05	0.07	0.18	0.12	0.35	0.01	0.04	0.01	0.07	0.29	0.29
Na <sub>2</sub> O	0.18	0.08	0.17	0.98	0.16	0.13	0.17	0.09	0.15	6.54	6.54
K <sub>2</sub> O	16.64	17.17	17.41	16.04	17.11	14.24	13.29	14.41	14.06	0.12	0.12
total	99.02	98.51	98.94	99.05	99.08	100.69	98.27	100.76	100.50	91.65	91.65
D=	2.84	2.86	2.85	2.82	2.84	2.73	2.78	2.73	2.73	2.93	2.93
Si	2.99	2.98	2.98	2.99	2.98	2.92	2.93	2.93	2.94	2.79	2.79
Al	0.95	0.97	0.97	0.95	0.95	1.12	1.14	1.13	1.11	0.98	0.98
Fe	0.05	0.04	0.03	0.02	0.03	0.03	0.02	0.02	0.02	0.17	0.17
Mg	0.04	0.02	0.01	0.03	0.04	0.02	0.01	0.00	0.01	0.45	0.45
Mn	0.00	0.00	0.00	0.00	0.00	0.00	0.00	0.00	0.00	0.00	0.00
Ca	0.00	0.00	0.01	0.01	0.02	0.00	0.00	0.00	0.00	0.02	0.02
Na	0.02	0.01	0.02	0.09	0.01	0.01	0.02	0.01	0.01	0.62	0.62
K	1.00	1.04	1.05	0.96	1.03	0.83	0.79	0.83	0.81	0.01	0.01
Σ Ions	5.04	5.06	5.07	5.06	5.07	4.93	4.90	4.93	4.92	5.04	5.04

mineral	fsp	fsp	fsp	fsp	fsp	fsp	fsp	fsp	fsp	fsp	fsp
Sample	EH0410	EH0410	EH0410	EH0410	EH0410	EH0410	EH0410	EH0410	EH0426/I	EH0426/I	S1025B
SiO <sub>2</sub>	67.34	63.19	66.95	64.20	62.43	62.68	67.92	62.60	64.49	62.05	63.68
Al <sub>2</sub> O <sub>3</sub>	18.93	19.02	18.65	18.31	18.47	17.12	18.62	17.27	17.40	17.92	17.87
FeO	0.39	1.05	0.45	0.66	0.54	0.14	0.19	0.02	0.15	1.05	0.18
MgO	0.22	0.18	0.18	0.17	0.30	0.18	0.03	0.00	0.00	0.16	0.03
MnO	0.00	0.00	0.02	0.00	0.00	0.02	0.13	0.00	0.00	0.05	0.00
CaO	0.15	2.34	0.08	1.62	0.62	0.05	0.20	0.00	0.12	2.06	0.05
Na <sub>2</sub> O	11.39	9.26	9.81	6.84	0.02	0.02	10.74	1.11	0.14	0.06	0.17
K <sub>2</sub> O	0.01	2.42	2.37	5.79	17.09	17.87	0.06	16.00	16.51	13.84	18.83
total	98.43	97.46	98.51	97.59	99.47	98.08	97.89	97.00	98.81	97.19	100.81
D=	2.67	2.76	2.69	2.77	2.83	2.87	2.67	2.88	2.82	2.86	2.80
Si	2.99	2.90	3.00	2.96	2.94	2.99	3.02	3.00	3.02	2.95	2.97
Al	0.99	1.03	0.98	0.99	1.02	0.96	0.98	0.97	0.96	1.01	0.98
Fe	0.01	0.04	0.02	0.03	0.02	0.01	0.01	0.00	0.01	0.04	0.01
Mg	0.01	0.01	0.01	0.01	0.02	0.01	0.00	0.00	0.00	0.01	0.00
Mn	0.00	0.00	0.00	0.00	0.00	0.00	0.00	0.00	0.00	0.00	0.00
Ca	0.01	0.12	0.00	0.08	0.03	0.00	0.01	0.00	0.01	0.11	0.00
Na	0.98	0.82	0.85	0.61	0.00	0.00	0.93	0.10	0.01	0.01	0.02
K	0.00	0.14	0.14	0.34	1.03	1.09	0.00	0.98	0.99	0.84	1.12
Σ Ions	5.00	5.07	5.00	5.02	5.06	5.07	4.95	5.05	5.00	4.97	5.10

## Plagioclase EMPA-data:

Mineral	ab	ab	ab	ab	ab	ab	ab	ab	ab	ab	ab	ab	ab	ab
Sample	C8902	C8902	C8902	C8902	C8902	C8902	C8902	C8902	C8902	C8902	C8902	C8902	C8902	C8902
SiO2	67.68	67.33	65.12	66.37	67.63	66.02	66.57	66.73	67.08	66.64	67.03	67.60	64.63	60.50
Al2O3	18.81	19.10	18.28	18.54	19.13	18.79	18.25	18.63	18.96	18.51	18.68	18.84	17.81	17.67
FeO	0.13	0.14	0.62	0.02	0.05	0.07	0.13	0.11	0.00	0.04	0.12	0.12	0.20	0.47
MnO	0.00	0.03	0.09	0.02	0.00	0.00	0.21	0.00	0.00	0.00	0.00	0.00	0.05	0.00
MgO	0.01	0.00	0.24	0.01	0.00	0.04	0.03	0.00	0.03	0.02	0.04	0.00	0.02	0.06
CaO	0.13	0.10	1.43	0.18	0.02	0.15	0.13	0.04	0.08	0.21	0.14	0.21	0.14	0.80
Na2O	10.92	10.60	10.08	11.36	11.20	10.71	11.24	11.41	11.51	10.57	11.11	10.77	11.03	10.18
K2O	0.02	0.05	0.07	0.11	0.03	0.05	0.04	0.05	0.02	0.05	0.04	0.00	0.04	0.10
Total	97.70	97.35	95.93	96.61	98.06	95.83	96.60	96.97	97.68	96.04	97.16	97.54	93.92	89.78
Si	3.02	3.01	2.98	3.00	3.01	3.00	3.01	3.01	3.00	3.02	3.01	3.02	3.01	2.96
Al	0.99	1.01	0.99	0.99	1.00	1.01	0.97	0.99	1.00	0.99	0.99	0.99	0.98	1.02
Fe	0.00	0.01	0.02	0.00	0.00	0.00	0.00	0.00	0.00	0.00	0.00	0.00	0.01	0.02
Mn	0.00	0.00	0.00	0.00	0.00	0.00	0.01	0.00	0.00	0.00	0.00	0.00	0.00	0.00
Mg	0.00	0.00	0.02	0.00	0.00	0.00	0.00	0.00	0.00	0.00	0.00	0.00	0.00	0.00
Ca	0.01	0.00	0.07	0.01	0.00	0.01	0.01	0.00	0.00	0.01	0.01	0.01	0.01	0.04
Na	0.94	0.92	0.89	1.00	0.97	0.94	0.99	1.00	1.00	0.93	0.97	0.93	1.00	0.97
K	0.00	0.00	0.00	0.01	0.00	0.00	0.00	0.00	0.00	0.00	0.00	0.00	0.00	0.01
Σ Ions	4.96	4.95	4.98	5.00	4.98	4.97	5.00	5.00	5.00	4.95	4.98	4.95	5.00	5.02
An-1 (Ca) %	0.65	0.52	7.24	0.86	0.10	0.77	0.63	0.19	0.38	1.08	0.69	1.07	0.69	4.14
An-2 (Al) %	-1.18	0.61	-1.48	-1.16	0.19	0.68	-2.71	-1.11	-0.12	-1.15	-1.16	-0.91	-2.32	1.93
An-average	-0.26	0.56	2.88	-0.15	0.15	0.72	-1.04	-0.46	0.13	-0.03	-0.24	0.08	-0.81	3.03

Mineral	ab	ab	ab	ab	ab	ab	ab	ab	ab	ab	ab	ab	ab	ab
Sample	C8902	C8906	C8906	C8906	C897A	C897A	C897A	C897A	C897A	C897A	C897A	C8913	C8913	C8913
SiO2	67.34	65.71	67.07	67.36	69.11	68.97	69.05	68.16	67.97	68.21	68.65	66.23	66.69	66.86
Al2O3	18.95	18.63	18.10	18.24	18.89	19.15	18.85	18.57	18.79	18.43	18.40	20.49	19.82	20.75
FeO	0.03	0.18	0.02	0.12	0.00	0.33	0.07	0.06	0.00	0.09	0.09	0.15	0.14	0.33
MnO	0.12	0.00	0.00	0.07	0.06	0.07	0.00	0.00	0.01	0.00	0.00	0.00	0.04	0.03
MgO	0.00	0.03	0.00	0.03	0.00	0.02	0.00	0.03	0.03	0.00	0.00	0.00	0.00	0.00
CaO	0.21	0.15	0.19	0.05	0.38	0.11	0.02	0.17	0.26	0.08	0.02	1.76	0.73	1.64
Na2O	11.33	11.37	10.94	11.32	10.53	11.00	11.31	11.52	10.51	10.86	10.65	10.62	9.66	9.64
K2O	0.06	0.01	0.00	0.01	0.05	0.01	0.05	0.03	0.04	0.17	0.07	0.03	0.02	0.05
Total	98.04	96.08	96.32	97.20	99.02	99.66	99.35	98.54	97.61	97.84	97.88	99.28	97.10	99.30
Si	3.00	2.99	3.03	3.02	3.03	3.02	3.03	3.02	3.03	3.03	3.05	2.93	2.99	2.94
Al	1.00	1.00	0.96	0.97	0.98	0.99	0.97	0.97	0.99	0.97	0.96	1.07	1.05	1.08
Fe	0.00	0.01	0.00	0.00	0.00	0.01	0.00	0.00	0.00	0.00	0.00	0.01	0.01	0.01
Mn	0.00	0.00	0.00	0.00	0.00	0.00	0.00	0.00	0.00	0.00	0.00	0.00	0.00	0.00
Mg	0.00	0.00	0.00	0.00	0.00	0.00	0.00	0.00	0.00	0.00	0.00	0.00	0.00	0.00
Ca	0.01	0.01	0.01	0.00	0.02	0.01	0.00	0.01	0.01	0.00	0.00	0.08	0.04	0.08
Na	0.98	1.00	0.96	0.99	0.90	0.93	0.96	0.99	0.91	0.94	0.92	0.91	0.84	0.82
K	0.00	0.00	0.00	0.00	0.00	0.00	0.00	0.00	0.00	0.01	0.00	0.00	0.00	0.00
Σ Ions	4.99	5.01	4.97	4.99	4.93	4.96	4.97	4.99	4.94	4.96	4.93	5.00	4.91	4.93
An-1 (Ca) %	1.01	0.72	0.95	0.24	1.95	0.55	0.10	0.81	1.35	0.40	0.10	8.38	4.00	8.57
An-2 (Al) %	-0.49	-0.05	-3.58	-3.53	-2.29	-1.30	-2.61	-3.09	-1.40	-3.35	-3.75	6.77	4.42	7.46
An-average	0.26	0.34	-1.31	-1.64	-0.17	-0.38	-1.26	-1.14	-0.03	-1.47	-1.82	7.57	4.21	8.01

## Plagioclase EMPA-data, continuation:

Mineral	ab	ab	ab	ab	ab	ab	ab	ab	ab	ab	ab	ab	ab	ab
Sample	C8913	C8922	C8922	C8922	C8922	C8928	C8928	C8928	C8928	C8928	C8931	C8940B	C8940B	C8940B
SiO2	65.86	69.73	67.34	66.85	68.80	67.39	67.49	68.07	67.52	67.63	66.59	67.25	67.16	67.67
Al2O3	20.57	20.42	19.76	20.72	19.58	19.31	19.18	19.35	19.40	18.75	18.96	18.68	18.61	19.56
FeO	0.28	0.01	0.23	0.31	0.12	0.00	0.03	0.10	0.04	0.20	0.32	0.34	0.54	0.36
MnO	0.00	0.03	0.10	0.00	0.00	0.04	0.00	0.00	0.00	0.00	0.02	0.00	0.00	0.00
MgO	0.00	0.00	0.00	0.12	0.08	0.04	0.02	0.00	0.00	0.01	0.00	0.15	0.24	0.00
CaO	1.61	0.24	0.40	0.77	0.43	0.15	0.27	0.41	0.35	0.24	0.27	0.24	0.25	0.40
Na2O	10.37	9.98	10.47	10.31	10.96	10.61	10.69	7.89	10.30	11.32	11.02	10.60	10.34	10.48
K2O	0.02	0.05	0.03	0.48	0.08	0.03	0.04	0.02	0.05	0.06	0.02	0.04	0.03	0.04
Total	98.71	100.46	98.33	99.56	100.05	97.57	97.72	95.84	97.66	98.21	97.20	97.30	97.17	98.51
Si	2.93	3.01	2.98	2.94	3.00	3.00	3.01	3.05	3.00	3.01	2.99	3.01	3.01	2.99
Al	1.08	1.04	1.03	1.07	1.01	1.01	1.01	1.02	1.02	0.98	1.00	0.99	0.98	1.02
Fe	0.01	0.00	0.01	0.01	0.00	0.00	0.00	0.00	0.00	0.01	0.01	0.01	0.02	0.01
Mn	0.00	0.00	0.00	0.00	0.00	0.00	0.00	0.00	0.00	0.00	0.00	0.00	0.00	0.00
Mg	0.00	0.00	0.00	0.01	0.01	0.00	0.00	0.00	0.00	0.00	0.00	0.01	0.02	0.00
Ca	0.08	0.01	0.02	0.04	0.02	0.01	0.01	0.02	0.02	0.01	0.01	0.01	0.01	0.02
Na	0.89	0.83	0.90	0.88	0.93	0.92	0.92	0.069	0.89	0.80	0.96	0.92	0.90	0.90
K	0.00	0.00	0.00	0.03	0.00	0.00	0.00	0.00	0.00	0.00	0.00	0.00	0.00	0.00
IonsΣ	4.98	4.89	4.95	4.98	4.96	4.95	4.95	4.78	4.93	4.99	4.99	4.96	4.95	4.95
An(Ca)%	7.89	1.31	2.06	3.85	2.11	0.77	1.37	2.79	1.84	1.15	1.33	1.23	1.32	2.06
An(Al)%	7.67	3.60	3.17	7.30	0.56	1.42	0.67	2.04	1.72	-1.72	0.45	-1.38	-1.62	1.96
average	7.78	2.45	2.62	5.57	1.34	1.10	1.02	2.41	1.78	-0.28	0.89	-0.07	-0.15	2.01

Mineral	ab	ab	ab	ab dkl	ab	ab	ab
Sample	CL1125AB	CL1125AB	CL1125AB	EH0214	EH0217	EH0217	EH0217
SiO2	63.74	64.83	63.55	69.05	69.44	68.67	69.89
Al2O3	19.72	19.85	19.91	19.44	19.32	19.25	19.45
FeO	0.12	0.14	0.22	0.06	0.21	0.15	0.35
MnO	0.00	0.00	0.00	0.00	0.00	0.14	0.00
MgO	0.04	0.06	0.11	0.00	0.09	0.00	0.00
CaO	1.91	1.37	3.03	0.28	0.22	0.45	0.38
Na2O	9.84	9.64	10.07	10.99	10.96	11.28	11.59
K2O	0.09	0.25	0.05	0.07	0.03	0.05	0.06
Total	95.46	96.15	96.95	99.89	100.27	99.99	101.72
Si	2.93	2.95	2.89	3.01	3.02	3.00	3.00
Al	1.07	1.06	1.07	1.00	0.99	0.99	0.99
Fe	0.00	0.01	0.01	0.00	0.01	0.01	0.01
Mn	0.00	0.00	0.00	0.00	0.00	0.01	0.00
Mg	0.00	0.00	0.01	0.00	0.01	0.00	0.00
Ca	0.09	0.07	0.15	0.01	0.01	0.02	0.02
Na	0.88	0.85	0.89	0.93	0.92	0.96	0.97
K	0.01	0.01	0.00	0.00	0.00	0.00	0.00
Σ Ions	4.98	4.95	5.02	4.96	4.95	4.98	4.99
An-1 (Ca) %	9.64	7.17	14.22	1.38	1.10	2.15	1.77
An-2 (Al) %	6.80	6.31	7.12	-0.12	-1.12	-0.86	-1.50
An-average	8.22	6.74	10.67	0.63	-0.01	0.64	0.14

## Plagioclase EMPA-data, continuation:

Mineral	ab	ab	ab	ab	ab	ab	ab	ab	ab	ab	ab	ab
Sample	EH0222	EH0401	EH0401	EH0409B	EH0409B	EH0409B	EH0409B	EH0409B	EH0409B	EH0409B	EH0409B	EH0409B
SiO <sub>2</sub>	66.50	68.72	68.77	69.70	69.33	67.48	65.79	69.36	68.50	69.76	68.43	68.53
Al <sub>2</sub> O <sub>3</sub>	18.33	20.00	19.96	18.97	18.85	18.74	17.99	19.09	19.03	18.82	18.80	18.78
FeO	0.01	0.28	0.28	0.38	0.15	0.70	2.54	0.51	0.95	0.09	0.27	1.16
MnO	0.00	0.00	0.04	0.00	0.00	0.00	0.00	0.06	0.01	0.21	0.04	0.09
MgO	0.00	0.03	0.01	0.00	0.02	0.08	0.08	0.00	0.03	0.00	0.08	0.00
CaO	0.07	0.66	0.64	0.13	0.04	0.91	0.07	0.16	0.35	0.15	0.11	0.14
Na <sub>2</sub> O	11.04	10.02	9.34	10.25	11.37	10.45	9.85	10.61	10.23	11.34	11.38	10.25
K <sub>2</sub> O	0.02	0.79	0.07	0.05	0.06	0.06	0.04	0.06	1.16	0.08	0.04	0.07
Total	95.97	100.50	99.11	99.48	99.82	98.42	96.36	99.85	100.26	100.45	99.15	99.02
Si	3.02	2.99	3.01	3.04	3.03	3.00	3.00	3.02	3.00	3.03	3.01	3.02
Al	0.98	1.02	1.03	0.98	0.97	0.98	0.97	0.98	0.98	0.96	0.98	0.98
Fe	0.00	0.01	0.01	0.01	0.01	0.03	0.10	0.02	0.03	0.00	0.01	0.04
Mn	0.00	0.00	0.00	0.00	0.00	0.00	0.00	0.00	0.00	0.01	0.00	0.00
Mg	0.00	0.00	0.00	0.00	0.00	0.01	0.01	0.00	0.00	0.00	0.01	0.00
Ca	0.00	0.03	0.03	0.01	0.00	0.04	0.00	0.01	0.02	0.01	0.01	0.01
Na	0.97	0.84	0.79	0.87	0.96	0.90	0.87	0.90	0.87	0.95	0.97	0.88
K	0.00	0.04	0.00	0.00	0.00	0.00	0.00	0.00	0.06	0.00	0.00	0.00
Σ Ions	4.98	4.94	4.88	4.91	4.97	4.96	4.95	4.93	4.97	4.97	4.99	4.93
AnCa%	0.35	3.34	3.63	0.69	0.19	4.57	0.39	0.82	1.73	0.72	0.53	0.75
An-Al%	-1.92	2.45	2.79	-2.42	-3.02	-1.84	-3.33	-1.87	-1.72	-3.72	-2.44	-2.41
average	-0.78	2.90	3.21	-0.86	-1.41	1.37	-1.47	-0.52	0.00	-1.50	-0.96	-0.83

Mineral	ab	ab	ab	ab	ab	ab	ab	ab	ab	ab	ab	ab
Sample	EH49B	EH49B	EH49B	EH0409B	EH0409B	EH0409B	EH0409B	EH0409B	EH0409B	EH0409B	EH0409B	EH0409B
SiO <sub>2</sub>	68.33	66.68	67.39	67.18	71.85	69.09	68.96	69.15	69.02	69.27	68.51	70.40
Al <sub>2</sub> O <sub>3</sub>	19.78	19.22	18.75	18.93	20.81	22.86	23.04	23.48	23.47	22.79	23.33	23.30
FeO	0.29	0.23	0.67	0.19	0.02	0.16	0.68	0.68	0.55	0.57	0.58	0.36
MnO	0.00	0.02	0.00	0.00	0.01	0.00	0.00	0.01	0.18	0.00	0.00	0.01
MgO	0.03	0.00	0.10	0.02	0.00	0.01	0.53	0.02	0.02	0.06	0.25	0.00
CaO	0.83	0.77	0.48	0.54	0.69	0.56	0.21	0.45	0.32	0.10	0.24	0.13
Na <sub>2</sub> O	11.10	10.77	11.07	11.42	10.47	11.13	10.36	11.39	11.30	11.11	10.05	10.11
K <sub>2</sub> O	0.02	0.05	0.07	0.01	0.05	0.02	0.14	0.24	0.25	0.13	0.45	0.06
Total	100.38	97.74	98.53	98.29	103.90	103.83	103.92	105.42	105.11	104.03	103.41	104.37
Si	2.98	2.98	3.00	2.99	3.00	2.91	2.90	2.88	2.88	2.91	2.89	2.93
Al	1.02	1.01	0.98	0.99	1.02	1.13	1.14	1.15	1.15	1.13	1.16	1.14
Fe	0.01	0.01	0.02	0.01	0.00	0.01	0.02	0.02	0.02	0.02	0.02	0.01
Mn	0.00	0.00	0.00	0.00	0.00	0.00	0.00	0.00	0.01	0.00	0.00	0.00
Mg	0.00	0.00	0.01	0.00	0.00	0.00	0.03	0.00	0.00	0.00	0.02	0.00
Ca	0.04	0.04	0.02	0.03	0.03	0.03	0.01	0.02	0.01	0.00	0.01	0.01
Na	0.94	0.93	0.95	0.99	0.85	0.91	0.84	0.92	0.91	0.91	0.82	0.82
K	0.00	0.00	0.00	0.00	0.00	0.00	0.01	0.01	0.01	0.01	0.02	0.00
Σ Ions	4.98	4.98	4.99	5.01	4.91	4.98	4.96	5.01	5.01	4.98	4.95	4.91
An-Ca%	3.96	3.79	2.33	2.55	3.50	2.70	1.10	2.11	1.52	0.49	1.27	0.70
An-Al%	1.60	1.33	-1.78	-0.67	2.43	12.84	13.58	14.77	14.94	12.39	15.29	13.30
average	2.78	2.56	0.27	0.94	2.96	7.77	7.34	8.44	8.23	6.44	8.28	7.00

## Plagioclase EMPA-data, continuation:

Mineral	ab	ab	ab	ab	ab	ab	ab	ab	ab	ab	ab	ab	ab
Sample	EH0409B	EH0409B	EH0409B	EH0410	EH0410	EH0410	EH0410	EH0410	EH0410	EH0410	EH0410	EH0410	EH0410
SiO2	66.35	69.78	69.38	69.14	68.44	67.66	67.37	67.04	62.84	69.59	68.57	68.57	68.01
Al2O3	19.04	22.99	22.70	20.63	20.15	18.95	18.91	18.45	17.72	18.91	18.76	18.76	18.80
FeO	0.13	0.43	0.35	0.16	0.14	0.21	0.23	0.48	0.82	0.18	0.17	0.17	0.39
MnO	0.00	0.00	0.00	0.00	0.00	0.00	0.10	0.11	0.13	0.02	0.03	0.06	0.02
MgO	0.02	0.03	0.01	0.00	0.00	0.06	0.00	0.07	0.07	0.08	0.00	0.00	0.05
CaO	0.45	0.13	0.13	0.29	0.11	0.12	0.19	0.32	1.37	0.05	0.22	0.22	0.20
Na2O	11.76	10.52	11.33	9.67	11.47	10.80	11.62	11.07	1.31	11.54	11.43	11.43	11.68
K2O	0.06	0.06	0.07	0.03	0.01	0.61	0.22	0.04	13.93	0.23	0.00	0.00	0.09
Total	97.81	103.94	103.97	99.92	100.32	98.51	98.65	97.60	98.08	100.61	99.21	99.21	99.24
Si	2.98	2.92	2.92	3.00	2.98	3.00	2.99	3.01	2.97	3.02	3.02	3.02	3.00
Al	1.01	1.13	1.12	1.05	1.03	0.99	0.99	0.98	0.99	0.97	0.97	0.97	0.98
Fe	0.00	0.02	0.01	0.01	0.01	0.01	0.01	0.02	0.03	0.01	0.01	0.01	0.01
Mn	0.00	0.00	0.00	0.00	0.00	0.00	0.00	0.00	0.00	0.00	0.00	0.00	0.00
Mg	0.00	0.00	0.00	0.00	0.00	0.00	0.00	0.00	0.00	0.01	0.00	0.00	0.00
Ca	0.02	0.01	0.01	0.01	0.01	0.01	0.01	0.02	0.07	0.00	0.01	0.01	0.01
Na	1.02	0.85	0.92	0.81	0.97	0.93	1.00	0.96	0.12	0.97	0.98	0.98	1.00
K	0.00	0.00	0.00	0.00	0.00	0.03	0.01	0.00	0.84	0.01	0.00	0.00	0.01
Σ Ions	5.03	4.94	4.99	4.88	4.99	4.98	5.02	4.99	5.02	4.99	4.98	4.98	5.01
An-Ca%	2.06	0.68	0.63	1.63	0.53	0.59	0.88	1.57	6.74	0.24	1.05	1.05	0.93
An-Al%	0.63	12.76	11.95	5.12	3.29	-0.83	-1.00	-2.55	-1.46	-3.29	-2.74	-2.74	-2.26
average	1.35	6.72	6.29	3.37	1.91	-0.12	-0.06	-0.49	2.64	-1.53	-0.84	-0.84	-0.66

Mineral	ab	ab	ab	ab	ab	ab	ab	ab	ab	ab	ab	ab	ab
Sample	EH0410	EH0410	EH0410	EH426I	EH426I	EH426I	EH426I	EH426I	EH426I	S1025B	S1025B	S1025B	S1025B
SiO2	69.26	68.39	68.42	69.37	69.36	67.86	69.23	69.84	67.64	68.33	68.17	68.44	68.59
Al2O3	19.19	19.26	18.80	18.80	18.92	18.47	18.66	18.80	18.34	19.59	19.94	19.63	18.99
FeO	0.18	0.16	0.13	0.22	0.19	0.23	0.07	0.14	0.06	0.35	0.51	0.23	0.00
MnO	0.05	0.02	0.00	0.06	0.07	0.00	0.00	0.00	0.00	0.00	0.13	0.10	0.00
MgO	0.01	0.01	0.00	0.00	0.00	0.00	0.00	0.00	0.01	0.00	0.03	0.03	0.00
CaO	0.24	0.24	0.13	0.02	0.27	0.27	0.14	0.09	0.14	0.72	0.95	0.66	0.44
Na2O	11.72	11.93	11.90	12.53	11.27	11.37	11.40	10.88	11.87	9.08	9.80	9.93	11.02
K2O	0.05	0.06	0.04	0.01	0.03	0.06	0.06	0.05	0.03	0.09	0.12	0.16	0.03
Total	100.70	100.07	99.42	101.01	100.11	98.26	99.56	99.80	98.09	98.17	99.64	99.18	99.07
Si	3.01	2.99	3.01	3.01	3.02	3.02	3.03	3.04	3.02	3.02	2.98	3.00	3.02
Al	0.98	0.99	0.97	0.96	0.97	0.97	0.96	0.96	0.96	1.02	1.03	1.02	0.98
Fe	0.01	0.01	0.00	0.01	0.01	0.01	0.00	0.01	0.00	0.01	0.02	0.01	0.00
Mn	0.00	0.00	0.00	0.00	0.00	0.00	0.00	0.00	0.00	0.00	0.00	0.00	0.00
Mg	0.00	0.00	0.00	0.00	0.00	0.00	0.00	0.00	0.00	0.00	0.00	0.00	0.00
Ca	0.01	0.01	0.01	0.00	0.01	0.01	0.01	0.00	0.01	0.03	0.04	0.03	0.02
Na	0.99	1.01	1.01	1.05	0.95	0.98	0.97	0.92	1.03	0.78	0.83	0.84	0.94
K	0.00	0.00	0.00	0.00	0.00	0.00	0.00	0.00	0.00	0.01	0.01	0.01	0.00
Σ Ions	5.00	5.02	5.01	5.04	4.97	4.99	4.97	4.94	5.02	4.86	4.92	4.92	4.96
An-Ca%	1.12	1.10	0.60	0.09	1.30	1.29	0.67	0.45	0.65	4.17	5.05	3.51	2.16
An-Al%	-1.85	-0.70	-2.59	-3.98	-2.87	-3.25	-3.75	-3.49	-3.71	1.86	2.83	1.48	-1.58
average	-0.37	0.20	-0.99	-1.95	-0.78	-0.98	-1.54	-1.52	-1.53	3.02	3.94	2.49	0.29

- End-

## Pumpellyite EMPA data

mineral	pmp	pmp	pmp	pmp	pmp	pmp	pmp	pmp	pmp	pmp	pmp
Sample	C8902	C8902	C8902	C8902	C8902	C8902	C8902	C8906	C8906	C8906	C8906
SiO2	33.92	36.40	36.64	35.58	35.50	36.30	36.88	35.12	34.70	34.30	34.41
TiO2	0.00	0.00	0.00	0.00	0.00	0.00	0.00	0.00	0.00	0.00	0.00
Al2O3	16.89	20.78	20.76	20.08	20.21	19.22	21.53	19.45	18.56	18.07	18.48
FeO	12.01	6.50	5.99	9.05	8.18	9.95	5.84	9.41	10.09	10.31	10.49
MnO	0.15	0.05	0.21	0.05	0.08	0.03	0.15	0.16	0.14	0.02	0.18
MgO	1.98	3.30	3.46	2.27	2.37	2.67	3.54	2.28	2.42	2.55	2.48
CaO	21.00	22.49	22.20	22.33	22.35	22.19	22.43	22.17	21.85	21.62	21.75
Na2O	0.03	0.02	0.07	0.00	0.02	0.01	0.00	0.02	0.00	0.04	0.00
K2O	0.13	0.00	0.00	0.01	0.03	0.01	0.00	0.02	0.00	0.00	0.01
TOTAL	86.11	89.54	89.33	89.37	88.74	90.38	90.37	88.63	87.76	86.91	87.80
Si	6.07	5.88	6.21	6.21	6.21	6.74	6.83	6.40	6.08	6.06	6.19
Ti	0.01	0.00	0.00	0.00	0.00	0.00	0.00	0.00	0.00	0.00	0.00
Altotal	3.79	3.73	4.21	4.21	4.21	4.02	4.03	4.89	4.10	3.65	3.57
Fetotal	1.42	2.03	0.98	0.98	0.98	0.30	0.23	0.01	1.21	1.76	1.64
Mn	0.02	0.00	0.02	0.02	0.02	0.00	0.00	0.00	0.00	0.02	0.00
Mg	0.57	0.25	0.43	0.43	0.43	0.24	0.47	0.15	0.41	0.42	0.39
Ca	3.93	3.85	3.81	3.81	3.81	4.30	3.96	4.16	3.96	3.77	3.86
Na	0.01	0.00	0.07	0.07	0.07	0.00	0.01	0.08	0.01	0.01	0.02
K	0.00	0.00	0.00	0.00	0.00	0.00	0.00	0.00	0.00	0.08	0.07
Σ Ions	15.82	15.74	15.73	15.73	15.73	15.60	15.54	15.69	15.77	15.77	15.74

mineral	pmp	pmp	pmp	pmp	pmp	pmp	pmp	pmp	pmp	pmp	pmp
Sample	C8906	C8906	C8907A	C8907A	C8907A	C8907A	C8907A	C8907A	C8907A	C8907A	C8907A
SiO2	35.26	35.41	36.45	36.11	36.05	36.66	35.67	36.37	36.88	36.68	35.26
TiO2	0.00	0.00	0.00	0.00	0.00	0.00	0.00	0.00	0.00	0.00	0.00
Al2O3	19.41	17.96	19.12	21.27	19.19	21.05	20.19	19.01	20.85	19.61	21.76
FeO	9.14	10.59	9.89	6.57	10.31	8.07	7.44	10.09	8.98	9.26	5.28
MnO	0.22	0.14	0.07	0.18	0.10	0.29	0.17	0.08	0.08	0.16	0.20
MgO	2.14	2.49	2.62	2.85	2.29	2.29	2.06	2.24	2.19	2.81	2.48
CaO	21.95	21.75	22.27	21.53	22.03	22.22	20.99	22.06	21.95	21.75	20.95
Na2O	0.00	0.01	0.03	0.01	0.00	0.06	0.13	0.00	0.00	0.02	0.03
K2O	0.02	0.01	0.00	0.00	0.05	0.02	0.05	0.00	0.01	0.03	0.02
TOTAL	88.14	88.36	90.45	88.52	90.02	90.66	86.70	89.85	90.94	90.32	85.98
Si	6.15	6.16	6.49	6.14	6.08	6.05	6.11	6.06	6.06	6.10	6.09
Ti	0.00	0.00	0.00	0.00	0.00	0.00	0.00	0.00	0.00	0.00	0.00
Altotal	4.26	4.25	4.15	3.22	3.37	3.43	3.60	3.93	4.03	4.63	4.01
Fetotal	0.81	0.73	0.79	2.07	1.90	1.88	1.69	1.44	1.26	0.54	1.08
Mn	0.00	0.06	0.05	0.01	0.00	0.00	0.01	0.02	0.01	0.02	0.02
Mg	0.50	0.86	0.60	0.37	0.45	0.40	0.41	0.40	0.56	0.74	0.70
Ca	4.08	3.76	3.45	3.92	3.96	4.04	3.91	3.88	3.87	3.78	3.96
Na	0.00	0.06	0.02	0.00	0.01	0.00	0.00	0.01	0.01	0.01	0.01
K	0.00	0.02	0.01	0.01	0.04	0.00	0.00	0.01	0.00	0.00	0.00
Σ Ions	15.81	15.90	15.55	15.72	15.81	15.80	15.74	15.76	15.80	15.82	15.87



## Pumpellyite EMPA data, continuation

mineral	pmp	pmp	pmp	pmp	pmp	pmp	pmp	pmp	pmp	pmp	pmp
Sample	C8907A	C8907A	C8907A	C8907A	C8907A	C8907B	C8907B	C8907B	C8907B	C8907B	C8907B
SiO2	36.74	36.72	35.67	36.11	36.82	37.02	36.16	36.34	36.07	36.22	36.14
TiO2	0.00	0.00	0.00	0.00	0.00	0.00	0.00	0.00	0.00	0.00	0.00
Al2O3	22.76	20.67	21.58	21.70	20.40	21.33	18.40	19.32	19.45	21.60	18.38
FeO	4.85	6.78	5.93	7.22	7.65	6.08	11.10	10.71	9.08	6.38	9.76
MnO	0.11	0.11	0.26	0.20	0.12	0.13	0.25	0.11	0.07	0.20	0.04
MgO	2.86	3.14	2.49	2.02	2.84	3.40	2.04	1.76	2.58	3.07	2.85
CaO	22.50	22.31	21.57	21.95	22.02	22.17	21.61	21.43	21.27	21.79	21.40
Na2O	0.00	0.00	0.02	0.00	0.03	0.00	0.00	0.01	0.03	0.05	0.00
K2O	0.00	0.01	0.00	0.01	0.01	0.00	0.03	0.01	0.07	0.00	0.23
TOTAL	89.82	89.74	87.52	89.21	89.89	90.13	89.59	89.69	88.62	89.31	88.80
Si	6.14	6.09	6.17	6.17	6.11	6.13	6.14	5.98	6.24	6.28	6.37
Ti	0.00	0.00	0.00	0.00	0.00	0.00	0.03	0.03	0.06	0.16	0.00
Altotal	3.99	4.58	3.76	3.48	4.04	3.32	3.17	4.83	3.29	3.29	3.40
Fetotal	1.05	0.39	1.48	1.70	1.44	1.69	2.00	0.55	1.62	2.18	1.81
Mn	0.00	0.02	0.02	0.01	0.01	0.00	0.01	0.04	0.00	0.01	0.02
Mg	0.72	1.01	0.52	0.41	0.48	1.06	0.85	0.40	0.93	0.62	0.96
Ca	3.92	3.83	3.70	3.96	3.55	3.64	3.54	3.96	3.53	2.76	2.95
Na	0.01	0.00	0.01	0.02	0.00	0.01	0.01	0.04	0.01	0.06	0.02
K	0.00	0.00	0.10	0.00	0.01	0.02	0.00	0.00	0.14	0.00	0.01
Σ Ions	15.84	15.92	15.76	15.75	15.65	15.88	15.75	15.82	15.82	15.36	15.54

mineral	pmp	pmp	pmp	pmp	pmp	pmp	pmp	pmp	pmp	pmp	pmp
Sample	C8907C	C8907C	C8907C	C8907C	C8907C	C8907C	C8907C	C8907C	C8907C	C8912	C8913
SiO2	36.05	35.72	35.71	35.99	35.48	35.87	34.82	36.62	35.34	40.81	35.27
TiO2	0.00	0.00	0.00	0.00	0.00	0.00	0.00	0.00	0.00	0.00	0.00
Al2O3	20.32	19.64	20.18	20.19	21.51	18.96	19.89	20.93	19.72	20.92	22.43
FeO	7.88	8.61	8.60	8.88	5.74	10.11	10.75	6.63	9.17	3.00	5.54
MnO	0.06	0.08	0.10	0.03	0.34	0.09	0.17	0.00	0.08	0.04	0.13
MgO	3.05	2.90	2.41	2.35	2.67	2.41	2.23	3.55	2.39	3.02	1.88
CaO	22.00	20.95	22.02	21.92	21.62	21.41	21.48	22.14	21.73	22.07	22.00
Na2O	0.00	0.04	0.00	0.01	0.01	0.00	0.00	0.00	0.03	0.09	0.07
K2O	0.12	0.12	0.13	0.16	0.02	0.00	0.02	0.07	0.06	0.01	0.00
TOTAL	89.48	88.06	89.15	89.53	87.39	88.85	89.36	89.94	88.52	89.96	87.32
Si	5.81	5.87	6.05	6.04	6.05	6.07	6.04	6.10	5.93	6.29	6.02
Ti	0.01	0.00	0.00	0.01	0.00	0.00	0.02	0.01	0.01	0.01	0.00
Altotal	4.07	3.74	4.06	4.18	4.20	4.18	4.24	4.27	3.93	4.07	3.97
Fetotal	1.67	1.91	1.21	1.03	1.06	1.01	0.97	0.86	1.95	0.94	1.37
Mn	0.00	0.00	0.05	0.02	0.03	0.02	0.01	0.01	0.01	0.02	0.01
Mg	0.44	0.66	0.50	0.59	0.51	0.64	0.66	0.67	0.36	0.60	0.63
Ca	3.81	3.61	3.94	3.99	3.95	3.89	3.89	3.90	3.41	3.67	3.82
Na	0.01	0.01	0.00	0.01	0.01	0.01	0.01	0.00	0.02	0.22	0.00
K	0.01	0.00	0.00	0.00	0.01	0.00	0.00	0.01	0.02	0.00	0.00
Σ Ions	15.83	15.80	15.81	15.86	15.82	15.83	15.84	15.83	15.63	15.81	15.82

## Pumpellyite EMPA data, continuation

mineral	pmp	pmp	pmp	pmp	pmp	pmp	pmp	pmp	pmp	pmp	pmp
Sample	C8913	C8913	C8913	C8913	C8913	C8913	C8913	C8922	C8922	C8922	C8922
SiO2	36.36	35.56	36.87	35.98	35.29	35.64	35.82	37.21	36.24	35.72	34.92
TiO2	0.00	0.00	0.00	0.00	0.00	0.00	0.00	0.00	0.00	0.00	0.00
Al2O3	25.18	17.66	20.59	22.56	16.85	21.45	21.71	23.34	23.69	23.58	22.41
FeO	2.86	12.64	7.38	5.27	14.47	7.32	6.96	4.71	3.90	3.67	4.50
MnO	0.22	0.13	0.17	0.06	0.04	0.20	0.17	0.16	0.23	0.11	0.24
MgO	1.72	2.37	3.24	2.28	1.99	1.92	1.84	5.56	2.52	2.68	5.44
CaO	23.29	21.91	22.30	21.95	21.86	22.11	22.12	19.97	22.00	21.92	19.17
Na2O	0.00	0.00	0.01	0.07	0.06	0.00	0.00	0.07	0.03	0.03	0.04
K2O	0.00	0.02	0.00	0.00	0.01	0.01	0.00	0.01	0.02	0.02	0.00
TOTAL	89.63	90.29	90.56	88.17	90.57	88.65	88.62	91.03	88.63	87.73	86.72
Si	6.10	6.02	6.08	6.15	6.05	6.75	6.71	6.03	6.02	6.02	6.00
Ti	0.00	0.00	0.00	0.00	0.02	0.01	0.05	0.00	0.00	0.02	0.00
Altotal	4.39	4.47	4.50	4.46	4.23	3.94	3.97	4.16	3.95	4.37	3.99
Fetotal	0.76	0.86	0.83	0.76	0.89	0.38	0.34	1.03	1.26	0.68	1.22
Mn	0.01	0.03	0.04	0.03	0.04	0.01	0.00	0.02	0.01	0.02	0.02
Mg	0.70	0.60	0.58	0.69	0.65	0.71	0.56	0.63	0.65	0.78	0.62
Ca	3.85	3.84	3.72	3.65	3.99	3.76	3.93	3.99	3.99	4.05	4.04
Na	0.01	0.02	0.01	0.01	0.01	0.04	0.01	0.01	0.00	0.01	0.01
K	0.00	0.00	0.00	0.00	0.01	0.03	0.05	0.00	0.00	0.00	0.00
Σ Ions	15.83	15.83	15.76	15.75	15.88	15.62	15.62	15.87	15.88	15.94	15.90

mineral	pmp	pmp	pmp	pmp	pmp	pmp	pmp	pmp	pmp	pmp	pmp
Sample	C8922	C8922	C8931	C8931	C8931	C8938	C8938	C8940B	C8940B	C8940B	C8940B
SiO2	37.18	35.61	35.66	38.99	35.61	36.07	35.31	35.86	36.07	35.30	35.63
TiO2	0.00	0.00	0.17	0.03	0.03	0.18	0.03	0.00	0.00	0.00	0.00
Al2O3	22.73	23.60	21.99	20.97	19.85	21.40	20.69	22.54	22.22	19.77	22.47
FeO	4.61	3.33	4.79	8.99	8.90	6.32	7.25	5.89	5.32	9.64	6.09
MnO	0.15	0.22	0.12	0.06	0.08	0.27	0.17	0.29	0.21	0.06	0.22
MgO	2.55	2.62	3.09	1.28	2.58	2.62	2.46	2.31	2.73	2.48	2.38
CaO	21.73	21.47	22.38	21.76	22.03	22.22	21.81	20.53	19.99	20.92	21.24
Na2O	0.08	0.05	0.02	0.01	0.01	0.02	0.03	0.03	0.04	0.01	0.06
K2O	0.05	0.00	0.01	0.00	0.00	0.03	0.00	0.00	0.00	0.00	0.00
TOTAL	89.08	86.90	88.23	92.09	89.09	89.13	87.75	87.45	86.58	88.18	88.09
Si	6.04	6.30	6.00	6.00	6.02	5.94	6.05	6.05	6.02	6.06	6.17
Ti	0.01	0.00	0.00	0.00	0.00	0.00	0.00	0.00	0.00	0.00	0.00
Altotal	4.63	3.99	4.55	4.63	4.45	4.49	4.66	4.72	4.68	4.68	4.44
Fetotal	0.48	1.21	0.72	0.52	0.64	0.64	0.54	0.47	0.52	0.48	0.64
Mn	0.03	0.01	0.01	0.02	0.02	0.03	0.03	0.03	0.02	0.04	0.02
Mg	0.69	0.31	1.17	0.95	1.34	1.38	0.63	0.66	0.67	0.75	0.63
Ca	4.02	3.77	3.41	3.80	3.46	3.49	3.93	3.91	3.96	3.84	3.86
Na	0.02	0.00	0.01	0.00	0.02	0.01	0.01	0.02	0.01	0.01	0.03
K	0.00	0.00	0.01	0.00	0.00	0.00	0.00	0.00	0.00	0.00	0.01
Σ Ions	15.92	15.59	15.88	15.92	15.95	16.00	15.86	15.86	15.88	15.86	15.80

## Pumpellyite EMPA data, continuation

mineral	pmp	pmp	pmp	pmp	pmp	pmp	pmp	pmp	pmp	pmp	pmp
Sample	C8940B	D5614	D5614	D5614	D5714	D5742VB	D5742VB	EH0207	EH0207	EH0207	EH0207
SiO2	35.63	37.78	36.74	36.65	36.07	42.91	43.04	36.48	36.48	36.48	35.61
TiO2	0.00	0.00	0.00	0.00	0.00	0.00	0.00	0.00	0.00	0.00	0.04
Al2O3	21.77	21.22	23.48	23.64	19.42	21.75	21.56	20.99	20.99	20.99	18.89
FeO	5.31	10.68	2.84	3.87	14.94	2.30	1.75	6.92	6.92	6.92	9.94
MnO	0.10	0.05	0.13	0.14	0.03	0.00	0.00	0.15	0.15	0.15	0.14
MgO	2.75	1.98	4.07	2.98	1.01	1.02	1.99	1.69	1.69	1.69	2.26
CaO	20.99	20.50	21.56	21.24	22.07	25.56	23.29	20.91	20.91	20.91	21.52
Na2O	0.03	0.01	0.00	0.02	0.01	0.00	0.02	0.21	0.21	0.21	0.02
K2O	0.00	0.05	0.02	0.01	0.00	0.01	0.00	0.02	0.02	0.02	0.00
TOTAL	86.58	92.27	88.84	88.55	93.55	93.53	91.65	87.37	87.37	87.37	88.42
Si	6.12	6.01	6.03	6.05	6.08	5.99	6.08	6.05	6.02	6.08	6.08
Ti	0.00	0.00	0.00	0.00	0.00	0.00	0.00	0.00	0.00	0.00	0.00
Alttotal	4.56	3.95	4.01	4.01	3.94	3.96	4.00	4.32	4.31	3.79	4.09
Fetotal	0.62	1.30	1.21	1.10	1.23	1.36	1.16	0.82	0.93	1.43	0.92
Mn	0.04	0.01	0.01	0.01	0.01	0.01	0.01	0.05	0.03	0.01	0.00
Mg	0.63	0.61	0.61	0.76	0.74	0.64	0.71	0.68	0.67	0.61	0.88
Ca	3.82	3.96	3.98	3.95	3.82	3.89	3.87	3.95	3.88	3.89	3.94
Na	0.00	0.01	0.00	0.00	0.01	0.00	0.00	0.00	0.01	0.00	0.00
K	0.01	0.01	0.03	0.03	0.03	0.00	0.00	0.00	0.00	0.00	0.01
Σ Ions	15.80	15.87	15.88	15.91	15.85	15.85	15.84	15.88	15.86	15.81	15.92

mineral	pmp	pmp	pmp	pmp	pmp	pmp	pmp	pmp	pmp	pmp	pmp
Sample	EH0401	EH0401	EH0401	EH0401	EH0401	EH0409B	EH0409B	EH0409B	EH0409B	EH0409B	EH0409B
SiO2	36.65	42.12	36.63	41.84	38.39	38.09	36.16	34.29	37.61	35.85	36.63
TiO2	0.04	0.39	0.01	0.08	0.07	0.00	0.00	0.00	1.25	0.22	0.45
Al2O3	21.40	21.14	21.58	20.73	21.11	17.26	20.60	15.76	16.74	15.73	16.39
FeO	7.33	2.55	7.65	2.80	6.88	12.95	8.67	11.31	15.64	14.01	11.37
MnO	0.13	0.01	0.20	0.08	0.12	0.17	0.35	0.03	0.08	0.05	0.00
MgO	2.60	2.36	2.09	2.95	2.44	3.86	1.99	3.99	2.51	3.32	3.67
CaO	21.94	23.01	22.32	21.76	20.92	16.49	22.01	19.00	15.46	19.33	19.37
Na2O	0.04	0.04	0.02	0.14	0.69	0.05	0.01	0.04	0.18	0.03	0.03
K2O	0.00	0.23	0.05	0.13	0.02	0.04	0.00	0.08	0.00	0.02	0.63
TOTAL	90.13	91.85	90.55	90.51	90.64	88.91	89.79	84.50	89.47	88.56	88.54
Si	5.89	6.15	6.04	6.05	6.10	6.11	6.14	6.10	6.08	6.05	6.12
Ti	0.00	0.00	0.00	0.00	0.00	0.00	0.00	0.00	0.00	0.00	0.00
Alttotal	3.97	3.58	3.99	3.78	3.82	3.88	3.67	3.66	3.81	4.25	4.15
Fetotal	1.52	1.45	1.25	1.39	1.50	1.29	1.38	1.57	1.27	0.89	0.84
Mn	0.02	0.00	0.00	0.01	0.02	0.01	0.01	0.04	0.02	0.03	0.02
Mg	0.56	0.66	0.59	0.71	0.44	0.65	0.72	0.51	0.76	0.76	0.84
Ca	3.89	3.97	3.94	3.92	3.85	3.86	3.89	3.91	3.93	3.90	3.92
Na	0.00	0.02	0.00	0.00	0.00	0.01	0.00	0.00	0.01	0.02	0.00
K	0.00	0.04	0.03	0.00	0.00	0.02	0.05	0.01	0.00	0.00	0.00
Σ Ions	15.86	15.87	15.85	15.87	15.74	15.82	15.86	15.79	15.88	15.89	15.89

## Pumpellyite EMPA data, continuation

mineral	pmp	pmp	pmp	pmp	pmp	pmp	pmp	pmp	pmp	pmp	pmp
Sample	EH0410	EH0426/I	EH0426/I	EH0426/I	EH0426/I	EH0426/I	EH0426/I	EH0426/I	EH0426/I	EH0426/I	EH0426/I
SiO2	36.28	36.34	36.18	37.12	35.79	33.29	36.72	34.34	36.60	30.50	36.72
TiO2	0.24	0.00	0.00	0.00	0.00	0.00	0.00	0.00	0.00	0.00	0.00
Al2O3	24.85	20.02	18.12	17.78	17.24	14.82	20.27	16.16	20.63	16.54	20.52
FeO	3.97	10.31	12.00	12.25	13.30	13.44	7.51	12.84	9.09	4.46	7.81
MnO	0.28	0.15	0.07	0.05	0.00	0.04	0.00	0.03	0.10	0.25	0.16
MgO	1.61	1.61	1.63	1.64	1.57	1.33	2.89	1.72	2.27	1.89	2.84
CaO	22.40	21.74	21.64	22.24	22.33	19.85	21.91	20.87	21.81	15.12	22.28
Na2O	0.11	0.04	0.00	0.06	0.01	0.00	0.04	0.04	0.02	0.04	0.02
K2O	0.00	0.04	0.00	0.00	0.00	0.03	0.01	0.17	0.02	0.03	0.00
TOTAL	89.74	90.25	89.64	91.14	90.24	82.80	89.35	86.17	90.54	68.83	90.35
Si	6.12	6.15	6.09	6.07	6.05	6.10	6.08	6.10	6.10	6.13	6.08
Ti	0.00	0.00	0.00	0.00	0.00	0.00	0.00	0.00	0.00	0.00	0.00
Alttotal	4.05	4.21	4.42	4.33	3.79	3.76	3.76	4.06	3.84	4.00	4.05
Fetotal	0.94	0.79	0.76	0.84	1.45	1.41	1.38	0.92	1.29	1.06	1.24
Mn	0.02	0.02	0.03	0.04	0.01	0.01	0.01	0.02	0.02	0.02	0.01
Mg	0.78	0.76	0.64	0.63	0.57	0.56	0.65	0.79	0.70	0.70	0.54
Ca	3.98	3.92	3.87	3.93	3.96	3.96	3.98	4.01	3.87	3.92	3.87
Na	0.00	0.01	0.01	0.01	0.00	0.00	0.01	0.02	0.01	0.01	0.00
K	0.00	0.00	0.00	0.00	0.01	0.00	0.00	0.01	0.01	0.00	0.00
Σ Ions	15.89	15.85	15.83	15.85	15.84	15.81	15.86	15.92	15.84	15.85	15.78

mineral	pmp	pmp	pmp	pmp	pmp	pmp
Sample	EH0426/I	S1025B	S1025B	S1025B	S1025B	S1025B
SiO2	36.94	35.89	36.50	36.67	35.95	34.91
TiO2	0.00	0.00	0.00	0.00	0.00	0.00
Al2O3	19.11	20.55	17.89	21.56	18.40	22.65
FeO	10.60	8.58	11.60	5.79	12.48	0.07
MnO	0.11	0.00	0.00	0.00	0.13	0.00
MgO	2.10	1.63	1.55	2.01	1.67	0.56
CaO	20.71	21.83	21.23	22.68	20.87	21.18
Na2O	0.02	0.03	0.06	0.01	0.04	0.23
K2O	0.47	0.00	0.32	0.00	0.36	0.01
TOTAL	90.06	88.50	89.14	88.72	89.90	79.61
Si	6.15	6.15	6.08	6.05	6.06	6.07
Ti	0.00	0.00	0.00	0.00	0.00	0.00
Alttotal	3.97	4.10	4.22	4.28	4.10	4.43
Fetotal	0.98	1.07	0.92	1.01	1.12	0.67
Mn	0.01	0.02	0.03	0.03	0.04	0.02
Mg	0.84	0.53	0.71	0.50	0.56	0.70
Ca	3.92	3.87	3.88	3.94	3.93	3.98
Na	0.00	0.04	0.00	0.00	0.02	0.00
K	0.00	0.01	0.00	0.00	0.00	0.00
Σ Ions	15.88	15.80	15.85	15.81	15.84	15.88

Pumpellyite EMPA data – end -

## Prehnite EMPA-data:

Mineral Sample	prh C8912	prh C8912	prh C8912	prh C8912	prh C8912	prh C8912	prh C8912	prh C8912	prh C8912	prh C8912	prh C8912
SiO2	42.45	43.62	43.47	43.32	43.73	42.94	43.63	42.87	42.71	42.43	42.01
TiO2	0.00	0.00	0.00	0.00	0.00	0.00	0.00	0.00	0.00	0.00	0.00
Al2O3	19.85	20.91	21.17	21.67	21.65	20.93	20.85	20.59	19.32	20.16	18.59
FeO	4.51	2.01	2.23	2.10	2.06	2.15	2.35	3.51	4.83	3.88	5.48
MnO	0.00	0.03	0.00	0.01	0.03	0.02	0.05	0.00	0.01	0.08	0.00
MgO	0.01	0.00	0.03	0.06	0.21	0.00	0.00	0.00	0.00	0.22	0.00
CaO	24.91	25.03	24.34	24.32	24.72	24.41	23.25	25.68	25.43	24.76	24.80
Na2O	0.03	0.13	0.05	0.07	0.06	0.13	0.06	0.02	0.09	0.01	0.05
K2O	0.00	0.00	0.01	0.00	0.01	0.02	0.02	0.02	0.01	0.02	0.02
total	91.76	91.73	91.30	91.55	92.47	90.60	90.21	92.69	92.40	91.56	90.95
Si	6.49	6.56	6.56	6.51	6.52	6.54	6.64	6.46	6.51	6.48	6.52
Ti	0.00	0.00	0.00	0.00	0.00	0.00	0.00	0.00	0.00	0.00	0.00
Al	3.57	3.71	3.76	3.84	3.80	3.76	3.74	3.66	3.47	3.63	3.40
Fe	0.58	0.25	0.28	0.26	0.26	0.27	0.30	0.44	0.62	0.50	0.71
Mn	0.00	0.00	0.00	0.00	0.00	0.00	0.01	0.00	0.00	0.01	0.00
Mg	0.00	0.00	0.01	0.01	0.05	0.00	0.00	0.00	0.00	0.05	0.00
Ca	4.08	4.03	3.93	3.92	3.95	3.98	3.79	4.15	4.15	4.05	4.13
Na	0.01	0.04	0.01	0.02	0.02	0.04	0.02	0.01	0.03	0.00	0.02
K	0.00	0.00	0.00	0.00	0.00	0.00	0.00	0.00	0.00	0.00	0.00
Σ cations	14.73	14.60	14.56	14.57	14.59	14.60	14.50	14.71	14.77	14.71	14.78

Mineral Sample	prh C8912	prh C8912	prh C8912	prh C8902	prh C8902	prh C8902	prh C8902	prh C8902	prh C8902	prh C8902	prh C8902
SiO2	42.07	42.89	42.47	41.51	41.59	42.29	40.96	41.13	41.23	41.13	40.71
TiO2	0.00	0.00	0.00	0.00	0.00	0.00	0.00	0.00	0.00	0.00	0.00
Al2O3	18.52	21.46	19.63	18.13	18.60	21.21	17.96	17.47	17.38	17.38	17.38
FeO	5.76	2.15	5.12	6.20	6.22	1.66	6.42	7.02	6.93	7.16	7.30
MnO	0.00	0.11	0.06	0.00	0.00	0.00	0.01	0.00	0.04	0.00	0.05
MgO	0.00	0.00	0.57	0.00	0.00	0.00	0.00	0.00	0.00	0.00	0.00
CaO	25.31	26.13	24.47	26.16	25.45	25.70	25.31	25.92	25.69	26.23	25.90
Na2O	0.09	0.02	0.04	0.03	0.04	0.01	0.08	0.01	0.05	0.00	0.00
K2O	0.01	0.00	0.00	0.00	0.00	0.00	0.03	0.03	0.00	0.00	0.01
total	91.76	92.76	92.36	92.03	91.90	90.87	90.77	91.58	91.32	91.90	91.35
Si	6.50	6.42	6.47	6.44	6.44	6.44	6.44	6.44	6.47	6.43	6.41
Ti	0.00	0.00	0.00	0.00	0.00	0.00	0.00	0.00	0.00	0.00	0.00
Al	3.37	3.79	3.52	3.31	3.39	3.81	3.33	3.23	3.21	3.20	3.23
Fe	0.74	0.27	0.65	0.80	0.81	0.21	0.84	0.92	0.91	0.94	0.96
Mn	0.00	0.01	0.01	0.00	0.00	0.00	0.00	0.00	0.01	0.00	0.01
Mg	0.00	0.00	0.13	0.00	0.00	0.00	0.00	0.00	0.00	0.00	0.00
Ca	4.19	4.19	3.99	4.35	4.22	4.19	4.26	4.35	4.32	4.39	4.37
Na	0.03	0.01	0.01	0.01	0.01	0.00	0.02	0.00	0.02	0.00	0.00
K	0.00	0.00	0.00	0.00	0.00	0.00	0.01	0.01	0.00	0.00	0.00
Σ cations	14.83	14.69	14.78	14.91	14.87	14.66	14.91	14.95	14.93	14.97	14.98

## Prehnite EMPA-data, continuation:

Mineral Sample	prh C8902	prh C8902	prh C8902	prh C8902	prh C8902	prh C8902	prh C8902	prh C8902	prh C8902	prh C8913	prh C8913
SiO <sub>2</sub>	43.10	41.62	41.04	42.79	41.41	42.13	41.74	40.63	41.34	41.94	41.18
TiO <sub>2</sub>	0.00	0.00	0.00	0.00	0.00	0.00	0.00	0.00	0.00	0.00	0.00
Al <sub>2</sub> O <sub>3</sub>	22.55	18.53	19.73	19.38	20.38	22.33	22.03	17.95	18.62	20.43	15.88
FeO	0.39	5.46	4.21	5.64	3.18	0.15	0.84	7.20	5.63	3.63	9.60
MnO	0.04	0.00	0.01	0.04	0.03	0.00	0.05	0.01	0.10	0.06	0.00
MgO	0.00	0.00	0.00	0.00	0.00	0.00	0.00	0.02	0.00	0.00	0.00
CaO	25.95	25.85	26.00	24.28	26.48	26.27	26.40	25.04	25.42	26.06	25.22
Na <sub>2</sub> O	0.07	0.06	0.10	0.08	0.05	0.03	0.01	0.06	0.00	0.04	0.00
K <sub>2</sub> O	0.00	0.00	0.01	0.04	0.00	0.02	0.13	0.27	0.07	0.00	0.02
total	92.10	91.52	91.10	92.25	91.53	90.93	91.20	91.18	91.18	92.16	91.90
Si	6.42	6.45	6.36	6.53	6.35	6.37	6.33	6.40	6.44	6.39	6.51
Ti	0.00	0.00	0.00	0.00	0.00	0.00	0.00	0.00	0.00	0.00	0.00
Al	3.96	3.39	3.60	3.49	3.68	3.98	3.94	3.33	3.42	3.67	2.96
Fe	0.05	0.71	0.55	0.72	0.41	0.02	0.11	0.95	0.73	0.46	1.27
Mn	0.01	0.00	0.00	0.01	0.00	0.00	0.01	0.00	0.01	0.01	0.00
Mg	0.00	0.00	0.00	0.00	0.00	0.00	0.00	0.00	0.00	0.00	0.00
Ca	4.14	4.29	4.32	3.97	4.35	4.26	4.29	4.22	4.24	4.25	4.27
Na	0.02	0.02	0.03	0.02	0.01	0.01	0.00	0.02	0.00	0.01	0.00
K	0.00	0.00	0.00	0.01	0.00	0.00	0.03	0.05	0.01	0.00	0.00
Σ cation	14.60	14.86	14.85	14.74	14.81	14.64	14.71	14.97	14.86	14.78	15.01

Mineral Sample	prh CL1125A B	prh CL1125A B	prh CL1125A B	prh CL1125A B	prh CL1125A B	prh CL1125A B	prh CL1125A B	prh CL1125A B	prh CL1125A B	prh CL1125A B	prh CL1125A B
SiO <sub>2</sub>	41.44	42.50	41.96	42.16	42.57	43.05	42.36	41.14	41.81	42.30	41.56
TiO <sub>2</sub>	0.00	0.00	0.00	0.00	0.00	0.00	0.00	0.00	0.00	0.00	0.00
Al <sub>2</sub> O <sub>3</sub>	20.84	21.15	20.26	20.25	20.33	20.51	20.72	19.75	20.24	21.45	20.61
FeO	1.60	1.45	1.77	1.97	1.81	1.57	2.03	2.39	3.62	1.96	1.80
MnO	0.04	0.04	0.00	0.06	0.06	0.00	0.00	0.04	0.00	0.10	0.00
MgO	1.50	0.04	1.33	0.35	0.03	0.01	0.47	0.69	0.06	0.13	0.05
CaO	24.37	26.19	24.82	24.36	24.90	25.00	24.93	25.39	26.50	26.59	26.20
Na <sub>2</sub> O	0.04	0.11	0.08	0.15	0.13	0.17	0.08	0.09	0.00	0.02	0.01
K <sub>2</sub> O	0.01	0.00	0.06	0.02	0.00	0.03	0.02	0.03	0.00	0.00	0.02
total	89.84	91.47	90.30	89.32	89.82	90.34	90.61	89.53	92.22	92.54	90.25
Si	6.38	6.44	6.44	6.53	6.55	6.57	6.47	6.41	6.37	6.36	6.41
Ti	0.00	0.00	0.00	0.00	0.00	0.00	0.00	0.00	0.00	0.00	0.00
Al	3.78	3.77	3.66	3.69	3.69	3.69	3.73	3.63	3.64	3.80	3.74
Fe	0.21	0.18	0.23	0.25	0.23	0.20	0.26	0.31	0.46	0.25	0.23
Mn	0.01	0.01	0.00	0.01	0.01	0.00	0.00	0.01	0.00	0.01	0.00
Mg	0.34	0.01	0.30	0.08	0.01	0.00	0.11	0.16	0.01	0.03	0.01
Ca	4.02	4.25	4.08	4.04	4.10	4.09	4.08	4.24	4.33	4.28	4.33
Na	0.01	0.03	0.02	0.05	0.04	0.05	0.02	0.03	0.00	0.01	0.00
K	0.00	0.00	0.01	0.00	0.00	0.01	0.00	0.01	0.00	0.00	0.00
Σ cation	14.74	14.69	14.75	14.65	14.63	14.61	14.68	14.79	14.81	14.74	14.72

## Prehnite EMPA-data, continuation:

Mineral Sample	prh D5620V	prh D5714	prh D5714	prh D5714	prh D5714	prh D5714	prh D5714	prh D5714	prh D5714	prh D5742VB	prh D5742VB	prh D5742VB
SiO2	41.53	42.44	41.05	42.42	42.18	42.67	41.46	40.77	42.47	41.86	42.85	42.85
TiO2	0.00	0.00	0.00	0.00	0.00	0.00	0.00	0.00	0.00	0.00	0.00	0.00
Al2O3	22.44	20.69	18.44	20.97	21.04	21.20	18.20	18.30	21.38	22.08	19.48	19.48
FeO	0.57	3.37	5.74	1.83	2.24	1.60	6.22	5.45	1.72	2.05	5.65	5.65
MnO	0.09	0.07	0.04	0.05	0.02	0.04	0.00	0.03	0.00	0.00	0.13	0.13
MgO	0.42	1.07	0.02	0.10	0.20	0.01	0.00	0.00	1.07	0.63	0.74	0.74
CaO	24.33	24.08	25.84	25.42	25.50	25.77	26.02	25.46	25.14	25.74	25.90	25.90
Na2O	0.03	0.01	0.03	0.01	0.01	0.03	0.02	0.03	0.00	0.04	0.06	0.06
K2O	0.02	0.00	0.00	0.00	0.01	0.00	0.00	0.00	0.00	0.00	0.05	0.05
total	89.43	91.73	91.15	90.81	91.19	91.33	91.92	90.03	91.78	92.40	94.86	94.86
Si	6.37	6.43	6.41	6.47	6.42	6.46	6.43	6.43	6.40	6.29	6.40	6.40
Ti	0.00	0.00	0.00	0.00	0.00	0.00	0.00	0.00	0.00	0.00	0.00	0.00
Al	4.05	3.70	3.39	3.77	3.77	3.78	3.33	3.40	3.79	3.91	3.43	3.43
Fe	0.07	0.43	0.75	0.23	0.29	0.20	0.81	0.72	0.22	0.26	0.71	0.71
Mn	0.01	0.01	0.01	0.01	0.00	0.01	0.00	0.00	0.00	0.00	0.02	0.02
Mg	0.10	0.24	0.00	0.02	0.05	0.00	0.00	0.00	0.24	0.14	0.16	0.16
Ca	4.00	3.91	4.32	4.15	4.16	4.18	4.33	4.30	4.06	4.14	4.15	4.15
Na	0.01	0.00	0.01	0.00	0.00	0.01	0.01	0.01	0.00	0.01	0.02	0.02
K	0.00	0.00	0.00	0.00	0.00	0.00	0.00	0.00	0.00	0.00	0.01	0.01
Σ cations	14.61	14.72	14.90	14.65	14.69	14.65	14.90	14.87	14.70	14.76	14.89	14.89

Mineral Sample	prh D5742VB	prh D5742VB	prh EH0207	prh EH0207	prh EH0207	prh EH0207	prh EH0401	prh EH0401	prh EH0401	prh EH0401	prh EH0401	prh EH0401
SiO2	41.14	40.29	43.65	42.39	42.54	39.31	42.35	44.89	43.24	42.79	43.18	43.18
TiO2	0.00	0.00	0.00	0.00	0.00	0.00	0.09	0.17	0.00	0.00	0.15	0.15
Al2O3	18.27	20.82	23.19	22.66	22.62	21.73	18.39	21.50	22.27	21.67	20.92	20.92
FeO	7.63	2.27	0.13	0.08	0.06	0.12	6.27	2.11	0.66	1.12	2.10	2.10
MnO	0.00	0.09	0.05	0.10	0.11	0.13	0.04	0.02	0.01	0.00	0.03	0.03
MgO	1.79	4.12	0.01	0.01	0.00	0.00	0.02	0.09	0.20	0.02	0.01	0.01
CaO	23.86	22.27	25.41	25.68	25.17	26.00	24.87	24.51	25.57	25.85	25.95	25.95
Na2O	0.00	0.01	0.05	0.03	0.04	0.04	0.05	0.93	0.30	0.07	0.13	0.13
K2O	0.01	0.00	0.03	0.00	0.02	0.02	0.01	0.04	0.04	0.01	0.01	0.01
total	92.70	89.88	92.54	90.95	90.55	87.35	92.10	94.25	92.30	91.52	92.48	92.48
Si	6.34	6.20	6.45	6.39	6.43	6.23	6.52	6.57	6.44	6.45	6.48	6.48
Ti	0.00	0.00	0.00	0.00	0.00	0.00	0.02	0.04	0.00	0.00	0.03	0.03
Al	3.32	3.78	4.04	4.03	4.03	4.06	3.34	3.71	3.91	3.85	3.70	3.70
Fe	0.98	0.29	0.02	0.01	0.01	0.02	0.81	0.26	0.08	0.14	0.26	0.26
Mn	0.00	0.01	0.01	0.01	0.01	0.02	0.01	0.00	0.00	0.00	0.00	0.00
Mg	0.41	0.95	0.00	0.00	0.00	0.00	0.00	0.02	0.04	0.00	0.00	0.00
Ca	3.94	3.67	4.02	4.15	4.07	4.41	4.10	3.84	4.08	4.17	4.17	4.17
Na	0.00	0.00	0.01	0.01	0.01	0.01	0.01	0.26	0.09	0.02	0.04	0.04
K	0.00	0.00	0.01	0.00	0.00	0.00	0.00	0.01	0.01	0.00	0.00	0.00
Σ cations	15.00	14.91	14.54	14.60	14.57	14.75	14.82	14.71	14.65	14.64	14.69	14.69

Prehnite EMPA-data, continuation:

stab 7

Mineral Sample	prh EH0401	prh EH0401	prh EH0401	prh EH0401	prh EH0401	prh S1025B	prh S1025B	prh S1025B
SiO2	42.78	43.20	43.13	43.34	43.00	42.91	43.13	39.92
TiO2	0.00	0.00	0.00	0.04	0.00	0.00	0.00	0.00
Al2O3	18.23	22.80	22.54	22.32	22.16	21.75	20.82	24.31
FeO	6.56	0.06	0.60	0.10	0.55	2.30	2.16	8.72
MnO	0.07	0.06	0.00	0.07	0.09	0.00	0.00	0.00
MgO	0.05	0.00	0.02	0.00	0.01	1.02	0.12	0.98
CaO	24.84	26.09	25.72	25.69	25.55	25.56	26.55	20.89
Na2O	0.03	0.03	0.09	0.00	0.08	0.00	0.05	1.12
K2O	0.00	0.00	0.01	0.01	0.02	0.01	0.02	0.00
total	92.55	92.24	92.10	91.58	91.45	93.53	92.85	95.93
Si	6.56	6.42	6.43	6.48	6.46	6.36	6.46	5.92
Ti	0.00	0.00	0.00	0.01	0.00	0.00	0.00	0.00
Al	3.29	3.99	3.96	3.93	3.92	3.80	3.67	4.25
Fe	0.84	0.01	0.07	0.01	0.07	0.29	0.27	1.08
Mn	0.01	0.01	0.00	0.01	0.01	0.00	0.00	0.00
Mg	0.01	0.00	0.00	0.00	0.00	0.23	0.03	0.22
Ca	4.08	4.15	4.11	4.11	4.11	4.06	4.26	3.32
Na	0.01	0.01	0.03	0.00	0.02	0.00	0.01	0.32
K	0.00	0.00	0.00	0.00	0.00	0.00	0.00	0.00
Σ cations	14.80	14.59	14.60	14.56	14.60	14.74	14.71	15.11

Prehnite EMPA-data – end.



## Phyllosilicate EMPA data

Sample	AH813	AH823v	AH823v	C8913	C8922	C8931	C8933b	C8933b	C8933b	C8933b	C8933b
Min	cln	cln	cln	cln	cln	cln	cln	cln	cln	cln	cln
SiO2	32.31	32.80	30.33	31.41	34.11	32.96	32.84	32.20	32.59	32.53	31.85
TiO2	0.00	0.00	0.00	0.00	0.00	0.03	0.00	0.00	0.00	0.00	0.00
Al2O3	14.03	14.63	14.09	15.03	13.00	14.42	14.44	14.26	13.36	14.39	13.89
FeO	12.62	13.31	13.11	16.65	7.34	9.89	10.89	11.06	10.43	11.35	11.42
MnO	0.31	0.29	0.30	0.40	0.29	0.34	0.31	0.33	0.40	0.37	0.33
MgO	24.29	24.53	23.36	20.99	29.73	26.20	26.80	26.58	27.16	26.86	26.73
CaO	0.35	0.08	1.29	0.55	1.07	0.36	0.07	0.12	0.06	0.11	0.08
Na2O	0.02	0.05	0.02	0.00	0.05	0.00	0.00	0.00	0.02	0.00	0.02
K2O	0.04	0.01	0.05	0.03	0.07	0.02	0.01	0.00	0.00	0.00	0.00
Total	83.97	85.70	82.55	85.06	85.66	84.22	85.36	84.55	84.02	85.61	84.32
Si	6.61	6.58	6.38	6.49	6.67	6.62	6.54	6.49	6.59	6.48	6.46
Ti	0.00	0.00	0.00	0.00	0.00	0.00	0.00	0.00	0.00	0.00	0.00
Al(tot)	3.38	3.46	3.49	3.66	3.00	3.41	3.39	3.39	3.18	3.38	3.32
Fe2+	2.16	2.23	2.31	2.88	1.20	1.66	1.81	1.86	1.76	1.89	1.94
Mn	0.05	0.05	0.05	0.07	0.05	0.06	0.05	0.06	0.07	0.06	0.06
Mg	7.41	7.34	7.33	6.46	8.67	7.84	7.96	7.99	8.19	7.98	8.08
Ca	0.08	0.02	0.29	0.12	0.22	0.08	0.01	0.03	0.01	0.02	0.02
Na	0.02	0.04	0.02	0.00	0.04	0.00	0.00	0.00	0.02	0.00	0.02
K	0.01	0.00	0.01	0.01	0.02	0.01	0.00	0.00	0.00	0.00	0.00
Cations	19.71	19.71	19.89	19.69	19.86	19.68	19.77	19.81	19.82	19.83	19.89

Sample	C8938	C8938	C8938	C8938	C8938	C8938	C8938	C8938	C8938	C8938	C8938
Min	cln	cln	cln	cln	cln	cln	cln	cln	cln	cln	cln
SiO2	31.34	30.59	32.10	30.95	30.59	32.27	31.94	32.33	31.88	29.93	30.54
TiO2	0.00	0.07	0.00	0.06	0.00	0.16	0.05	0.08	0.00	0.00	0.00
Al2O3	17.51	15.47	15.54	17.46	15.84	15.31	15.38	16.39	15.32	14.64	15.08
FeO	15.93	14.21	13.61	16.28	14.95	13.85	13.14	13.84	13.04	13.17	13.03
MnO	0.57	0.41	0.43	0.54	0.57	0.60	0.52	0.44	0.54	0.45	0.56
MgO	20.83	21.10	23.11	20.74	21.10	23.42	23.40	24.35	24.58	23.97	25.12
CaO	0.44	0.47	0.51	0.44	0.71	0.50	0.38	0.39	0.47	0.55	0.49
Na2O	0.01	0.01	0.00	0.03	0.02	0.04	0.12	0.06	0.02	0.01	0.05
K2O	0.02	0.02	0.01	0.00	0.03	0.05	0.04	0.03	0.08	0.05	0.05
Total	86.65	82.35	85.31	86.50	83.81	86.20	84.97	87.91	85.93	82.77	84.92
Si	6.31	6.45	6.49	6.26	6.37	6.48	6.47	6.35	6.40	6.28	6.23
Ti	0.00	0.01	0.00	0.01	0.00	0.02	0.01	0.01	0.00	0.00	0.00
Al(tot)	4.16	3.84	3.70	4.16	3.89	3.62	3.67	3.79	3.63	3.62	3.63
Fe2+	2.68	2.50	2.30	2.75	2.60	2.32	2.23	2.27	2.19	2.31	2.22
Mn	0.10	0.07	0.07	0.09	0.10	0.10	0.09	0.07	0.09	0.08	0.10
Mg	6.26	6.63	6.97	6.26	6.55	7.01	7.07	7.13	7.36	7.49	7.64
Ca	0.09	0.11	0.11	0.10	0.16	0.11	0.08	0.08	0.10	0.12	0.11
Na	0.01	0.01	0.00	0.02	0.02	0.03	0.09	0.05	0.02	0.01	0.04
K	0.01	0.01	0.00	0.00	0.01	0.01	0.01	0.01	0.02	0.01	0.01
Cations	19.61	19.63	19.66	19.66	19.70	19.71	19.73	19.77	19.80	19.92	19.98

## Phyllosilicate EMPA data, continuation:

Sample Min	C8940b cln	C8940b cln	C8940b cln	C8940b cln	C8940b cln	C8940b cln	C8940b cln	C1125b cln	C1125b cln	C1125b cln	C1125b cln
SiO2	33.13	29.51	31.82	32.56	31.97	30.21	30.32	30.21	30.21	29.9	29.9
TiO2	0	0	0	0	0	0	0	0	0	0	0
Al2O3	14.21	15.75	12.81	12.8	12.72	14.88	16.39	14.88	14.88	15.36	15.36
FeO	14.75	16.32	10.78	10.84	10.82	16.63	16.87	16.63	16.63	18.71	18.71
MnO	0.44	0.54	0.41	0.36	0.35	0.68	0.68	0.68	0.68	0.41	0.41
MgO	22.95	20.82	26.24	27.05	26.94	21.52	22.34	21.52	21.52	21.21	21.21
CaO	0.5	0.47	0.05	0.04	0.06	0.39	0.31	0.39	0.39	0.42	0.42
Na2O	0.02	0.01	0.01	0.02	0	0.05	0.04	0.05	0.05	0.05	0.05
K2O	0.12	0.06	0.02	0	0.01	0.13	0.1	0.13	0.13	0.08	0.08
Total	86.12	83.48	82.14	83.67	82.87	84.49	87.05	84.49	84.49	86.14	86.14
Si	6.68	6.23	6.61	6.63	6.58	6.32	6.15	6.32	6.32	6.19	6.19
Ti	0.00	0.00	0.00	0.00	0.00	0.00	0.00	0.00	0.00	0.00	0.00
Al(tot)	3.37	3.92	3.13	3.07	3.09	3.67	3.92	3.67	3.67	3.75	3.75
Fe2+	2.49	2.88	1.87	1.85	1.86	2.91	2.86	2.91	2.91	3.24	3.24
Mn	0.08	0.10	0.07	0.06	0.06	0.12	0.12	0.12	0.12	0.07	0.07
Mg	6.89	6.56	8.12	8.21	8.27	6.71	6.75	6.71	6.71	6.55	6.55
Ca	0.11	0.11	0.01	0.01	0.01	0.09	0.07	0.09	0.09	0.09	0.09
Na	0.02	0.01	0.01	0.02	0.00	0.04	0.03	0.04	0.04	0.04	0.04
K	0.03	0.02	0.01	0.00	0.00	0.03	0.03	0.03	0.03	0.02	0.02
Cations	19.66	19.82	19.83	19.84	19.88	19.89	19.92	19.89	19.89	19.96	19.96

Sample Min	C1125b cln	C1125b cln	C11430v cln	C11483b cln	C11483b cln	C11483b cln	D5614 cln	D5614 cln	D5614 cln	D5620v cln	D5707v cln
SiO2	29.66	29.66	34.08	32.51	33.48	31.9	32.61	32.36	32.23	33.78	32.87
TiO2	0	0	0	0	0	0	0	0	0	0	0
Al2O3	15.44	15.44	10.75	11.03	12.04	11.73	15.04	15.57	15.4	11.69	16.15
FeO	18.29	18.29	19.62	11.92	14.5	15.27	9.02	12.77	12.17	19.53	10.91
MnO	0.59	0.59	0.15	0.23	0.14	0.07	0.32	0.22	0.28	0.04	0.33
MgO	21.6	21.6	21.31	24.46	24.59	25.45	25.64	25.27	25.59	21.12	25.46
CaO	0.4	0.4	0.34	0.67	0.38	0.19	0.24	0.24	0.28	0.37	0.28
Na2O	0.05	0.05	0	0.07	0.03	0.02	0.04	0.03	0.03	0.04	0.01
K2O	0.12	0.12	0	0	0	0	0.07	0.13	0.12	0.14	0
Total	86.15	86.15	86.25	80.89	85.16	84.63	82.98	86.59	86.1	86.71	86.01
Si	6.14	6.14	7.03	6.90	6.81	6.59	6.61	6.42	6.41	6.92	6.48
Ti	0.00	0.00	0.00	0.00	0.00	0.00	0.00	0.00	0.00	0.00	0.00
Al(tot)	3.77	3.77	2.61	2.76	2.89	2.86	3.59	3.64	3.61	2.82	3.75
Fe2+	3.17	3.17	3.38	2.11	2.47	2.64	1.53	2.12	2.03	3.35	1.80
Mn	0.10	0.10	0.03	0.04	0.02	0.01	0.05	0.04	0.05	0.01	0.06
Mg	6.67	6.67	6.55	7.74	7.46	7.84	7.74	7.47	7.59	6.45	7.49
Ca	0.09	0.09	0.08	0.15	0.08	0.04	0.05	0.05	0.06	0.08	0.06
Na	0.04	0.04	0.00	0.06	0.02	0.02	0.03	0.02	0.02	0.03	0.01
K	0.03	0.03	0.00	0.00	0.00	0.00	0.02	0.03	0.03	0.04	0.00
Cations	20.01	20.01	19.67	19.75	19.76	19.99	19.62	19.79	19.81	19.70	19.64

## Phyllosilicate EMPA data, continuation:

Sample	D5707v	D5707v	D5707v	D5707v	D5714	D5714	D5714	D5724b	D5742vb	D5742vb	D5742vb
Min	cln	cln	cln	cln	cln	cln	cln	cln	cln	cln	cln
SiO2	31.62	31.58	30.42	29.4	32.28	30.48	29.89	32.36	33.68	32.46	31.18
TiO2	0	0	0.05	0	0	0	0	0	0	0	0
Al2O3	15.39	15.72	14.53	14.8	15.02	16.76	17.72	14.45	14.1	13.95	14.22
FeO	10.6	11.04	11.04	10.78	7.89	7.8	8.3	11.39	8.39	8.65	7.6
MnO	0.34	0.23	0.42	0.36	0.41	0.35	0.47	0.48	0.23	0.29	0.25
MgO	24.66	25.09	23.82	25.03	28.29	28.7	28.55	25.25	27.44	26.91	27.69
CaO	0.24	0.28	0.3	0.14	0.16	0.13	0.19	0.58	0.42	0.35	0.27
Na2O	0.01	0.04	0.1	0.03	0	0.01	0	0.06	0.03	0.04	0.01
K2O	0.02	0	0.02	0	0	0	0	0	0.01	0	0.02
Total	82.88	83.98	80.7	80.54	84.05	84.23	85.12	84.57	84.3	82.65	81.24
Si	6.48	6.40	6.44	6.25	6.44	6.08	5.93	6.54	6.69	6.60	6.44
Ti	0.00	0.00	0.01	0.00	0.00	0.00	0.00	0.00	0.00	0.00	0.00
Al(tot)	3.72	3.75	3.63	3.71	3.53	3.94	4.14	3.44	3.30	3.34	3.46
Fe2+	1.82	1.87	1.95	1.91	1.32	1.30	1.38	1.92	1.39	1.47	1.31
Mn	0.06	0.04	0.08	0.06	0.07	0.06	0.08	0.08	0.04	0.05	0.04
Mg	7.53	7.58	7.52	7.93	8.41	8.54	8.44	7.61	8.13	8.16	8.52
Ca	0.05	0.06	0.07	0.03	0.03	0.03	0.04	0.13	0.09	0.08	0.06
Na	0.01	0.03	0.08	0.02	0.00	0.01	0.00	0.05	0.02	0.03	0.01
K	0.01	0.00	0.01	0.00	0.00	0.00	0.00	0.00	0.00	0.00	0.01
Cations	19.67	19.74	19.78	19.91	19.80	19.95	20.00	19.76	19.67	19.74	19.84

Sample	EH410	EH410	EH410	EH410	EH410	EH410	EH410	EH410	EH410	EH410	EH410
Min	cln	cln	cln	cln	cln	cln	cln	cln	cln	cln	cln
SiO2	31.23	29.64	31.93	30.98	28.68	30.45	31.38	29.74	30.37	30.75	29.33
TiO2	0.01	0.05	0.04	0.03	0	0	0	0.01	0.04	0.06	0
Al2O3	14.84	16.98	16.07	14.85	17	15.36	15.09	17.47	15.55	15.52	16.57
FeO	19.64	22.17	20.52	20.55	22.18	20.98	20.4	21.67	20.92	20.25	22.34
MnO	0.39	0.54	0.62	0.43	0.5	0.48	0.44	0.47	0.4	0.43	0.52
MgO	19.28	16.59	19.4	18.77	16.4	18.13	19.65	17.96	18.79	19.72	17.26
CaO	0.46	0.38	0.46	0.39	0.23	0.33	0.29	0.36	0.36	0.51	0.38
Na2O	0	0.05	0.06	0.04	0	0.05	0.07	0.02	0.03	0.02	0.06
K2O	0.06	0.04	0.05	0.08	0.05	0.06	0.04	0.09	0.13	0.08	0.06
Total	85.91	86.44	89.15	86.12	85.04	85.84	87.36	87.79	86.59	87.34	86.52
Si	6.49	6.21	6.41	6.46	6.12	6.39	6.43	6.12	6.31	6.31	6.16
Ti	0.00	0.01	0.01	0.00	0.00	0.00	0.00	0.00	0.01	0.01	0.00
Al(tot)	3.63	4.19	3.80	3.65	4.28	3.80	3.64	4.23	3.81	3.76	4.10
Fe2+	3.41	3.88	3.44	3.58	3.96	3.68	3.50	3.73	3.64	3.48	3.92
Mn	0.07	0.10	0.11	0.08	0.09	0.09	0.08	0.08	0.07	0.07	0.09
Mg	5.97	5.18	5.80	5.83	5.22	5.67	6.00	5.51	5.82	6.04	5.40
Ca	0.10	0.09	0.10	0.09	0.05	0.07	0.06	0.08	0.08	0.11	0.09
Na	0.00	0.04	0.05	0.03	0.00	0.04	0.06	0.02	0.02	0.02	0.05
K	0.02	0.01	0.01	0.02	0.01	0.02	0.01	0.02	0.03	0.02	0.02
Cations	19.70	19.71	19.72	19.74	19.74	19.74	19.78	19.79	19.80	19.82	19.82

## Phyllosilicate EMPA data, continuation:

Sample	EH410	EH410	EH410	EH410	EH410	EH410	EH410	EH410	EH410	EH410	EH410
Min	cln	cln	cln	cln	cln	cln	cln	cln	cln	cln	cln
SiO2	29.99	32.38	30.18	30.05	31.23	29.67	30.47	28.69	29.05	29.43	29.38
TiO2	0.01	0.06	0.03	0.00	0.00	0.01	0.05	0.04	0.01	0.00	0.00
Al2O3	15.88	14.36	15.25	16.31	15.14	16.01	13.79	15.03	15.53	15.46	16.67
FeO	20.11	16.91	20.76	20.49	20.46	19.77	19.46	21.69	23.12	22.81	21.94
MnO	0.37	0.56	0.58	0.52	0.43	0.38	0.43	0.38	0.46	0.49	0.49
MgO	19.24	23.57	18.98	19.11	19.86	18.91	20.43	17.36	17.38	17.99	18.39
CaO	0.30	0.23	0.40	0.37	0.51	0.61	0.22	0.36	0.17	0.13	0.37
Na2O	0.05	0.00	0.04	0.06	0.08	0.07	0.00	0.03	0.00	0.00	0.01
K2O	0.06	0.00	0.06	0.08	0.11	0.15	0.01	0.08	0.02	0.01	0.05
Total	86.01	88.07	86.28	86.99	87.82	85.58	84.86	83.66	85.74	86.32	87.30
Si	6.25	6.47	6.30	6.21	6.38	6.22	6.43	6.23	6.19	6.21	6.10
Ti	0.00	0.01	0.00	0.00	0.00	0.00	0.01	0.01	0.00	0.00	0.00
Al(tot)	3.90	3.38	3.75	3.97	3.64	3.95	3.43	3.85	3.90	3.85	4.08
Fe2+	3.50	2.82	3.63	3.54	3.49	3.47	3.43	3.94	4.12	4.03	3.81
Mn	0.07	0.09	0.10	0.09	0.07	0.07	0.08	0.07	0.08	0.09	0.09
Mg	5.98	7.02	5.91	5.88	6.05	5.91	6.43	5.62	5.52	5.66	5.69
Ca	0.07	0.05	0.09	0.08	0.11	0.14	0.05	0.08	0.04	0.03	0.08
Na	0.04	0.00	0.03	0.05	0.06	0.06	0.00	0.03	0.00	0.00	0.01
K	0.02	0.00	0.02	0.02	0.03	0.04	0.00	0.02	0.01	0.00	0.01
Cationes	19.83	19.84	19.84	19.84	19.84	19.85	19.85	19.86	19.86	19.87	19.87

Sample	EH410	EH410	EH410	EH410	EH410	EH410	EH410	EH410	EH410	EH410	EH410
Min	cln	cln	cln	cln	cln	cln	cln	cln	cln	cln	cln
SiO2	29.63	31.21	28.32	29.63	29.40	31.17	28.28	28.34	30.17	29.32	29.30
TiO2	0.00	0.00	0.00	0.16	0.00	0.00	0.00	0.00	0.00	0.01	0.03
Al2O3	15.05	13.57	15.68	15.51	15.52	14.21	16.39	15.88	14.41	16.81	14.44
FeO	22.28	17.96	22.07	22.22	21.14	18.63	23.32	22.74	19.89	22.11	21.73
MnO	0.51	0.34	0.42	0.67	0.50	0.40	0.51	0.22	0.44	0.55	0.45
MgO	18.08	22.20	17.12	18.41	18.32	21.97	16.78	17.40	20.00	18.45	18.60
CaO	0.30	0.24	0.36	0.26	0.39	0.23	0.25	0.19	0.48	0.24	0.31
Na2O	0.03	0.00	0.03	0.03	0.09	0.00	0.00	0.00	0.02	0.06	0.01
K2O	0.08	0.03	0.07	0.03	0.05	0.03	0.07	0.05	0.09	0.07	0.04
Total	85.96	85.55	84.07	86.92	85.41	86.64	85.60	84.82	85.50	87.62	84.91
Si	6.27	6.47	6.14	6.20	6.22	6.40	6.05	6.10	6.34	6.07	6.27
Ti	0.00	0.00	0.00	0.03	0.00	0.00	0.00	0.00	0.00	0.00	0.00
Al(tot)	3.75	3.31	4.01	3.82	3.87	3.44	4.14	4.03	3.57	4.10	3.64
Fe2+	3.94	3.11	4.00	3.89	3.74	3.20	4.17	4.09	3.49	3.83	3.89
Mn	0.09	0.06	0.08	0.12	0.09	0.07	0.09	0.04	0.08	0.10	0.08
Mg	5.70	6.86	5.53	5.74	5.78	6.72	5.36	5.58	6.27	5.69	5.93
Ca	0.07	0.05	0.08	0.06	0.09	0.05	0.06	0.04	0.11	0.05	0.07
Na	0.02	0.00	0.03	0.02	0.07	0.00	0.00	0.00	0.02	0.05	0.01
K	0.02	0.01	0.02	0.01	0.01	0.01	0.02	0.01	0.02	0.02	0.01
Cationes	19.88	19.88	19.88	19.88	19.88	19.89	19.89	19.90	19.90	19.91	19.91

## Phyllosilicate EMPA data, continuation:

Sample	EH410	EH410	EH410	EH410	EH410	EH410	EH411V	EH411V	EH426I	EH426I	EH426I
Min	cln	cln	cln	cln	cln	cln	cln	cln	cln	cln	cln
SiO2	28.91	28.71	28.80	27.95	29.51	28.64	24.88	26.31	30.09	29.56	28.44
TiO2	0.00	0.00	0.00	0.00	0.00	0.00	0.00	0.00	0.00	0.00	0
Al2O3	15.10	15.23	14.77	16.11	13.41	16.08	17.45	13.53	15.19	14.39	15.86
FeO	20.77	24.30	23.14	24.85	22.74	23.34	19.33	17.01	23.32	24.00	25.11
MnO	0.39	0.18	0.41	0.43	0.41	0.42	0.36	0.24	0.57	0.34	0.39
MgO	18.73	17.11	17.94	16.53	18.98	18.48	14.44	16.05	16.78	17.22	16.34
CaO	0.35	0.10	0.08	0.10	0.31	0.16	0.08	0.32	0.46	0.25	0.19
Na2O	0.05	0.02	0.02	0.03	0.00	0.01	0.02	0.10	0.00	0.01	0.02
K2O	0.08	0.06	0.05	0.06	0.04	0.07	0.00	0.00	0.03	0.03	0.02
Total	84.38	85.71	85.21	86.06	85.40	87.20	76.56	73.56	86.44	85.80	86.37
Si	6.20	6.16	6.19	6.00	6.32	6.01	5.87	6.38	6.36	6.32	6.09
Ti	0.00	0.00	0.00	0.00	0.00	0.00	0.00	0.00	0.00	0.00	0.00
Al(tot)	3.81	3.85	3.74	4.08	3.38	3.98	4.85	3.87	3.78	3.63	4.00
Fe2+	3.72	4.36	4.16	4.46	4.07	4.10	3.81	3.45	4.12	4.29	4.49
Mn	0.07	0.03	0.07	0.08	0.07	0.07	0.07	0.05	0.10	0.06	0.07
Mg	5.98	5.47	5.75	5.29	6.06	5.78	5.08	5.80	5.28	5.49	5.21
Ca	0.08	0.02	0.02	0.02	0.07	0.04	0.02	0.08	0.10	0.06	0.04
Na	0.04	0.02	0.02	0.02	0.00	0.01	0.02	0.09	0.00	0.01	0.02
K	0.02	0.02	0.01	0.02	0.01	0.02	0.00	0.00	0.01	0.01	0.01
Cationes	19.93	19.93	19.96	19.98	19.99	20.01	19.72	19.73	19.76	19.87	19.93

Sample	EH426I	EH426I	EH426I	EH426I	EH426I	EH426I	EH49b	EH49b	EH49b	EH49b	EH49b
Min	cln	cln	cln	cln	cln	cln	cln	cln	cln	cln	cln
SiO2	28.26	28.99	28.74	28.58	28.20	27.90	29.40	29.18	29.04	27.99	29.9
TiO2	0.00	0.00	0.00	0.00	0.00	0.00	0.00	0.05	0.04	0.12	0
Al2O3	15.30	15.45	15.21	15.19	14.92	15.05	19.37	19.51	17.96	21.07	16.75
FeO	25.27	25.83	25.19	25.56	25.05	26.30	13.73	14.32	28.85	15.31	28.33
MnO	0.50	0.47	0.62	0.38	0.36	0.44	0.66	0.93	0.38	0.88	0.27
MgO	16.23	16.88	16.75	17.02	17.20	16.53	20.43	19.94	12.28	19.50	13.45
CaO	0.06	0.15	0.16	0.07	0.05	0.04	0.23	0.21	0.34	0.16	0.2
Na2O	0.00	0.01	0.03	0.00	0.01	0.00	0.01	0.01	0.00	0.01	0.04
K2O	0.00	0.00	0.00	0.01	0.02	0.00	0.07	0.07	0.06	0.09	0.07
Total	85.62	87.78	86.70	86.81	85.81	86.26	83.90	84.22	88.95	85.13	89.01
Si	6.12	6.12	6.14	6.10	6.09	6.03	6.06	6.02	6.11	5.75	6.26
Ti	0.00	0.00	0.00	0.00	0.00	0.00	0.00	0.01	0.01	0.02	0.00
Al(tot)	3.90	3.84	3.83	3.82	3.79	3.84	4.71	4.74	4.45	5.10	4.13
Fe2+	4.57	4.56	4.50	4.56	4.52	4.76	2.37	2.47	5.08	2.63	4.96
Mn	0.09	0.08	0.11	0.07	0.07	0.08	0.12	0.16	0.07	0.15	0.05
Mg	5.24	5.31	5.33	5.42	5.53	5.33	6.28	6.13	3.85	5.97	4.20
Ca	0.01	0.03	0.04	0.02	0.01	0.01	0.05	0.05	0.08	0.04	0.04
Na	0.00	0.01	0.02	0.00	0.01	0.00	0.01	0.01	0.00	0.01	0.03
K	0.00	0.00	0.00	0.00	0.01	0.00	0.02	0.02	0.02	0.02	0.02
Cationes	19.93	19.96	19.96	19.99	20.02	20.05	19.60	19.61	19.66	19.70	19.70

## Phyllosilicate EMPA data, continuation:

Sample	EH49b	EH49b	EH49b	EH49b	EH49b	EH49b	EH49b	EH49b	EH49b	EH49b	EH49b
Min	cln	cln	cln	cln	cln	cln	cln	cln	cln	cln	cln
SiO2	28.94	28.84	29.81	29.55	28.18	29.27	30.23	28.44	29.89	30.22	28.54
TiO2	0.00	0.03	0.03	0.00	0.00	0.00	0.03	0.04	0.11	0.00	0.09
Al2O3	18.24	17.73	14.20	14.09	14.67	16.79	16.05	16.92	16.33	15.85	17.84
FeO	30.30	16.26	26.73	27.94	24.33	28.38	27.39	15.68	28.57	27.96	29.72
MnO	0.19	1.01	0.19	0.33	0.14	0.17	0.14	0.71	0.35	0.15	0.24
MgO	12.20	19.54	14.27	13.72	14.23	13.43	15.13	20.04	14.13	14.95	12.81
CaO	0.24	0.14	0.20	0.33	0.22	0.28	0.22	0.12	0.24	0.30	0.33
Na2O	0.02	0.00	0.03	0.00	0.06	0.05	0.00	0.00	0.00	0.00	0.01
K2O	0.01	0.07	0.14	0.00	0.12	0.07	0.10	0.04	0.11	0.06	0.07
Total	90.14	83.62	85.60	85.96	81.95	88.44	89.29	81.99	89.73	89.49	89.65
Si	6.04	6.08	6.47	6.44	6.34	6.18	6.28	6.10	6.23	6.29	5.99
Ti	0.00	0.00	0.00	0.00	0.00	0.00	0.00	0.01	0.02	0.00	0.01
Al(tot)	4.49	4.40	3.63	3.62	3.89	4.18	3.93	4.28	4.01	3.89	4.42
Fe2+	5.29	2.87	4.85	5.09	4.58	5.01	4.76	2.81	4.98	4.86	5.22
Mn	0.03	0.18	0.03	0.06	0.03	0.03	0.02	0.13	0.06	0.03	0.04
Mg	3.80	6.14	4.62	4.46	4.77	4.23	4.69	6.41	4.39	4.64	4.01
Ca	0.05	0.03	0.05	0.08	0.05	0.06	0.05	0.03	0.05	0.07	0.07
Na	0.02	0.00	0.03	0.00	0.05	0.04	0.00	0.00	0.00	0.00	0.01
K	0.00	0.02	0.04	0.00	0.03	0.02	0.03	0.01	0.03	0.02	0.02
Cationes	19.72	19.72	19.74	19.75	19.75	19.76	19.76	19.76	19.77	19.78	19.80

Sample	EH49b	EH49b	EH49b	EH49b	EH49b	EH49b	EH49b	EH49b	EH49b	EH49b	EH49b
Min	cln	cln	cln	cln	cln	cln	cln	cln	cln	cln	cln
SiO2	30.52	27.62	27.16	27.12	29.34	28.78	27.84	27.50	29.46	29.73	28.68
TiO2	0.00	0.03	0.00	0.00	0.14	0.00	0.00	0.00	0.01	0.01	0.08
Al2O3	13.08	18.28	18.85	19.48	16.12	17.66	18.23	19.20	16.10	15.03	17.06
FeO	28.96	29.66	30.84	30.07	28.37	28.47	30.19	30.44	28.54	28.34	29.67
MnO	0.37	0.42	0.25	0.26	0.38	0.37	0.16	0.30	0.29	0.22	0.3
MgO	14.24	11.99	11.24	11.71	14.30	13.58	12.11	12.15	14.52	14.93	13.49
CaO	0.28	0.26	0.19	0.18	0.25	0.40	0.16	0.05	0.24	0.18	0.29
Na2O	0.02	0.03	0.02	0.03	0.02	0.03	0.06	0.01	0.02	0.00	0.04
K2O	0.07	0.03	0.00	0.00	0.00	0.10	0.02	0.00	0.03	0.03	0.03
Total	87.54	88.32	88.55	88.85	88.92	89.39	88.77	89.65	89.21	88.47	89.64
Si	6.56	5.90	5.82	5.76	6.17	6.03	5.92	5.80	6.18	6.29	6.03
Ti	0.00	0.00	0.00	0.00	0.02	0.00	0.00	0.00	0.00	0.00	0.01
Al(tot)	3.31	4.61	4.76	4.88	4.00	4.36	4.57	4.77	3.98	3.75	4.23
Fe2+	5.20	5.30	5.53	5.34	4.99	4.99	5.37	5.37	5.01	5.01	5.21
Mn	0.07	0.08	0.05	0.05	0.07	0.07	0.03	0.05	0.05	0.04	0.05
Mg	4.56	3.82	3.59	3.71	4.49	4.24	3.84	3.82	4.54	4.71	4.23
Ca	0.06	0.06	0.04	0.04	0.06	0.09	0.04	0.01	0.05	0.04	0.07
Na	0.02	0.02	0.02	0.02	0.02	0.02	0.05	0.01	0.02	0.00	0.03
K	0.02	0.01	0.00	0.00	0.00	0.03	0.01	0.00	0.01	0.01	0.01
Cationes	19.80	19.81	19.81	19.81	19.81	19.82	19.82	19.82	19.84	19.84	19.87

## Phyllosilicate EMPA data, continuation:

Sample	EH49b	EH49b	EH49b	EH49b	G710V	G710V	G710V	G710V	G76B	G76B	G76B
Min	cln	cln	cln	cln	cln	cln	cln	cln	cln	cln	cln
SiO2	28.60	27.41	29.25	25.51	30.71	31.82	28.72	28.95	31.02	30.55	30.12
TiO2	0.00	0.10	0.00	0.00	0.00	0.03	0.08	0.05	0.00	0.10	0.03
Al2O3	11.53	17.77	11.34	15.53	14.39	14.38	13.48	13.90	14.83	14.90	15.11
FeO	29.34	29.35	29.48	34.01	13.28	14.20	13.04	14.29	19.79	19.64	20.44
MnO	0.11	0.21	0.04	0.27	0.20	0.40	0.27	0.27	0.47	0.39	0.40
MgO	15.38	12.86	16.04	10.20	24.11	24.78	23.82	23.78	18.65	19.89	19.28
CaO	0.09	0.18	0.09	0.21	0.08	0.08	0.09	0.08	0.80	0.45	0.23
Na2O	0.01	0.32	0.02	0.05	0.02	0.02	0.01	0.01	0.00	0.01	0.02
K2O	0.00	0.40	0.00	0.02	0.02	0.02	0.03	0.00	0.03	0.06	0.03
Total	85.06	88.60	86.26	85.80	82.81	85.73	79.54	81.33	85.59	85.99	85.66
Si	6.39	5.84	6.43	5.82	6.41	6.44	6.27	6.22	6.49	6.36	6.32
Ti	0.00	0.02	0.00	0.00	0.00	0.00	0.01	0.01	0.00	0.02	0.00
Al(tot)	3.04	4.46	2.94	4.18	3.54	3.43	3.47	3.52	3.66	3.65	3.74
Fe2+	5.48	5.23	5.42	6.49	2.32	2.40	2.38	2.57	3.46	3.42	3.59
Mn	0.02	0.04	0.01	0.05	0.04	0.07	0.05	0.05	0.08	0.07	0.07
Mg	5.13	4.09	5.26	3.47	7.50	7.47	7.76	7.62	5.81	6.17	6.03
Ca	0.02	0.04	0.02	0.05	0.02	0.02	0.02	0.02	0.18	0.10	0.05
Na	0.01	0.26	0.02	0.04	0.02	0.02	0.01	0.01	0.00	0.01	0.02
K	0.00	0.11	0.00	0.01	0.01	0.01	0.01	0.00	0.01	0.02	0.01
Cationes	20.09	20.10	20.10	20.11	19.83	19.85	19.99	20.01	19.69	19.81	19.82

Sample	G76B	G76B	G76B	G76B	G76B	G76B	G76B	G76B	G76B	S1025b	S1025b
Min	cln	cln	cln	cln	cln	cln	cln	cln	cln	cln	cln
SiO2	30.90	30.31	29.89	30.16	29.95	30.56	29.34	29.15	27.97	29.97	28.83
TiO2	0.15	0.00	0.00	0.00	0.10	0.15	0.00	0.00	0.00	0.00	0.00
Al2O3	15.16	14.96	14.74	14.90	15.16	14.76	16.02	15.33	15.74	15.45	16.39
FeO	20.18	19.43	20.31	19.89	20.86	19.84	20.54	22.21	23.28	25.67	26.17
MnO	0.39	0.44	0.31	0.35	0.40	0.31	0.36	0.33	0.29	0.21	0.28
MgO	20.19	20.11	19.48	19.91	19.57	20.62	19.26	18.74	18.26	14.52	14.33
CaO	0.32	0.29	0.22	0.36	0.19	0.39	0.25	0.42	0.05	0.59	0.55
Na2O	0.02	0.01	0.01	0.02	0.00	0.00	0.02	0.00	0.02	0.05	0.02
K2O	0.07	0.05	0.01	0.06	0.03	0.08	0.02	0.00	0.00	0.09	0.08
Total	87.38	85.60	84.97	85.65	86.26	86.71	85.81	86.18	85.61	86.55	86.65
Si	6.34	6.33	6.32	6.31	6.26	6.31	6.15	6.15	5.99	6.39	6.17
Ti	0.02	0.00	0.00	0.00	0.02	0.02	0.00	0.00	0.00	0.00	0.00
Al(tot)	3.66	3.68	3.67	3.68	3.73	3.59	3.96	3.81	3.97	3.88	4.13
Fe2+	3.46	3.39	3.59	3.48	3.64	3.43	3.60	3.92	4.17	4.58	4.68
Mn	0.07	0.08	0.06	0.06	0.07	0.05	0.06	0.06	0.05	0.04	0.05
Mg	6.17	6.26	6.14	6.21	6.10	6.35	6.02	5.90	5.83	4.62	4.57
Ca	0.07	0.06	0.05	0.08	0.04	0.09	0.06	0.09	0.01	0.13	0.13
Na	0.02	0.01	0.01	0.02	0.00	0.00	0.02	0.00	0.02	0.04	0.02
K	0.02	0.01	0.00	0.02	0.01	0.02	0.01	0.00	0.00	0.02	0.02
Cationes	19.83	19.84	19.85	19.86	19.87	19.87	19.88	19.94	20.03	19.70	19.78

## Phyllosilicate EMPA data, continuation:

Sample Min	S1025b cln	S1025b cln	S1025b cln	S1025b cln	S1025b cln	S1025b cln	S1025b cln	S1025b cln	S1025b cln	S1025b cln	S1025b cln
SiO2	28.49	30.03	30.01	28.78	28.17	29.93	27.24	28.12	26.88	27.94	27.97
TiO2	0.00	0.00	0.00	0.00	0.00	0.00	0.02	0.00	0.20	0.00	0.00
Al2O3	16.33	16.58	15.34	16.71	16.39	13.84	15.77	15.67	14.78	15.86	12.25
FeO	26.86	26.66	27.05	26.50	27.20	28.09	26.27	26.01	26.13	26.57	26.36
MnO	0.22	0.36	0.36	0.51	0.59	0.67	0.47	0.56	0.69	0.55	0.69
MgO	14.02	15.67	15.27	14.64	14.69	15.51	14.41	15.51	14.21	14.98	15.16
CaO	0.26	0.43	0.65	0.50	0.42	0.25	0.44	0.43	0.47	0.41	0.22
Na2O	0.03	0.01	0.01	0.03	0.01	0.02	0.02	0.00	0.02	0.06	0.04
K2O	0.01	0.06	0.04	0.07	0.01	0.03	0.00	0.01	0.00	0.04	0.00
Total	86.22	89.80	88.73	87.74	87.48	88.34	84.64	86.31	83.38	86.41	82.69
Si	6.15	6.19	6.29	6.10	6.02	6.36	6.02	6.07	6.05	6.04	6.36
Ti	0.00	0.00	0.00	0.00	0.00	0.00	0.00	0.00	0.03	0.00	0.00
Al(tot)	4.15	4.03	3.79	4.17	4.13	3.46	4.11	3.99	3.92	4.04	3.28
Fe2+	4.85	4.59	4.74	4.69	4.86	4.99	4.85	4.69	4.92	4.80	5.01
Mn	0.04	0.06	0.06	0.09	0.11	0.12	0.09	0.10	0.13	0.10	0.13
Mg	4.51	4.82	4.77	4.62	4.68	4.91	4.75	4.99	4.77	4.83	5.14
Ca	0.06	0.09	0.15	0.11	0.10	0.06	0.10	0.10	0.11	0.09	0.05
Na	0.03	0.01	0.01	0.02	0.01	0.02	0.02	0.00	0.02	0.05	0.04
K	0.00	0.02	0.01	0.02	0.00	0.01	0.00	0.00	0.00	0.01	0.00
Cations	19.79	19.81	19.82	19.84	19.92	19.92	19.93	19.94	19.96	19.97	20.02

Sample Min	S1025b cln	S1070v cln	S1070v cln	S1070v cln	S1070v cln	S1070v cln	S1070v cln	S1070v cln	S1070v cln	S1070v cln	S1070v cln
SiO2	26.68	33.13	33.13	34.07	34.07	29.51	29.51	32.26	32.26	30.32	30.32
TiO2	0.00	0.00	0.00	0.00	0.00	0.00	0.00	0.00	0.00	0.00	0.00
Al2O3	15.34	14.21	14.21	10.57	10.57	15.75	15.75	13.46	13.46	16.39	16.39
FeO	26.45	14.75	14.75	17.90	17.90	16.32	16.32	11.64	11.64	16.87	16.87
MnO	0.35	0.44	0.44	0.25	0.25	0.54	0.54	0.46	0.46	0.68	0.68
MgO	15.07	22.95	22.95	22.36	22.36	20.82	20.82	26.61	26.61	22.34	22.34
CaO	0.39	0.50	0.50	0.58	0.58	0.47	0.47	0.11	0.11	0.31	0.31
Na2O	0.01	0.02	0.02	0.00	0.00	0.01	0.01	0.01	0.01	0.04	0.04
K2O	0.02	0.12	0.12	0.02	0.02	0.06	0.06	0.04	0.04	0.10	0.10
Total	84.31	86.12	86.12	85.75	85.75	83.48	83.48	84.59	84.59	87.05	87.05
Si	5.94	6.68	6.68	7.02	7.02	6.23	6.23	6.53	6.53	6.15	6.15
Ti	0.00	0.00	0.00	0.00	0.00	0.00	0.00	0.00	0.00	0.00	0.00
Al(tot)	4.02	3.37	3.37	2.57	2.57	3.92	3.92	3.21	3.21	3.92	3.92
Fe2+	4.92	2.49	2.49	3.08	3.08	2.88	2.88	1.97	1.97	2.86	2.86
Mn	0.07	0.08	0.08	0.04	0.04	0.10	0.10	0.08	0.08	0.12	0.12
Mg	5.00	6.89	6.89	6.86	6.86	6.56	6.56	8.03	8.03	6.75	6.75
Ca	0.09	0.11	0.11	0.13	0.13	0.11	0.11	0.02	0.02	0.07	0.07
Na	0.01	0.02	0.02	0.00	0.00	0.01	0.01	0.01	0.01	0.03	0.03
K	0.01	0.03	0.03	0.01	0.01	0.02	0.02	0.01	0.01	0.03	0.03
Cations	20.06	19.66	19.66	19.70	19.70	19.82	19.82	19.87	19.87	19.92	19.92



## Phyllosilicate EMPA data, continuation:

Sample Min	St724v cln	St724v cln	St724v cln	St724v cln	St77b cln	St77b cln	St77b cln	St77b cln	St77b cln	St77b cln	St77b cln
SiO2	31.16	30.04	29.05	26.34	31.46	30.46	28.09	30.67	30.46	29.78	29.86
TiO2	0.00	0.00	0.00	0.00	0.23	0.00	0.03	0.00	0.00	0.03	0.00
Al2O3	13.97	14.49	15.17	12.99	14.39	14.64	16.24	14.56	14.93	14.52	15.43
FeO	17.45	16.67	16.69	15.04	18.68	18.90	18.13	19.61	19.03	19.36	20.55
MnO	0.36	0.29	0.38	0.59	0.58	0.37	0.52	0.44	0.60	0.50	0.57
MgO	22.90	22.49	21.97	20.16	20.41	19.52	18.07	19.84	19.72	19.57	19.47
CaO	0.22	0.25	0.29	0.27	0.34	0.20	0.16	0.14	0.14	0.12	0.08
Na2O	0.02	0.05	0.02	0.07	0.00	0.00	0.02	0.00	0.04	0.02	0.01
K2O	0.00	0.00	0.03	0.00	0.02	0.04	0.01	0.01	0.02	0.03	0.00
Total	86.08	84.28	83.60	75.46	86.11	84.13	81.27	85.27	84.94	83.93	85.97
Si	6.40	6.29	6.15	6.19	6.50	6.45	6.16	6.43	6.39	6.35	6.25
Ti	0.00	0.00	0.00	0.00	0.04	0.00	0.00	0.00	0.00	0.00	0.00
Al(tot)	3.38	3.57	3.78	3.60	3.50	3.65	4.20	3.60	3.69	3.65	3.81
Fe2+	3.00	2.92	2.95	2.95	3.22	3.35	3.32	3.44	3.34	3.45	3.60
Mn	0.06	0.05	0.07	0.12	0.10	0.07	0.10	0.08	0.11	0.09	0.10
Mg	7.01	7.02	6.93	7.06	6.28	6.16	5.91	6.20	6.17	6.22	6.07
Ca	0.05	0.06	0.07	0.07	0.08	0.05	0.04	0.03	0.03	0.03	0.02
Na	0.02	0.04	0.02	0.06	0.00	0.00	0.02	0.00	0.03	0.02	0.01
K	0.00	0.00	0.01	0.00	0.01	0.01	0.00	0.00	0.01	0.01	0.00
Cations	19.92	19.95	19.97	20.05	19.72	19.73	19.75	19.77	19.78	19.83	19.85

Sample Min	St77b cln	St77b cln	St77b cln	St77b cln	St77b cln	St77b cln
SiO2	27.9	28.7	27.7	29.1	28.9	28.0
TiO2	0.0	0.0	0.0	0.0	0.0	0.0
Al2O3	14.0	17.3	16.9	15.1	14.8	14.7
FeO	19.4	21.8	22.2	21.5	21.5	22.5
MnO	0.5	0.5	0.7	0.6	0.5	0.6
MgO	18.2	18.5	17.0	19.2	19.1	18.6
CaO	0.2	0.1	0.2	0.1	0.1	0.1
Na2O	0.0	0.0	0.0	0.0	0.0	0.0
K2O	0.0	0.0	0.0	0.0	0.0	0.0
Total	80.2	86.9	84.8	85.6	84.8	84.4
Si	6.3	6.0	6.0	6.2	6.2	6.1
Ti	0.0	0.0	0.0	0.0	0.0	0.0
Al(tot)	3.7	4.2	4.3	3.8	3.7	3.8
Fe2+	3.6	3.8	4.0	3.8	3.8	4.1
Mn	0.1	0.1	0.1	0.1	0.1	0.1
Mg	6.1	5.8	5.4	6.1	6.1	6.0
Ca	0.0	0.0	0.0	0.0	0.0	0.0
Na	0.0	0.0	0.0	0.0	0.0	0.0
K	0.0	0.0	0.0	0.0	0.0	0.0
Cations	19.9	19.9	19.9	20.0	20.0	20.1

## Phyllosilicate EMPA data, continuation:

Sample Min	St724v cln	St724v cln	St724v cln	St724v cln	St77b cln	St77b cln	St77b cln	St77b cln	St77b cln	St77b cln	St77b cln
SiO2	31.16	30.04	29.05	26.34	31.46	30.46	28.09	30.67	30.46	29.78	29.86
TiO2	0.00	0.00	0.00	0.00	0.23	0.00	0.03	0.00	0.00	0.03	0.00
Al2O3	13.97	14.49	15.17	12.99	14.39	14.64	16.24	14.56	14.93	14.52	15.43
FeO	17.45	16.67	16.69	15.04	18.68	18.90	18.13	19.61	19.03	19.36	20.55
MnO	0.36	0.29	0.38	0.59	0.58	0.37	0.52	0.44	0.60	0.50	0.57
MgO	22.90	22.49	21.97	20.16	20.41	19.52	18.07	19.84	19.72	19.57	19.47
CaO	0.22	0.25	0.29	0.27	0.34	0.20	0.16	0.14	0.14	0.12	0.08
Na2O	0.02	0.05	0.02	0.07	0.00	0.00	0.02	0.00	0.04	0.02	0.01
K2O	0.00	0.00	0.03	0.00	0.02	0.04	0.01	0.01	0.02	0.03	0.00
Total	86.08	84.28	83.60	75.46	86.11	84.13	81.27	85.27	84.94	83.93	85.97
Si	6.40	6.29	6.15	6.19	6.50	6.45	6.16	6.43	6.39	6.35	6.25
Ti	0.00	0.00	0.00	0.00	0.04	0.00	0.00	0.00	0.00	0.00	0.00
Al(tot)	3.38	3.57	3.78	3.60	3.50	3.65	4.20	3.60	3.69	3.65	3.81
Fe2+	3.00	2.92	2.95	2.95	3.22	3.35	3.32	3.44	3.34	3.45	3.60
Mn	0.06	0.05	0.07	0.12	0.10	0.07	0.10	0.08	0.11	0.09	0.10
Mg	7.01	7.02	6.93	7.06	6.28	6.16	5.91	6.20	6.17	6.22	6.07
Ca	0.05	0.06	0.07	0.07	0.08	0.05	0.04	0.03	0.03	0.03	0.02
Na	0.02	0.04	0.02	0.06	0.00	0.00	0.02	0.00	0.03	0.02	0.01
K	0.00	0.00	0.01	0.00	0.01	0.01	0.00	0.00	0.01	0.01	0.00
Cations	19.92	19.95	19.97	20.05	19.72	19.73	19.75	19.77	19.78	19.83	19.85

Sample Min	St77b cln	St77b cln	St77b cln	St77b cln	St77b cln	St77b cln
SiO2	27.9	28.7	27.7	29.1	28.9	28.0
TiO2	0.0	0.0	0.0	0.0	0.0	0.0
Al2O3	14.0	17.3	16.9	15.1	14.8	14.7
FeO	19.4	21.8	22.2	21.5	21.5	22.5
MnO	0.5	0.5	0.7	0.6	0.5	0.6
MgO	18.2	18.5	17.0	19.2	19.1	18.6
CaO	0.2	0.1	0.2	0.1	0.1	0.1
Na2O	0.0	0.0	0.0	0.0	0.0	0.0
K2O	0.0	0.0	0.0	0.0	0.0	0.0
Total	80.2	86.9	84.8	85.6	84.8	84.4
Si	6.3	6.0	6.0	6.2	6.2	6.1
Ti	0.0	0.0	0.0	0.0	0.0	0.0
Al(tot)	3.7	4.2	4.3	3.8	3.7	3.8
Fe2+	3.6	3.8	4.0	3.8	3.8	4.1
Mn	0.1	0.1	0.1	0.1	0.1	0.1
Mg	6.1	5.8	5.4	6.1	6.1	6.0
Ca	0.0	0.0	0.0	0.0	0.0	0.0
Na	0.0	0.0	0.0	0.0	0.0	0.0
K	0.0	0.0	0.0	0.0	0.0	0.0
Cations	19.9	19.9	19.9	20.0	20.0	20.1

## Phyllosilicate EMPA data, continuation:

Sample	AH813	AH813	C8902	C8902	C8906	C8906	C8906	C8906	C8906	C8906	C8906
Min	corr	corr	corr	corr	corr	corr	corr	corr	corr	corr	corr
SiO2	37.91	37.91	36.32	35.23	36.45	36.46	35.47	35.21	35.69	34.92	35.23
TiO2	0.00	0.00	0.00	0.00	0.00	0.00	0.00	0.00	0.00	0.00	0.00
Al2O3	10.54	10.54	12.24	12.53	12.27	11.88	11.72	12.89	12.08	12.88	12.28
FeO	13.70	13.70	9.81	10.22	9.00	9.24	8.99	8.77	9.11	9.47	9.21
MnO	0.35	0.35	0.33	0.28	0.28	0.38	0.42	0.36	0.26	0.39	0.34
MgO	22.75	22.75	26.12	25.96	24.75	25.16	24.55	25.05	25.15	25.63	26.39
CaO	1.17	1.17	0.82	0.59	0.76	0.82	0.83	0.62	1.33	0.74	0.75
Na2O	0.03	0.03	0.03	0.06	0.05	0.02	0.02	0.03	0.12	0.10	0.06
K2O	0.13	0.13	0.15	0.08	0.14	0.05	0.11	0.05	0.14	0.07	0.06
Total	86.58	86.58	85.82	84.95	83.70	84.01	82.11	82.98	83.88	84.20	84.32
Si	7.50	7.50	7.12	7.00	7.28	7.27	7.24	7.10	7.15	6.98	7.02
Ti	0.00	0.00	0.00	0.00	0.00	0.00	0.00	0.00	0.00	0.00	0.00
Al(tot)	2.46	2.46	2.83	2.93	2.89	2.79	2.82	3.06	2.85	3.03	2.88
Fe <sup>2+</sup>	2.27	2.27	1.61	1.70	1.50	1.54	1.53	1.48	1.53	1.58	1.54
Mn	0.06	0.06	0.05	0.05	0.05	0.06	0.07	0.06	0.04	0.07	0.06
Mg	6.71	6.71	7.64	7.69	7.37	7.48	7.47	7.53	7.51	7.64	7.84
Ca	0.25	0.25	0.17	0.13	0.16	0.18	0.18	0.13	0.29	0.16	0.16
Na	0.02	0.02	0.02	0.05	0.04	0.02	0.02	0.02	0.09	0.08	0.05
K	0.03	0.03	0.04	0.02	0.04	0.01	0.03	0.01	0.04	0.02	0.02
Cationes	19.30	19.30	19.49	19.56	19.32	19.35	19.37	19.39	19.49	19.55	19.57

Sample	C8906	C8913	C8913	C8913	C8913	C8913	C8913	C8913	C8913	C8922	C8922
Min	corr	corr	corr	corr	corr	corr	corr	corr	corr	corr	corr
SiO2	34.85	36.44	35.45	33.88	34.75	34.48	33.74	32.83	33.44	36.82	37.40
TiO2	0.00	0.00	0.00	0.00	0.00	0.00	0.00	0.00	0.00	0.00	0.00
Al2O3	13.26	14.03	12.82	13.43	13.37	13.12	13.46	14.38	13.64	13.78	13.34
FeO	10.13	13.42	13.49	12.58	13.71	13.31	17.21	15.68	17.19	7.23	7.33
MnO	0.30	0.31	0.32	0.29	0.33	0.23	0.44	0.23	0.37	0.25	0.24
MgO	25.19	22.27	22.33	22.31	22.30	23.08	20.74	21.78	21.43	25.48	26.07
CaO	1.04	1.07	0.92	0.84	0.89	0.99	0.91	0.75	0.94	0.79	0.79
Na2O	0.11	0.13	0.00	0.00	0.02	0.04	0.02	0.01	0.05	0.05	0.03
K2O	0.20	0.09	0.06	0.02	0.02	0.08	0.10	0.02	0.07	0.04	0.03
Total	85.08	87.76	85.39	83.35	85.39	85.33	86.62	85.68	87.13	84.44	85.23
Si	6.93	7.09	7.12	6.95	6.99	6.94	6.84	6.68	6.75	7.20	7.25
Ti	0.00	0.00	0.00	0.00	0.00	0.00	0.00	0.00	0.00	0.00	0.00
Al(tot)	3.11	3.22	3.03	3.25	3.17	3.11	3.22	3.45	3.24	3.18	3.05
Fe2+	1.68	2.18	2.27	2.16	2.31	2.24	2.92	2.67	2.90	1.18	1.19
Mn	0.05	0.05	0.05	0.05	0.06	0.04	0.08	0.04	0.06	0.04	0.04
Mg	7.46	6.46	6.69	6.83	6.69	6.93	6.27	6.60	6.45	7.43	7.53
Ca	0.22	0.22	0.20	0.18	0.19	0.21	0.20	0.16	0.20	0.17	0.16
Na	0.08	0.10	0.00	0.00	0.02	0.03	0.02	0.01	0.04	0.04	0.02
K	0.05	0.02	0.02	0.01	0.01	0.02	0.03	0.01	0.02	0.01	0.01
Cationes	19.59	19.36	19.37	19.43	19.43	19.53	19.57	19.61	19.66	19.24	19.24

## Phyllosilicate EMPA data, continuation:

Sample	C8922	C8922	C8922	C8922	C8922	C8928	C8928	C8928	C8928	C8928	C8931
Min	corr	corr	corr	corr	corr	corr	corr	corr	corr	corr	corr
SiO2	35.04	35.98	35.91	37.12	32.54	36.89	36.05	35.10	35.97	35.24	36.46
TiO2	0.00	0.00	0.00	0.00	0.00	0.09	0.04	0.00	0.00	0.00	0.09
Al2O3	15.94	13.94	13.55	13.44	17.12	13.77	13.46	12.98	13.47	14.01	13.50
FeO	8.67	7.42	7.67	7.27	9.26	7.11	7.23	6.66	7.06	6.95	10.25
MnO	0.34	0.24	0.42	0.30	0.24	0.33	0.24	0.22	0.27	0.26	0.29
MgO	23.63	25.38	25.36	27.36	23.51	26.69	27.68	27.04	27.43	28.55	25.41
CaO	0.85	0.72	0.95	0.88	0.53	0.89	0.79	0.71	0.72	0.58	0.88
Na2O	0.02	0.00	0.04	0.03	0.01	0.08	0.01	0.06	0.10	0.00	0.02
K2O	0.01	0.02	0.05	0.08	0.02	0.06	0.06	0.07	0.06	0.09	0.08
Total	84.50	83.70	83.95	86.48	83.23	85.91	85.56	82.84	85.08	85.68	86.98
Si	6.91	7.11	7.11	7.11	6.56	7.10	6.99	7.01	7.00	6.83	7.06
Ti	0.00	0.00	0.00	0.00	0.00	0.01	0.01	0.00	0.00	0.00	0.01
Al(tot)	3.70	3.25	3.16	3.03	4.07	3.12	3.08	3.06	3.09	3.20	3.08
Fe2+	1.43	1.23	1.27	1.16	1.56	1.14	1.17	1.11	1.15	1.13	1.66
Mn	0.06	0.04	0.07	0.05	0.04	0.05	0.04	0.04	0.04	0.04	0.05
Mg	6.95	7.48	7.48	7.81	7.06	7.66	8.00	8.05	7.96	8.25	7.33
Ca	0.18	0.15	0.20	0.18	0.11	0.18	0.16	0.15	0.15	0.12	0.18
Na	0.02	0.00	0.03	0.02	0.01	0.06	0.01	0.05	0.08	0.00	0.02
K	0.00	0.01	0.01	0.02	0.01	0.01	0.01	0.02	0.01	0.02	0.02
Cations	19.25	19.27	19.33	19.39	19.42	19.36	19.48	19.49	19.49	19.58	19.41

Sample	C8931	C8931	C8938	C8938	C8938	C8938	C8938	C8938	C8938	C8938	C8938
Min	corr	corr	corr	corr	corr	corr	corr	corr	corr	corr	corr
SiO2	35.35	36.06	34.17	33.71	34.21	33.77	34.36	31.25	32.45	32.16	32.16
TiO2	0.00	0.03	0.14	0.04	0.03	0.00	0.00	0.01	0.00	0.10	0.10
Al2O3	13.12	13.85	14.27	14.91	13.84	14.88	14.74	17.14	15.38	15.15	15.15
FeO	10.00	10.15	14.59	13.86	13.81	13.88	13.64	15.66	13.65	13.67	13.67
MnO	0.40	0.33	0.56	0.51	0.52	0.59	0.59	0.54	0.55	0.56	0.56
MgO	24.36	25.42	21.46	21.87	22.26	22.32	22.92	20.36	21.57	21.42	21.42
CaO	0.97	0.84	0.95	0.62	0.89	0.93	0.83	0.36	0.47	0.49	0.49
Na2O	0.04	0.02	0.02	0.02	0.04	0.03	0.03	0.01	0.13	0.17	0.17
K2O	0.11	0.06	0.03	0.05	0.10	0.04	0.12	0.02	0.02	0.01	0.01
Total	84.35	86.76	86.19	85.59	85.70	86.44	87.23	85.35	84.22	83.73	83.73
Si	7.07	7.00	6.86	6.78	6.88	6.74	6.78	6.38	6.64	6.62	6.62
Ti	0.00	0.00	0.02	0.01	0.00	0.00	0.00	0.00	0.00	0.02	0.02
Al(tot)	3.09	3.17	3.38	3.53	3.28	3.50	3.43	4.12	3.71	3.68	3.68
Fe2+	1.67	1.65	2.45	2.33	2.32	2.32	2.25	2.67	2.33	2.35	2.35
Mn	0.07	0.05	0.10	0.09	0.09	0.10	0.10	0.09	0.10	0.10	0.10
Mg	7.26	7.35	6.42	6.56	6.68	6.64	6.74	6.20	6.58	6.58	6.58
Ca	0.21	0.17	0.20	0.13	0.19	0.20	0.18	0.08	0.10	0.11	0.11
Na	0.03	0.02	0.02	0.02	0.03	0.02	0.02	0.01	0.10	0.14	0.14
K	0.03	0.01	0.01	0.01	0.03	0.01	0.03	0.01	0.01	0.00	0.00
Cations	19.42	19.43	19.45	19.46	19.50	19.53	19.53	19.56	19.56	19.59	19.59

## Phyllosilicate EMPA data, continuation:

Sample	C8938	C8938	C8938	C8938	C8938	C8940b	C8940b	C8940b	C8940b	C897A	C897A
Min	corr	corr	corr	corr	corr	corr	corr	corr	corr	corr	corr
SiO2	32.72	33.07	32.28	32.28	32.71	33.58	33.58	31.45	33.02	36.26	35.71
TiO2	0.03	0.00	0.05	0.05	0.13	0.00	0.00	0.00	0.00	0.00	0.00
Al2O3	15.62	15.75	15.07	15.07	15.17	13.80	13.80	13.47	14.16	12.99	13.67
FeO	13.44	13.37	13.70	13.70	13.16	14.76	14.76	14.31	14.90	9.86	9.66
MnO	0.64	0.54	0.49	0.49	0.56	0.34	0.34	0.34	0.53	0.30	0.33
MgO	22.46	23.24	22.56	22.56	23.35	22.26	22.26	21.43	22.61	25.43	25.56
CaO	0.41	0.37	0.42	0.42	0.38	0.81	0.81	0.48	0.88	0.60	0.54
Na2O	0.10	0.12	0.15	0.15	0.19	0.04	0.04	0.02	0.07	0.05	0.02
K2O	0.03	0.00	0.00	0.00	0.00	0.15	0.15	0.15	0.15	0.03	0.03
Total	85.45	86.46	84.72	84.72	85.65	85.74	85.74	81.65	86.32	85.52	85.52
Si	6.59	6.57	6.57	6.57	6.57	6.79	6.79	6.69	6.66	7.12	7.01
Ti	0.00	0.00	0.01	0.01	0.02	0.00	0.00	0.00	0.00	0.00	0.00
Al(tot)	3.71	3.69	3.62	3.62	3.59	3.29	3.29	3.38	3.36	3.00	3.16
Fe2+	2.26	2.22	2.33	2.33	2.21	2.50	2.50	2.55	2.51	1.62	1.59
Mn	0.11	0.09	0.08	0.08	0.10	0.06	0.06	0.06	0.09	0.05	0.05
Mg	6.74	6.89	6.85	6.85	6.99	6.71	6.71	6.80	6.80	7.44	7.48
Ca	0.09	0.08	0.09	0.09	0.08	0.18	0.18	0.11	0.19	0.13	0.11
Na	0.08	0.09	0.12	0.12	0.15	0.03	0.03	0.02	0.05	0.04	0.02
K	0.01	0.00	0.00	0.00	0.00	0.04	0.04	0.04	0.04	0.01	0.01
Cations	19.59	19.63	19.67	19.67	19.69	19.60	19.60	19.65	19.71	19.40	19.42

Sample	C897C	Cl1125b	Cl1125b	Cl1125b	Cl1125b	Cl1125b	Cl1125b	Cl1125b	Cl1125b	Cl1125b	Cl1125b
Min	corr	corr	corr	corr	corr	corr	corr	corr	corr	corr	corr
SiO2	36.17	36.15	36.15	34.70	34.19	34.83	34.83	34.79	33.79	35.32	35.32
TiO2	0.00	0.00	0.00	0.00	0.10	0.00	0.00	0.00	0.00	0.00	0.00
Al2O3	10.58	10.34	10.34	13.48	13.73	9.76	9.76	13.39	13.70	10.91	10.91
FeO	11.51	19.39	19.39	5.76	6.32	19.25	19.25	6.82	6.84	20.69	20.69
MnO	0.35	0.00	0.00	0.27	0.34	0.10	0.10	0.33	0.28	0.10	0.10
MgO	23.90	19.76	19.76	27.69	27.19	19.51	19.51	27.60	26.66	19.50	19.50
CaO	0.69	1.07	1.07	0.51	0.72	1.07	1.07	0.72	0.87	1.06	1.06
Na2O	0.11	0.05	0.05	0.03	0.03	0.07	0.07	0.01	0.04	0.06	0.06
K2O	0.07	0.19	0.19	0.00	0.00	0.18	0.18	0.05	0.00	0.15	0.15
Total	83.38	86.95	86.95	82.44	82.62	84.77	84.77	83.71	82.18	87.79	87.79
Si	7.36	7.36	7.36	6.93	6.85	7.30	7.30	6.90	6.83	7.18	7.18
Ti	0.00	0.00	0.00	0.00	0.02	0.00	0.00	0.00	0.00	0.00	0.00
Al(tot)	2.54	2.48	2.48	3.17	3.24	2.41	2.41	3.13	3.26	2.61	2.61
Fe2+	1.96	3.30	3.30	0.96	1.06	3.37	3.37	1.13	1.16	3.52	3.52
Mn	0.06	0.00	0.00	0.05	0.06	0.02	0.02	0.06	0.05	0.02	0.02
Mg	7.25	5.99	5.99	8.25	8.12	6.10	6.10	8.16	8.03	5.91	5.91
Ca	0.15	0.23	0.23	0.11	0.15	0.24	0.24	0.15	0.19	0.23	0.23
Na	0.09	0.04	0.04	0.02	0.02	0.06	0.06	0.01	0.03	0.05	0.05
K	0.02	0.05	0.05	0.00	0.00	0.05	0.05	0.01	0.00	0.04	0.04
Cations	19.42	19.45	19.45	19.49	19.52	19.55	19.55	19.55	19.55	19.56	19.56

## Phyllosilicate EMPA data, continuation:

Sample	CI1125b	CI1125b	CI1125b	CI1125b	CI1125b	CI1125b	CI1430v	CI1430v	D5620v	D5620v	D5620v
Min	corr	corr	corr	corr	corr	corr	corr	corr	corr	corr	corr
SiO2	34.76	34.76	33.95	33.97	33.99	33.46	34.63	33.53	33.58	35.05	33.02
TiO2	0.00	0.00	0.08	0.00	0.00	0.00	0.00	0.00	0.00	0.00	0.00
Al2O3	10.53	10.53	13.17	13.01	14.08	14.24	10.03	9.94	13.80	10.72	14.16
FeO	19.65	19.65	6.27	6.01	6.64	7.87	17.91	18.83	14.76	19.71	14.90
MnO	0.21	0.21	0.22	0.39	0.49	0.25	0.05	0.13	0.34	0.10	0.53
MgO	19.53	19.53	27.78	28.03	28.12	27.14	20.93	20.26	22.26	20.75	22.61
CaO	1.11	1.11	0.72	0.63	0.67	0.78	0.71	0.53	0.81	0.90	0.88
Na2O	0.04	0.04	0.01	0.04	0.00	0.05	0.04	0.04	0.04	0.04	0.07
K2O	0.19	0.19	0.00	0.03	0.00	0.03	0.01	0.00	0.15	0.23	0.15
Total	86.02	86.02	82.20	82.11	83.99	83.82	84.31	83.26	85.74	87.50	86.32
Si	7.20	7.20	6.84	6.85	6.73	6.68	7.23	7.15	6.79	7.13	6.66
Ti	0.00	0.00	0.01	0.00	0.00	0.00	0.00	0.00	0.00	0.00	0.00
Al(tot)	2.57	2.57	3.13	3.09	3.28	3.35	2.47	2.50	3.29	2.57	3.36
Fe2+	3.40	3.40	1.06	1.01	1.10	1.31	3.13	3.36	2.50	3.35	2.51
Mn	0.04	0.04	0.04	0.07	0.08	0.04	0.01	0.02	0.06	0.02	0.09
Mg	6.03	6.03	8.35	8.43	8.30	8.07	6.52	6.44	6.71	6.29	6.80
Ca	0.25	0.25	0.16	0.14	0.14	0.17	0.16	0.12	0.18	0.20	0.19
Na	0.03	0.03	0.01	0.03	0.00	0.04	0.03	0.03	0.03	0.03	0.05
K	0.05	0.05	0.00	0.01	0.00	0.01	0.00	0.00	0.04	0.06	0.04
Cations	19.56	19.56	19.59	19.62	19.63	19.67	19.55	19.62	19.60	19.64	19.71

Sample	D5707v	D5742vb	D5742vb	D5742vb	EH41	EH41	EH41	EH410	EH410	EH410	EH410
Min	corr	corr	corr	corr	corr	corr	corr	corr	corr	corr	corr
SiO2	33.82	35.35	36.65	34.57	34.60	36.15	35.63	35.10	32.46	29.55	30.35
TiO2	0.00	0.00	0.00	0.00	0.00	0.05	0.00	0.14	0.00	0.13	0.08
Al2O3	15.71	15.21	16.48	14.83	17.23	15.01	15.51	9.91	17.14	13.58	14.09
FeO	10.98	8.30	7.70	7.80	14.39	10.43	11.67	12.54	22.07	19.86	24.43
MnO	0.43	0.38	0.34	0.22	0.20	0.13	0.20	0.12	0.39	0.36	0.31
MgO	24.99	22.84	26.21	26.53	21.85	25.22	25.95	22.25	16.04	18.84	17.04
CaO	0.19	0.26	0.21	1.85	0.70	1.15	0.91	0.89	0.27	2.20	0.22
Na2O	0.02	0.02	0.02	0.02	0.02	0.01	0.02	0.07	0.60	0.04	0.81
K2O	0.00	0.02	0.01	0.07	0.23	0.21	0.07	0.13	0.03	0.15	0.17
Total	86.14	82.38	87.62	85.89	89.22	88.36	89.96	81.15	89.00	84.71	87.50
Si	6.65	7.11	6.91	6.74	6.66	6.90	6.72	7.40	6.52	6.32	6.35
Ti	0.00	0.00	0.00	0.00	0.00	0.01	0.00	0.02	0.00	0.02	0.01
Al(tot)	3.64	3.60	3.66	3.41	3.91	3.38	3.45	2.46	4.06	3.43	3.48
Fe2+	1.80	1.40	1.21	1.27	2.32	1.66	1.84	2.21	3.71	3.55	4.28
Mn	0.07	0.06	0.05	0.04	0.03	0.02	0.03	0.02	0.07	0.07	0.05
Mg	7.32	6.85	7.37	7.71	6.27	7.18	7.30	6.99	4.80	6.01	5.32
Ca	0.04	0.06	0.04	0.39	0.14	0.24	0.18	0.20	0.06	0.50	0.05
Na	0.02	0.02	0.01	0.02	0.01	0.01	0.01	0.06	0.47	0.03	0.66
K	0.00	0.01	0.00	0.02	0.06	0.05	0.02	0.03	0.01	0.04	0.05
Cations	19.54	19.10	19.27	19.58	19.42	19.44	19.57	19.40	19.69	19.98	20.25

## Phyllosilicate EMPA data, continuation:

Sample Mineral	C8928 corr	C8928 corr	C8928 corr	C8928 corr	C8931 corr	C8931 corr	C8931 corr	C8931 corr	C8938 corr	C8938 corr	C8938 corr
SiO2	35.10	36.05	35.97	35.24	36.46	35.35	36.06	32.96	34.17	33.71	34.21
TiO2	0.00	0.04	0.00	0.00	0.09	0.00	0.03	0.03	0.14	0.04	0.03
Al2O3	12.98	13.46	13.47	14.01	13.50	13.12	13.85	14.42	14.27	14.91	13.84
FeO	6.66	7.23	7.06	6.95	10.25	10.00	10.15	9.89	14.59	13.86	13.81
MnO	0.22	0.24	0.27	0.26	0.29	0.40	0.33	0.34	0.56	0.51	0.52
MgO	27.04	27.68	27.43	28.55	25.41	24.36	25.42	26.20	21.46	21.87	22.26
CaO	0.71	0.79	0.72	0.58	0.88	0.97	0.84	0.36	0.95	0.62	0.89
Na2O	0.06	0.01	0.10	0.00	0.02	0.04	0.02	0.00	0.02	0.02	0.04
K2O	0.07	0.06	0.06	0.09	0.08	0.11	0.06	0.02	0.03	0.05	0.10
Total	82.84	85.56	85.08	85.68	86.98	84.35	86.76	84.22	86.19	85.59	85.70
Si(tot)	7.02	6.99	7.01	6.83	7.06	7.07	7.00	6.62	6.86	6.78	6.88
Ti	0.00	0.01	0.00	0.00	0.01	0.00	0.00	0.00	0.02	0.01	0.00
Al(tot)	3.06	3.08	3.09	3.20	3.08	3.09	3.17	3.41	3.38	3.54	3.28
Fe2	1.11	1.17	1.15	1.13	1.66	1.67	1.65	1.66	2.45	2.33	2.32
Mn	0.04	0.04	0.04	0.04	0.05	0.07	0.05	0.06	0.10	0.09	0.09
Mg	8.06	8.00	7.97	8.24	7.33	7.26	7.35	7.84	6.42	6.56	6.67
Ca	0.15	0.16	0.15	0.12	0.18	0.21	0.17	0.08	0.20	0.13	0.19
Na	0.02	0.00	0.04	0.00	0.01	0.02	0.01	0.00	0.01	0.01	0.02
K	0.02	0.01	0.01	0.02	0.02	0.03	0.01	0.01	0.01	0.01	0.03
ΣCation	19.47	19.47	19.47	19.58	19.40	19.41	19.42	19.67	19.44	19.45	19.49

Sample Mineral	C8938 corr	C8938 corr	C8938 corr	C8938 corr	C8938 corr	C8938 corr	C8938 corr	C8938 corr	C8938 corr	C8938 corr	C8940b corr
SiO2	34.36	33.77	32.45	32.16	32.16	32.72	33.07	32.28	32.28	32.71	30.32
TiO2	0.00	0.00	0.00	0.10	0.10	0.03	0.00	0.05	0.05	0.13	0.00
Al2O3	14.74	14.88	15.38	15.15	15.15	15.62	15.75	15.07	15.07	15.17	16.39
FeO	13.64	13.88	13.65	13.67	13.67	13.44	13.37	13.70	13.70	13.16	16.87
MnO	0.59	0.59	0.55	0.56	0.56	0.64	0.54	0.49	0.49	0.56	0.68
MgO	22.92	22.32	21.57	21.42	21.42	22.46	23.24	22.56	22.56	23.35	22.34
CaO	0.83	0.93	0.47	0.49	0.49	0.41	0.37	0.42	0.42	0.38	0.31
Na2O	0.03	0.03	0.13	0.17	0.17	0.10	0.12	0.15	0.15	0.19	0.04
K2O	0.12	0.04	0.02	0.01	0.01	0.03	0.00	0.00	0.00	0.00	0.10
Total	87.23	86.44	84.22	83.73	83.73	85.45	86.46	84.72	84.72	85.65	85.73
Si(tot)	6.78	6.74	6.64	6.63	6.63	6.59	6.58	6.58	6.58	6.57	6.79
Ti	0.00	0.00	0.00	0.02	0.02	0.00	0.00	0.01	0.01	0.02	0.00
Al(tot)	3.43	3.50	3.71	3.68	3.68	3.71	3.69	3.62	3.62	3.59	3.29
Fe2	2.25	2.32	2.34	2.36	2.36	2.27	2.22	2.34	2.34	2.21	2.50
Mn	0.10	0.10	0.10	0.10	0.10	0.11	0.09	0.08	0.08	0.10	0.06
Mg	6.74	6.64	6.58	6.58	6.58	6.75	6.89	6.85	6.85	6.99	6.71
Ca	0.18	0.20	0.10	0.11	0.11	0.09	0.08	0.09	0.09	0.08	0.18
Na	0.01	0.01	0.05	0.07	0.07	0.04	0.05	0.06	0.06	0.07	0.02
K	0.03	0.01	0.01	0.00	0.00	0.01	0.00	0.00	0.00	0.00	0.04
ΣCation	19.52	19.52	19.53	19.55	19.55	19.57	19.60	19.63	19.63	19.65	19.59

## Phyllosilicate EMPA data, continuation:

Sample	EH49b	EH49b	EH49b	EH49b	EH49b	EH49b	G76B	S1070v	S1070v	S1070v	S1070v
Min	corr	corr	corr	corr	corr	corr	corr	corr	corr	corr	corr
SiO2	29.78	30.78	28.32	32.79	29.37	30.51	30.79	36.15	34.06	34.55	34.55
TiO2	0.07	0.00	0.00	0.04	0.00	0.00	0.03	0.12	0.00	0.00	0.00
Al2O3	13.53	17.08	20.50	16.20	15.01	12.31	14.01	10.66	10.67	10.70	10.70
FeO	26.76	12.95	13.03	14.71	29.81	24.72	18.49	17.65	18.61	17.95	17.95
MnO	0.37	0.40	0.77	0.56	0.39	0.35	0.38	0.14	0.03	0.12	0.12
MgO	10.47	20.79	19.70	22.23	11.15	14.74	18.74	19.28	19.46	20.23	20.23
CaO	0.36	0.68	0.27	0.60	1.96	2.27	1.71	0.82	0.46	0.56	0.56
Na2O	0.09	0.07	0.03	0.02	0.00	0.06	0.02	0.09	0.00	0.01	0.01
K2O	0.07	0.07	0.04	0.06	0.09	0.07	0.00	0.03	0.01	0.03	0.03
Total	81.50	82.82	82.66	87.21	87.78	85.03	84.17	84.94	83.30	84.15	84.15
Si	6.81	6.39	5.91	6.52	6.36	6.66	6.53	7.44	7.22	7.22	7.22
Ti	0.01	0.00	0.00	0.01	0.00	0.00	0.00	0.02	0.00	0.00	0.00
Al(tot)	3.65	4.18	5.04	3.79	3.83	3.17	3.50	2.59	2.67	2.64	2.64
Fe2+	5.12	2.25	2.27	2.44	5.40	4.51	3.28	3.04	3.30	3.14	3.14
Mn	0.07	0.07	0.14	0.09	0.07	0.06	0.07	0.02	0.01	0.02	0.02
Mg	3.57	6.44	6.13	6.59	3.60	4.80	5.93	5.92	6.15	6.31	6.31
Ca	0.09	0.15	0.06	0.13	0.45	0.53	0.39	0.18	0.10	0.13	0.13
Na	0.08	0.06	0.02	0.02	0.00	0.05	0.02	0.07	0.00	0.01	0.01
K	0.02	0.02	0.01	0.02	0.02	0.02	0.00	0.01	0.00	0.01	0.01
Cations	19.41	19.55	19.59	19.60	19.74	19.79	19.72	19.29	19.45	19.47	19.47

Sample	S1070v	S1070v	S1070v	S1070v	S1070v	St720v	St720v	St720v	St720v	St751b	St751b
Min	corr	corr	corr	corr	corr	corr	corr	corr	corr	corr	corr
SiO2	35.58	33.22	34.44	33.39	33.07	36.05	36.50	35.20	35.93	34.90	34.47
TiO2	0.05	0.00	0.02	0.00	0.00	0.00	0.03	0.00	0.00	0.00	0.00
Al2O3	10.68	10.61	10.71	11.32	10.48	11.82	11.53	12.02	11.57	11.76	11.79
FeO	17.73	18.00	17.36	18.49	17.31	11.53	11.84	12.53	12.11	13.60	13.73
MnO	0.24	0.15	0.02	0.17	0.09	0.50	0.40	0.42	0.38	0.26	0.20
MgO	20.97	19.57	21.52	20.37	21.16	22.92	23.21	23.54	24.60	23.68	24.17
CaO	0.84	0.63	0.59	0.44	0.64	0.91	0.94	0.66	0.81	0.69	0.81
Na2O	0.11	0.03	0.03	0.04	0.01	0.01	0.04	0.02	0.07	0.04	0.00
K2O	0.02	0.02	0.03	0.09	0.03	0.00	0.00	0.02	0.03	0.00	0.01
Total	86.22	82.23	84.72	84.31	82.79	83.74	84.49	84.41	85.50	84.93	85.18
Si	7.24	7.14	7.13	7.01	7.04	7.30	7.33	7.12	7.16	7.07	6.98
Ti	0.01	0.00	0.00	0.00	0.00	0.00	0.00	0.00	0.00	0.00	0.00
Al(tot)	2.56	2.69	2.61	2.80	2.63	2.82	2.73	2.87	2.72	2.81	2.81
Fe2+	3.02	3.23	3.01	3.25	3.08	1.95	1.99	2.12	2.02	2.30	2.32
Mn	0.04	0.03	0.00	0.03	0.02	0.09	0.07	0.07	0.06	0.04	0.03
Mg	6.36	6.27	6.65	6.38	6.72	6.92	6.95	7.10	7.31	7.15	7.29
Ca	0.18	0.15	0.13	0.10	0.15	0.20	0.20	0.14	0.17	0.15	0.18
Na	0.09	0.02	0.02	0.03	0.01	0.01	0.03	0.02	0.05	0.03	0.00
K	0.01	0.01	0.01	0.02	0.01	0.00	0.00	0.01	0.01	0.00	0.00
Cations	19.51	19.53	19.57	19.62	19.65	19.29	19.31	19.45	19.51	19.55	19.62



## Phyllosilicate EMPA data, continuation:

Sample	AH813	AH813	AH823v	AH823v	C8902	C8906	C8906	C8906	C8922	C8922	C8922	St720v
Min	smc	smc	smc	smc	smc	smc	smc	smc	smc	smc	smc	smc
SiO2	39.89	37.47	38.43	35.80	38.63	36.79	37.58	36.44	36.08	34.79	35.46	37.36
TiO2	0.00	0.00	0.00	0.13	0.00	0.00	0.00	0.00	0.00	0.00	0.00	0.15
Al2O3	10.07	10.48	12.01	12.94	9.16	11.89	11.78	11.77	15.60	15.04	12.78	12.01
FeO	10.51	11.53	14.93	14.79	10.95	9.26	8.78	9.08	7.54	8.65	7.21	11.41
MnO	0.17	0.37	0.09	0.30	0.19	0.40	0.41	0.18	0.20	0.14	0.30	0.38
MgO	22.20	21.63	18.09	19.39	23.70	23.82	24.39	23.92	23.72	21.23	25.32	23.39
CaO	1.30	1.00	1.16	0.92	1.05	0.85	0.99	0.89	0.77	2.98	1.52	0.77
Na2O	0.16	0.03	0.05	0.05	0.08	0.01	0.04	0.04	0.03	0.10	0.15	0.29
K2O	0.19	0.12	0.00	0.01	0.20	0.08	0.14	0.11	0.04	0.07	0.21	0.00
Total	84.49	82.63	84.76	84.33	83.96	83.10	84.11	82.43	83.98	83.00	82.95	85.76
Si	7.90	7.67	7.74	7.30	7.75	7.40	7.45	7.38	7.09	7.03	7.11	7.35
Ti	0.00	0.00	0.00	0.02	0.00	0.00	0.00	0.00	0.00	0.00	0.00	0.02
Al(tot)	2.35	2.53	2.85	3.11	2.17	2.82	2.75	2.81	3.61	3.58	3.02	2.79
Fe2+	1.74	1.97	2.52	2.52	1.84	1.56	1.46	1.54	1.24	1.46	1.21	1.88
Mn	0.03	0.06	0.02	0.05	0.03	0.07	0.07	0.03	0.03	0.02	0.05	0.06
Mg	6.55	6.60	5.43	5.90	7.09	7.14	7.21	7.23	6.95	6.39	7.57	6.86
Ca	0.28	0.22	0.25	0.20	0.23	0.18	0.21	0.19	0.16	0.64	0.33	0.16
Na	0.12	0.02	0.04	0.04	0.06	0.01	0.03	0.03	0.02	0.08	0.12	0.22
K	0.05	0.03	0.00	0.00	0.05	0.02	0.04	0.03	0.01	0.02	0.05	0.00
Cationes	19.01	19.10	18.85	19.14	19.22	19.20	19.21	19.24	19.12	19.23	19.46	19.34

Sample	Cl1125b	Cl1430v	Cl1430v	Cl1430v	Cl1430v	Cl1430v	EH41	EH41	EH41	EH49b	St720v	St720v
Min	smc	smc	smc	smc	smc	smc	smc	smc	smc	smc	smc	smc
SiO2	39.11	39.27	39.28	37.66	38.51	39.68	37.23	36.04	33.92	35.99	38.95	36.99
TiO2	0.00	0.10	0.20	0.00	0.00	0.00	0.04	0.00	0.06	0.08	0.00	0.10
Al2O3	8.98	8.82	8.79	8.13	9.28	9.89	15.49	15.19	14.51	18.44	12.70	11.49
FeO	17.26	16.70	17.79	16.54	17.62	18.97	15.45	13.34	12.81	12.40	11.56	11.97
MnO	0.18	0.03	0.16	0.04	0.10	0.03	0.33	0.18	0.21	0.48	0.37	0.38
MgO	18.37	18.85	18.84	18.59	19.43	20.59	18.47	21.34	19.96	21.59	22.44	21.76
CaO	1.98	1.24	1.10	1.44	1.15	1.14	1.42	0.95	0.77	0.68	0.84	0.97
Na2O	0.08	0.02	0.04	0.03	0.02	0.06	0.00	0.04	0.03	0.96	0.04	0.05
K2O	0.20	0.01	0.01	0.04	0.00	0.01	0.13	0.73	1.50	0.23	0.00	0.05
Total	86.16	85.04	86.21	82.47	86.11	90.37	88.56	87.81	83.77	90.85	86.90	83.76
Si	7.91	7.98	7.93	7.93	7.79	7.67	7.23	7.03	6.98	6.70	7.53	7.48
Ti	0.00	0.02	0.03	0.00	0.00	0.00	0.01	0.00	0.01	0.01	0.00	0.02
Al(tot)	2.14	2.11	2.09	2.02	2.21	2.25	3.54	3.49	3.52	4.05	2.89	2.74
Fe2+	2.92	2.84	3.00	2.91	2.98	3.07	2.51	2.17	2.20	1.93	1.87	2.03
Mn	0.03	0.01	0.03	0.01	0.02	0.00	0.05	0.03	0.04	0.08	0.06	0.07
Mg	5.54	5.71	5.67	5.84	5.86	5.94	5.35	6.20	6.12	5.99	6.47	6.56
Ca	0.43	0.27	0.24	0.33	0.25	0.24	0.30	0.20	0.17	0.14	0.17	0.21
Na	0.06	0.02	0.03	0.02	0.02	0.04	0.00	0.03	0.02	0.69	0.03	0.04
K	0.05	0.00	0.00	0.01	0.00	0.00	0.03	0.18	0.39	0.05	0.00	0.01
Cationes	19.08	18.96	19.02	19.07	19.12	19.22	19.01	19.33	19.46	19.64	19.03	19.16

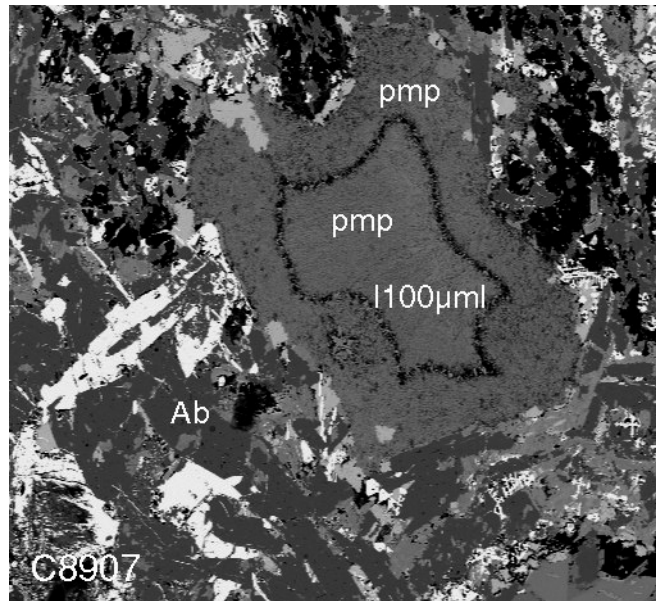
Phyllosilicate EMPA data – end.

**Appendix**  
-  
**BSE & SEM images**

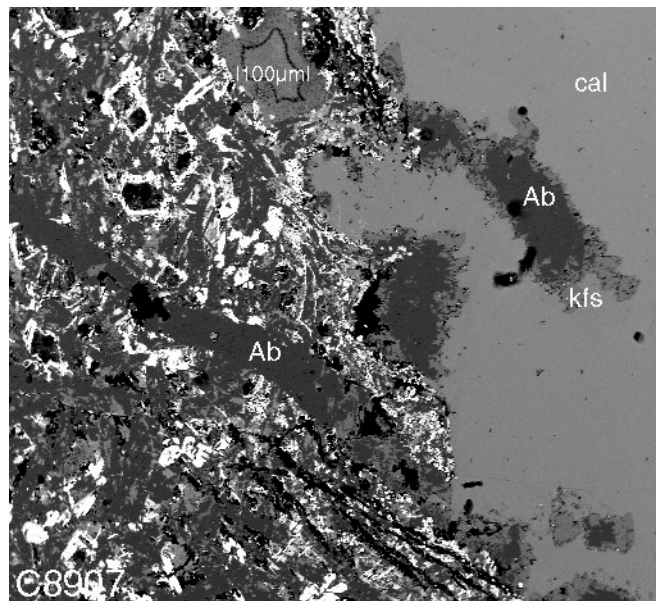
Mineral abbreviations (according to Kretz, 1983)

Ab	: albite
Cal	: calcite
Cln	: clinocllore
Dat	: datolite
Epi	: epidote
Fsp, kfsp, kfs	: potassium feldspar
Lmt	: laumontite
Phy	: phyllosilicate
Pmp	: pumpellyite
Prh	: prehnite
Px	: pyroxene
Qtz	: quartz
Zeo	: zeolite

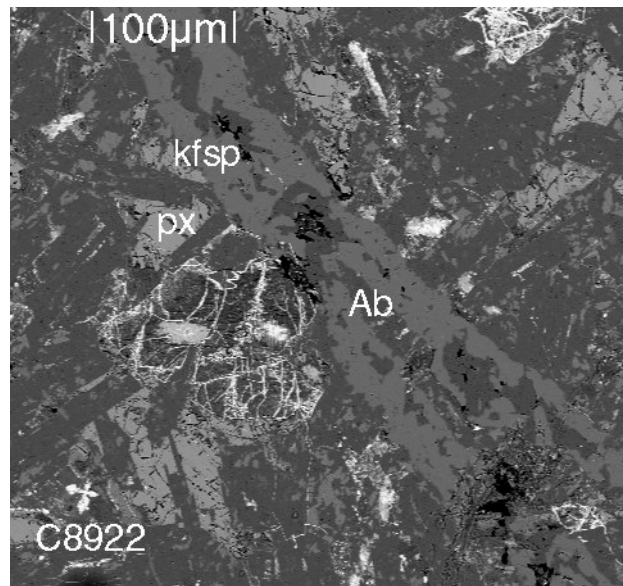
Selection of BSE images of typical and exotic minerals



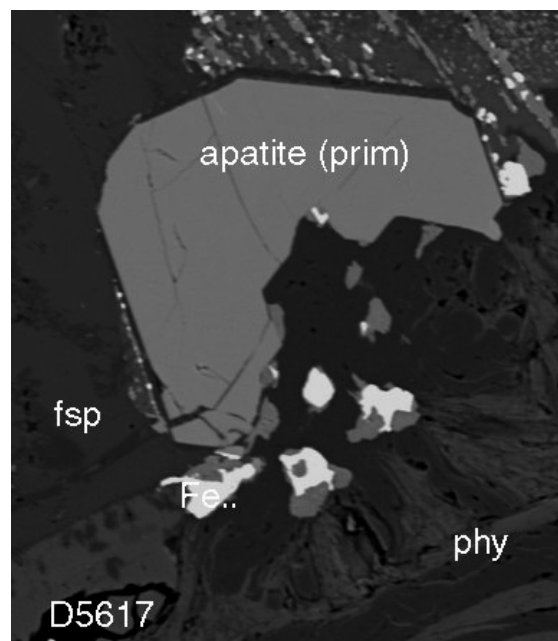
Amygdule infilling with two pumpellyite (pmp) generations (C8907)



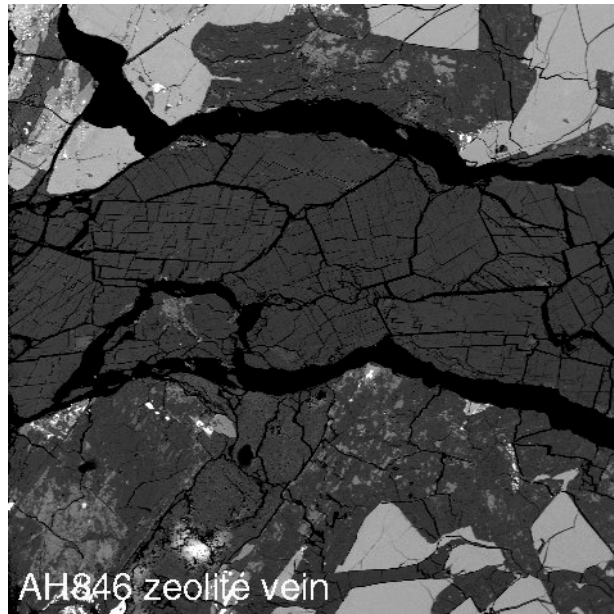
Early vein showing albite with potassium feldspar overgrowth. Amygdule finally filled by calcite (C8907).



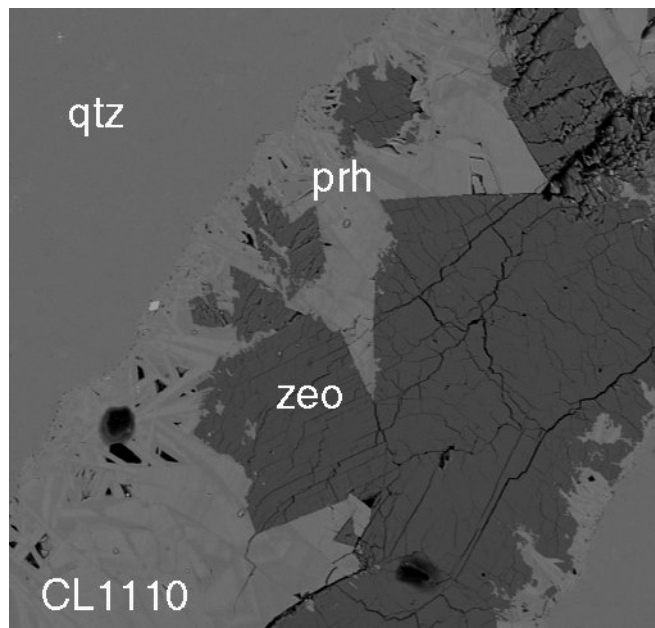
Matrix of massive flow showing secondary albite and potassium feldspar (C8922).



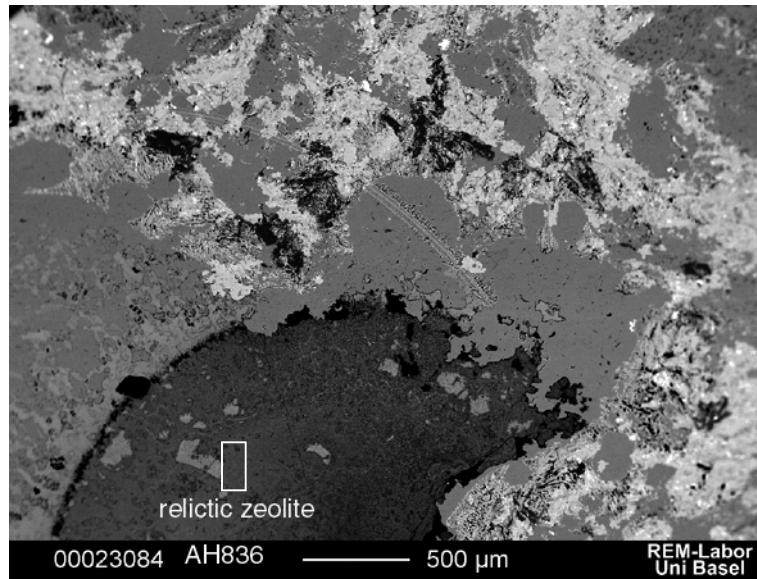
Primary relictic apatite (D5617)



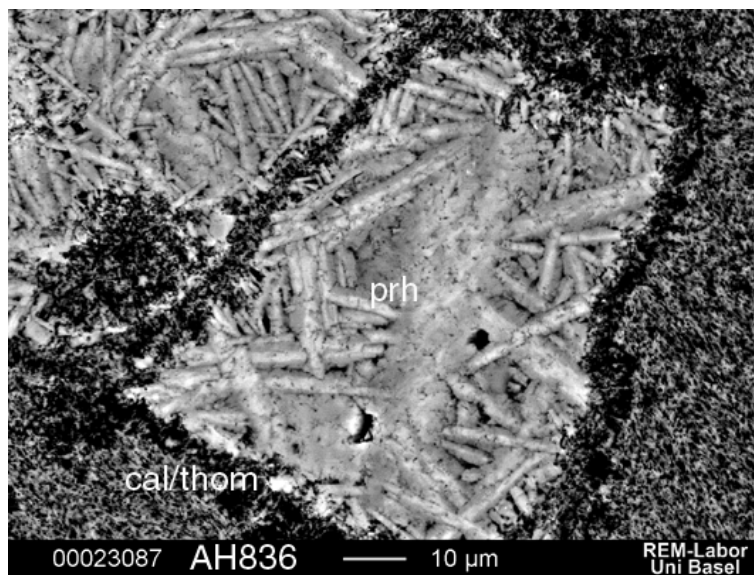
Late zeolite (laumontite) vein of stage three of the low-grade metamorphic history (AH846).



Vein with different alteration stages, quartz from the early stage, prehnite from the second stage. Vein reopened during stage three and was finally filled by laumontite (CL1110).

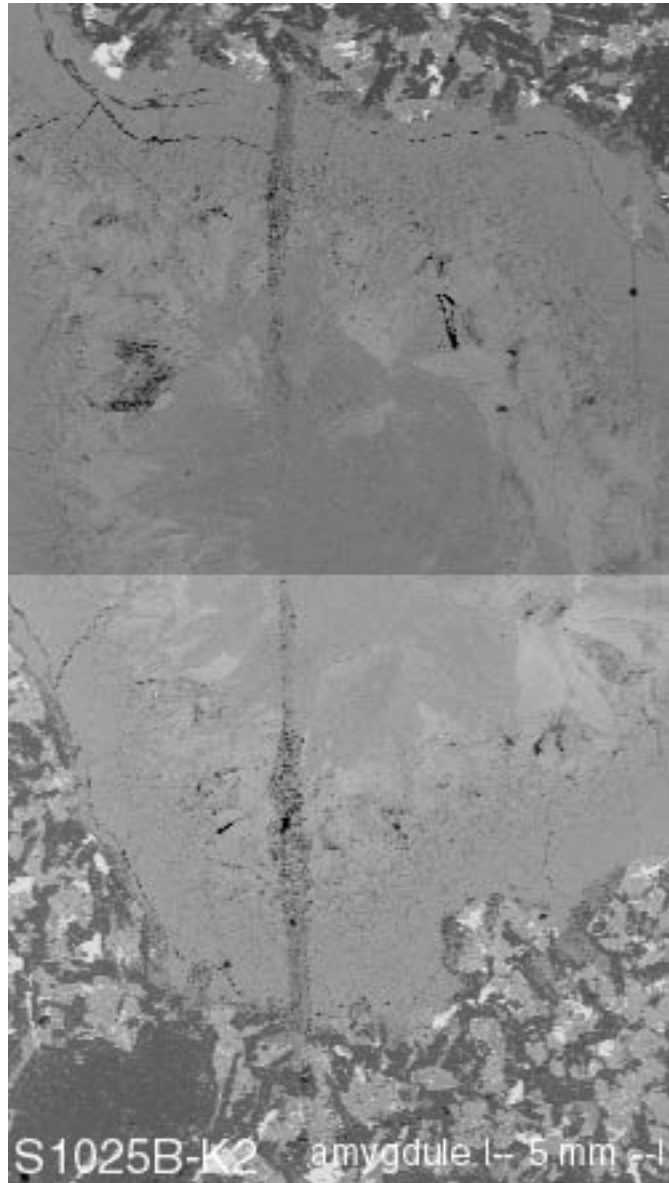


Single occurrence of relictic zeolite (AH836), quadrangle indicates location of image below.

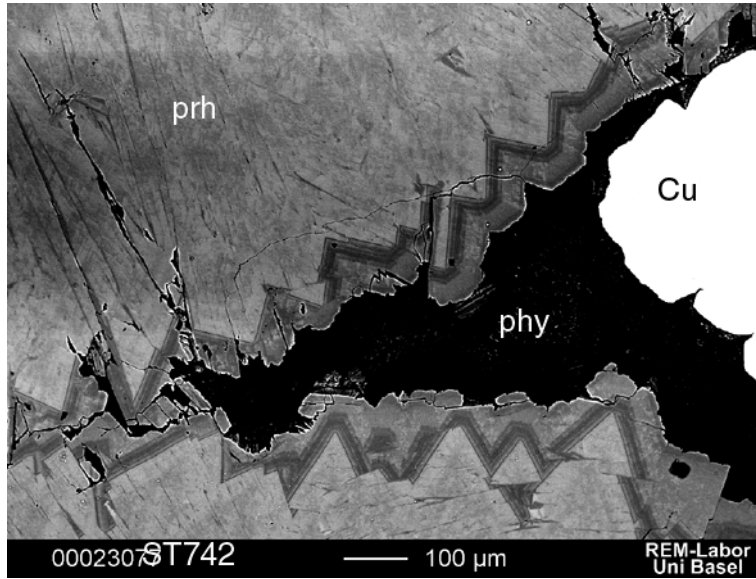


The detailed look discovers a total replacement by prehnite and calcite (AH836).

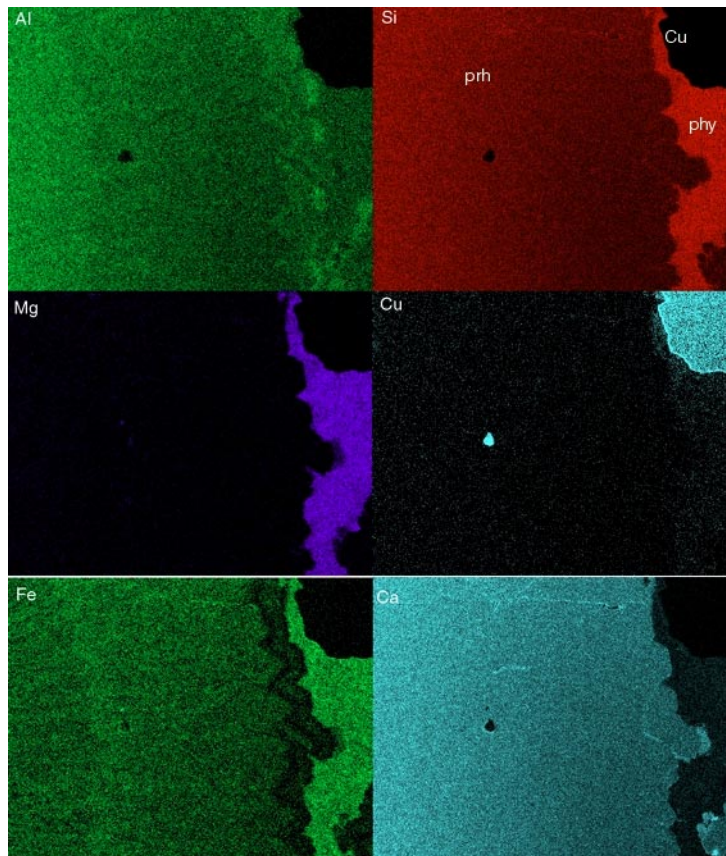
Typical BSE images of phyllosilicate occurrence:



Typical phyllosilicate (chlorite) filling of an amygdale. The rim shows a fine crystalline structure, whereas the center displays a botryoidal growth (S1025).

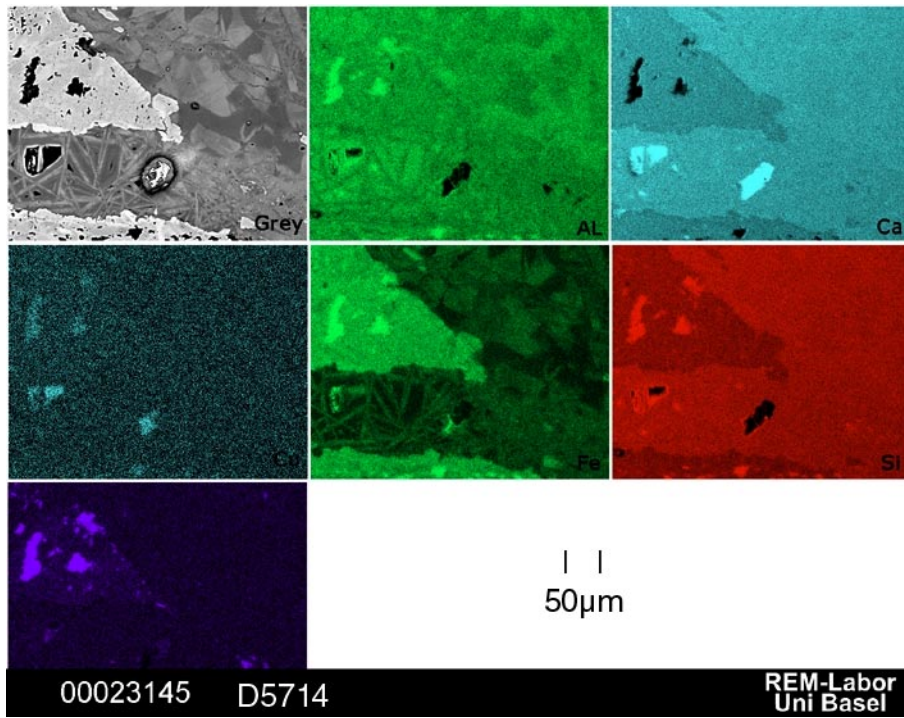


Native copper surrounded by late phyllosilicates and prehnite (ST742).

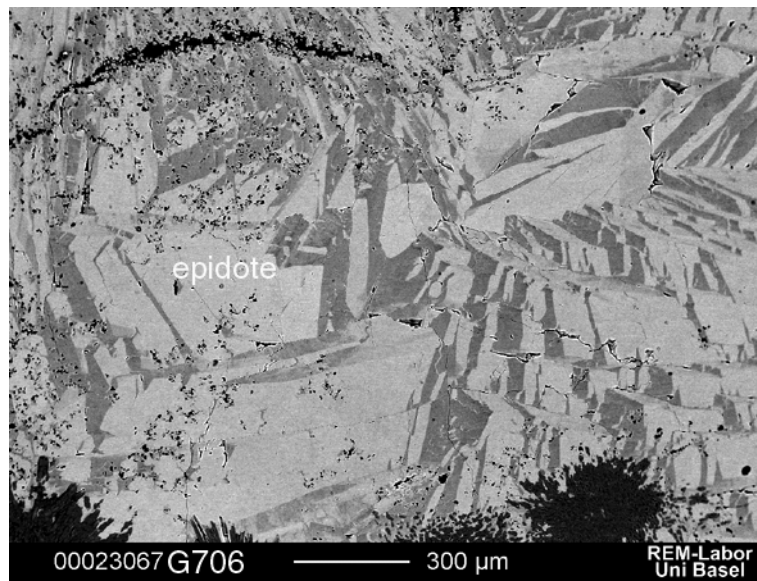


SEM-X-ray map of a similar location.

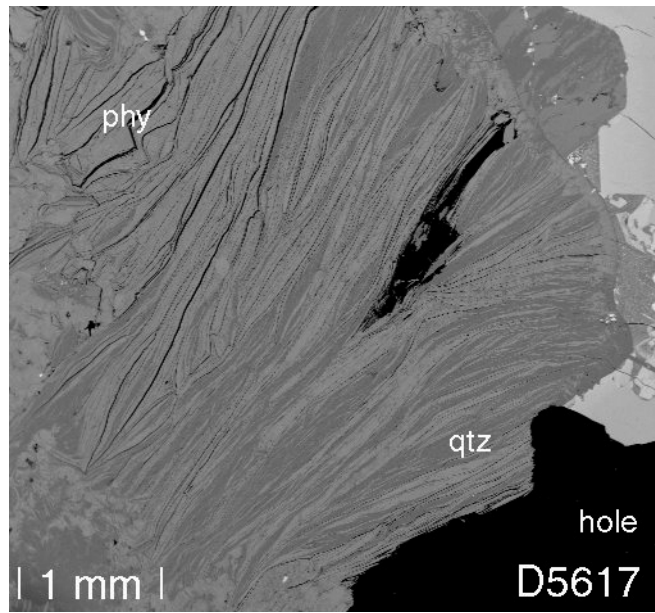




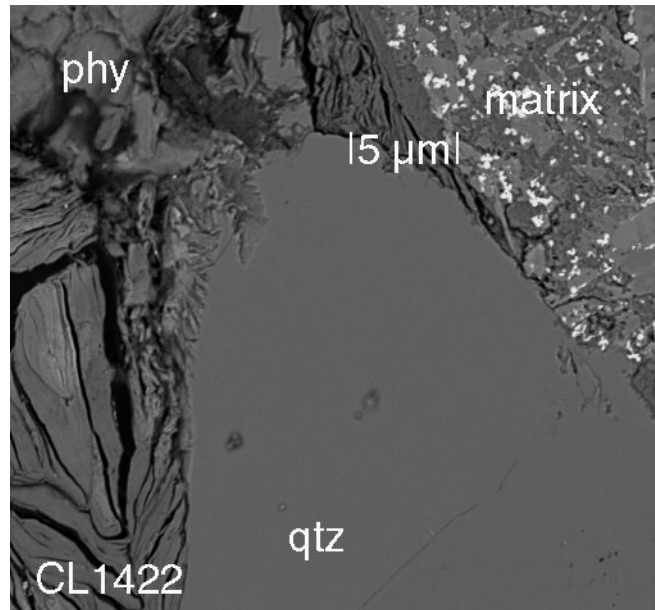
X-ray map of a epidote meta-domain with cross cutting prehnite veins of similar chemical composition.



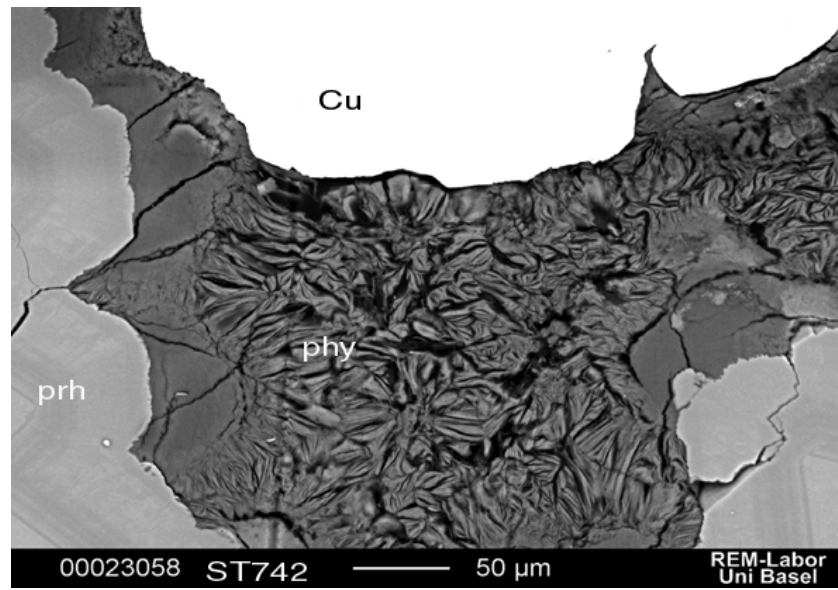
Early epidote in amygdale showing variation in the iron composition.  
(Lighter grey indicates higher Fe content(> z element))



Phyllosilicate of high Mg content intergrown with quartz in a matrix setting (D5617).

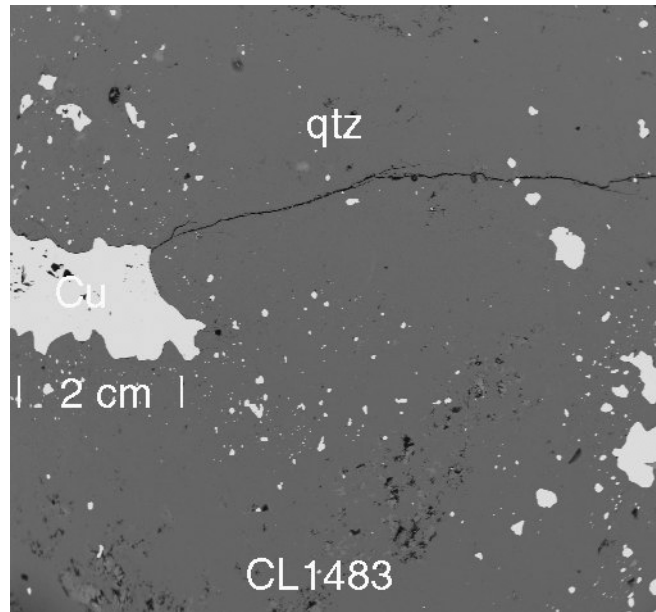


Detailed view of an amygdule rim with quartz being dissolved by alteration processes and transformed to phyllosilicates (CL1422).

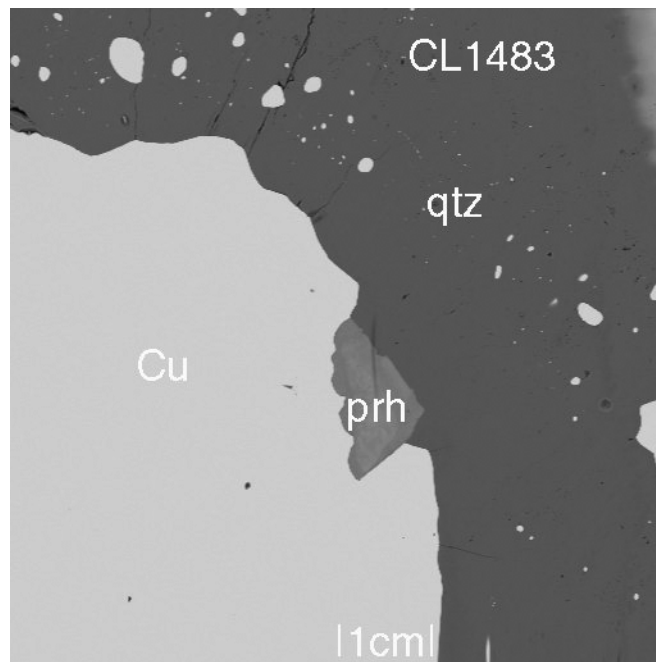


Third stage phyllosilicate in a setting with native copper and prehnite (ST742).

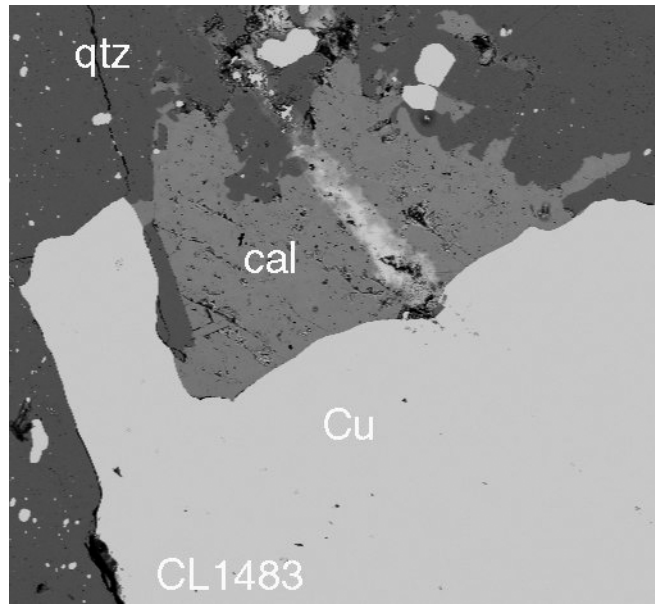
Native copper occurrence in BSE images:



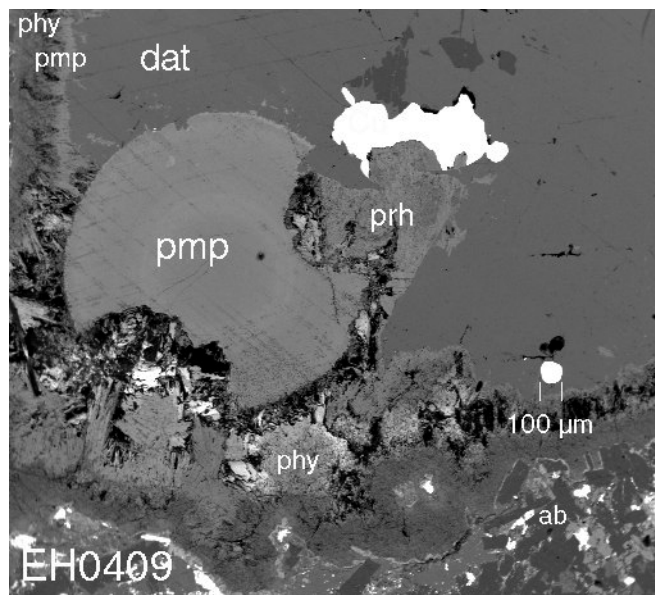
Droplets and irregular bodies of native copper in quartz vein, (CL1483).



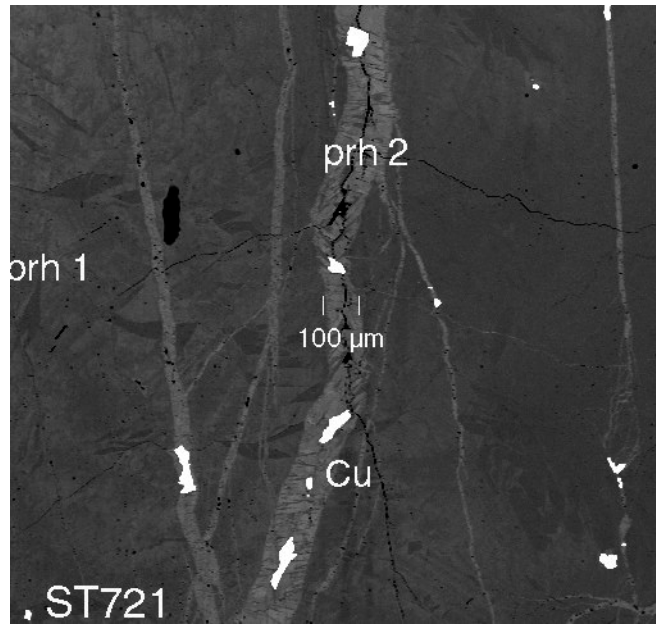
Droplets and irregular bodies of native copper in quartz vein, relictic corroded prehnite indicates preceding corrosive event (CL1483).



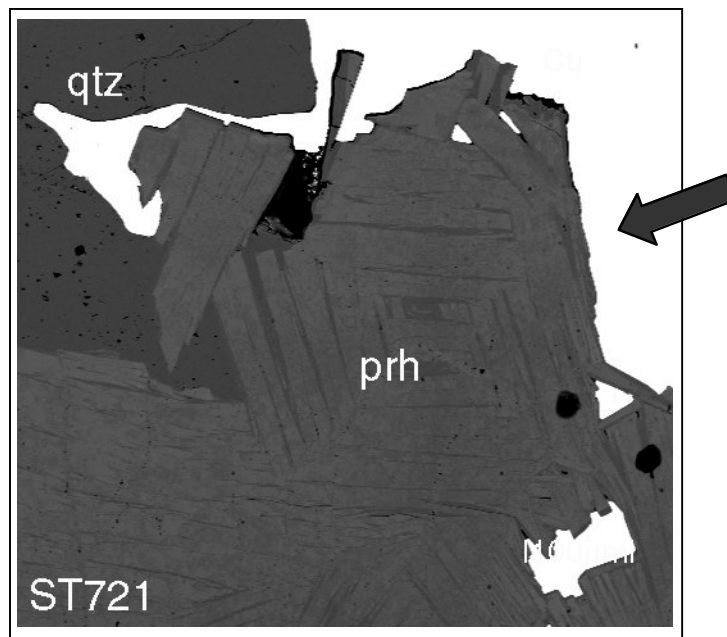
Native copper precipitation in quartz vein, relict calcite occurrence (CL1483).



Rare native copper occurrence in amygdale of the transition zone. Surrounding minerals are: phyllosilicates (phy), pumpellyite (pmp), datholite (dat), prehnite (prh) and in the matrix albite (ab) (EH0409).

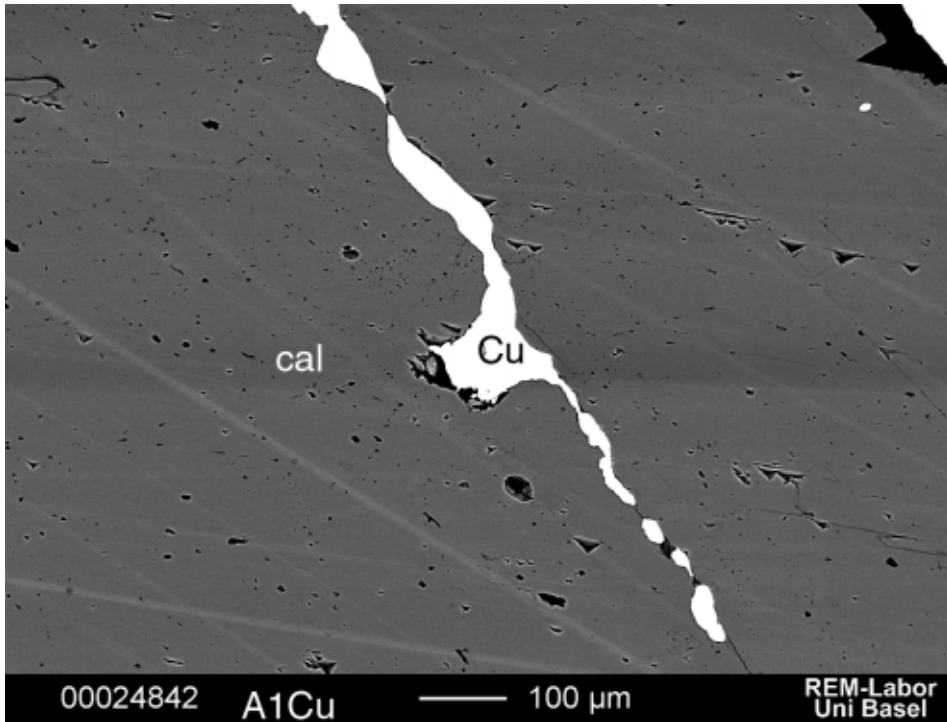


Typical native copper precipitation on second stage prehnite veins. Prehnite of stage two indicates with the lighter gray in the BSE image higher iron contents (ST721).

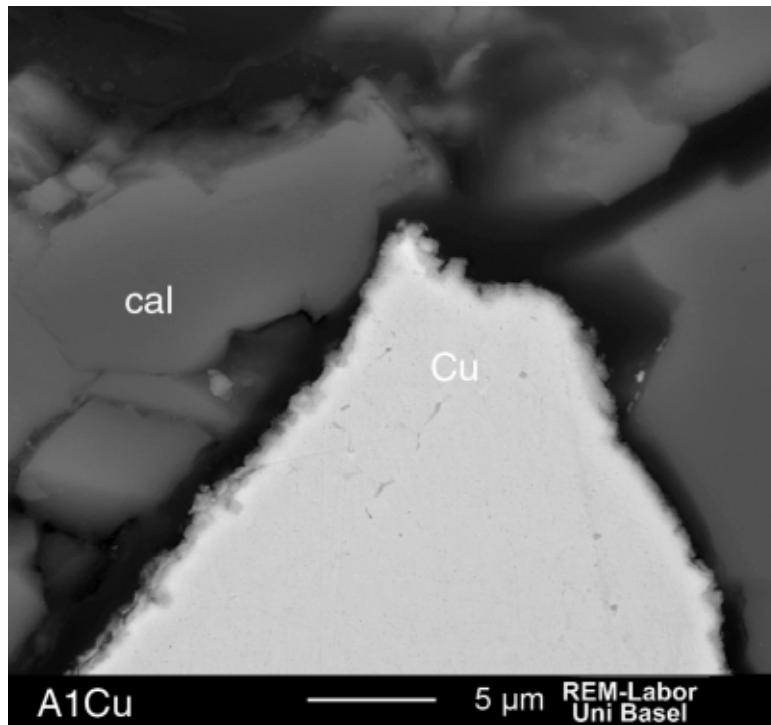


Native copper precipitation in vein. The corrosive character of the native copper fluid is indicated by corroded prehnite (arrow) (ST721).

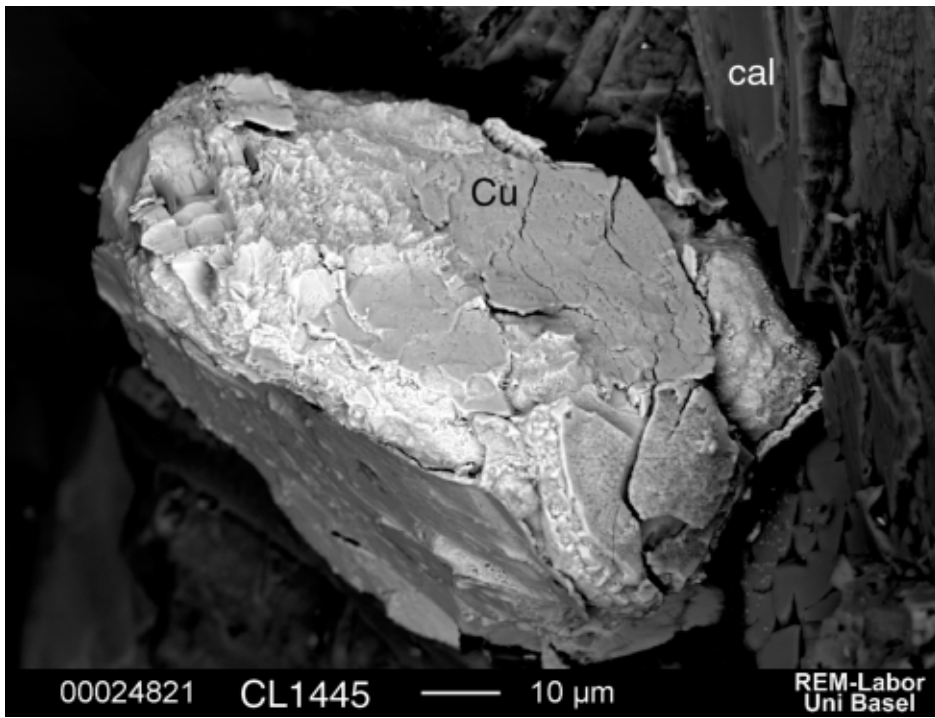
SEM images of typical native copper occurrence in the PLV:



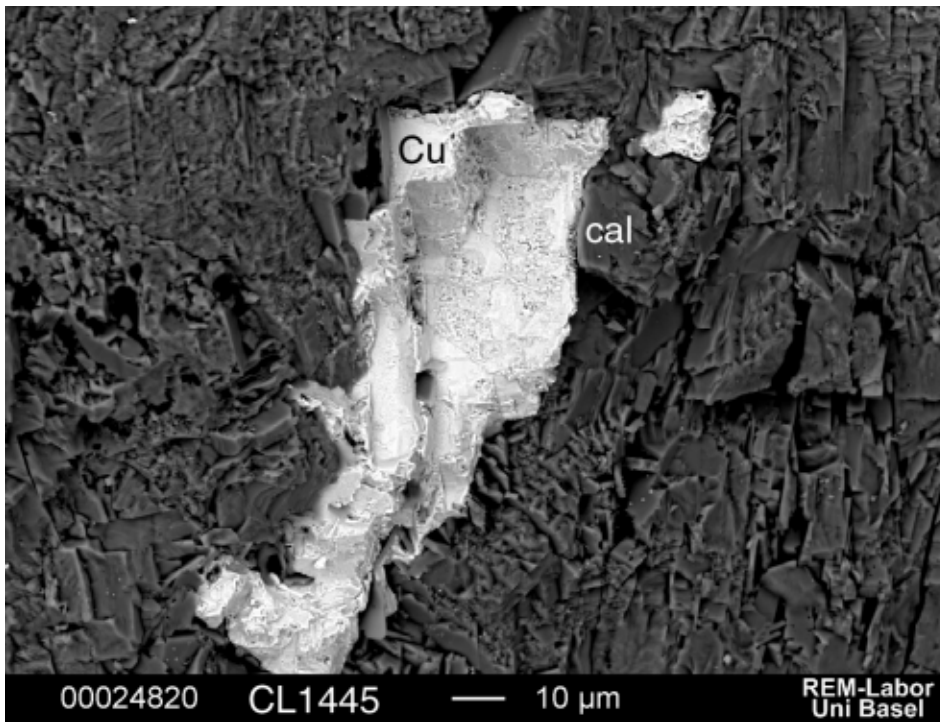
Native copper in secondary stage calcite. Precipitation on traces opened by corrosive fluids. (A1Cu = Sample from mine on the Keweenaw Peninsula).



Contact of native copper (Cu) and calcite (cal)  
(A1Cu = Sample from mine on the Keweenaw Peninsula).

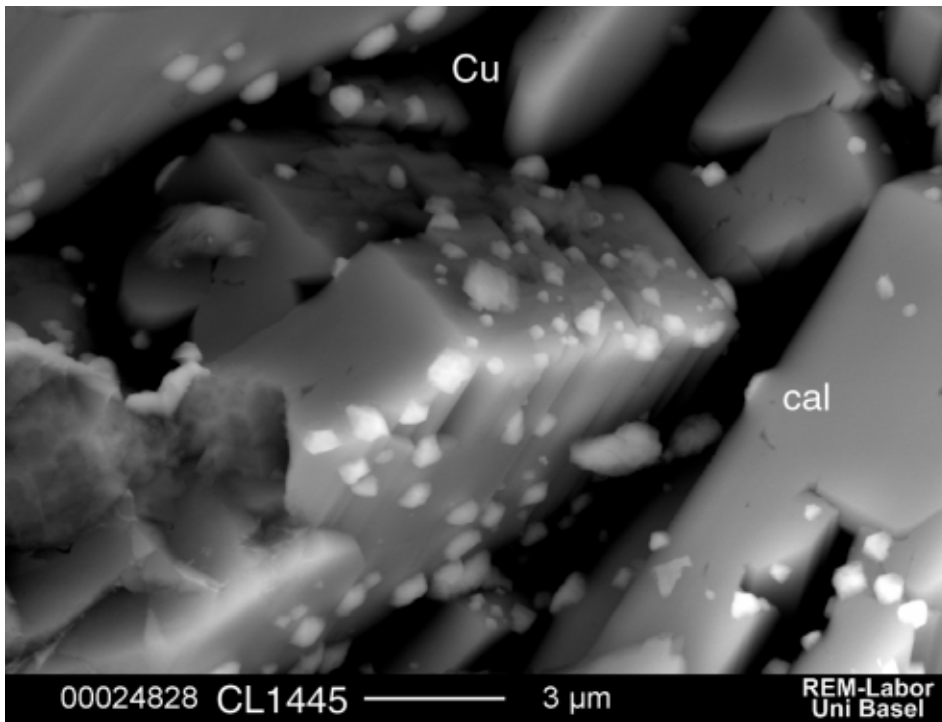


Sub-rounded native copper nugget in calcite (CL1445).

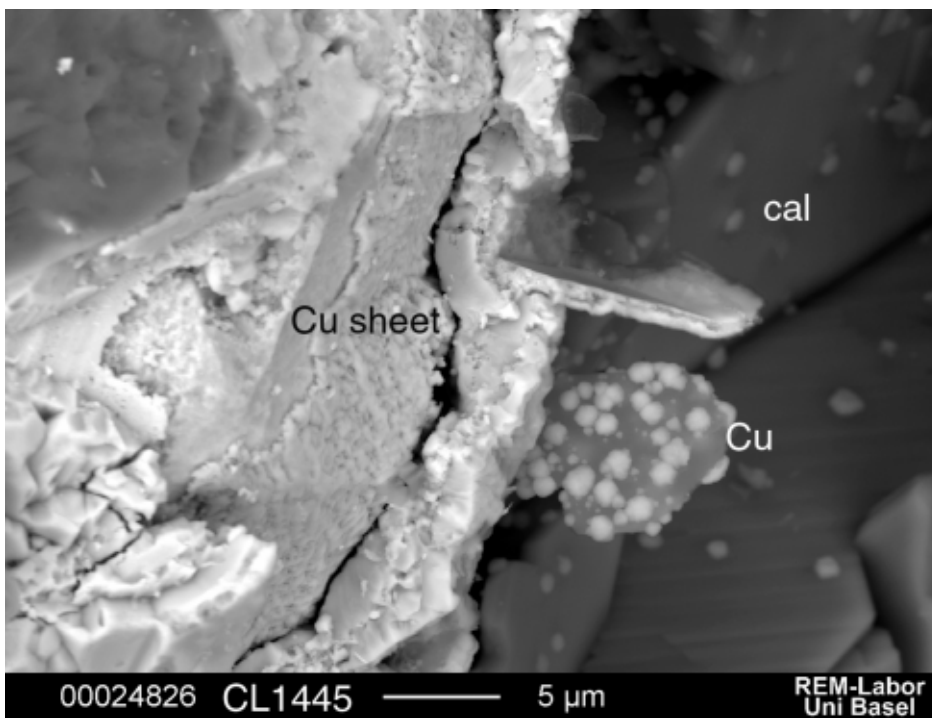


Native copper sheet located in vein calcite, on the mineral cleavage and inter-crystal spaces.  
Evidence of non-corrosive native copper precipitation (CL1445).

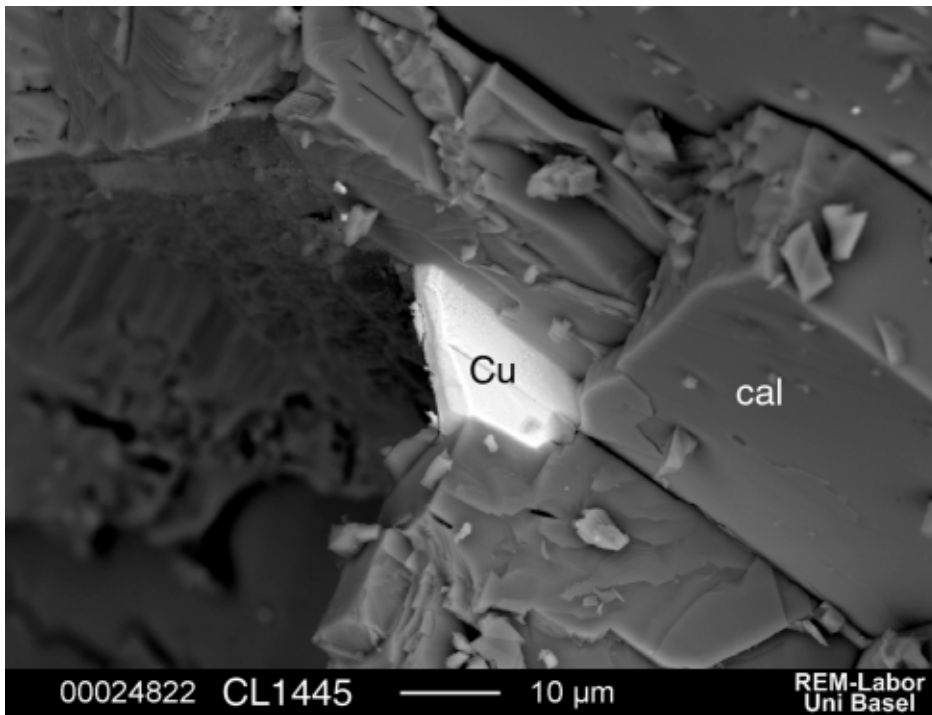




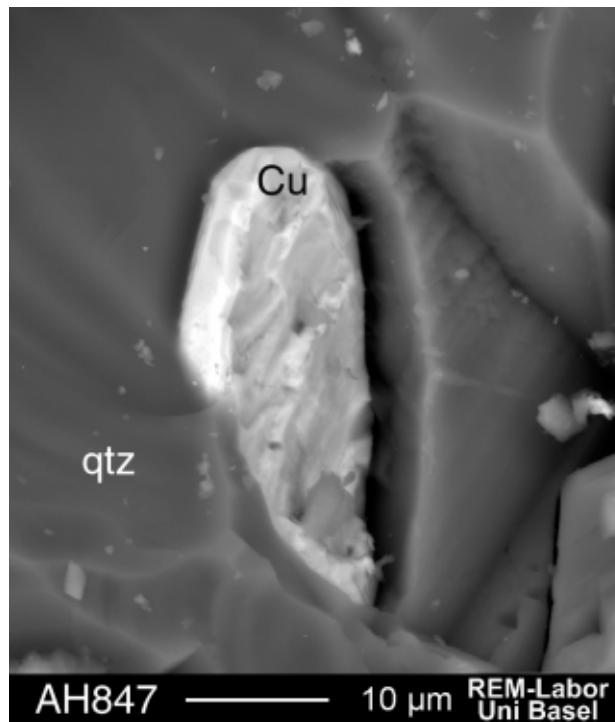
Native copper grown on calcite crystals and/or on the mineral cleavage. Precipitation not preceded by a corrosion of the calcite (CL1445).



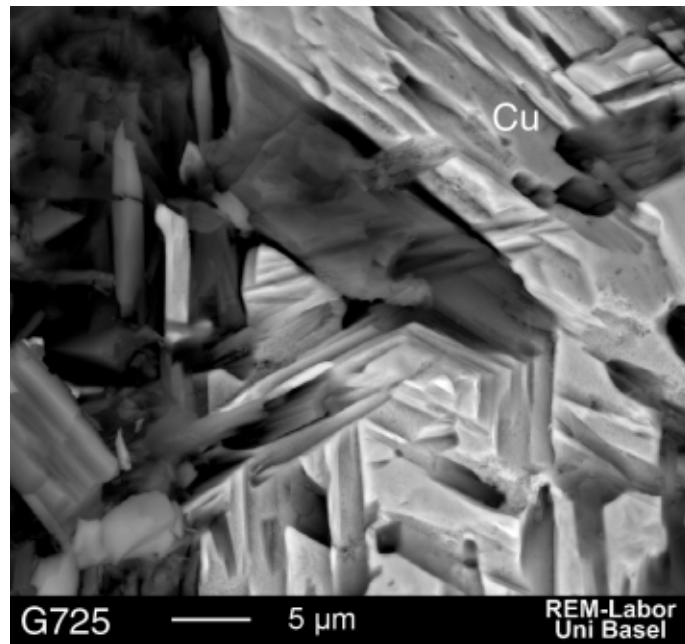
Native copper sheets on the mineral cleavage of calcite and an initial stage of native copper sheet formation. Precipitation not preceded by a corrosion of the calcite (CL1445).



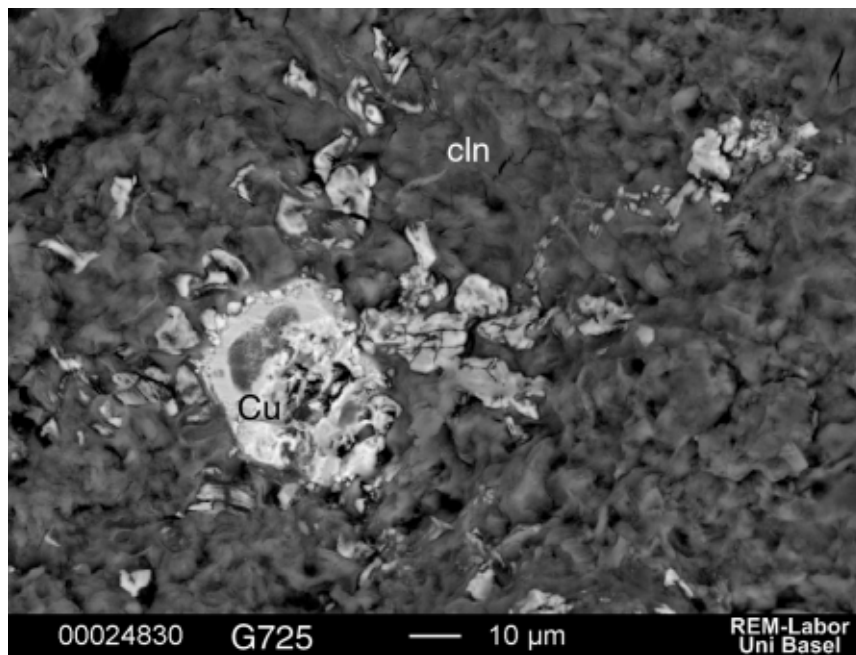
Native copper sheet on the cleavage of calcite. Precipitation not preceded by a corrosion of the calcite (CL1445).



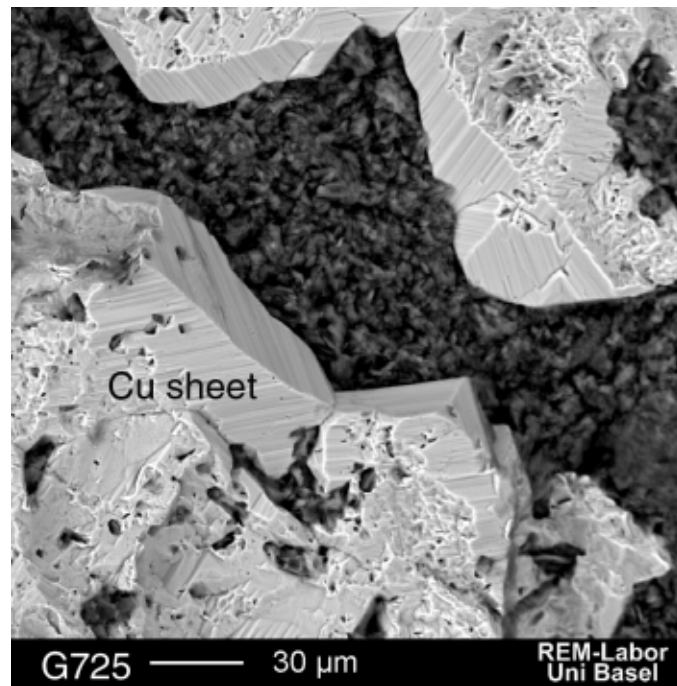
Native copper droplet (Cu) in quartz (qtz) matrix of conglomerate (AH847, host rock: Kingston conglomerate)



Native copper displaying the negative imprint of surrounding Mineral shapes (G725, host rock: massive flow interior).



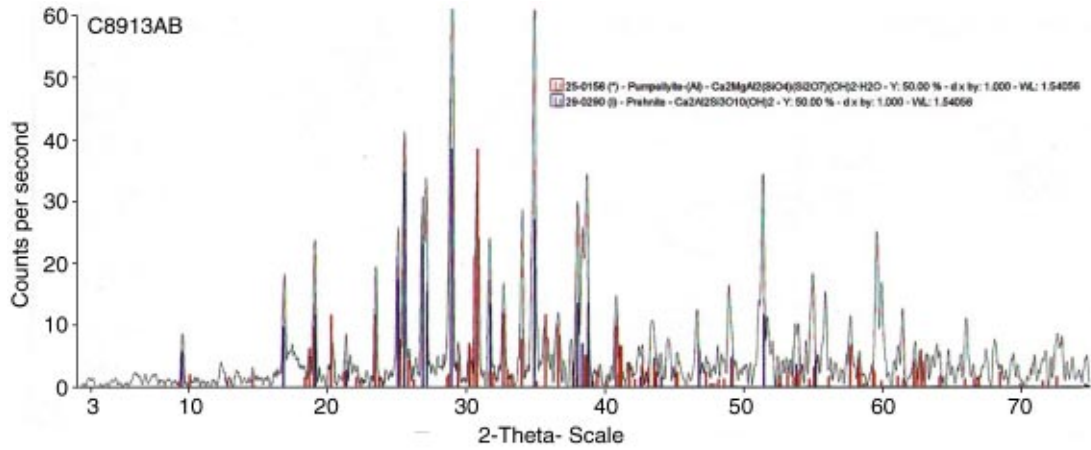
Native copper in massive flow interior, surrounded by third stage phyllosilicates (G725, host rock: massive flow interior).



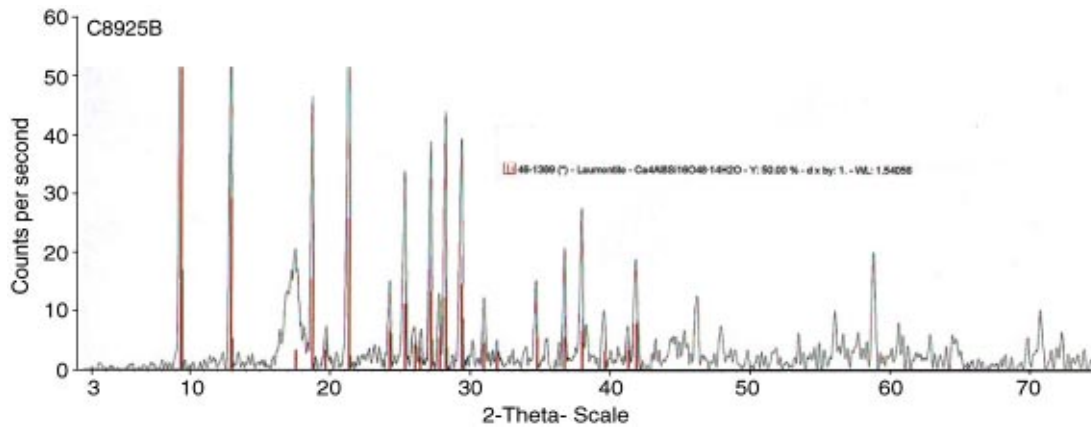
Massive flow interior: native copper showing the former walls of the vein, surrounded by third stage phyllosilicates (G725, host rock: massive flow interior).

**Appendix C**  
-  
**XRD – diffractograms (selection)**

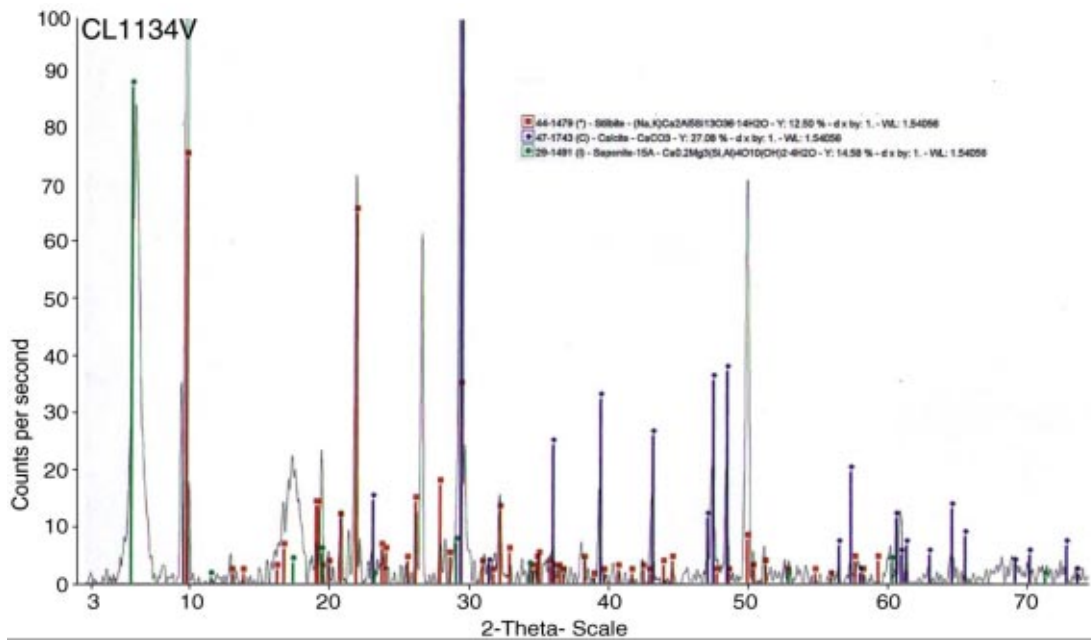
Selection of common and exotic X-ray diffractograms:



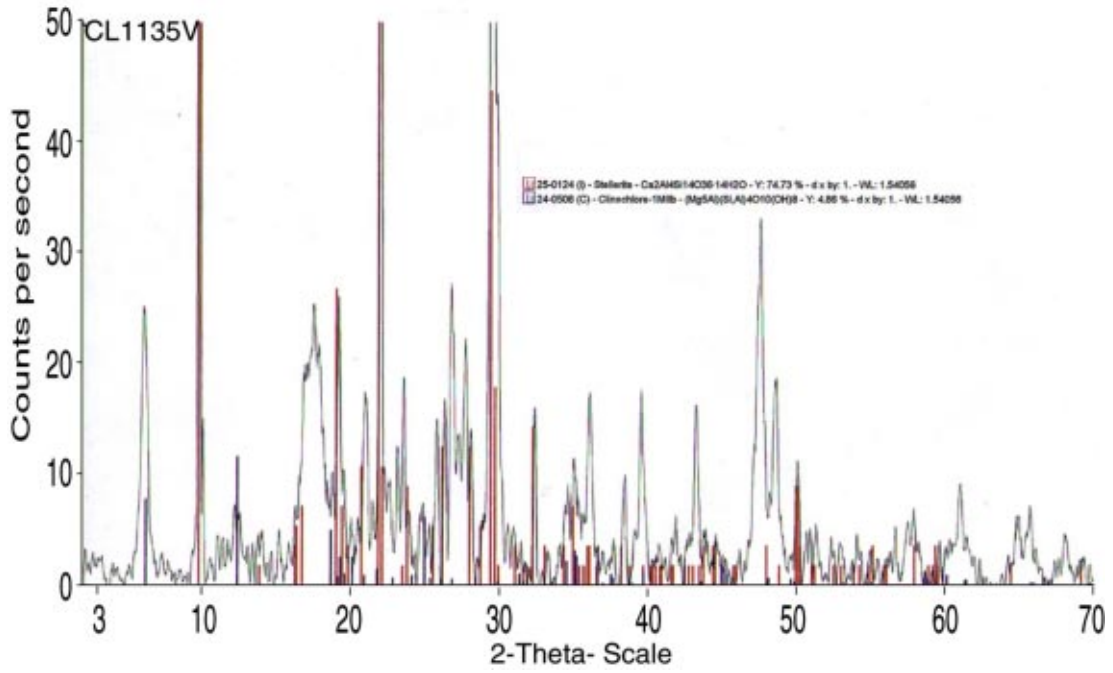
Typical amygdule mineral assemblage, red lines indicate pumpellyite and blue lines prehnite



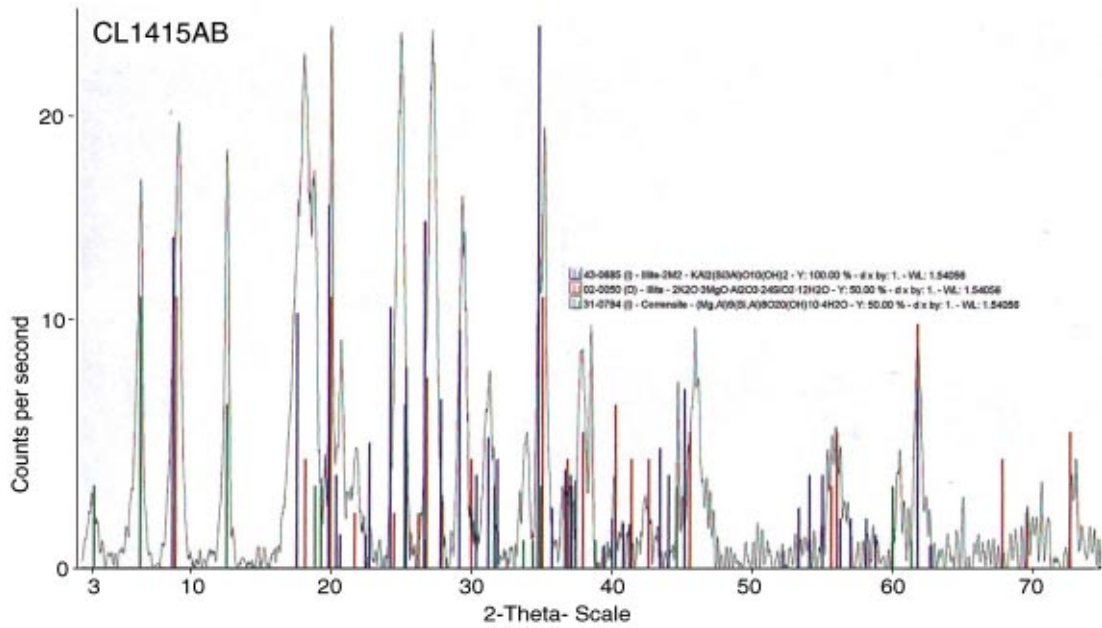
Laumontite diffractogram (C8925)



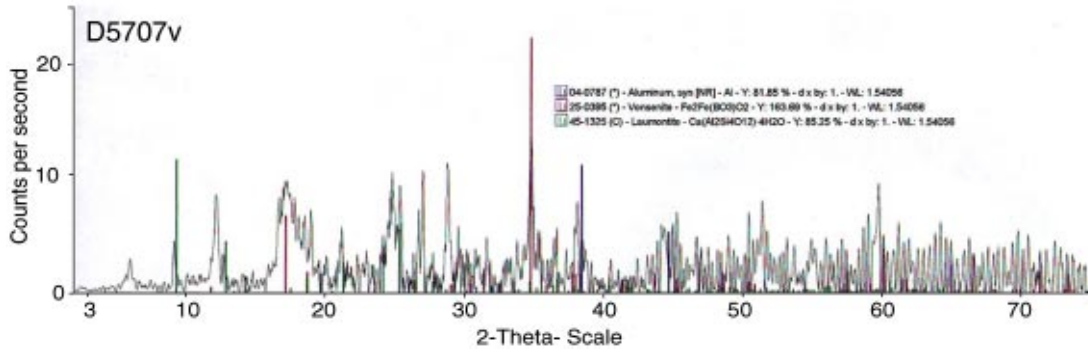
Third stage vein assemblage, red lines indicate stilbite, blue lines calcite, green lines saponite



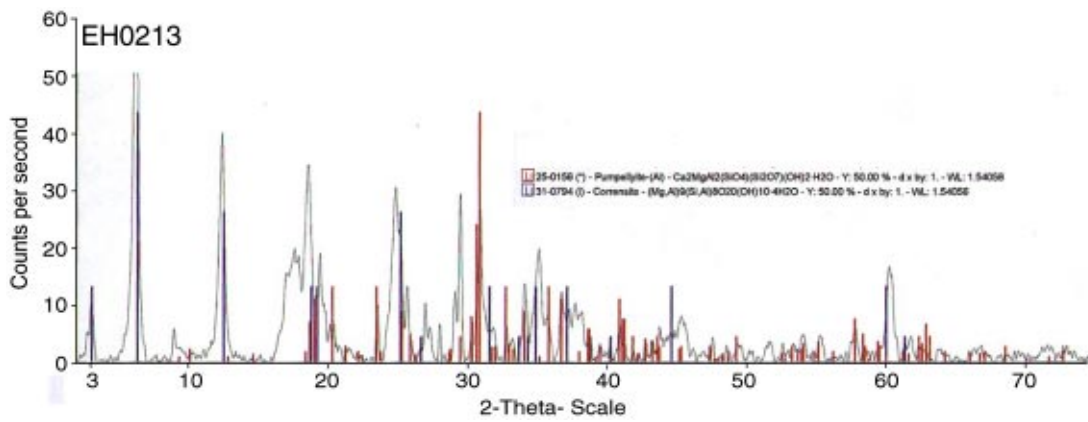
Third stage vein assemblage, red lines indicate stellerite, blue lines clinochlore.



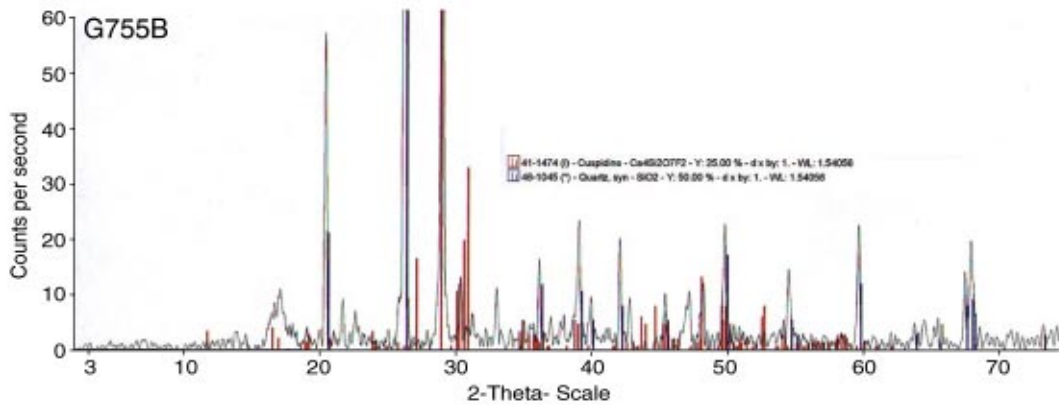
Amygdule phyllosilicate assemblage (air dry) blue illite, red illite, green corrensite (CL1415).



Late vein mineral assemblage, red lines indicate vonsenite, green lines laumontite, blue lines Aluminum of the special sample holder.

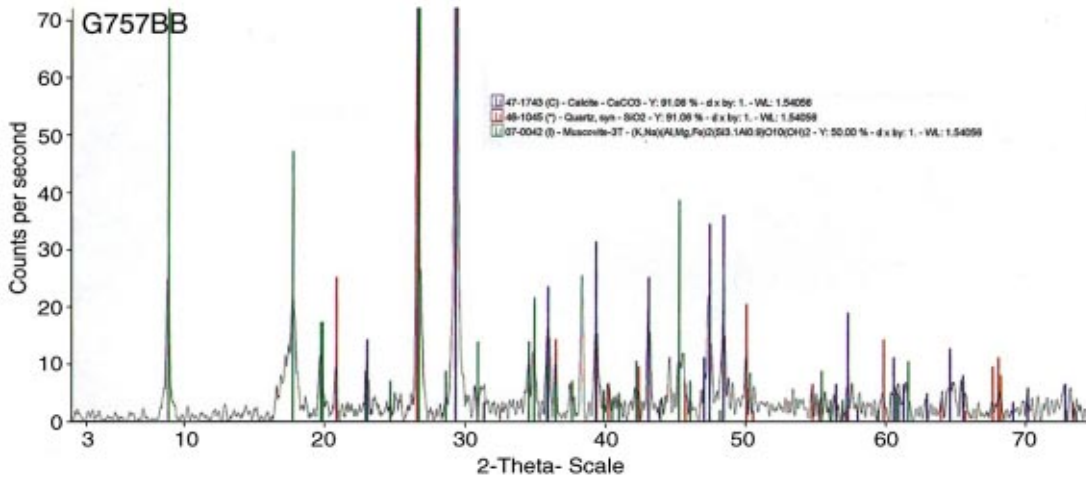


Amygdule assemblage red lines indicate pumpellyite, blue lines corrensite (EH0213).

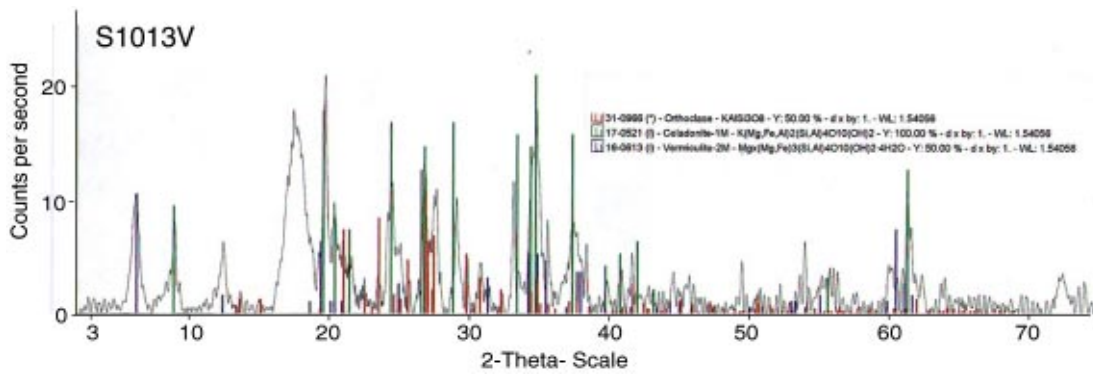


Exotic mineral red lines indicate cuspidine in an assemblage with quartz (blue lines).

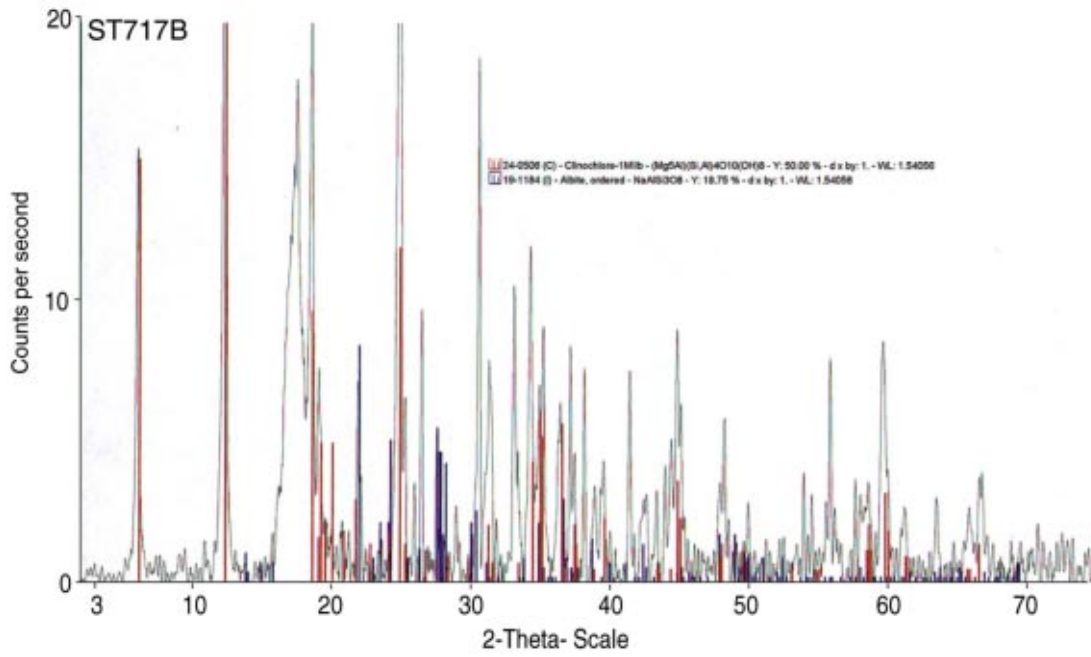




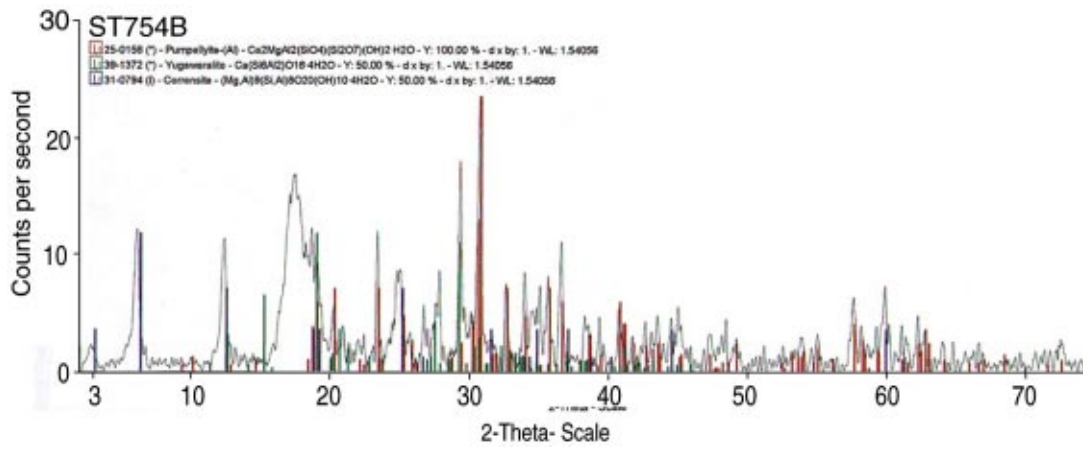
Green lines indicate muscovite, blue lines illite and red lines calcite.



Vein bulk analysis of potassium feldspar (red lines), and phyllosilicates celadonite (green lines) and vermiculite (blue lines).



Amygdule assemblage red clinocllore, and blue albitc (ST717).



Amygdule bulk analysis of pumpellyite (red lines), yugawaraitc (green lines) (zeolite), corrensite (blue lines).

**Appendix D**  
-  
**Fluid inclusion data**

Legend

HR: host rock; FT: flow top, TZ: transition zone

Real depth: depth under today's surface [m]; N.D.: no data

T<sub>1MP</sub>: first melting temperature of ice (eutectic temperature)

T<sub>MP</sub>: melting temperature of ice

T<sub>hom</sub>: homogenization temperature of fluid inclusion, (liquid + vapor = liquid)

NaCl<sub>equ</sub>: NaCl equivalents [w %] (after Potter et al. 1977)

## Fluid inclusion data:

HR	real depth	Drill	Location	Host minl	min stage	fluid inclusion size [μm]	Gas bubble [V %]	T <sub>1.MP</sub>	T <sub>MP</sub>	T <sub>nom</sub>	NaCl <sub>equ</sub>
FT	N.D.	MineKP	A1	cal	II	6.0	12.0		-0.1		0.18
FT	N.D.	MineKP	A1	cal	II	6.0	12.0		-0.1		0.18
FT	N.D.	MineKP	A1	cal	II	6.0	12.0		-0.1		0.18
FT	N.D.	MineKP	A1	cal	II	10.0	25.0		-0.1		0.18
FT	N.D.	MineKP	A1	cal	II	6.0	12.0		-0.1		0.18
FT	N.D.	MineKP	A1	cal	II	6.0	12.0		-0.1		0.18
FT	N.D.	MineKP	A1	qtz	I	7.0	3.0			151	
FT	N.D.	MineKP	A1	qtz	I	7.0	3.0			151	
FT	N.D.	MineKP	A1	qtz	I	5.0	20.0		-1.2	161	2.06
FT	N.D.	MineKP	A1	qtz	I	15.0	7.0	-22.0	-1.3	161	2.23
FT	N.D.	MineKP	A1	qtz	I	12.0	4.0	-17.3	-1.2	161	2.06
FT	N.D.	MineKP	A1	qtz	I	13.0	10.0		-1.2	161	2.06
FT	N.D.	MineKP	A1	qtz	I	10.0	7.0	-20.0	-1.2	161	2.06
FT	N.D.	MineKP	A1	qtz	I	20.0	15.0	-22.0	-1.7	161	2.89
FT	N.D.	MineKP	A1	qtz	I	7.0	5.0		-1.3	161	2.23
FT	N.D.	MineKP	A1	qtz	I	15.0	5.0		-1.3	161	2.23
FT	N.D.	MineKP	A1	qtz	I	10.0	5.0			170	
FT	N.D.	MineKP	A1	qtz	I	10.0	12.0		-1.0	174	1.90
FT	N.D.	MineKP	A1	qtz	I	5.0	9.0		-0.2	174	0.35
FT	N.D.	MineKP	A1	qtz	I	5.0	9.0		-0.2	174	0.35
FT	N.D.	MineKP	A1	qtz	I	7.0	5.0		-1.0	186	1.90
FT	N.D.	MineKP	A1	qtz	I	8.0	4.0			186	
FT	N.D.	MineKP	A1	qtz	I	8.0	5.0			186	
FT	N.D.	MineKP	A1	qtz	I	8.0	6.0		-2.1	186	3.53
FT	N.D.	MineKP	A1	qtz	I	7.0	6.0		-2.1	186	3.53
FT	N.D.	MineKP	A1	qtz	I	7.0	5.0			186	
FT	N.D.	MineKP	A1	qtz	I	10.0	12.0	-11.0	-2.7	186	4.48
FT	N.D.	MineKP	A1	qtz	I	2.5	5.0		-1.0	186	1.90
FT	N.D.	MineKP	A1	qtz	I	7.0	5.0		-1.0	186	1.90
FT	N.D.	MineKP	A1	qtz	I	10.0	5.0	-19.0	-1.0	186	1.90
FT	N.D.	MineKP	A1	qtz	I	30.0	30.0		-1.0	285	1.90
FT	N.D.	MineKP	A1	qtz	I	10.0	4.0		-0.1		0.18
FT	N.D.	MineKP	A1	qtz	I	10.0	3.0		-0.1		0.18
FT	N.D.	MineKP	A1	qtz	I	5.0	5.0		-0.1		0.18
FT	N.D.	MineKP	A1	qtz	I	2.5	7.0		-0.8		1.39
FT	N.D.	MineKP	A1	qtz	I	2.5	6.0		-0.8		1.39
FT	N.D.	MineKP	A1	qtz	I	12.0	7.0		-0.7		1.22
FT	N.D.	MineKP	A1	qtz	I	7.5	6.0		-0.8		1.39
FT	N.D.	MineKP	A1	qtz	I	7.0	4.5		-2.7		4.48

Appendix - D

HR	real depth	Drill	Location	Host min	min stage	fluid inclusion size [μm]	Gas bubble [V %]	T <sub>1,MP</sub>	T <sub>MP</sub>	T <sub>hom</sub>	NaCl <sub>equ</sub>
FT	N.D.	MineKP	A1	qtz	I	2.5	6.0		-0.8		1.39
FT	N.D.	MineKP	A1	qtz	I	2.5	6.0		-0.8		1.39
FT	N.D.	MineKP	A1	qtz	I	7.0	6.0	-19.0	-0.2		0.35
FT	N.D.	MineKP	A1	qtz	I	25.0	5.0		-0.2		0.35
FT	N.D.	MineKP	A1	qtz	I	7.0	20.0	-19.0	-0.2		0.35
FT	N.D.	MineKP	A1	qtz	I	10.0	6.0	-19.0	-0.2		0.35
FT	N.D.	MineKP	A1	qtz	I	12.0	20.0	-18.7	-0.5		0.37
FT	N.D.	MineKP	A1	qtz	I	30.0	10.0	-18.7	-0.4		0.70
FT	N.D.	MineKP	A1	qtz	I	20.0	5.0	-23.3	-0.4		0.70
FT	N.D.	CalMine	A3	qtz	I	8.0	7.0		-1.1	122	1.90
FT	N.D.	CalMine	A3	qtz	I	8.0	4.0		-0.1	151	0.18
FT	N.D.	CalMine	A3	qtz	I	10.0	5.0		-1.0	182	1.90
FT	N.D.	CalMine	A3	qtz	I	24.0	40.0	-17.0	-1.0	350	1.90
FT	N.D.	CalMine	A3	qtz	I	10.0	30.0	-17.0	-1.8	352	3.05
FT	N.D.	CalMine	A3	qtz	I	10.0	30.0	-17.0	-1.8	352	3.05
FT	N.D.	CalMine	A3	qtz	I	10.0	30.0	-17.0	-1.8	352	3.05
FT	N.D.	CalMine	A3	qtz	I	10.0	5.0	-17.0	-0.1		0.18
FT	N.D.	CalMine	A3	qtz	I	12.0	5.0	-17.0	-0.1		0.18
FT	N.D.	CalMine	A3	qtz	I						
FT	N.D.	CalMine	A3	qtz	I	3.0	10.0				
FT	N.D.	CalMine	A3	qtz	I	30.0	5.0	-11.0	-0.9		1.56
FT	N.D.	CalMine	A3	qtz	I	7.0	20.0	-17.0	-1.0		1.90
FT	N.D.	CalMine	A3	qtz	I	10.0	5.0		-1.1		1.90
FT	N.D.	CalMine	A3	qtz	I	7.0	10.0	-17.0	-1.0		1.90
FT	N.D.	CalMine	A3	qtz	I	4.0	8.0	-17.0	-1.0		1.90
FT	N.D.	CalMine	A3	qtz	I	5.0	7.0	-17.0	-1.0		1.90
FT	242	AH8	AH821	cal	II		5.5	-65.0	-25.1	56	30.00
FT	242	AH8	AH821	cal	II		5.5		-25.7	92	30.00
FT	242	AH8	AH821	cal	II		5.5		-25.1	105	30.00
FT	242	AH8	AH821	cal	II		5.5		-14.2	121	18.10
FT	242	AH8	AH821	cal	II		5.5		-25.7		30.00
FT	242	AH8	AH821	cal	II		5.5		-25.7		30.00
FT	242	AH8	AH821	cal	II		5.5		-25.1		30.00
FT	242	AH8	AH821	cal	II		5.5		-20.0		22.70
FT	242	AH8	AH821	qtz	II		4.5		-6.1	78	9.34
FT	242	AH8	AH821	qtz	II		6.5		-20.3	104	22.87
FT	242	AH8	AH821	qtz	II		6.5	-59.0	-1.0	104	1.90
FT	242	AH8	AH821	qtz	II				-7.0		10.49
FT	242	AH8	AH821	qtz	II		5.0		-1.0		1.90
FT	242	AH8	AH821	qtz	II		5.0		-0.5		0.37
FT	242	AH8	AH821	qtz	II		5.0		-4.8		7.40
FT	242	AH8	AH821	qtz	II		5.0		-2.0		3.37
FT	242	AH8	AH821	qtz	II				-25.8		30.00
FT	242	AH8	AH821	qtz	II				-8.1		11.80

Appendix - D

HR	real depth	Drill	Location	Host min	min stage	fluid inclusion size [μm]	Gas bubble [V %]	T <sub>1.MP</sub>	T <sub>MP</sub>	T <sub>hom</sub>	NaCl <sub>equ</sub>
FT	242	AH8	AH821	qtz	II		5.0		-25.0		30.00
TZ	345	AH8	AH832	cal	III	6.0	5.0		-23.1	183	30.00
TZ	345	AH8	AH832	cal	III	6.0	5.0		-14.0	183	17.90
TZ	345	AH8	AH832	cal	III	6.0	5.5		-23.1	183	30.00
TZ	345	AH8	AH832	cal	III	6.0	5.0		-14.0	186	17.90
TZ	345	AH8	AH832	cal	III	6.0	4.5		-23.4		30.00
TZ	345	AH8	AH832	cal	III	6.0	5.5		-15.6		19.30
TZ	345	AH8	AH832	cal	III	6.0	6.0		-13.1		17.20
TZ	345	AH8	AH832	cal	III	6.0	4.5		-28.0		30.00
TZ	345	AH8	AH832	cal	III	6.0	5.0		-18.6		21.70
TZ	345	AH8	AH832	cal	III	6.0	5.5		-20.7		23.15
TZ	345	AH8	AH832	cal	III	6.0	4.5		-16.2		19.80
TZ	345	AH8	AH832	cal	III	6.0	5.0		-17.0		20.40
FT	102	AH8	AH8J	cal	II		7.5		-19.6	160	22.40
FT	102	AH8	AH8J	cal	II		6.5		-19.3	206	22.20
FT	102	AH8	AH8J	cal	II		7.5		-28.0		30.00
FT	102	AH8	AH8J	cal	II		4.5		-4.4		7.01
FT	102	AH8	AH8J	cal	II		7.0		-5.5		8.54
FT	102	AH8	AH8J	cal	II		7.5		-18.9		21.90
FT	102	AH8	AH8J	cal	II		7.5		-19.6		22.40
FT	102	AH8	AH8J	qtz	II		4.5		-13.7	136	17.70
FT	102	AH8	AH8J	qtz	II		6.5		-11.7	170	15.80
FT	102	AH8	AH8J	qtz	II		5.0		-13.0	174	17.10
FT	102	AH8	AH8J	qtz	II		5.5		-15.3	175	19.00
FT	102	AH8	AH8J	qtz	II		5.0		-15.3	182	19.00
FT	102	AH8	AH8J	qtz	II		5.5		-11.6	188	15.70
FT	102	AH8	AH8J	qtz	II		5.0		-15.6	188	19.30
FT	102	AH8	AH8J	qtz	II		6.5		-18.5	188	21.60
FT	102	AH8	AH8J	qtz	II		4.0		-20.3		22.87
FT	102	AH8	AH8J	qtz	II		5.0		-10.4		14.40
FT	102	AH8	AH8J	qtz	II		5.5	-59.0	-18.5		21.60
FT	102	AH8	AH8J	qtz	II		5.0		-20.1		22.70
FT	102	AH8	AH8J	qtz	II		5.5		-19.7		22.50
FT	102	AH8	AH8J	qtz	II		5.0		-16.2		19.80
TZ	412	CL14	CL1481	cal	II				-36.0	31	30.00
TZ	412	CL14	CL1481	cal	II			-71.0	-36.0	44	30.00
TZ	412	CL14	CL1481	cal	II	40.0	3.0	-74.0	-37.0	44	30.00
TZ	412	CL14	CL1481	cal	II		2.5		-34.0	45	30.00
TZ	412	CL14	CL1481	cal	II	17.0		-76.0	-28.0	46	30.00
TZ	412	CL14	CL1481	cal	II	44.0	3.5	-55.0	-1.5	48	2.56
TZ	412	CL14	CL1481	cal	II		2.5	-75.0	-35.0	53	30.00
TZ	412	CL14	CL1481	cal	II				-24.0	55	30.00
TZ	412	CL14	CL1481	cal	II				-37.0	55	30.00
TZ	412	CL14	CL1481	cal	II		3.5			58	

Appendix - D

HR	real depth	Drill	Location	Host min	min stage	fluid inclusion size [μm]	Gas bubble [V %]	T <sub>1.MP</sub>	T <sub>MP</sub>	T <sub>hom</sub>	NaCl <sub>equ</sub>
TZ	412	CL14	CL1481	cal	II		2.5		-34.0	58	30.00
TZ	412	CL14	CL1481	cal	II		2.5			59	
TZ	412	CL14	CL1481	cal	II	7.0	3.5			62	
TZ	412	CL14	CL1481	cal	II		2.5	-73.0	-35.0	65	30.00
TZ	412	CL14	CL1481	cal	II		2.5	-77.0	-33.0	66	30.00
TZ	412	CL14	CL1481	cal	II		3.5			67	
TZ	412	CL14	CL1481	cal	II		3.5		-2.6	68	4.32
TZ	412	CL14	CL1481	cal	II		3.5			70	
TZ	412	CL14	CL1481	cal	II		3.5		-2.3	71	3.85
TZ	412	CL14	CL1481	cal	II		3.5		-2.2	72	3.69
TZ	412	CL14	CL1481	cal	II		3.5			77	
TZ	412	CL14	CL1481	cal	II			-75.0			
TZ	412	CL14	CL1481	cal	II		2.5	-75.0			
TZ	412	CL14	CL1481	cal	II		3.5		-0.5		0.37
TZ	412	CL14	CL1481	cal	II		2.5		-35.0		30.00
TZ	412	CL14	CL1481	cal	II				-26.0		30.00
TZ	412	CL14	CL1481	cal	II				-27.0		30.00
TZ	412	CL14	CL1481	cal	II				-26.0		30.00
TZ	412	CL14	CL1481	cal	II		2.5	-74.0	-29.0		30.00
TZ	412	CL14	CL1481	cal	II		3.5		-1.1		1.90
TZ	412	CL14	CL1481	qtz	II			-77.0	-30.0		30.00
TZ	412	CL14	CL1481	qtz	II				-29.0		30.00
TZ	412	CL14	CL1481	qtz	II				-35.0		30.00
TZ	412	CL14	CL1481	qtz	II	45.0					
TZ	412	CL14	CL1481	qtz	II				-31.0		30.00
TZ	412	CL14	CL1481	qtz	II				-33.0		30.00
TZ	412	CL14	CL1481	qtz	II				-44.0		30.00
TZ	412	CL14	CL1481	qtz	II	17.0					
TZ	412	CL14	CL1481	qtz	II	80.0		-87.0	-23.0		30.00
TZ	412	CL14	CL1481	qtz	II			-79.0	-28.0		30.00
TZ	412	CL14	CL1481	qtz	II				-27.0		30.00
TZ	412	CL14	CL1481	qtz	II				-34.0		30.00
TZ	347	G7	G746	cal	II				-17.0	63	20.40
TZ	347	G7	G746	cal	II					68	
TZ	347	G7	G746	cal	II			-79.0	-10.0	82	14.00
TZ	347	G7	G746	cal	II				-20.0	83	22.70
TZ	347	G7	G746	cal	II	6.0	3.5	-68.0		83	
TZ	347	G7	G746	cal	II	6.0	3.5	-70.0	-23.0	87	30.00
TZ	347	G7	G746	cal	II					91	
TZ	347	G7	G746	cal	II	12.0		-81.0		93	
TZ	347	G7	G746	cal	II	5.0	3.5		-8.0	94	11.70
TZ	347	G7	G746	cal	II					98	
TZ	347	G7	G746	cal	II			-79.0	-11.0	104	15.00
TZ	347	G7	G746	cal	II	4.0					

Appendix - D

HR	real depth	Drill	Location	Host min	min stage	fluid inclusion size [μm]	Gas bubble [V %]	T <sub>1.MP</sub>	T <sub>MP</sub>	T <sub>hom</sub>	NaCl <sub>equ</sub>
TZ	347	G7	G746	cal	II					-11.0	15.00
TZ	347	G7	G746	cal	II	10.0					
TZ	347	G7	G746	qtz	II				-3.0	60	4.94
TZ	347	G7	G746	qtz	II			-53.0	-2.8	65	4.63
TZ	347	G7	G746	qtz	II				-3.0	66	4.94
TZ	347	G7	G746	qtz	II			-53.0	-2.2	70	3.69
TZ	347	G7	G746	qtz	II				-2.0	72	3.37
FT	251	S10	S1037.2	cal	II		4.5	-68.0	-15.0	99	18.70
FT	251	S10	S1037.2	cal	II	9.0	4.5	-65.0	-14.0	101	17.90
FT	251	S10	S1037.2	cal	II		4.5	-50.0	-4.0	102	6.43
FT	251	S10	S1037.2	cal	II	11.0	4.5		-8.0	106	11.70
FT	251	S10	S1037.2	cal	II	30.0	4.5		-8.0	108	11.70
FT	251	S10	S1037	cal	II		5.5		-4.0	115	6.43
FT	251	S10	S1037	cal	II	5.0	5.0		-5.9	122	9.07
FT	251	S10	S1037	cal	II	6.0	6.5		-6.8	142	10.24
FT	251	S10	S1037	cal	II	20.0	3.5		-7.9	156	11.60
FT	251	S10	S1037	cal	II	6.0	7.0	-54.5	-3.7	156	5.99
FT	251	S10	S1037	cal	II		6.5			188	
FT	251	S10	S1037	cal	II	4.0	7.0		-4.6		7.30
FT	251	S10	S1037	cal	II		5.0		-4.6		7.30
FT	251	S10	S1037	cal	II		5.0		-4.6		7.30
FT	251	S10	S1037	cal	II	6.0	3.5		-8.7		12.50
FT	251	S10	S1037	cal	II		5.0		-5.2		8.13
FT	251	S10	S1037	cal	II		4.0		-16.2		19.80
FT	251	S10	S1037	cal	II		8.5		-0.9		1.56
FT	251	S10	S1037	cal	II	8.0	5.0		-3.7		5.99
FT	251	S10	S1037	cal	II		8.0		-10.0		14.00
FT	251	S10	S1037	cal	II	8.0	7.0		-3.7		5.99
FT	251	S10	S1037	cal	II		7.0	-56.5	-6.0		9.21
FT	251	S10	S1037	cal	II		5.0		-7.6		11.20
FT	251	S10	S1037	cal	II		5.0		-7.6		11.20
FT	251	S10	S1037	cal	II		5.5		-7.6		11.20
FT	251	S10	S1037	cal	II	10.0	5.0		-7.9		11.60
FT	251	S10	S1037	cal	II		7.0		-8.0		11.70
FT	251	S10	S1037	cal	II		4.0		-7.6		11.20
FT	251	S10	S1037	cal	II	40.0	5.0		-6.8		10.24
FT	251	S10	S1037	cal	II		6.0		-8.0		11.70
FT	251	S10	S1037	cal	II		7.0		-6.4		9.88
FT	251	S10	S1037	cal	II		6.5		-7.6		11.20
FT	251	S10	S1037	cal	II		5.5		-7.3		10.90
FT	251	S10	S1037	cal	II	7.0	4.5		-6.9		10.37
FT	251	S10	S1037	cal	II				-15.0	110	18.70
FT	251	S10	S1037	cal	II				-11.0	120	15.00
TZ	7	ST7	ST721	cal	II	30.0	5.0	-79.0	-43.0	46	30.00
TZ	7	ST7	ST721	cal	II		5.0			51	



Appendix - D

HR	real depth	Drill	Location	Host min	min stage	fluid inclusion size [ $\mu\text{m}$ ]	Gas bubble [V %]	$T_{1.MP}$	$T_{MP}$	$T_{hom}$	$\text{NaCl}_{\text{equ}}$
TZ	7	ST7	ST721	cal	II		5.0			53	
TZ	7	ST7	ST721	cal	II		5.0			54	
TZ	7	ST7	ST721	cal	II	11.0	5.0		-44.0	55	30.00
TZ	7	ST7	ST721	cal	II		5.0			59	
TZ	7	ST7	ST721	cal	II	7.0	5.0			62	
TZ	7	ST7	ST721	cal	II		5.0		-45.0	62	30.00
TZ	7	ST7	ST721	cal	II		5.0			62	
TZ	7	ST7	ST721	cal	II		5.0			63	
TZ	7	ST7	ST721	cal	II		5.0			67	
TZ	7	ST7	ST721	cal	II		5.0			67	
TZ	7	ST7	ST721	cal	II	16.0	5.0			68	
TZ	7	ST7	ST721	cal	II		5.0	-74.0		69	
TZ	7	ST7	ST721	cal	II		5.0			69	
TZ	7	ST7	ST721	cal	II		5.0	-82.0	-17.0		20.40
TZ	7	ST7	ST721	cal	II		5.0		-16.0		19.80
TZ	7	ST7	ST721	cal	II	10.0	5.0		-17.0		20.40
TZ	7	ST7	ST721	cal	II		5.0		-20.0		22.70
TZ	7	ST7	ST721	cal	II		5.0		-19.0		22.00
TZ	7	ST7	ST721	cal	II	20.0	5.0		-7.0		10.49
TZ	7	ST7	ST721	cal	II		5.0 N.D.				
TZ	7	ST7	ST721	cal	II	17.0	5.0		-13.0		17.10
TZ	7	ST7	ST721	cal	II		5.0		-13.0		17.10
TZ	7	ST7	ST721	cal	II		5.0		-13.0		17.10
TZ	180	ST7	ST742	cal	I		4.5		-14.7	149	18.50
TZ	180	ST7	ST742	cal	I		4.5		-5.2	149	8.13
TZ	180	ST7	ST742	cal	I		5.0		-12.4	204	16.40
TZ	180	ST7	ST742	cal	I		5.5		-8.1		11.80
TZ	180	ST7	ST742	cal	I		6.5		-6.4		9.88
TZ	180	ST7	ST742	cal	I		5.0		-6.2		9.47
TZ	180	ST7	ST742	cal	I		5.0		-14.5		18.40
TZ	180	ST7	ST742	cal	I		4.5		-16.0		19.60
TZ	180	ST7	ST742	cal	I		5.0		-8.4		12.20
TZ	180	ST7	ST742	cal	I		4.5		-10.2		14.20

---

## Curriculum Vitae

Name : Ulrich Richard Püschner  
Birth date : 18<sup>th</sup> of April 1972  
Place of birth : Frankfurt-Höchst/Main  
Nationality : German  
Profession : Geologist - Dipl. Univ.

### Education

1982-1991 : Wieland Gymnasium (D-88 400 Biberach/Riss) final exam: Abitur

### Obligatory service of Germany

1991 –1992 : Civil service in a sheltered workshop and a church community (15 months)

### Academic studies

1992-1994 : Basic study in Geology & Paleontology at University of Würzburg  
1994-1995 : Main studies in Engineering Geology at Technical University of Munich  
1996-1997 : Main studies in Geology & Paleontology at University of Würzburg  
03.08.1997 : Diploma exams at the University of Würzburg  
01.11.1997 : Ph.D. student and half-assistant position at the University of Basel  
08.10.2001 : Defence of the Ph.D.

### Internships & advanced training

08-09/1993 : Geodesy Institute U. Ender, Biberach/Germany  
03/1995 : Geo-Technical Institute Prof. Magar & Partner, Würzburg/Germany  
05-07/1995 : Material Testing Institute, Technical University of Munich/Germany  
09-10/1995 : English Language School, Auckland/New Zealand  
05-06/1997 : Geo-Technical Lab of the Geological Survey Rheinland-Pfalz, Mainz/Germany  
1997 – 2001 : Assistant for the electron microprobe and optical microscopy classes at the Mineralogic- Petrographic Institute, University of Basel/Switzerland  
03-08/2000 : Stable Isotope Lab of the Department of Geology at Indiana University of Bloomington/USA

### Award

07.05.1999 : Best Student Paper Award, Institute on Lake Superior Geology, 45<sup>th</sup> Annual Meeting

### Published Abstracts

**Püschner U.** and Schmidt S. Th., 1999, Low-grade metamorphism and hydrothermal alteration of the Keweenaw Portage Lake Volcanics, Michigan, *in* European Union of Geoscience, Strasbourg, France, v. 4, p. 791.  
**Püschner U.**, Schmidt S. Th. and Bornhorst Th. J., 1999, Low-grade metamorphism and hydrothermal alteration of the Upper Keweenaw Portage Lake Volcanics, Michigan, *in* Institute on Lake Superior Geology, Proceedings, Marquette, Michigan, v. 45, p. 49-50.  
**Püschner U.** and Schmidt S. Th., 1999, Phyllosilicates in the Keweenaw Portage Lake Volcanics, Michigan as a result of hydrothermal alteration ad very low-grade metamorphism, *in* Euroclay 1999, Krakow, Poland, p. 124.

- 
- Püschner U.** and Schmidt S. Th., 1999, Secondary mineralisation as a result of very low-grade metamorphism and hydrothermal alteration of the Keweenaw (Precambrian) Portage Lake Volcanics, Lake Superior, Michigan, USA, *in* Jahrestagung der Schweizerischen Naturforschenden Gesellschaft, Luzern, Switzerland.
- Püschner U.** and Schmidt S. Th., 2000, Low-grade metamorphic zonation of the Keweenaw Portage Lake Volcanics on the Keweenaw Peninsula, Michigan, *in* Annual Meeting of Institute on Lake Superior Geology, Thunder Bay, Ontario, v. 46, p. 53-55.
- Püschner U.** and Schmidt S. Th., 2000, The very low-grade metamorphic zonation of the Keweenaw Portage Lake Volcanics, Michigan, USA., *in* 78. Jahrestagung der Deutschen Mineralogischen Gesellschaft, Heidelberg, Germany, v. 12, p. 160.
- Pueschner U. R.**, Schmidt S. Th., Ripley E. M. and Park Y.-R., 2000, Low-grade metamorphism and stable isotope composition of alteration minerals in the Portage Lake Volcanics, Upper Peninsula, Michigan, *in* Annual Meeting of the Geological Society of America, Reno, Nevada, v. 32, p. A-365.
- Pueschner U.**, Schmidt S. Th. and Mullis J., 2001, The very low-grade metamorphism of the Portage Lake Volcanics, Keweenaw Peninsula/Michigan/USA – Results based on stable isotopes (O, H, C) and fluid inclusions, *in* European Union of Geo-Sciences, Strasbourg, France, v. 6, p. 237.

### **Supervisors and Referents**

P.D. Dr.

Susanne Th. Schmidt : Department of Mineralogy, Geneva University  
Email: Susanne.Schmidt@terre.unige.ch

Prof. Dr.

Martin Frey : Mineralogisch Petrographisches Insitut, Basel University  
died Sep. 2000

Prof. Dr.

Willem B. Stern : Mineralogisch Petrographisches Insitut, Basel University  
Email: W.Stern@unibas.ch

Prof. Dr.

Theodore J. Bornhorst: Department of Geological Engineering and Sciences,  
Michigan Technological University, Houghton/USA  
Email: tjb@mtu.edu